Distraction osteogenesis: mechanobiological modeling and numerical applications

A dissertation presented by

Esther Reina Romo

In partial fulfillment of the requirements for the degree of Doctor of Philosophy

Directed by

PhD Jaime Domínguez Abascal

and

PhD José Manuel García Aznar

UNIVERSITY OF SEVILLE, 2009

A mis padres

Acknowledgements

Son muchas las personas que han contribuido directa o indirectamente a esta tesis. Ante todo, a todas ellas muchísimas gracias por todo el apoyo tanto personal como profesional.

En primer lugar quisiera agradecer a mis directores de tesis, Jaime y Manu, su cercanía, consejos, así como su constante seguimiento e interacción durante esta tesis doctoral. A Jaime, que desde mis inicios en la carrera ha confiado en mi y por el que siento una gran admiración. A Manu, por su apoyo incondicional y seguimiento continuo que, a pesar de ser muchas veces a distancia, nos ha unido en una gran amistad.

A María José, a la que considero también mi directora de tesis y amiga, le agradezco de todo corazón su continua dedicación y disponibilidad. Su capacidad de trabajo así como su enorme paciencia, generosidad y talento han contribuido muy especialmente en mi formación personal y profesional. Muchas gracias Mariajo. Todo lo que pueda decir no es suficiente para expresar mi gratitud hacia ti.

Tampoco quisiera olvidarme del grupo GEMM de la Universidad de Zaragoza, que en todo momento me ha hecho sentir como en casa. Muy especialmente al profesor Manuel Doblaré, cuyo talento investigador es incalculable, siendo líder nacional en el campo de la bioingeniería y de reconocido prestigio internacional. Gracias a todos, en especial a Víctor, Pedro, Pas, Conchi, Fany, M^a Ángeles, José Felix, Elvio, Andrés Mena y Joan. Muchísimas gracias también a Ángel Sampietro por sus aportaciones y sugerencias en el marco de la biología.

Moreover I would like to express my gratitude to Dr Ian McCarthy, who let me take part of the UCL Institute of Orthopaedics and Musculoskeletal Science in the Royal National Orthopaedic Hospital of London. My three months internship has been very valuable as well as enriching, specially from the clinical point of view. Thanks also to all the BME group for their kind reception.

Asimismo quiero hacer extensible estos agradecimientos al grupo de Ingeniería Mecánica de la Universidad de Sevilla. En especial a mis compañeros de despacho pero sobre todo amigos Charo, Domingo y Joaquín que me han ayudado y

apoyado siempre que lo he necesitado.

También quisiera agradecer a todos mis amigos y familia todo el apoyo mostrado. Muy especialmente a mis abuelos, mi tía Sol, mi hermana y mis padres. A mi hermana Celia, que a pesar de estar lejos estos cuatro últimos años, la siento muy cerca. Y a mis padres, que me han mostrado un apoyo incondicional en todo lo que he hecho y que siempre serán un referente para mi.

Finalmente debo el agradecimiento más especial a José Antonio. Ha sido la persona que más me ha apoyado en los momentos difíciles de esta tesis así como la mejor recompensa de la misma. Sin su compresión e inestimable apoyo no hubiera sido posible finalizar esta tesis. ¡Gracias José!

Abstract

Distraction osteogenesis is a useful technique aimed at inducing bone formation through gradual traction of bony segments. Since its introduction by G. A. Ilizarov to the field of orthopedics in 1951, this technique has gained wide acceptance. It has been applied to many different situations and its use is continuously increasing for the treatment of limb or craniofacial deformities, reconstruction of large bony defects and fracture nonunions or malunions amongst others.

The purpose of this thesis is to apply numerical techniques to model this mechanobiologically regulated process. Very few works of distraction osteogenesis have been developed with mechanobiological rules. Therefore, this PhD thesis aims to predict the time-varying tissue evolution during distraction osteogenesis using a finite element framework. The main motivation is its potential interest to surgeons and biologists. In fact, accurate simulations of the process and patient specific models can help to the surgeon for a more precise pre-operative planning.

Therefore, in this document, a robust mathematical model that simulates the process of distraction osteogenesis is developed. This model considers the main cellular events underlying distraction osteogenesis namely cell proliferation, migration and differentiation as well as tissue growth and damage, and incorporates important effects such as the influence of the load history on tissue differentiation. The model is validated, to some extent, by analyzing the effect of the different distraction rates on the outcome of the distracted regenerate. The obtained results are compared with experimental data reported in the literature showing a close agreement.

Additionally to the above described new differentiation approach, another important feature of soft tissues, namely residual stresses is investigated in the field of bone lengthening. Therefore, a general macroscopic formulation able to consider residual stresses in living tissues is formulated. The fundamental aspect of this model is to assume that stress relaxation is regulated by the poroelastic behaviour of tissue matrix and tissue growth. This model is successfully validated with a clinical example that investigates the influence of residual stresses on the outcome of limb lengthening and is applied to different animal species and a human case to compare the pattern of limb lengthening in animals of

different sizes.

Due to the complexity of the distraction osteogenesis process, the above models have been applied to axisymmetrical geometries, showing the enormous potential of the mathematical rules proposed in 2D models. To test the reliability of the formulation in patient specific models, a three-dimensional approach of the process is performed. The 3-D study is based on data from a young male patient with unilateral mandibular hypoplasia of the right mandibular ramus, a type of hemifacial microsomia. Results show the ability of the model to predict tissue outcome in the interfragmentary gap and thus confirm the huge potential of mechanobiological models on clinical procedures.

Although further experimental validation is needed to completely corroborate the model, its ability to predict tissue outcome under different mechanical environments and within different types of bone indicates that distraction osteogenesis can be predicted by a model dependent on mechanobiological factors.

Keywords: Distraction osteogenesis, mechanobiology, Finite Element Method, residual stresses, tissue differentiation, tissue growth, load-history.

Resumen

La distracción osteogénica es una técnica que permite generar nuevo tejido óseo a partir de la separación gradual de dos fragmentos óseos. Desde que se introdujo en la ortopedia por G. A. Ilizarov, esta técnica ha ido ganando popularidad. De hecho, las aplicaciones de este proceso son muy numerosas: tratamiento de deformidades craneofaciales o de huesos largos, reconstrucción de grandes defectos óseos o tratamiento de no uniones entre otros.

El objetivo de esta tesis consiste en aplicar técnicas numéricas para simular este proceso. Hasta el momento se han implementado pocos modelos mecanobiológicos evolutivos para estudiar la distracción. Por lo tanto, esta tesis doctoral pretende predecir, desde un punto de vista computacional, la evolución temporo-espacial de los tejidos en el entorno de la osteotomía durante este proceso. La escasez de modelos computacionales en distracción osteogénica, así como el interés potencial que estos modelos ofrecen para la planificación pre-operatoria, es la principal razón y motivación de esta tesis.

Como primera aproximación, se desarrolla un modelo matemático que simula el proceso de distracción. El modelo implementado considera los distintos eventos celulares que tienen lugar durante el proceso: proliferación, migración y diferenciación celulares, así como el crecimiento y daño de los tejidos e incorpora efectos importantes como la influencia de la historia de carga en la diferenciación celular. Este modelo se valida de manera preliminar analizando el efecto de la velocidad de distracción en el tejido generado en el espacio interfragmentario y comparándolo con datos de la bibliografía.

Por otro lado, se ha investigado el efecto de las tensiones residuales en el marco de la distracción, ya que éstas constituyen una característica fundamental de todos los tejidos blandos. Para ello, se ha desarrollado e implementado una formulación general que incorpora las tensiones residuales en tejidos biológicos desde un punto de vista macroscópico. La hipótesis fundamental de este modelo se centra en suponer que la relajación de las tensiones está controlada por el comportamiento poroelástico de los tejidos y el crecimiento de los mismos. Se ha validado con éxito este modelo comparándolo en primer lugar con un caso clínico que investiga la influencia de las tensiones residuales en el proceso de distracción y posteriormente

analizando las diferencias existentes durante el proceso de elongación ósea entre distintas especies y el humano.

Dada la gran complejidad de la simulación del proceso de distracción ósea, los modelos han sido aplicados a geometrías axisimétricas, mostrando el enorme potencial de la formulación matemática propuesta en modelos bidimensionales. Sin embargo, con el fin de comprobar la fiabilidad del modelo en geometrías más realistas, se ha extendido también el modelo a un caso tridimensional. En concreto, el estudio se basa en los datos clínicos de un paciente pediátrico con hipoplasia mandibular unilateral de la rama derecha, un tipo de microsomía hemifacial. Se han predicho con éxito las distribuciones tisulares a lo largo del proceso, confirmando, por lo tanto, el enorme potencial de los modelos mecanobiológicos en el campo clínico.

A pesar de que una validación más exhaustiva del modelo es necesaria, se concluye del estudio que el modelo desarrollado permite determinar la evolución de los distintos tejidos en una gran variedad de ambientes mecánicos y de geometrías, y que por lo tanto este complejo proceso se puede predecir con un modelo dependiente de factores mecanobiológicos.

Palabras clave: Distracción osteogénica, mecanobiología, método de los elementos finitos, tensiones residuales, diferenciación tisular, crecimiento de tejidos, historia de carga.

Contents

Chapter 0

Distracción osteogénica: modelo y aplicaciones[1,2]

0.1 Introducción

La etimología del término distracción deriva de la palabra latina *distrahere* (de *dis*, separación, y *trahere*, echar hacia atrás) que significa tirar en varias direcciones. G. A. Ilizarov introdujo dicho concepto en el campo de la ortopedia en 1951 para describir el proceso de formación ósea que tiene lugar entre dos fragmentos óseos que se separan gradualmente. El profundo interés de Ilizarov en la influencia de la mecánica en los procesos biológicos le llevó a desarrollar su bien conocida ley de "*Tension-Stress*". Este principio describe cómo la tracción gradual de tejidos vivos genera unas tensiones que estimulan y mantienen la regeneración y crecimiento continuo de ciertas estructuras tisulares. Por lo tanto, el efecto de la mecánica en el proceso de distracción osteogénica es fundamental. Al igual que la distracción, existen numerosos procesos físicos regidos por estímulos mecánicos (e.g. consolidación ósea, osteoporosis y remodelación ósea). De hecho, estudios recientes de biología celular y molecular ponen de manifiesto la importancia de las fuerzas mecánicas en los procesos de diferenciación, desarrollo y remodelación tisular. Sin embargo, la identificación de los parámetros mecánicos y sus meca-

[1]Spanish translation of the most relevant contents of the English version of the dissertation.

[2]Traducción al español de los contenidos más relevantes de la versión escrita en inglés de la tesis.

nismos de acción aún son desconocidos y continúan siendo investigados.

Estas relaciones entre función y forma de muchos tejidos y órganos no es nueva y data de Galileo, que ya en 1638 estableció que tanto la gravedad como las fuerzas mecánicas son factores limitantes en el crecimiento y arquitectura de los órganos. En los últimos 150 años, Charles Darwin (1859), Karl Culmann (1864), G. Hermann von Meyer (1867), Julius Wolff (1892), Wilhelm Roux (1895), Gebhardt (1901), D'Arcy Thompson (1917), Friedrich Pauwels (1941), y Harrol Frost (1963) han reconocido la importancia de los factores mecánicos en el desarrollo y evolución de órganos y organismos.

Este concepto de regulación mecánica de los procesos biológicos es la principal premisa de la *mecanobiología*, un campo de investigación introducido en el siglo XX y que ha sido desarrollado en la década de los 90. A diferencia de la biomecánica (disciplina que trata del análisis y predicción de la mecánica de los seres vivos), este campo se centra en estudiar cómo el ambiente mecánico regula el comportamiento celular en los procesos biológicos, como por ejemplo, desarrollo, adaptación, crecimiento, remodelación, reparación, regeneración y diferenciación tisular. Incluye tanto modelos experimentales como analíticos, y permite entender la respuesta de los tejidos biológicos ante factores mecánicos (van der Meulen & Huiskes, 2002). Usualmente se divide en:

- *Mecanobiología experimental*, utilizada para examinar la diferenciación y adaptación de los tejidos ante cambios de carga, centrándose la mayoría de estos experimentos en la remodelación tisular ante cambios de estímulo mecánico. El experimento más habitual consiste en un dispositivo que aisla y controla el estímulo mecánico para así poder examinar la formación de distintos tejidos (Soballe *et al.*, 1992; Goodman *et al.*, 1994; Guldberg *et al.*, 1997; Tagil & Aspenberg, 1999; Altman *et al.*, 2002; Ng *et al.*, 2006).

- *Mecanobiología computacional*, cuyo principal objetivo es determinar cuantitativamente modelos matemáticos que relacionen la carga mecánica con la diferenciación, crecimiento, adaptación y mantenimiento de los tejidos. Primero se supone una posible regla de comportamiento y tras simularlo se determina si los resultados obtenidos concuerdan con las distribuciones tisulares reales (Claes & Heigele, 1999). Si los resultados de esta simulación

de prueba y error son satisfactorios, entonces se considera la regla propuesta como hipótesis de partida para ser evaluada de nuevo en condiciones diferentes.

El potencial que tiene la mecanobiología en el campo clínico es muy prometedor. Por ejemplo, patologías reguladas por factores mecánicos como la osteoporosis, neocondrogénesis, diferenciación tisular en las interfaces de implantes, consolidación ósea o distracción osteogénica contituyen hoy en día áreas de intensa investigación científica.

La mayoría de los procesos mecanobiológicos se pueden englobar en tres áreas principales: diferenciación tisular, crecimiento endocondral y crecimiento y adaptación ósea (Carter & Beaupré, 2001). En la Tabla 1 se enumeran aplicaciones de estas tres áreas, teniendo todas ellas en común que los factores mecánicos juegan un papel fundamental. Se puede observar cómo la distracción osteogénica es un claro ejemplo de proceso mecanobiológico, ya que queda englobado en las tres áreas: durante la elongación ósea se aplican fuerzas en el espacio interfragmentario que influyen significativamente en el crecimiento tisular y en la posterior osificación y remodelación ósea (Tabla 1).

Tabla 1: Regulación mecánica de los tejidos óseos y aplicaciones (adaptado de Carter & Beaupré (2001)) (Crec.=crecimiento; DO=distracción osteogénica).

Diferenciación tisular	Crecimiento y osificación endocondral	Crecimiento y adaptación óseos
Crec. y desarrollo	Crec. y desarrollo	Crec. y desarrollo
Regeneración tisular	**DO, fase consolidación**	**DO, fase remodelación**
Inicios consolidación	Formación articulaciones	Mantenimiento óseo
DO	Mantenimiento cartílago	Hipertrofia y atrofia óseas
Osteoartritis	Osteoartritis	Osteoporosis
Neocondrogénesis	Reparación cartílago	Osteoartritis
Fijaciones protésicas	Rehabilitación ósea	Remodelación peri-protésica
Rehabilitación ósea		Rehabilitación ósea

Entender la mecanobiología del proceso de distracción osteogénica a nivel tisular puede evitar complicaciones (e.g. no uniones) y promover la regeneración ósea a través de la estimulación mecánica en el espacio interfragmentario. Es

por ello, que en esta tesis se pretende desarrollar un modelo mecanobiológico que permita predecir el proceso de distracción ósea de manera precisa, desde un punto de vista computacional. Estas herramientas podrían ayudar en un futuro a los cirujanos ortopédicos en la planificación y desarrollo de operaciones y tratamientos.

0.2 Distracción osteogénica

La técnica de distracción osteogénica constituye un proceso biológico único de formación ósea entre dos fragmentos óseos que se separan gradualmente a través de una tracción incremental. Esta técnica se usa para corregir lesiones óseas severas y para alargar huesos. Los métodos tradicionales que trataban lesiones óseas severas han evolucionado desde los aparatos ortopédicos hasta la amputación y los injertos óseos. El primero es claramente visible y por lo tanto se rechaza frecuentemente por razones estéticas (Leung *et al.*, 2006). Los injertos óseos, clasificados en autógenos y autólogos, muestran limitaciones y presentan tasas de fallo del 22.5% al 38% (Ilizarov & Ledyaev, 1992). En los injertos autógenos, el tejido es proporcionado por el mismo individuo, mientras que en los injertos autólogos el tejido proviene de un donante. El primero consolida más rápidamente y es más fiable pero presenta complicaciones debidas a la provisión limitada y a la necrosis de la zona transplantada. El injerto autólogo en cambio puede propiciar una reacción inmunológica debida a las diferencias genéticas entre individuos y se induce el riesgo de padecer enfermedades infecciosas (Glowacki & Mulliken, 1985; Buck *et al.*, 1989). Los aloinjertos, injertos óseos procedentes de otras especies, tampoco son una opción válida debido al riesgo de transmisión de enfermedades y al rechazo inmunológico.

Por lo tanto, a la luz de estas limitaciones era necesaria una nueva metodología que solventara los problemas expuestos. Dentro de este contexto, la contribución de G. A. Ilizarov es indiscutible (Ilizarov & Soybelman, 1969; Ilizarov, 1988, 1989*a*,*b*). En base a su gran experiencia clínica y su intensa investigación científica, introdujo en el campo de la ortopedia lo que denominó distracción osteogénica.

La técnica de distracción osteogénica aprovecha el proceso natural de formación de hueso y de otros tejidos que tiene lugar en el cuerpo humano y,

por tanto, ofrece ventajas claras sobre los métodos tradicionales. Requiere mucho menos tiempo de operación que los injertos óseos, permite la elongación de cualquier tipo de hueso, la hospitalización rara vez supera las 24 horas, no existe necrosis de la zona transplantada, no es necesario realizar transfusiones de sangre y permite además la elongación de los tejidos blandos circundantes (Fonseca, 2000). Además de los beneficios médicos, los pacientes pueden mantener una vida próxima a la normalidad durante todo el tratamiento, permitiendo andar y trabajar a la mayoría de los pacientes (Heller, 1998). Con este tratamiento también se producen ahorros de 30,000 $ por paciente aproximadamente en comparación con los métodos convencionales, y de 345,000 $ por paciente en comparación con los costes de amputación debido al menor coste protésico durante el resto de la vida de los pacientes (Lieberman & Friedlaender, 2005). Las desventajas de este método incluyen la larga duración del tratamiento, la necesidad de una monotorización continua y la medicación frecuente (Kirienko *et al.*, 2003).

Las complicaciones potenciales de este método son comparables a las que presentan otras técnicas quirúrjicas. Entre ellas, la contracción muscular, la luxación de la articulación, los problemas asociados a los *pins*, desviación axial, lesiones neurológicas, lesiones vasculares, consolidación prematura, retrasos en la consolidación y no unión (Paley, 1990). Estas complicaciones pueden minimizarse con una técnica meticulosa y con una monitorización muy cuidadosa; pueden considerarse aceptables a la vista de los beneficios potenciales de esta técnica.

Debido a las ventajas que ofrece el proceso de distracción ósea respecto a los métodos convencionales, se ha aplicado esta técnica a las situaciones ortopédicas más desafiantes como la elongación de huesos largos, el transporte óseo y el tratamiento de no-uniones y deformidades (Paley *et al.*, 1989; Hyodo *et al.*, 1996; Aronson, 1997; Paley *et al.*, 1997). Además, en los últimos 20 años se ha introducido esta técnica al resto del organismo. Por ejemplo, en la región craneofacial se han abierto multitud de posibilidades en la corrección de deformidades craneofaciales así como de lesiones faciales resultantes de una situación de trauma. También se aplica para tratar deformaciones complejas del pie para las que no existe ningún otro tratamiento (Grant *et al.*, 1992; Paley, 1993; de la Huerta, 1994), para crear nuevos ligamentos (Aston *et al.*, 1992), corregir deformidades de los tejidos blandos (e.g. contracciones crónicas de la rodilla y del codo) (Cal-

houn *et al.*, 1992*a*; Haggland *et al.*, 1993; Herzenberg *et al.*, 1994*a*) o huesos planos como las vértebras (Lieberman & Friedlaender, 2005).

Algunas de las patologías que requieren el tratamiento con distracción osteogénica son muy comunes en la población. Por ejemplo, el 23% de la población presenta una diferencia en la longitud de las piernas de 1 cm y aproximadamente 1 de cada 1000 requerirá un dispositivo de corrección (Rozbruch & Ilizarov, 2006). Las personas afectadas le dan una importancia similar a los factores estéticos y a las limitaciones funcionales, que afectan tanto estática como dinámicamente a todo el sistema musculoesquelético y postural. Las causas de esas diferencias de longitud pueden ser congénitas o adquiridas. Los defectos congénitos constituyen las causas más comunes de acortamientos óseos como la deficiencia focal del fémur proximal, las hemimelias o las pseudoartrosis congénitas. Las patologías adquiridas son también frecuentes e involucran una gran pérdida de hueso y tejido blando. Pueden ser debidas a la resección de un tumor, a situaciones traumatológicas de alta energía o a fracturas no consolidadas. Por ejemplo, en Estados Unidos el 5-10 % (250,000 a 500,000) de las fracturas no consolidan o terminan en una mala unión (Rockwood *et al.*, 2006). La mayoría de esas no-uniones dan lugar a acortamientos óseos. Además, los defectos craneofaciales susceptibles de ser tratados con distracción son muy comunes. Por ejemplo, el 10% de la población presenta un resalte dental significante consecuencia de patologías congénitas o adquiridas (http://emedicine.medscape.com/article/844837-overview).

0.3 Teorías de diferenciación tisular

Los procesos de distracción osteogénica, consolidación ósea, adaptación a implantes óseos, regeneración y desarrollo óseo constituyen procesos de diferenciación de tejido óseo e involucran muchos tipos de células y tejidos. Durante esos procesos los tejidos están en constante cambio debido al crecimiento y a la respuesta al ambiente, tanto mecánico como químico o físico.

Una célula que es vital para esos cambios es la célula madre mesenquimal (MSCs). A lo largo de su diferenciación, las MSCs se dividen en “células hijas”, que tras sufrir una serie de cambios en su fenotipo terminan en la fabricación de un único tipo de tejido, ver Figura 1 (Caplan & Boyan, 1994). Sin embargo, el

programa de diferenciación de las MSCs se puede alterar como consecuencia de cambios en el estímulo mecánico y químico. Esto es lo que se conoce como plasticidad celular (Roder, 2003). Numerosos investigadores han intentado relacionar la excitación mecánica de un tejido sin diferenciar con el proceso de diferenciación que tiene lugar. Este concepto es antiguo y data de finales del siglo XIX, cuando William Roux, en sus estudios de morfología funcional, afirmó que a nivel de célula, los procesos biológicos están regulados por cargas mecánicas (Roux, 1895).

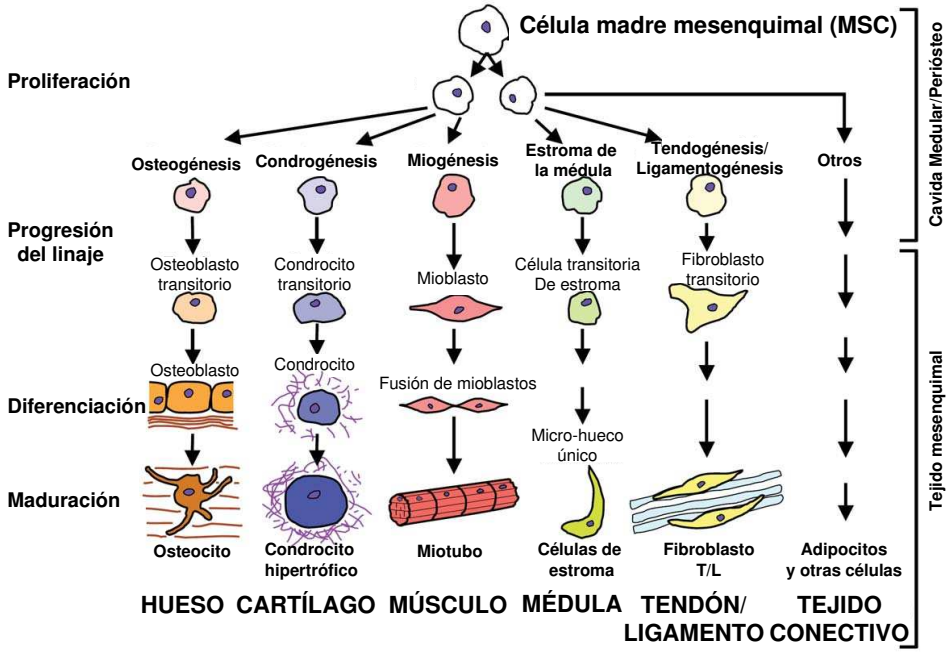

Figura 1: El proceso de diferenciación celular (Caplan & Boyan, 1994).

En base a estos trabajos previos, Pauwels (1941) propuso una de las primeras teorías de diferenciación celular en función de las condiciones mecánicas. Consideraba que la componente desviadora de la tensión controlaba la diferenciación de las células madre a fibroblastos y que la octaédrica es la que estimula la diferenciación de las células madre a condrocitos (Figura 2). Las combinaciones de estos estímulos darían lugar a fibrocartílago mientras que el tejido óseo sólo aparecería en ambientes mecánicos de bajo estímulo.

Posteriormente, Perren (1979) y Perren & Cordey (1980) propusieron un

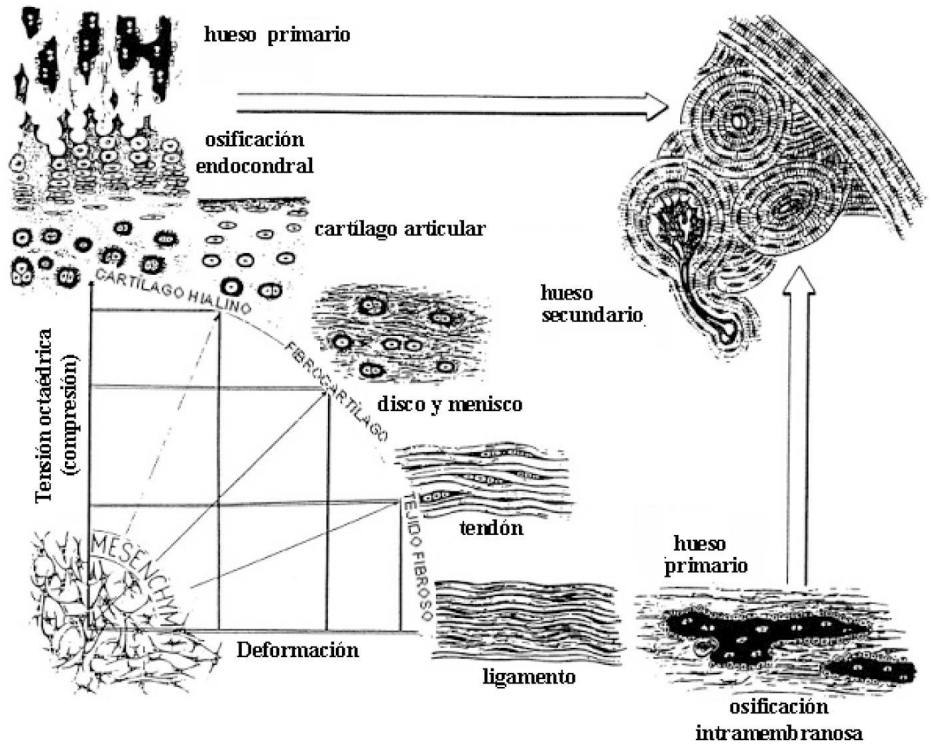

Figura 2: Esquema de diferenciación tisular propuesto por Pauwels (1941).

modelo de diferenciación controlado por la deformación interfragmentaria (IS). Esta deformación interfragmentaria fue definida como el cociente entre el movimiento longitudinal del espacio interfragmentario y el tamaño del mismo. Según esta teoría cada tejido puede soportar únicamente un rango de deformación específico, fuera del cual se iniciaría la diferenciación a otro tejido (Figura 3). Esta teoría, sin embargo, únicamente considera la deformación axial o longitudinal, no teniendo en cuenta efectos tridimensionales.

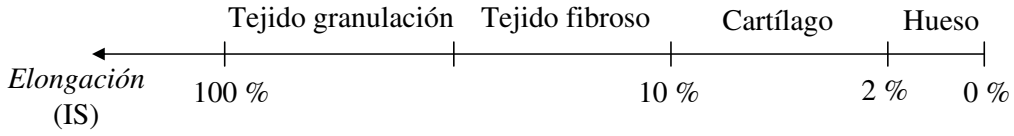

Figura 3: Concepto de diferenciación según Perren (1979).

Siguiendo la idea inicial de Pauwels, Carter formuló la diferenciación tisular en base al estado tensional tridimensional (Carter, 1987; Carter *et al.*, 1998). La

Figura 4 muestra cómo la componente octaédrica de compresión es la responsable de la formación de cartílago mientras que la desviadora favorece la aparición de tejido fibroso. Finalmente el hueso aparece en regiones de estado tensional bajo.

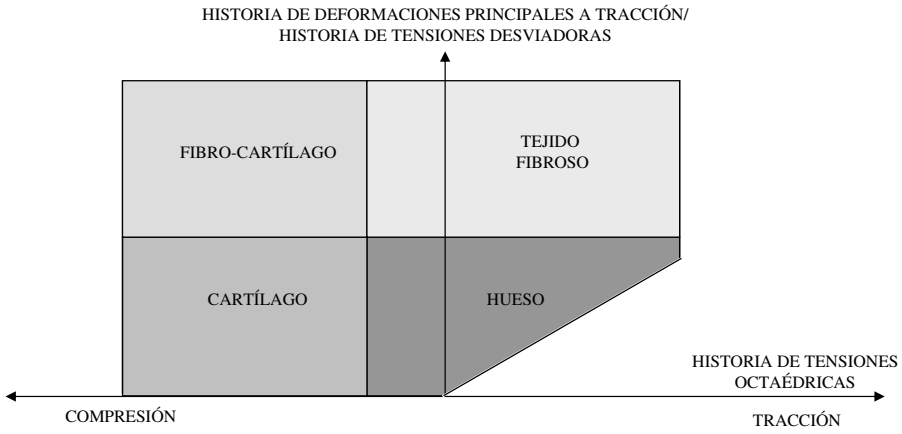

Figura 4: Esquema de diferenciación de Carter *et al.* (1998).

Posteriormente Claes & Heigele (1999), en base a sus estudios experimentales, propusieron una teoría mecanoreguladora muy similar a la de Carter (1987) pero formulada en términos cuantitativos (Figura 5).

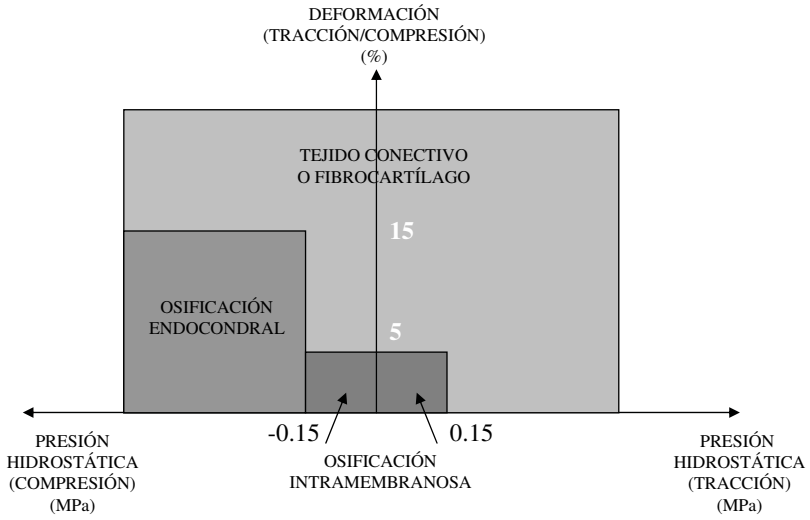

Figura 5: Modelo de diferenciación tisular según Claes & Heigele (1999).

Prendergast *et al.* (1997) propusieron para la interfaz hueso-implante, una ley

de diferenciación controlada por dos estímulos mecánicos: el nivel de deformaciones en la matriz y la velocidad relativa del fluido que circula en su interior (Figura 6).

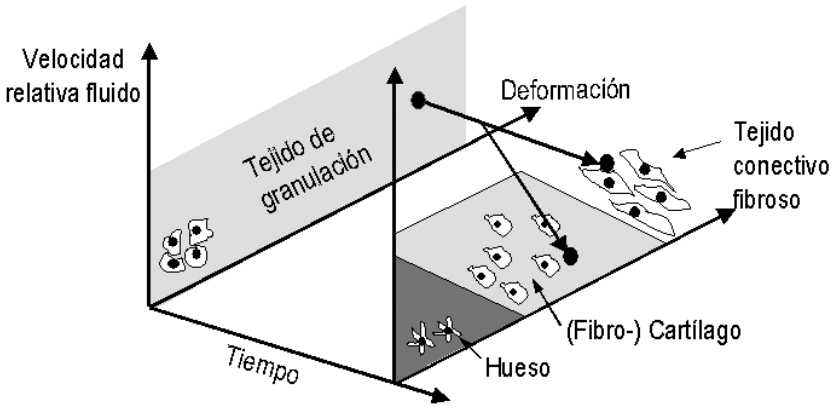

Figura 6: Teoría de diferenciación propuesta por Prendergast *et al.* (1997).

Finalmente Gómez-Benito *et al.* (2005), Doblaré & García-Aznar (2006) y García-Aznar *et al.* (2007) desarrollaron un modelo matemático regido exclusivamente por el segundo invariante del tensor desviador de deformaciones, asumiendo un comportamiento bifásico de los tejidos.

A pesar de que estas teorías son diferentes, presentan características comunes. En primer lugar, en todas ellas, un estímulo mecánico alto favorece la formación de fibrocartílago mientras que ambientes con bajo estímulo favorecen la aparición de hueso. En segundo lugar, todos ellos desarrollan leyes mecanobiológicas mediante teorías formuladas a partir de observaciones empíricas. En tercer lugar, ninguna teoría está suficientemente validada a pesar de poder reproducir el patrón característico del proceso de consolidación ósea en ambientes mecánicos específicos. Finalmente, todas las teorías están reguladas por un estímulo mecánico, considerando implícitamente los procesos biológicos pero sin incluirlos directamente.

0.3.1 Modelos de consolidación ósea

A pesar de que la gran mayoría de las teorías de diferenciación anteriormente descritas se desarrollaron con herramientas numéricas, como por ejemplo el método

de los elementos finitos (MEF), las más antiguas se iniciaron con la aparición de estas herramientas. Así, por ejemplo, Cheal *et al.* (1991) retomaron la hipótesis de la deformación interfragmentaria propuesta por Perren (1979). Compararon la histología del callo de fractura con la deformación del mismo usando el MEF para así poder determinar computacionalmente el campo de deformaciones en el callo en la primera etapa del proceso de consolidación. Además, aunque no demostraron el daño existente en los tejidos, sí que encontraron una correlación entre reabsorción ósea con altos niveles de deformación, así como, formación ósea con bajos niveles de deformación.

Ament & Hofer (1996, 2000) propusieron un modelo biomecánico basado en la lógica difusa para describir la diferenciación tisular durante la consolidación. Además del estímulo mecánico introdujeron un factor biológico, la vascularización, para así poder distinguir entre osificación intramembranosa y endocondral. El estímulo mecánico era la densidad energía de deformación. Predijeron con éxito la formación de cartílago, el crecimiento del callo, y la posterior reabsorción del mismo tras la osificación del espacio interfragmentario. Esta formulación ha sido retomada recientemente por Simon *et al.* (2003) y Shefelbine *et al.* (2005). Los autores simularon con el MEF y la lógica difusa, el proceso de consolidación ósea, basándose en la teoría de diferenciación de Claes & Heigele (1999).

Bailón-Plaza & van der Meulen (2001) plantearon el primer modelo mecanobiológico bidimensional que incluía los factores de crecimiento. Este modelo se modificó posteriormente para incorporar el efecto del estímulo mecánico en la diferenciación celular (Bailón-Plaza & van der Meulen, 2003). Recientemente Geris *et al.* (2006, 2008) extendieron este modelo introduciendo aspectos claves de la consolidación ósea, como la vascularización y compararon los resultados con datos experimentales.

Lacroix *et al.* (2002) propusieron un modelo de consolidación ósea basado en la teoría de diferenciación celular propuesta anteriormente por Prendergast *et al.* (1997). Este modelo ha sido utilizado posteriormente por Andreykiv *et al.* (2007) para incluir los procesos de difusión, proliferación y diferenciación de las poblaciones celulares (MSCs, fibroblastos, condrocitos y osteoblastos). Isaksson *et al.* (2008) propusieron un modelo similar para desarrollar una formulación mecánica de la diferenciación tisular durante la consolidación ósea, relacionando

mecanismos celulares con el estímulo mecánico.

Finalmente, Gómez-Benito *et al.* (2005), Doblaré & García-Aznar (2006) y García-Aznar *et al.* (2007) reprodujeron con éxito los principales eventos que ocurren durante la consolidación ósea: la proliferación, migración y diferenciación celular, así como el daño de los tejidos y la vascularización. Además, mejoraron los modelos numéricos existentes de consolidación (Ament & Hofer, 2000; Bailón-Plaza & van der Meulen, 2001; Lacroix & Prendergast, 2002*a*; Bailón-Plaza & van der Meulen, 2003) con la incorporación de una formulación matemática que describía el crecimiento del callo.

0.3.2 Modelos de distracción osteogénica

El fenómeno biológico que tiene lugar en la distracción es muy similar al de la consolidación ósea (Lammens *et al.*, 1998; Jensen, 2002) por lo que la mayoría de los modelos de distracción ósea parten de esquemas de diferenciación tisular ya propuestos para la consolidación.

Hasta el momento se han implementado pocos modelos para el caso de distracción, comparado con la gran cantidad de modelos de consolidación ósea. La mayoría de estos modelos analizan cómo la geometría, propiedades del material y carga afectan al ambiente mecánico del espacio interfragmentario en uno o varios instantes del proceso de distracción (Carter *et al.*, 1998; Samchukov *et al.*, 1998; Loboa *et al.*, 2005; Kofod *et al.*, 2005; Cattaneo *et al.*, 2005; Boccaccio *et al.*, 2006; Morgan *et al.*, 2006). Estos son los llamados modelos biomecánicos.

Por ejemplo, Samchukov *et al.* (1998) evaluaron desde el punto de vista biomecánico la orientación de distractores lineales con un modelo bidimensional de una mandíbula humana. Concluyeron que estos dispositivos deben estar orientados paralelos al eje de distracción.

Carter y sus colaboradores (Carter *et al.*, 1998; Morgan *et al.*, 2006) caracterizaron el ambiente biofísico del espacio interfragmentario durante la distracción. En primer lugar, Carter *et al.* (1998) obtuvieron en dos instantes concretos de la distracción los campos de deformación principal máxima y de tensión hidrostática. Posteriormente, Morgan *et al.* (2006) cuantificaron computacionalmente la distribución espacial y temporal de cuatro estímulos mecánicos para la diferen-

ciación tisular (presión, deformación principal máxima, velocidad del fluido y deformación octaédrica), concluyendo que la deformación octaédrica del tejido es clave para la regeneración ósea (Figura 7).

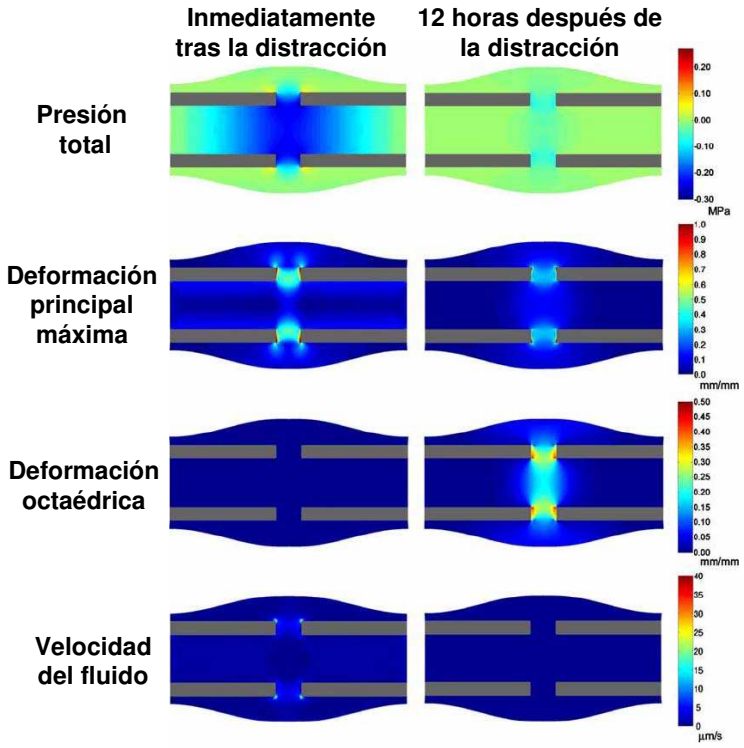

Figura 7: Valores de la presión, deformación principal máxima, deformación octaédrica y velocidad del fluido en el espacio interfragmentario (Morgan *et al.*, 2006).

En este mismo grupo de investigación, Loboa *et al.* (2005) implementaron un análisis tridimensional de elementos finitos de la mandíbula de una rata en distintos momentos del proceso. Determinaron la evolución de los campos de tensión hidrostática y de deformación durante el proceso y lo compararon con éxito con histologías previas.

Kofod *et al.* (2005) y Cattaneo *et al.* (2005) investigaron el campo de tensiones en la mandíbula y en la articulación temporomandibular (ATM) antes y después del proceso de distracción mediante el MEF. En base a sus resultados, sugirieron que la técnica de distracción osteogénica permite normalizar la distribución de tensiones en la ATM.

Boccaccio *et al.* (2006) estudiaron la respuesta mecánica de una mandíbula humana con distractores comparando los campos de desplazamientos y de tensiones en una mandíbula sana y en otra con una osteotomía. En concreto, analizaron el efecto de la masticación en la mandíbula no distraída, el efecto de una expansión progresiva del distractor y la velocidad de distracción (0.6 y 1.2 mm/día). Concluyeron que las respuestas mecánicas de la mandíbula sana y distraída son muy distintas y que una velocidad de 1.2 mm/día reproduce mejor el campo de desplazamientos impuesto por el distractor.

Sin embargo, los modelos evolutivos proporcionan mejores aproximaciones de la diferenciación tisular como función del ambiente mecánico a lo largo de todo el periodo de distracción. Hasta ahora, existen pocos modelos capaces de predecir la evolución temporo-espacial de los distintos tejidos en el espacio interfragmentario (Idelsohn *et al.*, 2006; Isaksson *et al.*, 2007; Boccaccio *et al.*, 2007, 2008). Todos ellos hacen uso del esquema de diferenciación propuesto por Prendergast *et al.* (1997) (véase Figura 6). Idelsohn *et al.* (2006) simularon las tres fases de la distracción en la mandíbula de un conejo. Analizaron la influencia de la frecuencia de distracción recomendando bajas frecuencias en la primera etapa del proceso. Isaksson *et al.* (2007) simularon la regeneración ósea en la tibia de una oveja durante todo el proceso de distracción osteogénica. Estos autores predijeron con éxito la distribución tisular con distintas frecuencias y velocidades de distracción pero no así la evolución de la fuerza necesaria para producir la distracción. Boccaccio *et al.* (2007, 2008) analizaron la influencia de la velocidad de distracción y la duración del periodo de latencia en el callo de fractura de una mandíbula humana sometida a distracción en la zona sinfisaria (Figura 8). En este trabajo se determinó un periodo máximo de latencia de 1 semana para evitar uniones prematuras y una velocidad óptima de distracción de 1.2 mm/día.

0.4 Motivación y objetivos del presente trabajo

El proceso de distracción osteogénica ha ido ganando popularidad debido su número elevado de aplicaciones. Sin embargo, hoy en día, la mayoría de los cirujanos son autodidactas dadas las instrucciones tan limitadas de las que disponen. Además, a pesar de la reducción en el número de complicaciones, se trata de

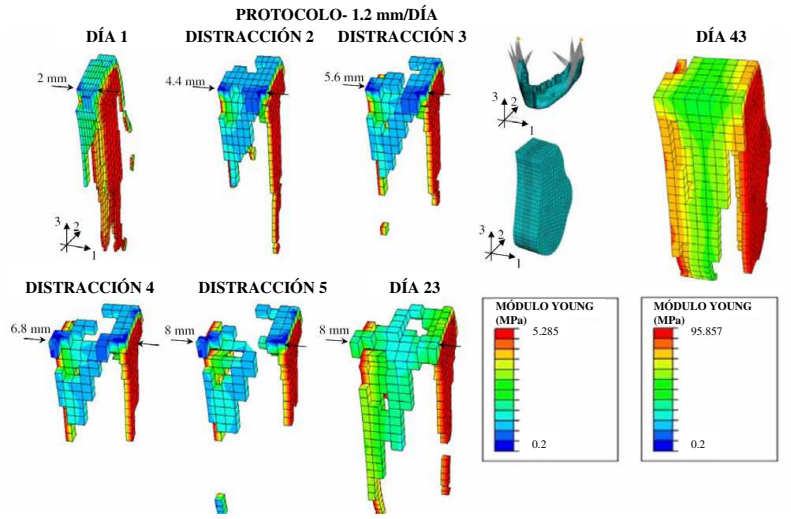

Figura 8: Proceso de regeneración ósea para una velocidad de distracción de 1.2 mm/día (Boccaccio *et al.*, 2007).

un proceso muy complejo con multitud de adversidades. Hace falta buen juicio, conocimiento exacto y una técnica meticulosa para la selección y diseño de los dispositivos, la realización de las corticotomías, maximizar la regeneración ósea, localizar la inserción de los *pins*, mantener la función articular y determinar el momento exacto para retirar el distractor (Dahl *et al.*, 1994).

Sin embargo, los nuevos avances a nivel celular, molecular y computacional, así como los nuevos diseños de los distractores externos e internos ayudan al perfeccionamiento de la técnica. Desde la década de los 80, con el desarrollo de los ordenadores, se ha producido un creciente interés por parte de los ingenieros, matemáticos y físicos en las áreas biomédicas, y en particular, en la última década, en la distracción osteogénica. En este aspecto, los ingenieros desempeñan un papel crucial en este campo tan incipiente ya que simulaciones precisas del proceso y modelos específicos para cada paciente mejorarían los tratamientos y operaciones clínicas.

En la actualidad existen numerosos modelos biomecánicos (Carter *et al.*, 1998; Samchukov *et al.*, 1998; Loboa *et al.*, 2005; Kofod *et al.*, 2005; Cattaneo *et al.*, 2005; Boccaccio *et al.*, 2006; Morgan *et al.*, 2006) en los que la geometría, propiedades del material y carga se analizan en uno o varios instantes del proceso

de distracción. Sin embargo, hasta el momento se han implementado pocos modelos mecanobiológicos evolutivos de distracción (Idelsohn *et al.*, 2006; Isaksson *et al.*, 2007; Boccaccio *et al.*, 2007, 2008).

La escasez de modelos computacionales en distracción osteogénica así como el interés potencial que éstos ofrecen para la planificación pre-operatoria es la principal razón y motivación de esta tesis. En particular, el primer objetivo es desarrollar un modelo mecanobiológico robusto capaz de predecir las principales características de la distracción en distintos ambientes mecánicos y en diferentes tipos de hueso. Así, por ejemplo, el efecto de la velocidad de distracción, las tensiones residuales, la rigidez del fijador, o la geometría del hueso han sido analizados en la distracción de huesos largos mientras que un caso clínico de microsomía hemifacial ha sido simulado en una mandíbula reconstruida a partir de la geometría del paciente. Diferentes protocolos clínicos han sido simulados y contrastados con datos experimentales. Para materializar estos objetivos, el documento se organiza como sigue.

En el capítulo dos, se describe brevemente la fisiología de los tejidos más importantes involucrados en la distracción y se analizan los principales principios biológicos que rigen el proceso. En particular, se tratan los siguientes tejidos: hueso, cartílago, tejido de granulación y tejido fibroso. Además, se detallan las distintas fases de la distracción osteogénica, la histología, medidas de fuerza necesarias para distraer, factores biomecánicos y aplicaciones del proceso.

En el capítulo tres, se presenta y describe un nuevo modelo matemático de distracción ósea. Este modelo considera los distintos procesos celulares que tienen lugar durante la distracción: proliferación, migración y diferenciación celulares, así como el crecimiento y daño de los tejidos e incorpora efectos importantes como la influencia de la historia de carga en la diferenciación celular. Dado que se ha visto que la mecánica influye profundamente en este proceso, en este capítulo se simula el modelo en distintos ambientes mecánicos y se comparan con datos experimentales. En concreto, se analiza el efecto de las siguientes velocidades de distracción: 1 mm/día, 0.3 mm/día y 2 mm/día.

En el capítulo cuatro se desarrolla una formulación general que considera las tensiones residuales en tejidos biológicos desde un punto de vista macroscópico. Posteriormente se particulariza al proceso de distracción osteogénica y se aplica

el modelo a un ejemplo clínico para validarlo de manera preliminar. Finalmente, también se implementa este modelo en distintas geometrías para comparar el proceso de distracción entre diferentes especies animales y el humano.

En el capítulo cinco se aplica el modelo a una mandíbula pediátrica afectada con microsomía hemifacial. El capítulo se subdivide en el análisis de esta patología y su tratamiento desde dos perspectivas: biomecánica y mecanobiológica. En primer lugar, se analiza el campo de deformaciones antes y después del proceso de distracción y se compara con un caso ideal sano. En segundo lugar, se extiende el modelo mecanobiológico para simular la evolución temporo-espacial de las poblaciones celulares y tejidos en una mandíbula tridimensional comparándose con los resultados clínicos.

Finalmente, en el capítulo seis, se presentan las conclusiones finales, el trabajo futuro y las aportaciones originales de este documento.

0.5 Conclusiones

En este trabajo se ha presentado un nuevo modelo de distracción osteogénica que permite predecir las principales características temporo-espaciales de los tejidos en el espacio interfragmentario. Se han implementado los procesos celulares que tienen lugar durante la distracción: proliferación, migración y diferenciación, así como el crecimiento y daño de los tejidos basándose en una formulación matemática previamente desarrollada para la consolidación ósea (Gómez-Benito *et al.*, 2005). Dicho modelo se ha extendido introduciendo nuevos aspectos en la formulación de la diferenciación celular.

En primer lugar, se ha incorporado el efecto de la historia de carga en la diferenciación a través de una ley lineal acumulativa similar a la regla de Miner de daño acumulado por fatiga (Miner, 1945). La idea se basa en la hipótesis de que las células evolucionan y maduran de forma paulatina en su proceso de diferenciación en función de la señalización percibida por las mismas que se encuentra regulada por los cambios producidos en el ambiente mecánico. Hasta que no se alcanza un grado de maduración las células pueden desdiferenciarse y diferenciarse a otros tipos celulares. Esta alteración potencial del proceso se conoce como *plasticidad celular* (Roder, 2003).

Para analizar la potencialidad del modelo, se ha estudiado una amplia variedad de condiciones mecánicas, comparando cualitativamente los resultados con datos experimentales. Se ha demostrado que el modelo, bajo esta nueva hipótesis, permite reproducir resultados recogidos en la bibliografía, como la influencia de la velocidad de distracción o las diferencias entre especies.

Además de la nueva ley propuesta de diferenciación, se ha investigado la influencia de las tensiones residuales en distracción ósea, al tratarse de una característica fundamental de todos los tejidos blandos. A diferencia de las simulaciones existentes hasta ahora, que consideraban una relajación completa de los tejidos tras el proceso de carga diario, en esta tesis, basándose en resultados experimentales, se ha considerado que una configuración libre de tensiones antes del proceso de distracción diario es improbable (Brunner *et al.*, 1994; Waanders *et al.*, 1998; Matsushita *et al.*, 1999; Richards *et al.*, 1999). En concreto, se ha propuesto un nuevo modelo de crecimiento que modela la relajación de tensiones como función de la producción de matriz. En este sentido, al igual que propone Humphrey & Rajagopal (2003), se considera que el campo de deformaciones depende de la variación de la cantidad de matriz producida.

Por otro lado, se ha implementado el modelo mecanobiológico de distracción en tres dimensiones. La simulación tridimensional se basa en los datos clínicos de un paciente pediátrico con hipoplasia mandibular en la rama derecha que fue tratado con distracción osteogénica. Se reconstruyó la mandíbula del paciente a partir de tomografías axiales computarizadas (TACs) y se simuló con éxito el protocolo clínico de distracción obteniéndose la evolución de tejidos y células en la rama distraída.

Las principales conclusiones de esta tesis son las siguientes:

- Se ha observado la importancia de considerar la historia de carga en la diferenciación celular para poder predecir el efecto de la velocidad de distracción en la regeneración ósea del espacio interfragmentario. Estudios existentes analizan con éxito bajas velocidades de distracción (Isaksson *et al.*, 2007), pero sin embargo no son capaces de predecir no uniones a altas velocidades, en las que el papel de la historia de carga es fundamental.

- Al simular el efecto de la velocidad de distracción, se ha corroborado com-

putacionalmente su importancia en la osificación del espacio interfragmentario: bajas velocidades de distracción resultan en uniones prematuras mientras que velocidades altas dan lugar a uniones fibrosas o no uniones.

- Se ha demostrado que la incorporación del efecto de las tensiones residuales en el modelado de la distracción ósea es fundamental ya que permite realizar una estimación adecuada de las fuerzas resultantes del proceso con unas propiedades del material acordes con la bibliografía. Hasta ahora, los modelos existentes hacían uso de propiedades del material elevadas para ser capaces de predecir la rigidización propia del proceso de distracción.

- A pesar de que es necesario incluir las tensiones residuales para poder predecir la evolución de la fuerza de reacción con propiedades del material realistas, las distribuciones tisulares no son tan dependientes de este efecto mostrando resultados similares con y sin fuerzas de pre-tracción.

- Modificando únicamente la geometría y maduraciones celulares, se han predicho las principales diferencias existentes entre distintas especies animales y el humano durante el proceso de elongación ósea: la fuerza de reacción es un orden de magnitud menor en el conejo en comparación con la del humano y la oveja, y mayores cantidades de cartílago son predichas en el conejo en comparación con los otros dos casos.

- El modelado tridimensional del proceso de distracción osteogénica mandibular ha permitido visualizar las similitudes entre el campo de deformaciones de la mandíbula tras el proceso de elongación ósea y el mismo campo de deformaciones del caso ideal sano. Sin embargo, las diferencias entre la mandíbula original y el caso ideal sano son significativas tanto cuantitativa como cualitativamente, corroborando el éxito del proceso clínico de distracción desde el punto de vista biomecánico.

0.6 Aportaciones originales

Para el desarrollo de esta tesis, se ha implementado el modelo de distracción ósea con el programa comercial de elementos finitos Abaqus®. En concreto, se utilizó

este software para resolver los análisis poroelástico, termoelástico y los dos de difusión descritos en la sección 3.4. El análisis poroelástico se implementó dentro de dos subrutinas diferentes. La primera consiste en una subrutina de usuario que define el comportamiento mecánico del material (UMAT) en el código de elementos finitos. En ella se incorporó la historia de carga al modelo previamente desarrollado para la consolidación ósea (Gómez-Benito *et al.*, 2005; García-Aznar *et al.*, 2007). En segundo lugar, para poder considerar las tensiones residuales fue necesario elaborar una subrutina de usuario (UEL) de Abaqus. Todas estas subrutinas fueron programadas en lenguaje Fortran 95. Por otro lado, el remallado diario llevado a cabo para evitar la excesiva distorsión de los elementos se implementó en Ansys® y Matlab®. Otros softwares fueron necesarios para el desarrollo de este trabajo. Por ejemplo, los TACS fueron tratados en Mimics®, la generación de la malla en Harpoon® y Ansys ICEM® y la visualización de los resultados en Tecplot®.

Las principales aportaciones de esta tesis son:

- Se ha formulado un nuevo concepto de diferenciación celular que tiene en cuenta la influencia de la historia de carga en el proceso de maduración hacia un fenotipo específico. Ello abandona la idea clásica de diferenciación directa de las células madre usado hasta ahora en modelos de consolidación y distracción ósea.

- Simulación computacional de modelos de distracción osteogénica bidimensionales y tridimensionales. Se han simulado tanto huesos largos como una mandíbula real de un paciente. En ambos casos se producen cambios geométricos importantes con las dificultades numéricas que esto implica.

- Análisis de distintos ambientes mecánicos durante el proceso de distracción osteogénica. En concreto, se ha estudiado el efecto de la velocidad de distracción en la regeneración tisular.

- Comparación de las distribuciones tisulares y fuerzas de reacción en distintas especies y el humano para evaluar el efecto de la geometría en el proceso de distracción.

- Formulación de un modelo que incluye las tensiones de pre-tracción en distracción osteogénica. Este modelo se simuló en casos de elongación de huesos largos asumiendo un estado de tensiones no nulo antes del proceso de carga diario.

0.7 Publicaciones

Fruto de esta tesis doctoral se han publicado los siguientes trabajos de investigación en revistas científicas y conferencias:

0.7.1 Revistas

- Reina-Romo E., Gómez-Benito M.J., García-Aznar J.M., Domínguez J., Doblaré, M. (2009). Modeling Distraction Osteogenesis: Analysis of the distraction rate. *Biomechanics and Modeling in Mechanobiology.* 8: 323-35.

- Reina-Romo E., Gómez-Benito M.J., García-Aznar J.M., Domínguez J., Doblaré, M. Growth mixture model of distraction osteogenesis: effect of pre-traction stresses. *Biomechanics and Modeling in Mechanobiology.* In Press, DOI: 10.1007/s10237-009-0162-5.

- Reina-Romo E., Gómez-Benito M.J., García-Aznar J.M., Domínguez J., Doblaré, M. An interspecies computational study on limb lengthening. *Enviado.*

- Reina-Romo E., Sampietro-Fuentes A., Gómez-Benito M.J., García-Aznar J.M., Domínguez J., Doblaré, M. Biomechanical response of a mandible in a patient affected with hemifacial microsomia before and after distraction osteogenesis. *Enviado.*

- Reina-Romo E., Sampietro-Fuentes A., Gómez-Benito M.J., García-Aznar J.M., Domínguez J., Doblaré, M. Three-dimensional simulation of mandibular distraction osteogenesis: mechanobiological analysis. *En preparación.*

0.7.2 Conferencias

- Reina E., Gómez-Benito M.J., García-Aznar J.M., Domínguez J., Doblaré, M. Modelo computacional de distracción ósea. CMNE/CILAMCE, Semni. Oporto, Portugal, Junio, 2007.

- Reina E., Gómez-Benito M.J., García-Aznar J.M., Domínguez J., Doblaré, M. Influence of distraction rate on the outcome of distraction osteogenesis: computational simulation. European Society of Biomechanichs Workshop 2007. Dublín, Irlanda, Agosto, 2007.

- Reina E., Gómez-Benito M.J., García-Aznar J.M., Domínguez J., Doblaré, M. Influencia de la velocidad de distracción en la regeneración ósea. Modelo computacional. 8^o Congreso Iberoamericano de Ingeniería Mecánica. Cusco, Perú, Octubre, 2007.

- Reina-Romo E., Gómez-Benito M.J., García-Aznar J.M., Domínguez J., Doblaré, M. Simulating limb lengthening in an interspecies' analysis. Biomechanics and Biology of Bone Healing. Berlín, Alemania, Mayo 2008.

- Reina-Romo E., Gómez-Benito M.J., García-Aznar J.M., Domínguez J., Doblaré, M. Different animal models of bone distraction. 5^{th} European Congress on Computational Methods in Applied Sciences and Engineeering (ECCOMAS 2008). Venecia, Italia, Julio 2008.

- Reina-Romo E., Gómez-Benito M.J., García-Aznar J.M., Domínguez J., Doblaré, M. Limb lengthening: Influence of the load history. 16^{th} Congress European Society of Biomechanics. Lucerna, Suiza, Julio 2008.

- A. Sampietro Fuentes, E. Reina-Romo, M Ferrer Molina. Análisis biomecánico de la distracción ósea en mandíbula: comparativa clínico-experimental. 55 Reunión de la Sociedad Española de Ortodoncia. Valencia, España, Junio 2009.

- Reina-Romo E., Sampietro-Fuentes A., Gómez-Benito M.J., García-Aznar J.M., Domínguez J., Doblaré, M. Estudio tensional antes y después de la

distracción osteogénica mandibular en una caso de microsomía hemifacial. Semni. Barcelona, España, Julio 2009.

- Reina-Romo E., Sampietro-Fuentes A., Gómez-Benito M.J., García-Aznar J.M., Domínguez J., Doblaré, M. Simulación numérica del proceso de distracción osteogénica mandibular en un caso de microsomía hemifacial. 9^o Congreso Iberoamericano de Ingeniería Mecánica, Las Palmas de Gran Canaria, España, Noviembre 2009.

0.8 Líneas de trabajo futuro

El proceso de distracción osteogénica constituye un campo muy activo que aún sigue siendo objeto de intensa investigación científica. De hecho, es uno de los fenómenos más desconocidos de la biología ósea. Además, los cirujanos carecen hoy en día de instrucciones establecidas que definan el protocolo más adecuado de distracción para cada paciente.

Por lo tanto, las posibles mejoras y desarrollo de este campo son innumerables, tanto desde el punto de vista computacional como experimental. En concreto, se han planificado algunas extensiones del modelo incorporando factores no considerados así como nuevas aplicaciones. Se resume como sigue:

1. Desarrollo futuro en la parte computacional:

    - Simular las fases de latencia y de remodelación en detalle.
    - El proceso de distracción osteogénica es claramente un problema de grandes deformaciones. Sin embargo, la falta de datos experimentales acerca del comportamiento real de los tejidos durante el proceso de distracción ósea limita sus aplicaciones numéricas. Por lo tanto, en un futuro se debe caracterizar el comportamiento mecánico de los tejidos del espacio interfragmentario en ambientes de grandes deformaciones.
    - Simular el proceso de elongación ósea en geometrías más complejas y desarrollar modelos específicos para cada paciente. De hecho, las simulaciones de elementos finitos del proceso de distracción osteogénica deberían desarrollarse en base a funciones que representen la geometría

exacta del modelo (análisis isogeométrico, NURBS). Estos análisis también se podrían extender y adaptar al proceso de distracción ósea. La malla podría adaptarse a los cambios geométricos que tienen lugar a lo largo del proceso de distracción evitando por lo tanto la inclusión del remallado.

- Otro aspecto que podría ser susceptible de mejora es la migración celular, que aquí ha sido simulada con una ecuación estándar de difusión. Sin embargo, es bien conocido que el movimiento de las células no es aleatorio o adireccional sino que contituye un proceso mucho más complejo. Por ejemplo, recientemente se ha demostrado que el movimiento celular se guía por la rigidez y deformación del sustrato (Lo *et al.*, 2000; Wong *et al.*, 2003; Schwarz & Bischofs, 2005; Moreo *et al.*, 2008; Sanz-Herrera *et al.*, 2009). Estos aspectos deberían estudiarse en un futuro puesto que la migración celular es fundamental en el proceso de distracción osteogénica.
- Se ha supuesto que las tensiones residuales están reguladas por la producción de matriz. Sin embargo, estudios futuros deberían también incluir un término adicional de relajación de tensiones debido al crecimiento volumétrico.
- Se ha simulado el cremiento como función de la proliferación de las MSCs y de la hipertrofia de los condrocitos (Gómez-Benito *et al.*, 2005). Sin embargo, el crecimiento volumétrico debido a la producción de matriz no es despreciable y debería ser incluido en modelos futuros para así obtener resultados más realistas.
- En relación con los aspectos anteriores, se podría extender el modelo con un planteamiento micro-macro y así reducir el número de parámetros. Se podrían simular los procesos de diferenciación, proliferación y migración celular en el nivel micro y después homogeneizar las variables y pasarlas al nivel macro.
- Además se quiere extender el modelo para estudiar teorías de diferenciación asimétricas. Hoy en día existe un intenso debate acerca de si las células de cartílago aparecen o no en ambientes a tracción como

la distracción ósea. Numerosos estudios demuestran que sólo existe osificación intramembranosa en el espacio interfragmentario durante la distracción (Ilizarov, 1989*a*,*b*; Aronson *et al.*, 1989; Delloye *et al.*, 1990; Shearer *et al.*, 1992; Ganey *et al.*, 1994; Schenck & Gatchter, 1994). Pero casi todos los modelos mecanobiológicos proponen reglas simétricas de diferenciación respecto del tipo de carga (Prendergast *et al.*, 1997; Gómez-Benito *et al.*, 2005) y por lo tanto consideran la formación de cartílago tanto a compresión como a tracción. El modelo de Claes & Heigele (1999), en cambio, incluye esta asimetría formándose cartílago sólo a compresión. En el apéndice B se ha aplicado esta teoría de diferenciación y se ha extendido al caso de distracción ósea para comprobar si formulaciones asimétricas ya existentes de diferenciación celular son capaces de predecir el proceso de distracción osteogénica de manera más realista. El modelo se ha validado de manera preliminar analizando el efecto de la rigidez del fijador durante la etapa de consolidación ósea. Sin embargo, este estudio requiere más análisis para validar completamente el modelo.

2. Desarrollo futuro en la parte experimental:

   - La insuficiente validación de los modelos de distracción osteogénica es una de las principales limitaciones de los mismos. Existen bastantes estudios experimentales de distracción en la bibliografía pero presentan una gran variabilidad en los resultados. Por lo tanto, se pretende llevar a cabo en un futuro cercano experimentos de distracción ósea para comprobar las hipótesis más relevantes del modelo, así como realizar una estimación de los parámetros del mismo. Para ello, es preciso en un futuro:

     – Definir y preparar los experimentos en animales, centrándose en la elección del tipo de especie, el procedimiento de distracción a realizar, el protocolo de distracción así como los parámetros a controlar durante el ensayo entre otros. Por ejemplo, se podrían medir las fuerzas producidas por el distractor sobre el hueso cada

vez que se produce un desplazamiento en el distractor, así como las tensiones residuales que mantiene el hueso sobre el distractor al final de cada día, y antes del siguiente paso de distracción.

- Diseño y fabricación del distractor. Se debe diseñar el distractor para asegurar la estabilidad del espacio interfragmentario así como unas condiciones clínicas óptimas.
- Desarrollo de la instrumentación electrónica necesaria para medir los parámetros de interés, como por ejemplo la carga.

En el marco de la validación experimental de los modelos se pone de manifiesto el carácter interdisciplinar de este proceso, ya que deben considerarse aspectos mecánicos, biológicos y médicos.

Con estos desarrollos futuros se contribuirá a la mejora de los tratamientos clínicos. Por ejemplo, hoy en día, se usan radiografías para determinar el momento de retirada del distractor. Sin embargo, la correlación entre la densidad ósea de la radiografía y la integridad biomecánica del nuevo hueso formado es muy pobre. Por lo tanto, son necesarios modelos fiables que permitan determinar cualitativa y cuantitativamente el protocolo óptimo de distracción.

Chapter 1

Introduction

1.1 Introduction

The Latin etymology of distraction, *distrahere* (from *dis*, apart, and *trahere*, to draw) means pulling in various directions (Burrill, 1998) and was introduced by G. A. Ilizarov to the field of orthopedics in 1951 to describe the induction of new-bone formation between two bone segments that are separated by gradual traction. The deep interest of Ilizarov in the fundamental role played by local mechanical parameters on biological processes has lead to his well known "*Law of Tension-Stress*" which states that gradual traction of living tissues creates stresses that can stimulate and maintain the regeneration and active growth of certain tissue structures. Therefore, in distraction osteogenesis, mechanical forces play a major role in the development of tissues within the distracted gap. As in distraction osteogenesis, a wide variety of physical phenomena are induced by mechanical stimuli (e.g. bone healing, osteoporosis and tissue remodeling). In fact, recent advances in cell and molecular biology take into account the central role of mechanical forces on tissue differentiation, development and remodeling. However, the identification of the mechanical parameters of importance and their mechanisms of action are unresolved and continue to be investigated.

These relationships between physical forces and the morphology of living things is not new and dates from Galileo. He hypothesized in 1638 that gravity and mechanical forces are limiting factors on the growth and architecture

of living organs. Over the last 150 years, Charles Darwin (1859), Karl Culmann (1864), G. Hermann von Meyer (1867), Julius Wolff (1892), Wilhelm Roux (1895), Gebhardt (1901), D'Arcy Thompson (1917), Friedrich Pauwels (1941), and Harrol Frost (1963) have recognized the importance of mechanical conditions in skeletal development and evolution.

This concept of mechanical regulation of biological processes is the main premise of *mechanobiology*, a research field introduced in the 20^{th} century and that has been developed in the 1990s. In contrast to biomechanics (mechanics applied to biosciences), this research field focuses on how the mechanical environment regulates the cell behavior in different biological processes, such as, development, adaptation, growth, remodeling, repair, regeneration and tissue differentiation pathways of biological tissues. It includes experimental and analytical models that help to understand the skeletal response to mechanical factors (van der Meulen & Huiskes, 2002), being usually divided into:

- *Experimental Mechanobiology*: it has been used to examine both tissue differentiation and adaptation to altered loading, with the majority of experiments examining tissue remodeling in response to mechanical stimuli. The most common experimental design is a device that isolates or controls the mechanical stimuli and then examines the tissues that form (Soballe *et al.*, 1992; Goodman *et al.*, 1994; Guldberg *et al.*, 1997; Tagil & Aspenberg, 1999; Altman *et al.*, 2002; Ng *et al.*, 2006).

- *Computational Mechanobiology*: its purpose is to determine the quantitative rules that govern the effects of mechanical loading on tissue differentiation, growth, adaptation and maintenance. A potential rule is hypothesized and the outcome of this hypothesis is modeled and compared against real tissue structures and morphologies (Claes & Heigele, 1999). If the results of this trial-and-error method correspond well, there might be an explanation for the mechanism being modeled.

The potential of mechanobiology to contribute to clinical progress is very promising. Mechanically based pathologies, such as, osteoporosis, neochondrogenesis, tissue differentiation at implant interfaces, bone healing or distraction

osteogenesis are nowadays areas of intense research activity. Table 1.1 lists different physiologic and pathologic conditions in which mechanical factors have been shown to play an important role (Carter & Beaupré, 2001). These mechanobiological examples are included within three main areas: tissue differentiation, endochondral growth and bone growth and adaptation. Distraction osteogenesis is a technique that falls within the three areas since during this process the application of mechanical forces at the site of tissue regeneration influences significantly tissue growth as well as bone formation and remodeling (Table 1.1). Thus, this technique is a clear example of mechanobiological process.

Table 1.1: Mechanobiological regulation of skeletal tissues and applications (adapted from Carter & Beaupré (2001)) (DO=Distraction osteogenesis; develop.=development).

Tissue differentiation	Endochondral growth and ossification	Bone growth and adaptation
Growth & develop.	Growth & develop.	Growth & develop.
Tissue regeneration	**DO, consolidation phase**	**DO, remodeling phase**
Initial fracture callus	Joint formation	Bone maintenance
DO	Cartilage maintenance	Bone hypertrophy, atrophy
Osteoarthritis	Osteoarthritis	Osteoporosis
Neochondrogenesis	Cartilage repair	Osteoarthritis
Prosthesis fixation	Skeletal rehabilitation	Peri-prosthetic remodeling
Skeletal rehabilitation		Skeletal rehabilitation

Understanding the mechanobiology of the distraction osteogenesis procedure at the tissue level may reduce complications (e.g., fibrous union) and enhance bone regeneration through the application of mechanical stimulation to guide differentiation of multipotent tissue within the distraction gap. Therefore, in this thesis we aim to develop a model, from a computational perspective, based on mechanobiologic concepts able to accurately simulate this process. This can provide powerful tools in designing patient-specific preoperative planning of this process and can help orthopaedic surgeons for accurate performance in this demanding field.

1.2 Distraction osteogenesis

Distraction osteogenesis is a unique biologic process of new bone formation between the surfaces of bone segments that are gradually separated by incremental traction. It is used to correct severe bone injuries and to lengthen bones. Traditional treatments for severe bone injuries have evolved through major stages that include high level amputation, shoe augmentation, orthotics and bone grafting. Shoe augmentation and orthotics, are clearly visible and are, therefore, mostly refused because they tarnish the external appearance (Leung *et al.*, 2006). Bone grafting, which is classified into autogenous or allogeneic bone grafting, exhibit limitations and have failure rates from 22.5% to 38% (Ilizarov & Ledyaev, 1992). In autogenous bone grafting, tissue is provided by the individual him/herself and in allogeneic bone grafting tissue is taken from a donor. The former heals quickest and more reliably but is limited in quantity and involves donor site morbidity whilst the latter could elicit an immunological response due to genetic differences and the risk of inducing transmissible diseases (Glowacki & Mulliken, 1985; Buck *et al.*, 1989). Xenografts, or bone grafts obtained from different species are also a poor option due to the danger of disease transmission or immunological rejection.

In light of these limitations, particular attention is paid to surgical techniques to lengthen the extremities or to bridge bone defects. In this respect, the contribution made by G. A. Ilizarov is undisputed (Ilizarov & Soybelman, 1969; Ilizarov, 1988, 1989*a*,*b*). Through systematic basic research and extensive clinical application he introduced to the field of orthopaedics in 1951 what he referred as distraction osteogenesis.

Distraction osteogenesis takes the advantage of the body's natural ability to regenerate bone and other tissues and therefore offers some distinct advantages over traditional methods. It requires much less operative time than bone grafts, allows the distraction of any bone type, hospitalization is rarely more than 24 hours, there is no donor site morbidity, blood transfusions are not necessary and it lengthens the associated skin, muscle and subcutaneous tissues, eliminating potentially deforming mechanisms from contracted soft tissues and abnormally directed muscle forces (Fonseca, 2000). Besides medical benefits, patients are also able to maintain a close to normal life style while under treatment, with

many patients fully ambulatory and able to work during the entire length of the treatment (Heller, 1998). It has also been shown to contribute to savings of approximately $30,000 per patient (Cierny & Zorn, 1994) when compared with conventional methods of treatment and to savings of approximately $345,000 per patient when compared to the costs of amputation due to the lower cost of prosthetic care for the remaining life of patients (Lieberman & Friedlaender, 2005). The disadvantages of this method include the long duration of treatment, the necessity of continual monitoring of the treatment device, the need for frequent medication and the continual radiographic monitoring to assess the progress of correction (Kirienko *et al.*, 2003).

Potential complications of the surgical method are comparable to those elicited by other surgical procedures. They include muscle contracture, joint luxation, pin site problems, axial deviation, neurologic injury, vascular injury, premature consolidation, delayed consolidation, nonunion and hardware failure (Paley, 1990). These complications can be minimized with meticulous technique and careful monitoring and can be considered acceptable in light of the potential benefits of this surgical procedure.

Due to the huge benefits of distraction osteogenesis over conventional methods, this technique has been successfully applied to some of the most challenging conditions in the orthopedic surgery such as limb lengthening, bone transport, treatment of nonunions and deformities (Paley *et al.*, 1989; Hyodo *et al.*, 1996; Aronson, 1997; Paley *et al.*, 1997). Furthermore, over the last 20 years this technique has also been introduced to the rest of the organism such as the craniofacial region, opening up new possibilities in the correction of severe craniofacial deformities as well as some facial injuries resulting from trauma. It is also applied to complex foot deformities for which other treatment options do not exist (Grant *et al.*, 1992; Paley, 1993; de la Huerta, 1994), to create new ligaments (Aston *et al.*, 1992), correct soft tissue deformities (e.g. chronic knee and elbow contracture) (Calhoun *et al.*, 1992*a*; Haggland *et al.*, 1993; Herzenberg *et al.*, 1994*a*) or flat bone such as vertebrae (Lieberman & Friedlaender, 2005).

Some of the pathologies well accepted for treatment of distraction osteogenesis are very common in the current population. For example, 23% of the general population has a leg length discrepancy of 1 cm and approximately 1

in 1000 requires a corrective device (Rozbruch & Ilizarov, 2006). Affected people often find that the associated aesthetic problem is just as debilitating as the functional limitations, which affect statically and dynamically the entire postural and musculoskeletal system. The causes of such differences in limb length can be either congenital or acquired. Congenital conditions or birth defects are the commonest causes of one side limb shortening such as proximal focal femoral deficiency, hemimelias or congenital pseudoarthrosis. Acquired pathologies with extensive loss of bone and soft tissue are also frequent and can be due to tumor resection tissue, to high energy trauma or malunited fractures. For instance, in the United States 5-10 % (250,000 to 500,000) of fractures go onto nonunion or delayed union (Rockwood *et al.*, 2006). Most of this large number of mal-united fractures lead to limb shortening. Additionally, craniofacial defects amenable to treatment with distraction osteogenesis are very common. For example, approximately 10% of the population has significant dental overjet (http://emedicine.medscape.com/article/844837-overview).

1.2.1 Tissue differentiation theories

Distraction osteogenesis, fracture healing, adaptation to skeletal implants, bone development and regeneration are skeletal tissue differentiation processes, which involve many cell and tissue types. During these processes, tissues are continually changing due to growth and response to the tissue environment, including the physical, chemical and mechanical environment.

One cell that is vital for these changes is the stem cell. There are two general types of stem cells: the embryonic stem cells (ESC) and the somatic tissue stem cells (TSC), which differ in their properties. ESC are pluripotent in nature, i.e., they are able to give rise to all tissues of an embryo, whilst TSC are multipotent, i.e., they have a differentiation potential which is restricted to the different lineages of a pre-specified tissue (Roder, 2003). The focus of this thesis is the influence of the differentiation of TSC (which will be called mesenchymal stem cells, MSCs) on the process of distraction osteogenesis.

During their differentiation, MSCs divide, and their "daughter cells" become committed to a specific and distinctive phenotypic pathway, a lineage with dis-

crete steps and, finally, end-stage cells involved with fabrication of a unique tissue type (Figure 1.1, Caplan & Boyan (1994)). However, during their differentiation, MSCs have the capacity to change their tissue specific differentiation program (Roder, 2003). This is the so called plasticity phenomena. Examples of tissues supplied by MSCs include adipose (Zuk *et al.*, 2001), synovial membrane (De Bari *et al.*, 2001), muscle (Bosch *et al.*, 2000), dermis (Young *et al.*, 2001), pericytes (Brighton *et al.*, 1992; Reilly *et al.*, 1998; Diefenderfer & Brighton, 2000) blood (Zvaifler *et al.*, 2000), bone marrow (Pittenger *et al.*, 1999), and, most recently, trabecular bone (Nöth *et al.*, 2002; Osyczka *et al.*, 2002), placenta, and cord blood.

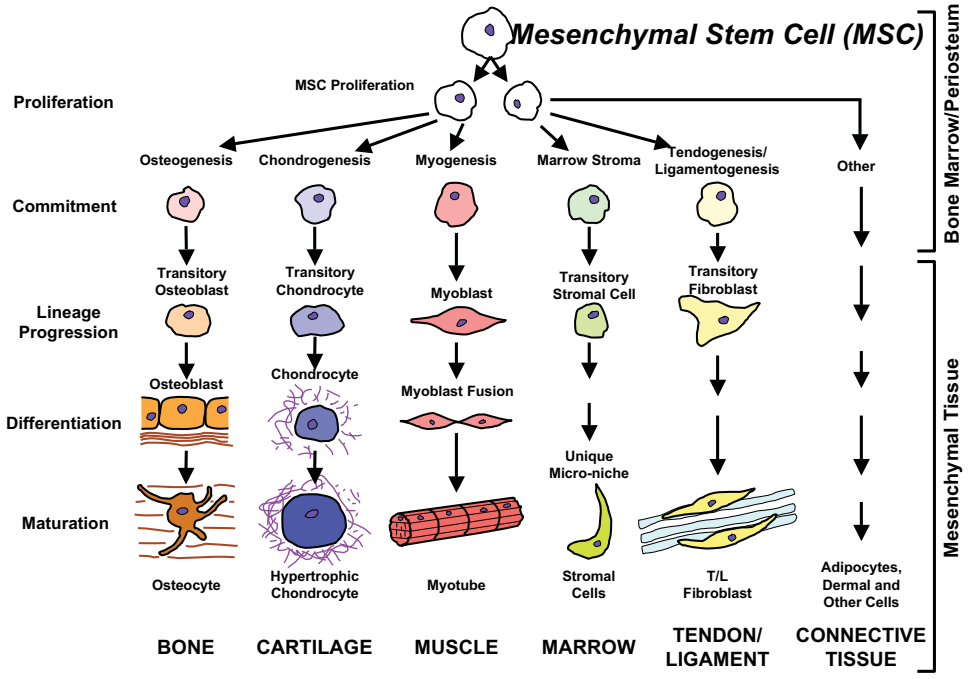

Figure 1.1: The mesengenic process (Caplan & Boyan, 1994).

It has been suggested that chemical and mechanical stimuli can control the differentiation of adult MSCs. Many researchers have attempted to establish the relationship between the mechanical level of an undifferentiated tissue and the ultimate tissue phenotype formed. However, the concept that biological processes at the cellular level can be regulated by mechanical loading dates back to the late 1800s when Roux introduced his theory of functional adaptation. He pro-

posed that the mechanical environment of "irritations" actually stimulated the formation of particular types of connective tissue (Roux, 1895). In particular, he postulated that compression stimulated the formation of bone, tension for connective tissue, and relative displacement in combination with compression or tension for cartilage.

Roux's hypothesis took some time before been taken up in orthopedics. It was only in the 1920s that his work was seriously considered again in relation to fracture healing. Pauwels (1941) proposed a more rigorous mechanoregulation theory based on continuum mechanics. His studies were largely based on clinical observation and logic. He hypothesized that the invariants of the strain and stress tensors guided the differentiation pathway, whereby deviatoric stresses stimulate the formation of fibrous connective tissue and hydrostatic, compressive stresses stimulate cartilage formation. No specific stimulus exists in this theory for the differentiation of bony tissue (Figure 1.2).

Later, a simpler idea, strain-based, was proposed by Perren (1979) and Perren & Cordey (1980) to predict the evolution of tissues in a bone fracture gap. They developed the concept of "interfragmentary strain (IFS)":

$$IFS = \frac{\Delta L}{L} \tag{1.1}$$

where L is the width of the fracture gap and ΔL is the change of the fracture gap after loading. Perren & Cordey (1980) believed that tissue differentiation was a result of tissue disruption. Therefore, if IFS exceeds the tissue strength or tissue elongation, the tissue resulted in rupture and would change its phenotype such that tissue failure would not occur. As observed in Figure 1.3, the strain tolerance is greatest for granulation tissue, intermediate for cartilage, and least for bone.

Based also on the ideas of Pauwels, Carter proposed a combination of octahedral shear stress and hydrostatic stress for his differentiation theory (Carter, 1987; Carter *et al.*, 1998). They postulated that the compressive hydrostatic stress history guides the formation of cartilage, whereas the tensile strain history guides the synthesis of fibrous connective tissue and bone is formed in regions without significant levels of both (Figure 1.4). Unlike Pauwels, they recognized

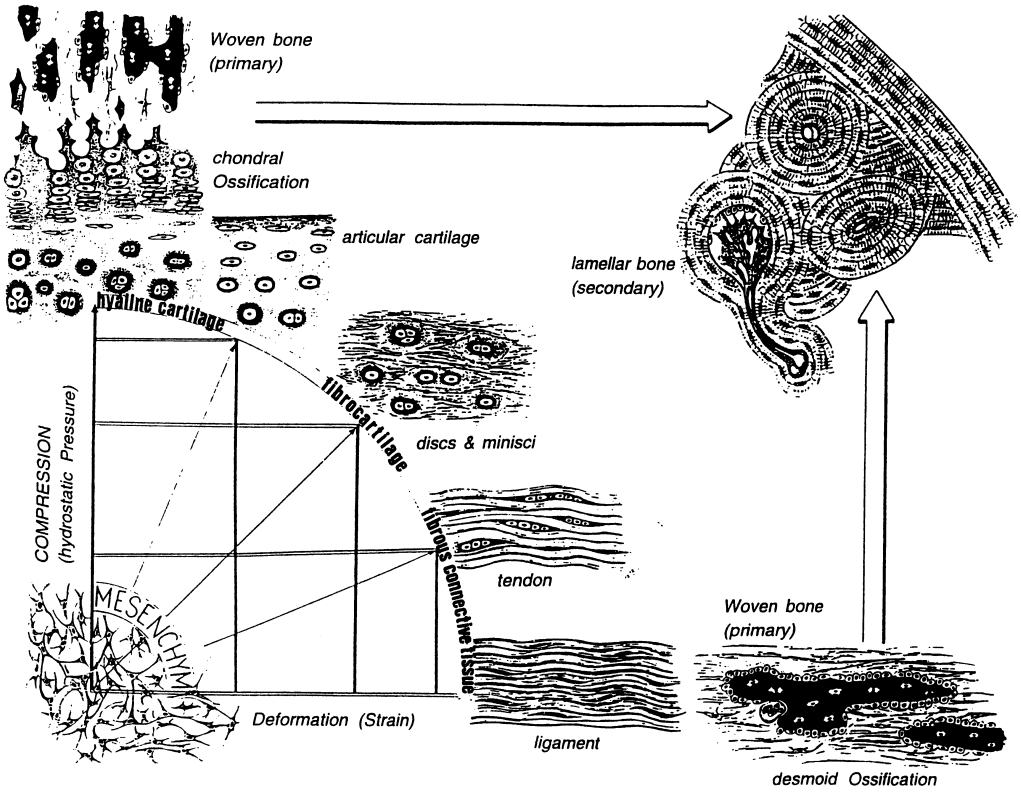

Figure 1.2: Pauwels (1941) concept of differentiation.

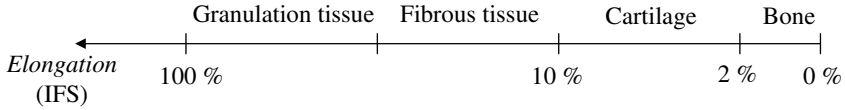

Figure 1.3: Perren (1979) concept of differentiation.

the influence of the vascularization and proposed that low oxygen tension favors chondrogenesis (Carter, 1987; Beaupré *et al.*, 1992). Carter's model (Carter, 1987; Carter *et al.*, 1998) was used in several computational studies to investigate oblique fracture healing (Blenman *et al.*, 1989), pseudarthrosis formation (Loboa *et al.*, 2001), asymmetric clinical fractures (Gardner *et al.*, 2006) and distraction osteogenesis (Morgan *et al.*, 2006).

Claes & Heigele (1999) using an elastic finite element model, proposed a mechanoregulation theory similar to that of Carter (1987) but presented in quan-

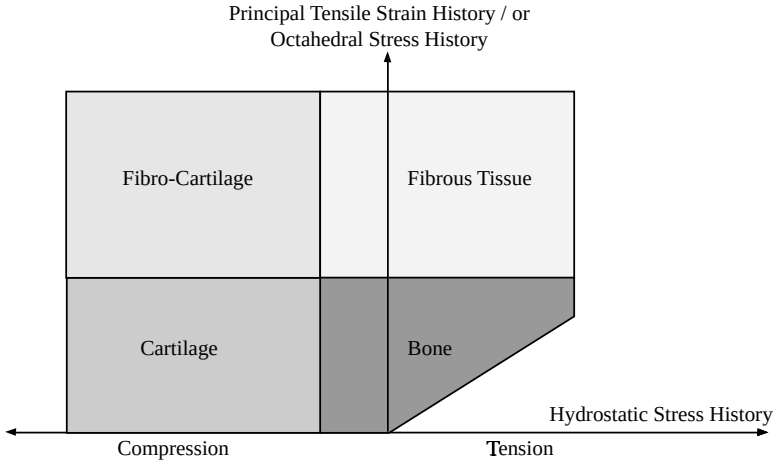

Figure 1.4: Relationship between loading history and tissue phenotype (Carter *et al.*, 1998).

titative terms (Figure 1.5). Their mechanical stimulus is dependent on both the tissue strain and hydrostatic pressure: very small tissue strains (less than 5 %) and hydrostatic pressures (below -0.15 MPa) would allow direct intramembranous ossification, larger values (less than 15 % of strain, greater than -0.15 MPa of hydrostatic pressure) would allow endochondral ossification, and tissue strains above 15% would lead to fibrocartilage and connective tissue preventing bone healing. The comparison of their finite element analysis with histological findings from *in vivo* experiments shows that the quantitative formulation did properly predict tissue differentiation events in the callus during healing.

Prendergast *et al.* (1997) developed a different mechanoregulation concept assuming that tissues are poroelastic and thus comprise both fluid and solid. They proposed a mechanoregulation pathway regulated by two biophysical stimuli, deviatoric strain of the solid and interstitial fluid velocity relative to the solid (Figure 1.6). They firstly demonstrated the consistency of the model at implant to bone interfaces (Prendergast *et al.*, 1997) and afterwards in a bone chamber (Geris *et al.*, 2003, 2004, 2009), osteochondral defects (Kelly & Prendergast, 2005), bone healing (Lacroix *et al.*, 2002; Isaksson *et al.*, 2008) and distraction osteogenesis (Idelsohn *et al.*, 2006; Isaksson *et al.*, 2007; Boccaccio *et al.*, 2007,

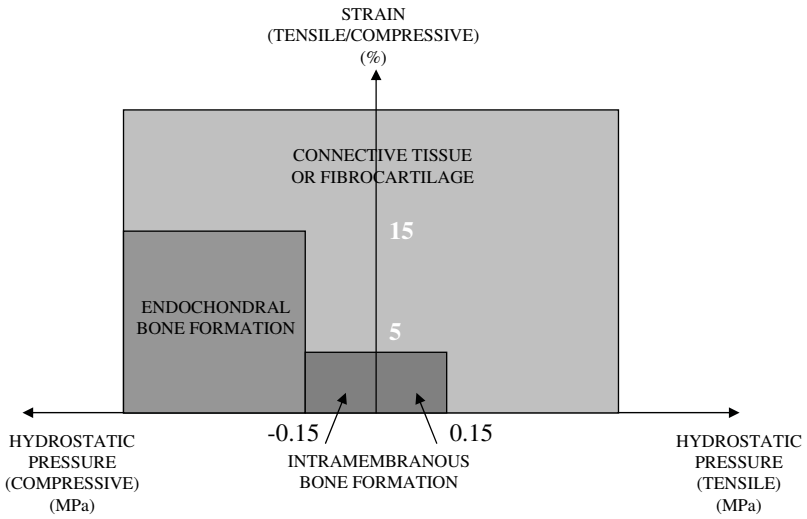

Figure 1.5: Relationship between mechanical stimuli and bone formation (adapted from Claes & Heigele (1999)).

2008).

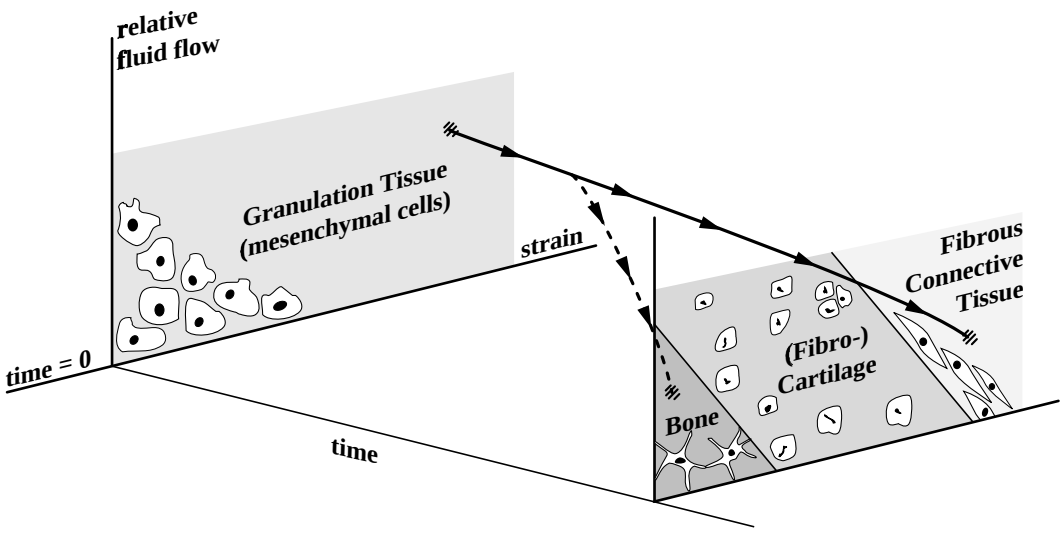

Figure 1.6: Mechanoregulation diagram for bone formation and resorption based on mechanical strain and fluid flow (Prendergast *et al.*, 1997).

Finally, Gómez-Benito *et al.* (2005), Doblaré & García-Aznar (2006) and

García-Aznar *et al.* (2007) proposed a mathematical model driven exclusively by the second invariant of the deviatoric strain tensor, assuming that tissues are poroelastic.

Although these theories are different in details, they share some characteristics. Firstly, they all propose that high mechanical stimulation favors the formation of fibrocartilage tissue, while non stimulated environments favor bone formation. Secondly, they all develop phenomenologic rules, with theories derived from empirical observations. Thirdly, they are not sufficiently validated despite being able to successfully reproduce the main patterns of fracture healing in specific mechanical environments. And finally, all these tissue differentiation theories are obviously related to mechanical stimuli, which is definitely executed by cells whose biological sensing and signaling activities are implicitly assumed but not directly considered.

Models of bone healing

Although most of the previous differentiation theories were developed within numerical frames, such as the finite element analysis (FEA), the older ones were taken up when these new tools emerged. For example, Cheal *et al.* (1991) took up the "interfragmentary strain hypothesis" proposed by Perren (1979). They compared the histology of fracture callus with magnitudes of strain using the FEA to determine computationally the strain distribution in the callus at the initial stage of healing. Although they did not demonstrate tissue damage, they found an association of high strain levels with bone resorption and low strain levels with bone formation.

Ament & Hofer (1996, 2000) proposed a biomechanical model based on a set of fuzzy logic rules to describe the tissue transformation during healing. They introduced a biological factor in addition to the mechanical stimulus. The biological factor was an osteogenic factor that accounted for the vascularization and therefore allowed the differentiation between intramembranous and chondral ossification. The mechanical stimulus was the strain energy density. They succeed in predicting bridging of the bone ends through cartilage, followed by the growth of a callus cuff, and finally, the resorption of callus after ossification of the interfragmentary gap. This approach has been taken up more recently by Simon

et al. (2003) and Shefelbine *et al.* (2005), who simulated, using finite element analysis and the fuzzy logic, fracture healing, based on local mechanical factors, as described by Claes & Heigele (1999), and the local vascularity.

Bailón-Plaza & van der Meulen (2001) presented the first two-dimensional temporo-spatial mathematical model of the bone healing process that considers the effect of the growth factors. This model was later modified to incorporate the effects of mechanical stimulation on cell differentiation (Bailón-Plaza & van der Meulen, 2003). More recently, Geris *et al.* (2006, 2008) developed this model further by including key aspects of healing, such as angiogenesis and directed cell migration and compared the simulation results with the experimental observations. They also demonstrated the potential therapeutical value of bone regeneration models (Geris *et al.*, 2008).

Lacroix *et al.* (2002) have developed a bone healing model based on the mechanoregulation theory early formulated by Prendergast *et al.* (1997). This model has been taken up by Andreykiv *et al.* (2007) to include diffusion, proliferation and differentiation of cell populations (mesenchymal stem cells, fibroblasts, chondrocytes and osteoblasts). A similar model was proposed by Isaksson *et al.* (2008). They develop a mechanistic model of tissue differentiation, which directly couples cellular mechanisms to mechanical stimuli during bone healing.

Finally, Gómez-Benito *et al.* (2005), Doblaré & García-Aznar (2006) and García-Aznar *et al.* (2007) succeed in simulating the main processes that occur during fracture healing, namely proliferation, migration and differentiation as well as tissue damage and vascularization. Moreover, they improved on existing numerical models of fracture healing (Ament & Hofer, 2000; Bailón-Plaza & van der Meulen, 2001; Lacroix & Prendergast, 2002*a*; Bailón-Plaza & van der Meulen, 2003) by providing a mathematical formulation of callus growth.

Models of distraction osteogenesis

Fracture and distraction repair proceed by the same cellular healing process (Lammens *et al.*, 1998; Jensen, 2002), and therefore, most existing models of distraction osteogenesis are based on existing models of fracture healing.

In fact, compared to the huge amount of bone healing models, only a small number of computational works have been developed in bone distraction. Most

of these previous computational studies are based on biomechanical models, analyzing how the geometry, material properties and loading conditions at a specific time point affect the mechanical environment around the osteotomy (Carter *et al.*, 1998; Samchukov *et al.*, 1998; Loboa *et al.*, 2005; Kofod *et al.*, 2005; Cattaneo *et al.*, 2005; Boccaccio *et al.*, 2006; Morgan *et al.*, 2006).

For example, Samchukov *et al.* (1998) evaluated the biomechanical effects of the orientation of linear distractors with a two-dimensional model of a human mandible and concluded that distraction appliances must be oriented parallel to the axis of distraction.

Carter and its coworkers (Carter *et al.*, 1998; Morgan *et al.*, 2006) characterized the local bio-physical environment created within the osteotomy gap during long bone distraction osteogenesis. Firstly, Carter *et al.* (1998) predicted the maximum principal tensile strain and hydrostatic stress patterns at two stages of distraction osteogenesis. Afterwards, Morgan *et al.* (2006) quantified computationally the spatial and temporal profiles of four mechanical stimuli for tissue differentiation (pressure, tensile strain, fluid flow and tissue dilatation) and concluded that tissue dilatation might be a key stimulus for bone regeneration (Figure 1.7).

In the same research group, Loboa *et al.* (2005) performed a three dimensional finite element analysis at different time points during mandibular distraction in a rat model. They determined the changes in hydrostatic stress and tensile strain fields throughout distraction and compared them successfully with previous histological findings.

Kofod *et al.* (2005) and Cattaneo *et al.* (2005) investigated the stress distribution in the mandible and the temporomandibular joint (TMJ) before and after skeletal correction by intraoral unilateral vertical mandibular ramus distraction, using a finite element model. Their results suggested that correction of the mandibular deformity by distraction osteogenesis tends to normalize the stress patterns in the TMJ.

Boccaccio *et al.* (2006) studied the mechanical response of a human mandible when distraction orthodontic devices are used by comparing the displacement field and the stress distribution in an osteotomized and healthy mandible. In particular, they analyzed the effect of mastication in the undistracted mandible,

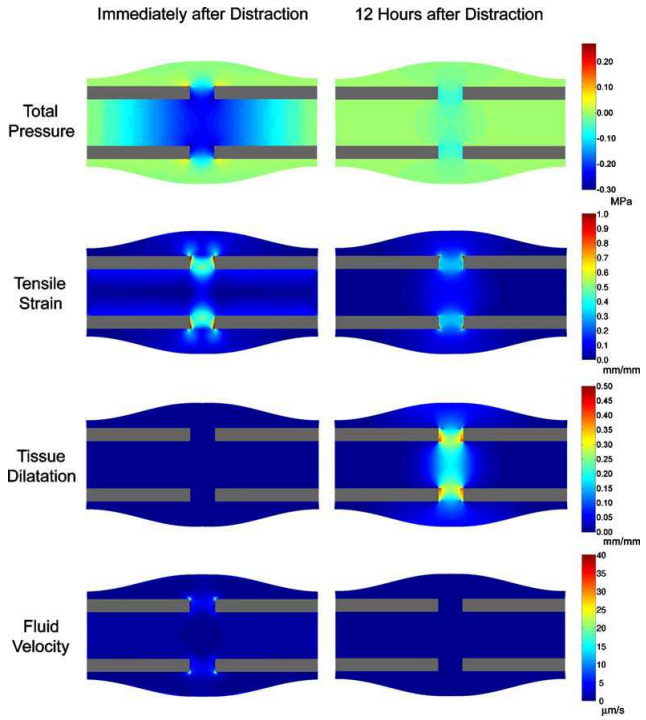

Figure 1.7: Magnitudes of total pressure, tensile strain (maximum principal tensile strain), tissue dilatation (volumetric strain) and fluid velocity in the regenerate (Morgan *et al.*, 2006).

the effect of a progressive expansion of the distractor and compared two distraction protocols with different expansion rates (0.6 and 1.2 mm/day). They found that the overall mechanical response of an osteotomized mandible is very different from the healthy one and that a rate of 1.2 mm/day reproduces better the displacement field imposed by the device.

However, time evolutive models provide more appropriate predictions of tissue differentiation as a function of the mechanical environment throughout the whole distraction period. To date, there are only a few evolutive models capable of predicting the spatial and temporal tissue differentiation patterns (Idelsohn *et al.*, 2006; Isaksson *et al.*, 2007; Boccaccio *et al.*, 2007, 2008). All these models are based on the mechanoregulation theory presented earlier by Prendergast *et al.* (1997). Firstly, Idelsohn *et al.* (2006) simulated the three phases of distraction osteogenesis in a rabbit mandible. They analyzed the influence of different

distraction frequencies and concluded that high frequencies of distraction are recommended for the first distraction period. Secondly, Isaksson *et al.* (2007) analyzed bone regeneration in an ovine tibia during the entire process of distraction osteogenesis. They successfully predicted tissue distribution during the entire period of distraction under different rates and frequencies of distraction. Nevertheless, they were not able to reproduce the evolution of the reaction force during the distraction period.

Finally, Boccaccio *et al.* (2007, 2008) examined the influence of the rate of distraction and the latency period duration within the fracture callus of a human mandible submitted to symphyseal distraction osteogenesis (Figure 1.8). They determined a maximum latency period of 1 week to avoid premature bony union and an optimal distraction rate of around 1.2 mm/day.

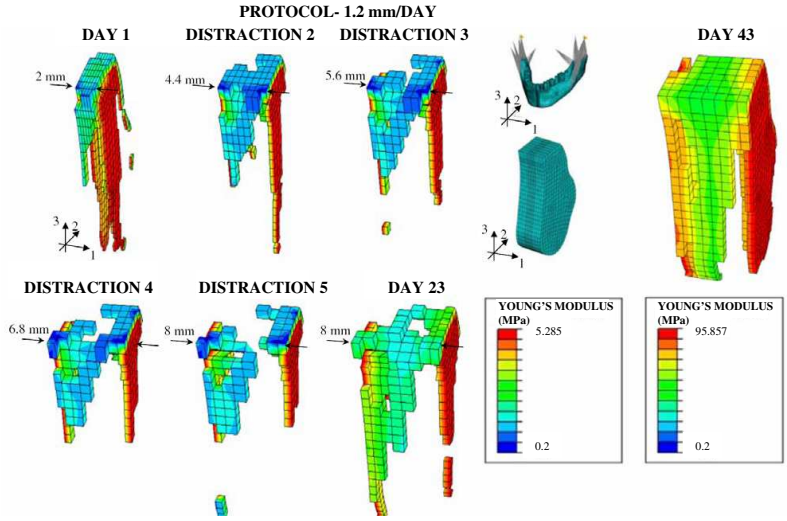

Figure 1.8: Bone regeneration process for a distraction rate of 1.2 mm/day (Boccaccio *et al.*, 2007).

1.3 Motivation and objectives of the present work

Distraction osteogenesis is an increasing demanding field due to the numerous applications it offers. However, currently, most of the surgeons are self-taught due to the limited instructions available. Moreover, despite a decreased rate of

complications, limb lengthening is a very complex process with numerous adversities. Good judgment, accurate knowledge and meticulous technique are necessary to select and design devices, perform corticotomies, maximize bone regeneration, manage pin sites, maintain articular function and time fixator removal (Dahl *et al.*, 1994).

The new developments in cellular, molecular and computational technologies, as well as the new designs of internal and external devices will help to improve the treatment of distraction osteogenesis. Since the late 80s, with the development of computers, there has been an increasing interest of engineers on biomedical fields, and in particular, in the last decade, in distraction osteogenesis. We believe that engineers play a crucial role in this emerging field since accurate simulations of the process and patient specific models can help the surgeon for a more precise performance.

Most of the existing models analyze specific instants of time (Carter *et al.*, 1998; Samchukov *et al.*, 1998; Loboa *et al.*, 2005; Kofod *et al.*, 2005; Cattaneo *et al.*, 2005; Boccaccio *et al.*, 2006; Morgan *et al.*, 2006). However, the temporospatial prediction of the process could be much valuable for the orthopaedic surgeons in terms of the distraction process planning. To date, there are only a few evolutive models capable of predicting the spatial and temporal tissue differentiation patterns from a qualitative point of view (Idelsohn *et al.*, 2006; Isaksson *et al.*, 2007; Boccaccio *et al.*, 2007, 2008).

This lack of mechanobiological models in bone distraction and its potential interest to surgeons is the main motivation of this work. Within this purpose, the first aim of this thesis is to develop a robust mechanobiological model able to predict the main features of distraction osteogenesis under different mechanical environments and within different types of bone. For example, the effect of the distraction rate, residual stresses, fixator stiffness, or geometry of the bone have been analyzed in long bone lengthening whilst a clinical case of hemifacial microsomia has been simulated in a mandible reconstructed from the patient geometry. Different clinical settings have been simulated and compared against experimental results. To perform these objectives, the manuscript is organized as follows.

In chapter two, the physiology of the most important tissues involved in dis-

traction osteogenesis is briefly described and the biological principles behind distraction are analyzed. In particular, the following tissues are described: bone, cartilage, granulation tissue and fibrous tissue. Moreover, the phases of distraction osteogenesis, the histology, the load measurements, the biomechanical factors and the main applications of this process are presented.

In chapter three, a new mathematical model of distraction osteogenesis is described. This model considers the main cellular events underlying distraction osteogenesis: cell proliferation, migration and differentiation as well as tissue growth and damage and incorporates important effects such as the influence of the load history on tissue differentiation. Since mechanical loading has profound influences on distraction osteogenesis, in this chapter the model is applied to different mechanical environments, comparing the results to experimental setups found in the literature. In particular, the effect of different distraction rates is analyzed: 1 mm/day, 0.3 mm/day and 2 mm/day.

In chapter four a general macroscopic formulation is presented, which is able to consider the effect of residual stresses in living tissues. Then, the model is particularized to the process of distraction osteogenesis and afterwards applied to a clinical example in order to investigate the influence of residual stresses on the outcome of limb lengthening. Finally, the pattern of limb lengthening is compared in different animal species and a human case.

In chapter five the model is applied to a pediatric mandible of a patient with hemifacial microsomia. This chapter is divided into the analysis of two different applications: biomechanical and mechanobiological. First, the pattern of stresses and strains is analyzed before and after the process of distraction and compared with a healthy idealized case. And secondly, a temporo-spatial analysis of the whole process of distraction is developed and the final outcome compared against actual clinical results.

Finally, in chapter six, the final conclusions, the future work as well as the main original contributions of this work are presented.

Chapter 2

Biological background of bone distraction

2.1 Introduction

Distraction osteogenesis is a unique biologic process of new bone formation between the surfaces of bone segments that are gradually separated. Under the influence of the tensional stress, the soft callus is maintained at the center of the distraction gap while routine fracture healing occurs at the periphery of the regenerate (Samchukov *et al.*, 2001). Many tissues besides bone have been observed to form under tension stress, including mucosa, skin, muscle, tendon, cartilage, blood vessels, and peripheral nerves (Ilizarov, 1989*a*,*b*; Cope *et al.*, 1999). Therefore, distraction osteogenesis involves a process of continuum tissue formation.

In the following sections, we review the tissue physiology of the connective tissues with a special emphasis on the most commonly found in distraction osteogenesis. Moreover, the process of distraction osteogenesis is described from a biological and mechanical perspective, detailing the main phases of the process as well as the mechanobiological factors involved. Finally, the main applications of this technique are discussed.

2.2 Connective tissue physiology

Connective tissues share a common origin from undifferentiated mesenchymal cells (Figure 1.1) and encompass the major structural constituents of the body. The different types of connective tissues are responsible of providing and maintaining form in the body. Functioning mechanically, they provide a matrix that connects and binds the cells and organs and ultimately give support to the body. Its structure is composed by ground substance, cells and fibers. Unlike the other tissues (epithelial, muscle an nerve), which are formed mainly by cells, the major constituent of the connective tissue is the extracellular matrix. Extracellular matrices consist of different combinations of protein fibers (collagen, reticular and elastic), most of which are collagen fibers and ground substance (Junqueira & Carneiro, 2005). Of the more than 20 types of collagen thus far identified, types I to III are found mainly in connective tissues (see Table 2.1).

Connective tissues include cartilage, tendons, ligaments, bone and the adipose tissues as well as skin, blood and lymph (Cowin, 1999). Here, we review the main tissue types that appear in the distracted gap, i.e., bone tissue, cartilage tissue, fibrous tissue and granulation tissue. The composition and the structure of the tissues that develop within the distracted gap is presented.

2.2.1 Bone tissue

Bone is a metabolically active tissue capable of adapting its structure to mechanical stimuli and repairing structural damage through the process of remodeling (Robling *et al.*, 2006). It has the capability of forming new osseous tissue at locations that are damaged or missing, such as in fracture healing, distraction osteogenesis or bone implants interface or removing bone matrix in case of disuse. This calcified, vascular connective tissue has many functions, including support, protection, mineral storage, blood cell production (hematopoiesis) and locomotion through the attachment of muscles.

Table 2.1: Fibril forming collagens (Hertling & Kessler, 2006).

Collagen type	Tissue distribution	Light microscopy	Ultrastructure	Site of synthesis	Interaction with GAGs	Function
Type I	Dermis, bone, tendon, dentin, fascias, sclera, organ capsules intervertebral disk	Closely packed, thick collagen fibers	Densely packed, thick fibrils with marked variation in diameter	Fibroblast, osteoblast, chondroblast, odontoblast	Intermediate level of interaction, especially with dermatan sulfate	Resistance to tension
Type II	Hyaline and elastic cartilages	Loose, collagenous network embbebed in abundant ECM	No fibers, very thin fibrils	Chondroblasts	High level of interaction mainly with chondrotin sulfates	Resistance to intermitent pressure
Type III	Smooth muscle, endoneurium, arteries, uterus, liver, spleen, kidney, lung	Loose network of thin reticular fibers	Loosely packed thin fibrils with uniform diameters	Smooth muscle, fibroblast, reticular cells, Schwann cells, hepatocytes	Intermediate level of interaction, mainly with heparin sulfate	Structural maintenance in expansible organs

Bone structure

At the gross structural level, mature bone can be classified into compact/cortical bone and cancellous/trabecular bone (Figure 2.1). *Cancellous bone* has large, open spaces surrounded by thin, anastomosing plates of bone. The large spaces contain red bone marrow and the plates of bone are trabeculae composed of several layers of lamellae (Figure 2.1). By contrast, *compact bone* is much more dense than cancellous bone, with spaces reduced in size and lamellar organization more precise and thicker (Figure 2.1).

Cancellous bone can be found in the epiphysis or heads of long bones whilst cortical bone is found in the diaphysis or shaft of the bone and outer layer of the trabecular bone. The epiphysis is an expanded portion at each end of the bone that articulates with another bone (Figure 2.1). With the exception of the articulating surfaces, the bone is completely enclosed by the periosteum, a tough, highly vascularized and innervated fibrous tissue really important in the healing of bone during distraction osteogenesis (Delloye *et al.*, 1990; Yasui *et al.*, 1991).

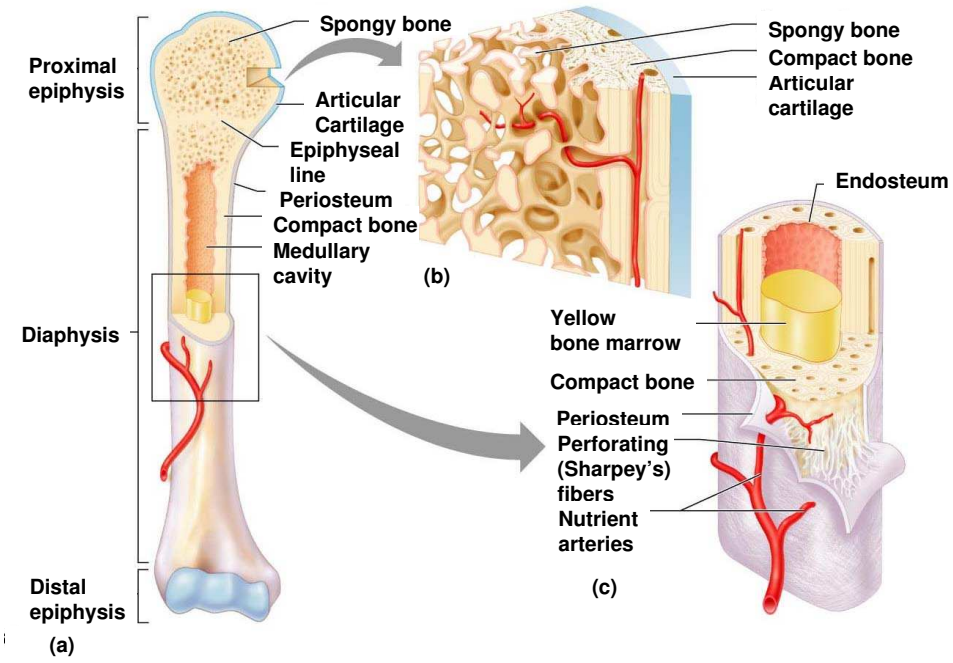

Figure 2.1: Long bone structure, a) human tibia, b) epiphysis, c) diaphysis (Marieb, 2004).

At the tissue level, bone may be divided into three wide categories:

- *Woven bone*: This type of bone is laid down rapidly as a disorganized arrangement of collagen fibers and osteocytes. The disorganized pattern and generally lower proportions of noncollagenous proteins decrease the mechanical strength of woven bone compared with the primary or secondary bone. The cell to bone volume ratio is high, confirming its role in providing temporary, rapid mechanical support, such as following traumatic injury. This type of bone is unique because it can be deposited without a preexisting membrane, bone or cartilaginous model (Martin *et al.*, 1998).

  In adult skeleton, this young regenerated bone can be found in a fracture callus, during distraction osteogenesis and in areas undergoing active endochondral ossification.

  Chemical analysis of this bone type has revealed constituents consistent with normal bone. The water (15%), lipid (5%), calcium (25%), phosphorus (12%), and collagen (24%) contents have been measured and compared favorably to normal bone specimen (Lieberman & Friedlaender, 2005).

- *Primary bone* or lamellar bone can exist in cortical and trabecular bone. Unlike woven bone, primary bone must replace a preexisting structure, either a cartilaginous model or previously deposited woven bone.

- *Secondary bone* is deposited only during remodeling and replaces primary cortical or trabecular bone. Differences between the developmental process of primary and secondary bone imply that a different controlling mechanism may be responsible for the endosteal and periosteal deposition of primary bone versus the intracortical deposition of secondary bone during remodeling.

Bone cells

Three main types of cell populations may be distinguished within the bone tissue:

- *Osteoblasts* are mononuclear bone cells of mesenchymal origin that secrete unmineralized bone matrix (osteoid), which eventually mineralizes to yield

mature bone. These are the most abundant bone cells that develop during the early stages of distraction osteogenesis. There are two variants of osteoblasts: *mesenchymal osteoblasts* or *bone lining cells* (Shapiro, 1988). The former are poorly differentiated cells that originate from the MSCs and synthesize woven matrix by secreting collagen fibrils circumferentially. These are crucial in the distraction osteogenesis procedure. The latter are essentially inactive osteoblasts. They array themselves in a well-polarized fashion along the woven bone surface and secrete fibrils in a parallel or lamellar orientation.

- *Osteocytes* are terminally differentiated osteoblasts that are completely surrounded by the mineralized collagen matrix. These cells are the most abundant cells in bone, can be in woven or lamellar bone and may act as sensors for the mechanical and chemical signals (Cowin *et al.*, 1991; Lanyon, 1993; Burger, 2001). They are distributed throughout the bone tissue volume and have the ability to communicate with other bone cells through an extensive network of cellular processes connected at gap junctions. Osteocytes response to mechanical stimuli includes changes in strain itself and strain generated changes in their fluid environment (Ehrlich & Lanyon, 2002). They then transduce the mechanical signals derived from mechanical loading into cues that eventually result in reduced bone loss or enhanced bone gain (Robling *et al.*, 2006).

- *Osteoclasts* are multinucleate cells derived from fusion of mononuclear haemopoietic precursors that resorb bone by secretion of acid and proteases.

Bone development

Normal bone develops via intramembranous or endochondral ossification. The former arises in a richly vascularized mesenchymal membrane where mesenchymal cells differentiate into osteoblasts without the mediation of a cartilage phase. The latter describes the synthesis of bone on a mineralized cartilage scaffold. Both types of bone formation occur within the regenerate during distraction osteogenesis and bone healing.

Intramembranous ossification occurs by direct differentiation of mesenchymal stem cells into bone cells that later secrete bone tissue. This type of bone formation begins when an ossification center appears in the fibrous connective tissue membrane (supporting structures). Selected centrally located mesenchymal cells form a group and differentiate into osteoblasts, forming an ossification center (Figure 2.2a). Osteoblasts begin to secrete osteoid, which is mineralized within a few days and trapped osteoblasts become osteocytes (Figure 2.2b). Accumulated osteoid is laid down between embryonic blood vessels, which form a random network. The result is a network of trabeculae (Figure 2.2c). Vascularized mesenchyme condenses on the external face of the woven bone and becomes the periosteum. Trabeculae just deep to the periosteum thicken, forming a woven bone collar that is later replaced with mature lamellar bone. Spongy bone (diploë), consisting of distinct trabeculae, persists internally and its vascular tissue becomes red marrow (Figure 2.2d).

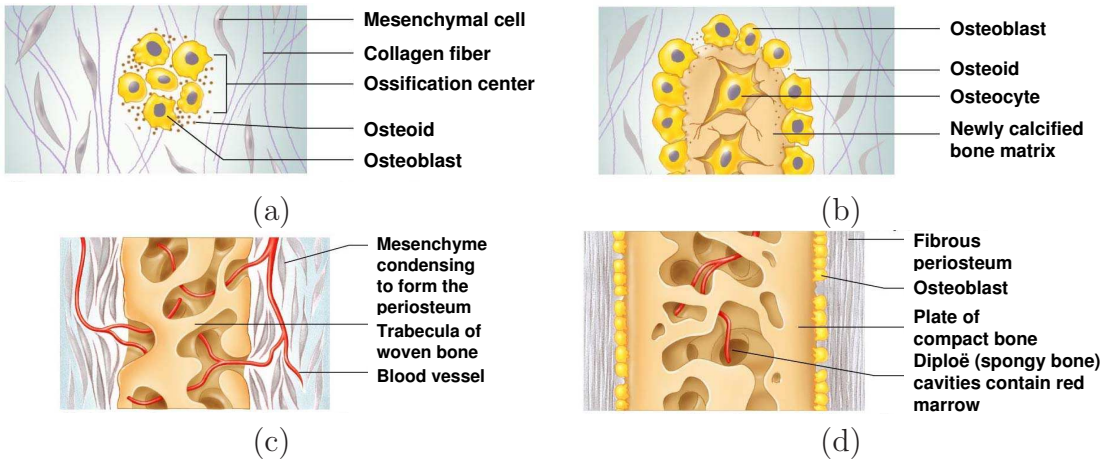

Figure 2.2: Bone formation by intramembranous ossification (Marieb, 2004).

Except for the clavicles and some bones of the skull such as the mandible, all bones of the skeleton form by *endochondral ossification*. This process which begins in the second month of the development uses hyaline cartilage "bones" formed earlier as models for bone construction. It is more complex than intramembranous ossification because the hyaline cartilage must be broken down as ossification proceeds.

The formation of a long bone typically begins in the primary center of ossifi-

cation, which is in the middle of diaphysis (Figure 2.3). First, the perichondrium covering the hyaline cartilage "bone" is infiltrated with blood vessels, converting it to a vascularized periosteum. The periosteum contains a layer of undifferentiated cells which later become osteoblasts (Figure 2.3). These osteoblasts secrete osteoid against the hyaline cartilage diaphysis, encasing it in a bone collar. This serves as a support for the new bone. As this bone collar forms, chondrocytes in the primary center of ossification begin to grow (hypertrophy) and signal the surrounding cartilage matrix to calcify. Since calcified cartilage is impermeable to diffusing nutrients, the chondrocytes undergo programmed death or apoptosis and the matrix begins to deteriorate. In month 3, the forming cavities are invaded by a collection of elements called the periosteal bud, which contains a nutrient artery and vein, lymphatics, nerve fibers, red marrow elements, osteoblasts and osteoclasts. Blood vessels forming the periosteal bud invade the cavity left by the chondrocytes and branch in opposite directions along the length of the shaft. The entering osteoclasts partially erode the calcified cartilage matrix, and the osteoblasts secrete osteoid around the remaining fragments of hyaline cartilage, forming bone covered cartilage trabeculae. As the primary ossification center enlarges, osteoclasts break down the newly formed spongy bone to form the bone marrow cavity in the center of the diaphysis. Shortly before or after birth, secondary ossification centers appear in one or both epiphyses. Cartilage cells undergo the same transformation as above and the epiphyses gain bony tissue. When secondary ossification is complete, hyaline cartilage remains only on the articular cartilages and at the epiphyseal plates (Marieb, 2004).

During infancy and youth, long bones lengthen by interstitial growth of the epiphyseal plates. Longitudinal bone growth is very similar to the events that take place during endochondral ossification. From a histologic point of view, five distinct zones can be distinguished in the epiphyseal plate (Figure 2.4):

- *Resting zone*: this zone contains normal, inactive hyaline cartilage.

- *Proliferative zone*: in this zone, chondrocytes undergo rapid mitosis pushing the epiphysis away from the diaphysis, causing the entire long bone to lengthen.

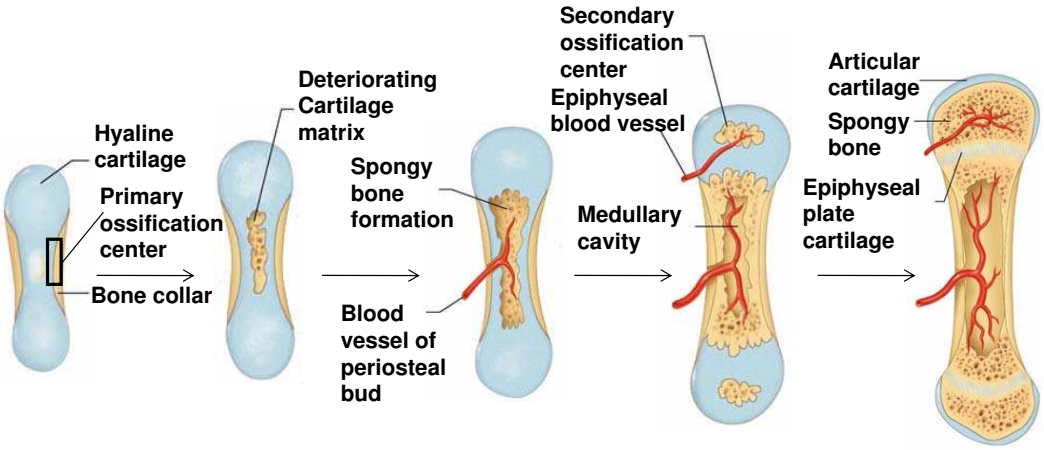

Figure 2.3: Endochondral ossification in a long bone (Marieb, 2004).

- *Hypertrophic zone*: it is in this zone that the chondrocytes undergo hypertrophy. Chondrocytes contain large amounts of glycogen and begin to secrete alkaline phosphatase.

- *Calcification zone*: in this zone, matrix becomes calcified and cartilage cells undergo apoptosis. This leaves long spicules of calcified cartilage at the epiphysis-diaphysis junction.

- *Ossification zone*: new bone formation is taking place. The cartilage spicules are partly eroded by osteoclasts and then quickly covered with bone matrix by osteoblasts, forming spongy bone.

During growth, the epiphyseal plate maintains a constant thickness because the rate of cartilage growth on the epiphysis is balanced by its replacement with bony tissue on the diaphysis. Longitudinal growth is accompanied by almost continuous remodeling of the epiphyseal ends to maintain the proper proportions between the diaphysis and epiphysis. At about 20 years of age the rate of chondrocyte proliferation diminishes and the epiphyseal plates become thinner until they are completely replaced by bone tissue.

However, adult bone can still increase in diameter or thickness by appositional growth when stressed by excessive muscle activity or body weight. Bone deposition occurs beneath the periosteum whilst osteoclasts resorption usually takes

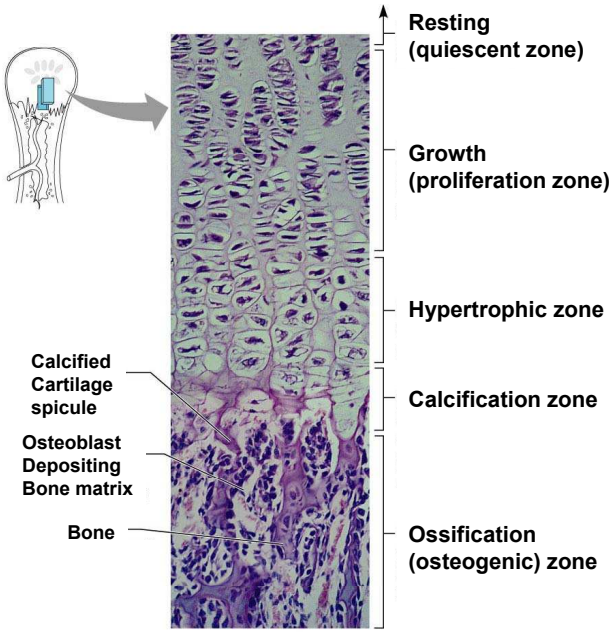

Figure 2.4: Growth in length of a long bone (Marieb, 2004).

place in the interior cavity to increase the diameter of the marrow. This process is maintained until the ultimate thickness and diameter is achieved.

Bone composition

Bone is a composite material with 70% of inorganic matrix, 20% of organic matrix and 10% of water. The detailed composition of bone depends on species, anatomical location, dietary history and either the absence or presence of disease (Kaplan *et al.*, 1994):

- *Inorganic phase*: The inorganic component of bone is primarily platelike crystalline hydroxyapatite, $Ca_5(PO_4)_3(OH)$ or HA (Kaplan *et al.*, 1994; Ying, 2001). Small amount of impurities may be present in the mineralized HA matrix; for example, carbonate may replace phosphate groups, whereas chloride and fluoride may replace hydroxil groups.

- *Organic phase*: Approximately 90% of the organic phase of bone is type I collagen; the remaining 10% consists of noncollagenous proteins, such

as lipids and other macromolecules, i.e., growth factors, cytokines, and adhesive proteins (Fung, 1993; Kaplan *et al.*, 1994; Ying, 2001). Growth factors and cytokines (such as insulinlike growth factors), proteins contained in serum, bone-inductive proteins (such as osteonectin, osteopontin and osteocalcin) and extracellular matrix compounds (such as bone sialoprotein, bone proteoglycans, and other phosphoproteins as well as proteolipids) are present in the mineralized matrix and may mediate bone cell function such as formation of new bone by osteoblasts and bone resorption by osteoclasts (Kaplan *et al.*, 1994; Ying, 2001).

The presence of crystals gives bone its rigidity and compressive strength, whereas collagen fibers confer tensile strength and toughness (Adams *et al.*, 2006). The water binding properties of proteoglycans enable them to "capture space" in developing tissue (Adams *et al.*, 2006).

2.2.2 Cartilage tissue

Cartilage is a type of connective tissue that stands up to both tension and compression and has qualities intermediate between dense connective tissue and bone. It is tough but flexible, providing resilient rigidity to the structures it supports. Cartilage lacks nerve fibers and unlike other connective tissues is avascular. It receives by diffusion from the blood vessels located in the connective tissue membrane surrounding it (Marieb & Hoehn, 2007). Thus, compared to other connective tissues, cartilage grows and repairs more slowly.

It is composed of specialized cells called chondrocytes and chondroblasts that produce a large amount of extracellular matrix composed of collagen fibers, abundant ground substance rich in proteoglycan, and elastin fibers.

Cartilage is classified in three types:

- *Hyaline cartilage* is the most abundant cartilage type in the body. It is a rather hard, translucent material rich in collagen and proteoglycan. It covers the end of bones to form the smooth articular surface of joints. It is also found in the nose, the larynx, between the ribs and the sternum and in the processes of bone healing and distraction osteogenesis. Bones grow via a

hyaline cartilage intermediate through the endochondral ossification during normal skeletal development and usually during distraction osteogenesis.

- *Elastic cartilage* is similar in appearance to hyaline cartilage, except for the presence of numerous branching elastic fibers within its matrix. It is stiff yet elastic, and is important to prevent tubular structures from collapsing. Elastic cartilage is found in the pinna of the ear, in tubular structures such as the auditory tubes and in the epiglottis.

- *Fibrocartilage* is characterized by large amounts of irregular and dense bundles of coarse collagen fibers in its matrix. In contrast to hyaline and elastic cartilage, fibrocartilage consists of alternating layers of cartilage matrix and thick dense layers of type I collagen fibers. It is a white, very tough material that provides high tensile strength and support. It contains more collagen and less proteoglycan than hyaline cartilage. Thus, its properties are closer to those of tendons than hyaline cartilage. It is present in areas most subjected to frequent stress like intervertebral discs, the symphysis pubis and the attachments of certain tendons and ligaments.

As hyaline cartilage is the type of cartilage which appears in the distracted callus, we are here mainly interested in this type of connective tissue. Its organic matrix is composed of a dense network of fine collagen fibrils (mostly type II collagen, with minor amounts of types V, VI, IX and XI) that are enmeshed in a concentrated solution of proteoglycans (PGs) (Bateman *et al.*, 1996). In normal articular cartilage the collagen content ranges from 15 to 22% by wet weight and the PG content from 4 to 7% by wet weight. The remaining 60 to 85% is water, inorganic salts and small amounts of other matrix proteins, glycoproteins and lipids (Mow & Ratcliffe, 1997). Collagen fibrils and PGs, each being capable of forming structural networks of significant strength (Kempson *et al.*, 1976; Broom & Silyn-Roberts, 1990), are the structural components supporting the internal mechanical stresses that result from loads being applied to the articular cartilage. Moreover, these structural components, together with water determine the mechanical behavior of this tissue (Mow & Ateshian, 1997).

2.2.3 Fibrous tissue

Fibrous connective tissue is a type of connective tissue which has relatively high tensile strength and great elasticity, due to a relatively high concentration of collagenous or elastic fibers. These fibers are embedded in a matrix which consists primarily on water, polysaccharides and proteins.

The cells of fibrous connective tissue are mostly fibroblasts, irregular, branching cells that secrete strong fibrous proteins as an extracellular matrix. There are several categories of fibrous connective tissue:

- *Loose connective tissue* (Figure 2.5) supports most epithelia and many organs that are required to expand like the lungs, arteries, and bladder. It also surrounds blood vessels and nerves and is found between muscles and in the distracted gap during the latency phase of the distraction process (Pietrzak, 2008). There are three subclasses: areolar, adipose and reticular (Marieb & Hoehn, 2007).

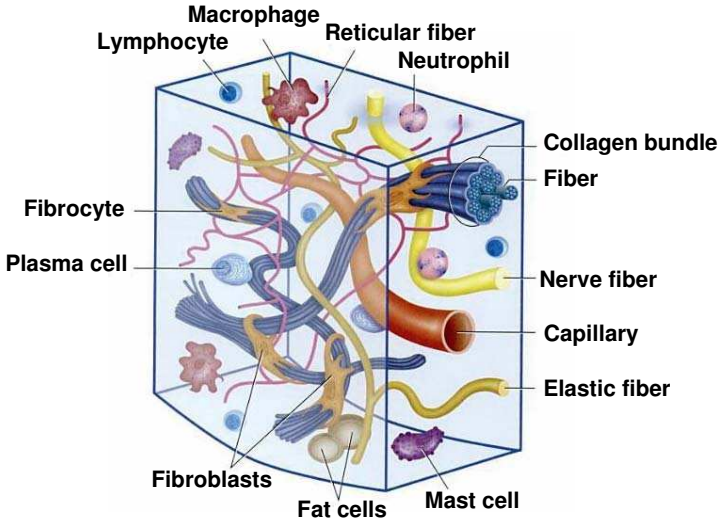

Figure 2.5: Loose connective tissue with its predominant cells and fibers (Eroschenko & di Fiore, 2007).

  - The functions of *areolar* connective tissue, shared by some but not all connective tissues, include supporting and binding other tissues, holding body fluids, defending against infection and storing nutrients as

fat. Fibroblast predominate, but macrophages, fat cells and occasional mast cells are also seen. The most obvious structural feature of this tissue is the loose arrangement of its fibers. Because of its loose nature, areolar connective tissue provides a reservoir of water and salts for surrounding body tissues. Areolar connective tissue is the most widely distributed connective tissue in the body and it serves as a kind of universal packing material between other tissues. It binds body parts together while allowing them to move freely, wraps small blood vessels and nerves, surrounds glands, forms the subcutaneous tissue and is present in all mucous membranes. This type of tissue is also the predominate type involved in wound inflammation and wound healing and during the latency phase of distraction osteogenesis (Bucci, 1995).

  - *Adipose* connective tissue is similar to areolar tissue in structure and function but its nutrient-storing ability is much greater. Consequently, adipocytes (fat cells) predominate and account for 90 % of this tissue mass. This tissue is highly vascularized indicating its high metabolic activity and is very abundant since it constitutes 18% of an average person body weight.
  - *Reticular* connective tissue resembles areolar connective tissue but the only fibers in its matrix are reticular fibers, which form a network along which fibroblasts called reticular cells lie scattered. This tissue forms supporting structures for many organs, such as the spleen and thymus.

- *Dense connective tissue* has collagen fibers as its main matrix element. There are two subclasses: regular or irregular.

  Dense regular connective tissue contains closely packed bundles of collagen fibers forming a uniaxial fiber network and thus providing a great tensile strength. Unlike areolar connective tissue, this tissue has few cells other than fibroblasts and is poorly vascularized. Dense regular tissue forms tendons (which attach muscles to bones) and flat, sheets like tendons called aponeuroses (which attach muscles to other muscles or to bones). It also forms fascia and ligaments.

Irregular connective tissue has the same structural elements as the regular variety. However, the bundles of collagen fibers are much thicker and they are arranged irregularly. This type of tissue forms sheets in areas where tension is exerted from many different directions. It is found in the skin and it forms fibrous joint capsules and the fibrous covering that surrounds some organs (kidneys, bone, cartilages, muscles and nerves).

When a non-union or pseudoarthrosis[1] takes place in distraction osteogenesis, two different fibrous tissues may appear in the distracted gap, according to the type of non-union (Ilizarov & Gracheva, 1971). When the pseudoarthrosis is stiff, the tissue between bone ends is dense fibrous or fibrocartilagenous tissue whereas in mobile pseudoarthrosis it is loose connective tissue (Khaleel & Pool, 2003).

2.2.4 Granulation tissue

Granulation tissue is a loosely organized connective tissue that replaces the fibrin clot during the latency phase in distraction osteogenesis or during the inflammatory phase in fracture healing and in wound healing. It is composed largely of MSCs, proliferating fibroblasts, macrophages, newly formed blood vessels and ground substance that includes collagen, glycoproteins and hyaluronic acid (a component of the cartilage) (Mulder *et al.*, 2002). The blood vessels need to be established as soon as possible to provide the growing tissue with nutrients, to take away cellular wastes, and transport new leukocytes to the area. Proliferating fibroblasts produce growth factors as well as new collagen fibers to bridge the gap. Some of these fibroblasts have contractile properties that pull the margins of the wound together (Marieb & Hoehn, 2007). The ground substance consists initially of a network of type III collagen, a weaker form of the structural protein that can be produced rapidly. This is later replaced by the stronger, long-stranded type I collagen. Granulation tissue has generally considerable numbers of active immune cells. The main ones are macrophages and neutrophils, although other leukocytes are also present. These work to phagocytize old or damaged tissue,

[1]Pseudarthrosis (or "non-union") is the formation of a false joint caused by the failure of the bones to fuse. This most commonly occurs when the bones do not heal properly after a fracture.

and protect the healing tissue from pathogenic insult. This is necessary both to aid the healing process and to protect against invading pathogens.

As explained above, experimentally, granulation tissue consists of many cell types, ground substance and blood vessels. In the initial phase of the distraction process, these cells are very difficult to distinguish within the distraction gap. In this thesis, when referring to this type of tissue, we will only consider one of the associated cells, as representative of all initial precursor cells: the mesenchymal stem cells. To avoid misunderstanding with the fibrous tissue created in non-unions, the loose fibrous connective tissue that appears in the latency phase of the distraction process will also be called in this thesis granulation tissue since they are very similar in composition and structure.

2.3 Biological basis of bone formation in distraction osteogenesis

Distraction osteogenesis is a surgical technique aimed to produce large amounts of bony tissue. Depending on the anatomical site where the tensional stress is induced, distraction osteogenesis techniques can be divided into callotasis (distraction of the fracture callus) or physeal distraction (distraction of the growth plate). Here, we focus on the former which consists on the gradual stretching of a reparative callus formed around bone segments surgically interrupted by an osteotomy (Murray, 1996). This method has been utilized as the predominant technique of distraction osteogenesis in experimental models and clinical applications due to the many complications associated to physeal distraction (Pietrzak, 2008).

2.3.1 Phases of distraction osteogenesis

In the distraction process, there are five fundamental sequential phases in which different biologic phenomena are produced (Figure 2.6):

- *Osteotomy.* In this phase the bone is surgically divided into two segments, resulting in a loss of continuity and mechanical integrity. Bone fragments

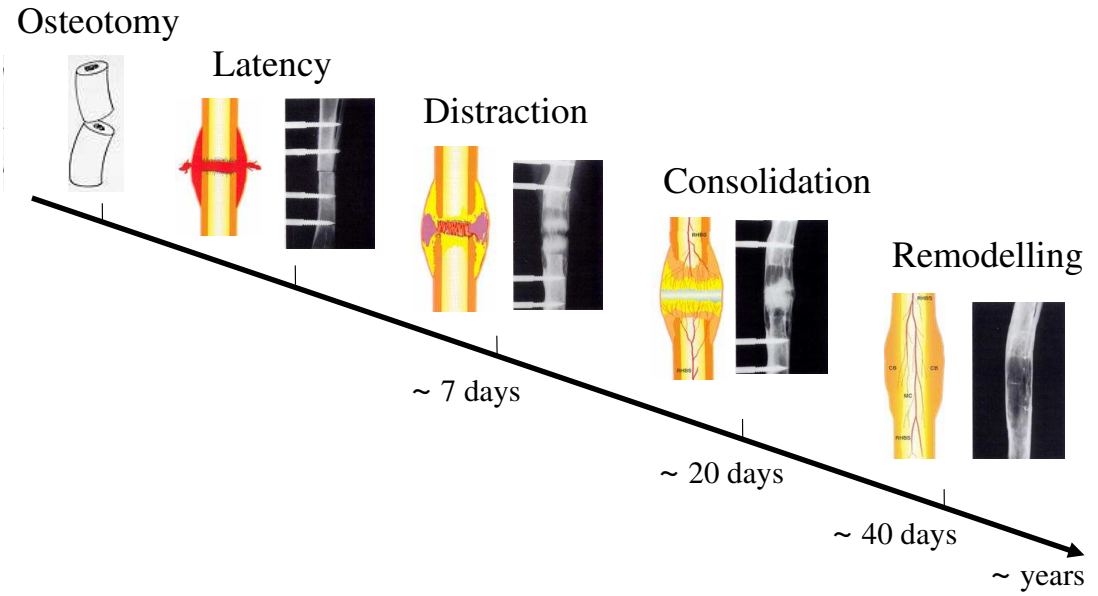

Figure 2.6: Phases of distraction osteogenesis (Samchukov *et al.*, 2001).

are then fixed by means of a distractor/external fixator to stabilize the new created gap. This process has been well described by Ilizarov & Ledyaev (1992). They emphasized the need to keep the incision and periosteal dissection to a minimum so that the medullary blood supply is preserved.

- *Latency phase*: it is the period between performance of osteotomy and start of the traction, during which soft callus is formed. This period coincides with the initial events in the normal process of bone healing.

  Histologically, the initial clotting is converted at 3 days into granulation tissue, which becomes increasingly fibrous due to the presence of collagen and increasingly vascular through the appearance of new capillaries. At this stage, recruitment of MSCs from the bone medulla and adjacent periosteum begins (Samchukov *et al.*, 2001). Currently, the periosteum, the surrounding soft tissues and the marrow space at the site of the damaged cortical bone tissue are considered to be the most accessible and enriched sources of MSCs (Gerstenfeld *et al.*, 2003).

- *Distraction*: it is the period in which the two ends of the osteotomized bone are gradually moved apart resulting in the formation of new bony

tissues within the progressively increasing interfragmentary gap. Through the application of tensional stress, a dynamic microenvironment is created (Delloye *et al.*, 1990). This environment stimulates changes at the cellular and subcellular level. These changes can be characterized as growth stimulating effect and shape forming effect (Kallio *et al.*, 1994; Holbein *et al.*, 1995; Mosheiff *et al.*, 1996):

- The growth stimulating effect of tension activates the biologic processes of the interfragmentary connective tissue. This includes the prolongation of angiogenesis with increased tissue oxygenation and the increased fibroblast proliferation with intensification of biosynthetic activity (Figure 2.7).

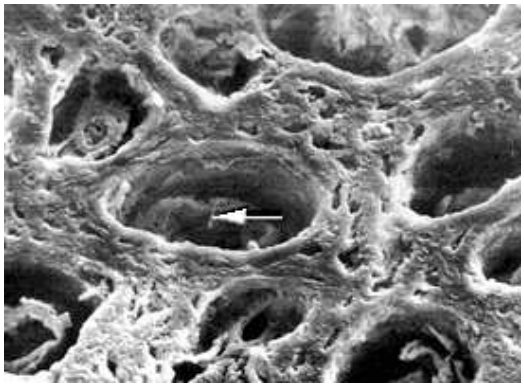

Figure 2.7: Newly formed vessels in the distraction regenerate, electron micrograph x500 (Ilizarov, 1992).

- The shape-forming effect causes an altered phenotypic expression of the cells: under the applied load, cells within the gap and their secreted collagen become longitudinally oriented along the axis of distraction (Figure 2.8).

- *Consolidation*: The consolidation period is the time between the cessation of traction forces and removal of the distraction device. This period represents the time required for complete mineralization of the regenerated tissue. After distraction finishes, the distracted gap gradually ossifies and one distinct zone of fiber bone completely bridges the gap.

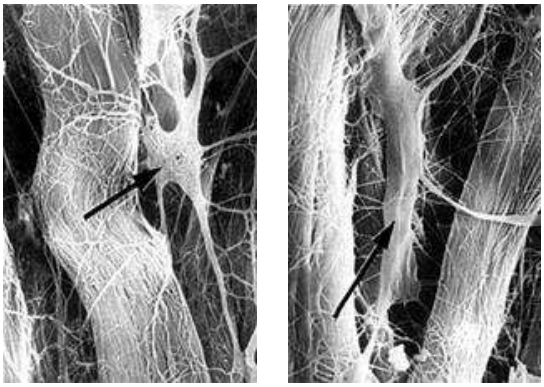

(a) (b)

Figure 2.8: Normal (a) and "distraction" (b) fibroblasts in the intefragmentary gap; electron micrographs, x1000 (Ilizarov, 1992).

- *Remodeling*: it is the time from the removal of the distraction device (and thus application of full functional loading) to the complete remodeling of the newly formed bone. During this period, the initially formed bony scaffold is reinforced by parallel-fibered lamellar bone. Both the cortical bone and marrow cavity are restored. Haversian remodeling, representing the last stage of cortical reconstruction, normalizes the bone structure (Tajana *et al.*, 1989). Although it takes a year or more before the structure of newly formed bony tissue is comparable to that of the preexisting bone, remodeling of the newly formed bone begins at the completion of distraction and continues throughout the consolidation period (Murray, 1996).

2.3.2 Histology of distraction

Histologically, distraction osteogenesis shares many of the features of fetal tissue growth and neonatal limb development as well as normal fracture gap healing (Ilizarov, 1992; Sato *et al.*, 1999) and has been studied extensively.

Many works report intramembranous ossification in the distracted gap (Ilizarov, 1989*a*,*b*; Aronson *et al.*, 1989; Delloye *et al.*, 1990; Shearer *et al.*, 1992; Ganey *et al.*, 1994; Schenck & Gatchter, 1994) whilst others demonstrated predominantly fibrocartilage in the distracted zone, resembling the endochondral sequence of mineralization (Kojimoto *et al.*, 1988; White & Kenwright, 1990; Waanders

et al., 1994). In addition, research on limb lengthening has not been limited to long bones or bones formed by endochondral ossification. Karp *et al.* (1990) and Komuro *et al.* (1994) examined distraction osteogenesis in the rat mandible, a bone formed embryologically without a cartilage anlage. Interestingly, Komuro *et al.* (1994) showed cartilage-like cells and endochondral ossification, whereas Karp *et al.* (1990) reported a purely intramembranous phenomenon. These differences in ossification patterns may be attributed to interspecies variation or other factors, such as the fixation stability, the distraction protocol, the method of osteotomy and the length of the latency period (Jazrawi *et al.*, 1998).

Histology of the distracted tissue shows an inflammatory reaction after the osteotomy, equal to that of fracture healing (Sevitt, 1981). During distraction, the regenerated tissue shows a specific longitudinal configuration: a central collagenous fibrous interzone (type I) in which the influence of tensional stress is maximal; two adjacent zones of vascular ingrowth, where proliferating and differentiating osteoblasts lay down longitudinal microcolumns of new bone (Figure 2.9b); and two peripherical zones with longitudinally oriented cylindrical primary osteons that grow toward each other. The collagen fibers of the fibrous interzone seem to play a critical role in bone formation during distraction by providing mechanical stability and facilitating the formation of early bone spicules extending from the osteotomy edges towards the centre of the distraction gap (Figure 2.9a) (Kojimoto *et al.*, 1988; Ilizarov, 1989*a*; Richards *et al.*, 1998; Bouletreau *et al.*, 2002*a*; Rozbruch & Ilizarov, 2006). When the distraction is stopped, the bone columns proceed across the collagenous interface to complete the bony bridge if the intramembranous ossification is the main mode of bone formation. Otherwise, cartilage islands would gradually be converted into bone through the endochondral ossification. Rapid remodelling to a normal macro and microstructure occurs, matching the host bone location, including the medullary bone marrow contents.

The rate of distraction osteogenesis (length of new bone segment per day) averages about 300 microns per day, which is similar to that of the growth rate of the fetal femur (400 microns/day) and much higher than that of the adolescent distal femoral physis growth rate (50 microns/day) (Rozbruch & Ilizarov, 2006).

Although the biomechanical, histological and ultrastructural changes associated with distraction osteogenesis have been widely described, the molecular

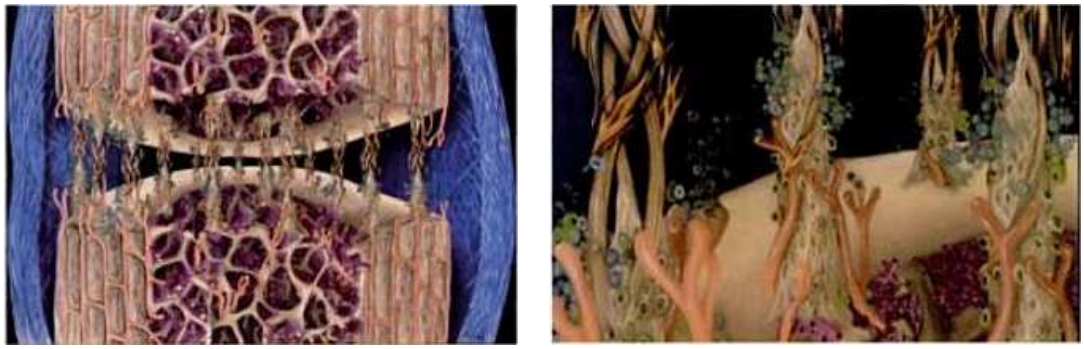

(a) (b)

Figure 2.9: a) Drawing of histological findings that shows multiple bone forming units (BFUs) bridging the entire cross-section of the two distraction surfaces; b) closer examination of the BFUs (Rozbruch & Ilizarov, 2006).

mechanisms governing the formation of new bone in the interfragmentary gap of gradually distracted bone segments remain largely unclear. A growing body of evidence has emphasized the contribution of both local bone or bone precursor cells and neovascularity to bone formation during distraction (Choi *et al.*, 2000). Recent studies have implicated a growing number of cytokines that are intimately involved in the regulation of bone synthesis and turnover during distraction procedures (Meyer *et al.*, 2001). The gene regulation of numerous cytokines (transforming growth factor-beta1 [TGF-β1], transforming growth factor-beta2 [TGF-β2], transforming growth factor-beta3 [TGF-β3], bone morphogenetic proteins [BMP], insulin-like growth factor 1, and fibroblast growth factor [FGF] 2) and extracellular matrix proteins (osteonectin, osteopontin) during distraction osteogenesis have been reviewed by Bouletreau *et al.* (2002*a*,*b*).

2.4 Mechanical basis of bone formation in distraction osteogenesis

Clinical and experimental observations have demonstrated that bone is a strain-sensitive tissue that reacts to the prevailing mechanical environment (Lanyon, 1987; Riddle & Donahue, 2009). In particular, in distraction osteogenesis the mechanical environment is imposed by the distractor device and influences the

subsequent pattern of healing. However, despite all the experimental findings performed within this orthopaedic process, the optimal mechanical environment for distraction osteogenesis has yet to be established.

To understand the role of mechanics on distraction osteogenesis it is useful to consider the history of limb lengthening which in fact represents the evolution of the external fixators. Also, load measurements during distraction osteogenesis are reviewed in this section. These are very important in the quantitative validation of models of limb lengthening due to the limited data available in the literature and the lack of histological studies in many works.

2.4.1 History of limb lengthening

Principles of mechanical manipulation of bone segments have been practiced in orthopedics since ancient times, when Hippocrates described the placement of traction forces on broken bones (Peltier, 1990). Further evolution of distraction osteogenesis involved the development and integration of traction, bone fixation, and osteotomy techniques (Paterson, 1990; Wiedemann, 1996; Murray, 1996). The first occurrence of continuous traction for long bone fractures can be traced to the work of Chauliac in the fourteenth century (Peltier, 1990). Barton, in 1826, is being credited with being the first to perform a surgical division of bone, or osteotomy (Barton, 2007). The development of external fixation dates from the middle of the nineteenth century when Malaigne constructed an apparatus that was directly attached to the bone (Figure 2.10, Malgaigne, 1847).

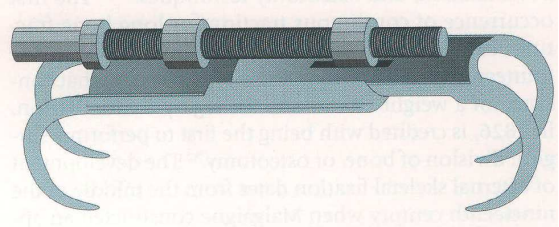

Figure 2.10: Malgaigne's external skeletal clamp (Samchukov *et al.*, 2001).

The combination of these techniques was first performed by Codivilla in 1905 when, after femoral osteotomy, he subjected the fragments to a strong tension

using nails fixed in the bone (Codivilla, 1905). His device used a traditional plaster cast, which was placed on the leg and cut in half at the level of the osteotomy (Figure 2.11). The proximal part of the cast was fastened to a stationary external frame, and the distal part was connected to a pin inserted to the calcaneous. Elongation was achieved in a single phase lengthening (up to 8 cm) by skeletal traction applied at the transcalcaneal pin (Samchukov *et al.*, 2001). This single phase lengthening was complicated by serious nerve lesions and persistent and uncontrollable convulsions (Codivilla, 1905).

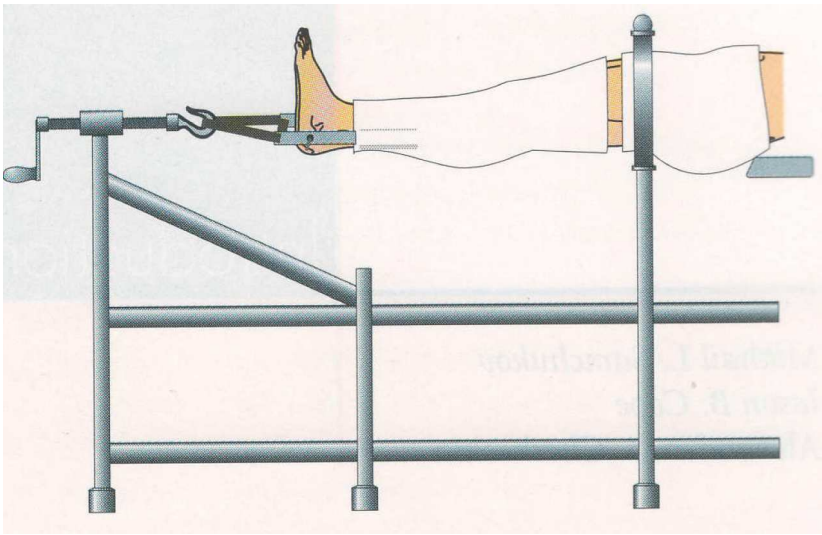

Figure 2.11: Codivilla's calcaneal pin traction plaster (Wiedemann, 1996).

Subsequent to Codivilla, various crude methods of limb lengthening were used but resulted in high complication rates. Not until the work of Putti (Putti, 1990, 1934) and Abbott (Abbott, 1927; Abbott & Saunders, 1939), in the 1920s and their painstaking operative technique did the results become verifiable. Abbott (1927) introduced the idea of the latency period to promote bone formation and Putti (1990) introduced a monolateral fixator he called the *osteoton* with half pin fixation (Figure 2.12).

During the 1930s, various modifications were introduced and the apparatus was simplified (Klapp & Block, 1930). Anderson (1936) reported several innovations for femoral lengthening, including the use of wires attached to the apparatus under tension and a technique for percutaneous osteotomy (Figure 2.13). Bost &

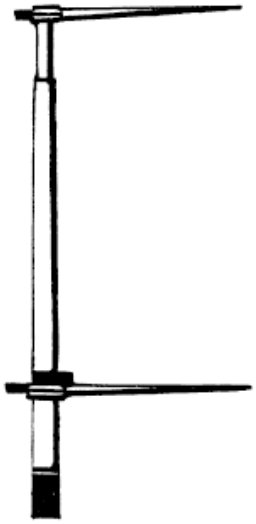

Figure 2.12: Putti's unilateral distraction frame (Wiedemann, 1996).

Larsen (1956) modified the technique further by performing femoral lengthening over an intramedullary rod after creation of an osteotomy with a power or Gigli saw. Although some femora united spontaneously, delayed unions were frequent.

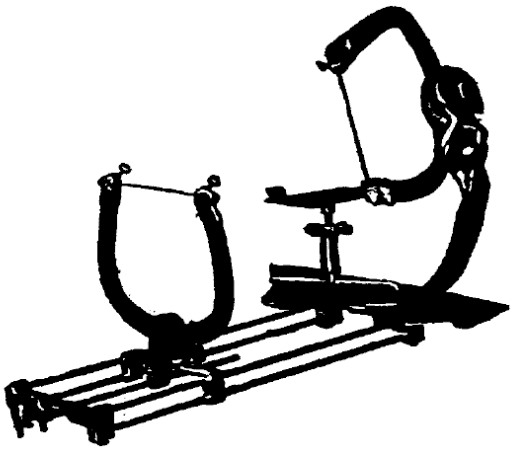

Figure 2.13: The Roger Anderson lengthening apparatus (Wiedemann, 1996).

In the 1950s, the Russian traumatologist Ilizarov was responsible for the major development of this technique. After World War II, antibiotics were scarce, and chronic osteomyelitis[2] associated with loss of bone, non-unions, and skeletal

[2]Osteomyelitis: infection of bone or bone marrow.

deformities were so common that Ilizarov found himself practicing orthopaedics although he had no formal training in that specialty. In 1951, he designed a new apparatus for bone fixation consisting of two metal rings joined together with three or four threaded rods, which is still used today (Figure 2.14). He later developed a low energy, subperiosteal osteotomy technique (corticotomy[3]) and a unique protocol for limb lengthening utilizing a 5- to 7-day latency period, followed by a distraction rate of 1 mm per day performed in four increments of 0.25 mm (Ilizarov, 1989*a*,*b*). Ilizarov also coined after World War II the term distraction osteogenesis to describe the regeneration of bone between vascularized bone surfaces that are separated by gradual distraction.

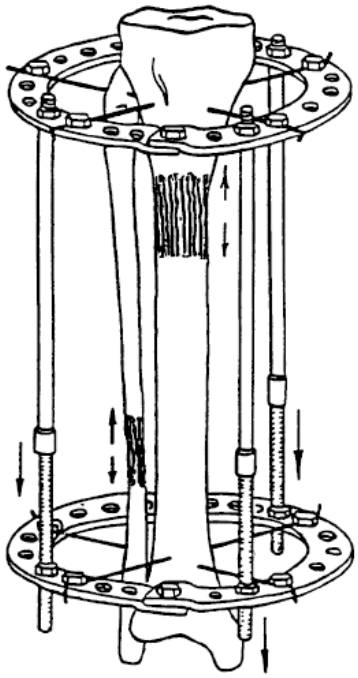

Figure 2.14: Ilizarov apparatus design.

Ilizarov's work remained unknown for some time outside Russia, and the technique mainly used in German speaking countries and later in the United States was that developed by Wagner (1971) (Figure 2.15). This method was technically simple but offered no major advantages regarding early mobilization of the

[3]Corticotomy: osteotomy performed with a narrow osteotome through a small skin incision so that the bones cortex is broken without either damaging the periosteal soft tissues or transecting the medullary canal contents.

patient. In addition, it disregarded the soft tissues and the biological principles, it required three sequential major operations, and led to numerous late complications (Paley, 1988).

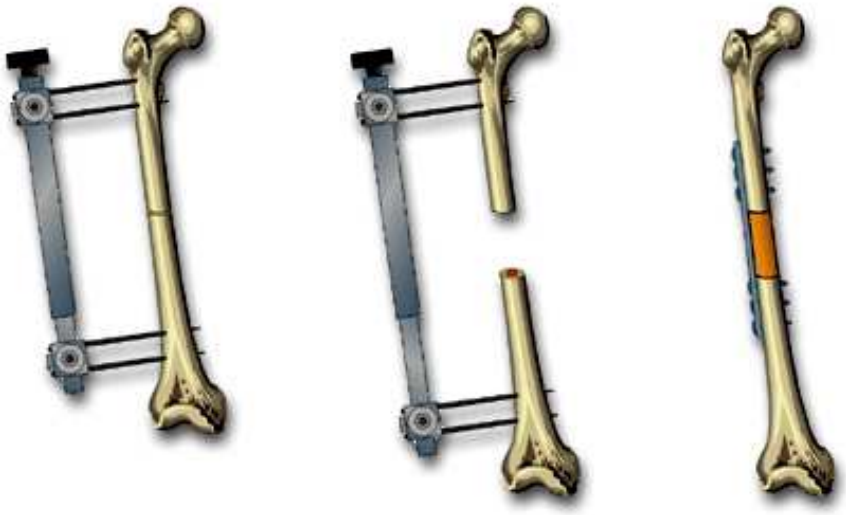

(a) (b) (c)

Figure 2.15: Wagner's limb lengthening technique (Samchukov *et al.*, 2001).

Devices used nowadays in long bones range from the ring external fixator with tensioned wires designed by Ilizarov to the monolateral, half-pins frames (Dahl & Fischer, 1991; Cañadell, 1993; de Pablos *et al.*, 1994) or even intramedullary rods (Brunner *et al.*, 1994). Each type of external fixator exhibits individual mechanical qualities that may or not enhance osteogenesis and generalized healing (Paley *et al.*, 1990; Calhoun *et al.*, 1992*b*; Podolsky & Chao, 1993; Hamanishi *et al.*, 1994). However, it is clear that the application of the Ilizarov ring fixator to some anatomic localizations as well as the correction of angular deformities is difficult. Uniplane deformities can be corrected by the use of hybrid fixators (Ilizarov ring fixator with half pins modifications) (Green, 1991; Green *et al.*, 1992) which promote gradual mechanical forces and movements of bone in any plane (frontal, sagittal or transverse) or direction (axial, angular, translational, rotational or any combination) at an unlimited number of treatment sides, including the potential to cross and protect active joints (Golyakhovsky & Frankel, 1991; de la Huerta, 1994; Herzenberg *et al.*, 1994*b*,*c*). However biplane or tri-

plane deformities, require the use of the specialized Taylor Spatial Frame fixator to generate motion in two or three planes at the same time (Figure 2.16).

Figure 2.16: Taylor Spatial Frame fixator design.

Similar to limb lengthening, the evolution of craniofacial distraction was based on the development and improvement of dentofacial traction, craniofacial osteotomies, and skeletal fixation methods.

The application of tensile and compressive forces to the bones of the craniofacial skeleton was reported as early as 1728, when Fauchard described the use of the expansion arch. The crowded dentition was broadened to a more normal form with an ideally shaped metal plate ligated to the teeth. This form of traction was limited to tooth movement only and have little effect on the shape of the bone.

The application of Ilizarov's principle to the craniofacial skeleton was first reported by Snyder *et al.* (1973) in a canine model. However, McCarthy *et al.* (1992) reported the first mandibular distraction in humans. They applied extraoral distraction osteogenesis on four children with congenital craniofacial anomalies such as hemifacial microsomia and Nager's syndrome. About the same time, Guerrero (1990) began developing his midsymphyseal mandibular widening technique and demonstrated successful results of mandibular widening on 11 patients with transverse deficiencies raging form 4 to 7 mm. Following the first reports of McCarthy and Guerrero, which demonstrated successful lengthening and widening of the human mandible by gradual distraction, the field of craniofacial distraction has rapidly gained popularity. Many authors have reported successful results with corrective osteotomies followed by gradual mandibular distraction for deformity

correction, lengthening, widening, bone transport and alveolar ridge augmentation (Block *et al.*, 1993; Habal, 1994; Havlik & Bartlett, 1994; Moore *et al.*, 1994; Block *et al.*, 1995; Chin & Toth, 1996; Weil *et al.*, 1997; Yen, 1997).

Different distraction devices are now available for oral and maxillofacial application, including mandibular, maxillary, midfacial, cranial, and alveolar distractors. They can all be classified in two types: external and internal. The external devices are attached to the bone by percutaneous pins connected externally to fixation clamps. The fixation clamps, in turn, are joined together by a distraction rod that, when activated, effectively pushes the clamps and the attached bone segments apart, generating new bone in its path. Relative to the direction of lengthening, they are divided into unidirectional, bidirectional, and multidirectional devices. The internal devices are located either subcutaneously or within the oral cavity (intraorally). The intraoral devices can be placed above (extramucosal) or below (submucosal) the soft tissue. These devices are attached to the bone (bone-borne), to the teeth (tooth-borne) or simultaneously to the teeth and bone (hybrid) (Samchukov *et al.*, 2001).

2.4.2 Load measurements during distraction

In vivo load measurements show that forces required to distract increase with time because gap tissues become gradually stiffer and therefore are indicative of the distraction process outcome (Figure 2.17) (Leong *et al.*, 1979; Jones *et al.*, 1989; White & Kenwright, 1990; Kenwright *et al.*, 1990; Wolfson *et al.*, 1990; Brunner *et al.*, 1994; Younger *et al.*, 1994; Simpson *et al.*, 1996; Forriol *et al.*, 1997; Waanders *et al.*, 1998; Matsushita *et al.*, 1999; Aarnes *et al.*, 2002; Singare *et al.*, 2006). Initially, the distracted bone surfaces are joined by a collagenous bridge that becomes progressively more mineralized and therefore stiffer as distraction proceeds. Most of the resistance is thus concentrated in shorter lengths of collagen, giving rise to higher loads over time. Therefore, the actual load measured during distraction correlates directly to the cross sectional area of this bridge and inversely to the length of the unmineralized portion (Figure 2.9a).

Forces involved in limb lengthening have been reported in animal (White & Kenwright, 1990; Brunner *et al.*, 1994; Forriol *et al.*, 1997; Waanders *et al.*,

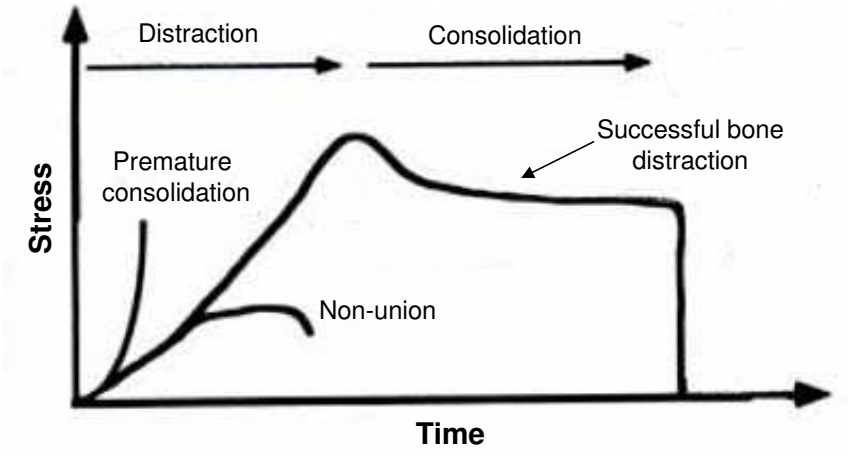

Figure 2.17: Evolution of the force required to distract during distraction osteogenesis. Premature consolidation, nonunion and normal load evolution are represented (Rozbruch & Ilizarov, 2006).

1998; Singare *et al.*, 2006) as well as in human studies (Leong *et al.*, 1979; Jones *et al.*, 1989; Wolfson *et al.*, 1990; Kenwright *et al.*, 1990; Younger *et al.*, 1994; Simpson *et al.*, 1996; Matsushita *et al.*, 1999; Aarnes *et al.*, 2002). However, there is a high variation of measured force levels in the literature due to the different animal characteristics, surgical techniques, fixator types, latency periods, distraction rates, distraction frequencies, patients age and bone type amongst others. This makes comparisons very difficult.

Human forces have been measured in a few studies. Leong *et al.* (1979) measured forces in two pediatric subjects who underwent tibial lengthening. Forces peaked at 122.6 N and 147 N respectively. Matsushita *et al.* (1999) measured forces around 500 N in fourteen human lower extremities using a Hifixator. Wolfson *et al.* (1990) measured pre-distraction forces of 233 N at the end of an Ilizarov tibial lengthening. Younger *et al.* (1994) measured forces during Ilizarov femoral lengthening and found peaks of 428 N, 447 N, and 673 N at the end of distraction. Simpson *et al.* (1996) measured axial forces during limb lengthening using either callotasis or the Wagner technique in a series of ten patients with varying pathologies. They recorded varying forces pattern according to the pathology. For example, in patients with congenitally short limbs they measured very high peak forces (in some cases over 1000 N). Aarnes *et al.* (2002) measured forces

between 431 and 542 N in four short statured patients undergoing tibial lengthening. Physeal lengthening required greater forces of 569 N to 804 N (Jones *et al.*, 1989; Kenwright *et al.*, 1990).

Distraction forces measured in sheep tibias are similar to human ones. For example, Brunner *et al.* (1994) measured forces of 350 N in sheep tibias at the end of transport and Younger (1997) recorded peak forces at an average of 285 N.

Lower forces are required to distract lamb and rabbit tibias. In a study on lambs the maximum force attained was between 80 and 100 N (Forriol *et al.*, 1997). In rabbit tibias, Waanders *et al.* (1998) measured an averaged distraction force on each day of distraction ranging from 5 to 24 N. Singare *et al.* (2006) showed that the latency period had a strong effect on the increase of the distraction force. In the immediate distraction group (0 day latency) the postdistraction force registered was 28.71 N, whereas in the 4-day delay distraction group, the tensile force was 30.51 N. In the 7-day delay distraction group, the tensile load was 39.86 N. These results are similar to those found by White & Kenwright (1990). The tension obtained at the end of distraction in the immediate distraction group was about 30 N, and in the 7-day delay distraction group was more than 50 N. These increasing loads in prolonged latency phases are due to the advanced mineralization of the bridge (Figure 2.9b).

In all cases, the force required to maintain a given tissue length decreases with time due to the relaxation effect: peak forces each day occur immediately after distraction, and are reduced progressively during the next 24 hours (Leong *et al.*, 1979; Brunner *et al.*, 1994; Forriol *et al.*, 1997; Waanders *et al.*, 1998; Matsushita *et al.*, 1999). Some studies reveal that the force obtained after the applied displacement decays exponentially during the 24 hours after distraction (Aarnes *et al.*, 2002). However, this relaxation is not complete and leads to a daily force accumulation due to three main effects: the mechanical elongation of the gap, the intrinsic viscoelastic nature of soft tissues in the interfragmentary gap (Simpson *et al.*, 1996; Nakamura *et al.*, 1997; Matsushita *et al.*, 1999; Richards *et al.*, 1999; Aarnes *et al.*, 2002; Leong & Morgan, 2008) and the tissue growth/differentiation inside the gap. Quantitative estimations of stress accumulation due to residual stresses during the process of distraction can be found in the literature (Brunner

et al., 1994; Waanders *et al.*, 1998; Matsushita *et al.*, 1999; Richards *et al.*, 1999).

2.5 Biomechanical factors

The optimal mechanical environment in which bone formation occurs clinically has not been fully determined yet. In fact, there are multiple mechanical and biological factors that affect to the quality and quantity of the regenerated bone. The basic parameters include:

- *Vascular supply*: Many studies have suggested that blood supply has a significant influence on the shape and mass of the resulting bone (Trueta & Trias, 1961; Ilizarov, 1989*a*; Aronson, 1994). If blood supply is inadequate to support normal or increased mechanical loading, then the bone cannot respond favorably, leading to atrophic or degenerative changes. By contrast, if blood supply is adequate to support increased mechanical loading, the bone will demonstrate compensatory hypertrophic changes. Ilizarov demonstrated that the periosteum, the bone marrow and the nutrient artery are equally important for new bone formation (Ilizarov, 1971; Ilizarov *et al.*, 1983; Ilizarov, 1989*a*) although many authors have indicated that the periosteum is the major contributor to osteogenesis during distraction (Delloye *et al.*, 1990; Yasui *et al.*, 1991; Cara del Rosal, 1992). Therefore, methods of bone separation that disrupt the periosteum, such as widely displaced corticotomies or osteotomies, can result in decreased osteogenesis (Frierson *et al.*, 1994).

- *Latency period.* It is generally agreed that a period of latency subsequent to a corticotomy enhances the formation of bone (White & Kenwright, 1991; Gil-Albarova *et al.*, 1992; Aronson, 1994; Aronson & Shen, 1994). The duration of the latency period in most clinical reports (Paley, 1990; Price & Mann, 1991; Dahl & Fischer, 1991; Bonnard *et al.*, 1993; Kenwright & White, 1993; Aronson, 1994; Fischgrund *et al.*, 1994) has ranged from three to ten days, with the shorter periods used with the classic Ilizarov corticotomy at metaphyseal locations and the longer periods needed for more traditional osteotomy techniques performed with an oscillating saw,

especially in diaphyseal bones. Experimentally, the limits of these periods have been tested further; good bone formation was seen in canine tibiae after no latency period, and the risk of premature consolidation of the gap increased with latency periods of fourteen to twenty-one days (Aronson & Shen, 1994).

- *Rate of distraction.* It represents the total amount of bone segment movement performed per day. A distraction rate of 1 mm/day remains the consensus for bone formation at any site (Ilizarov, 1989*a*,*b*, 1990; Aronson, 1993; Choi *et al.*, 1997; Farhadieh *et al.*, 2000; al Ruhaimi, 2001; King *et al.*, 2003), although a range of rates is clearly possible and even necessary for many treatments, such as angular lengthening. Rates ranging from 0.5 to 2 mm/day have been reliable for distraction (Figure 2.18). However, if the rate of distraction is less than 0.5 mm per day, the bone may consolidate prematurely (Rozbruch & Ilizarov, 2006). If the rate of distraction is more than 2 mm per day, local ischemia in the interzone and delayed ossification or pseudoarthrosis may result (Ilizarov, 1989*a*,*b*, 1990; Yasui *et al.*, 1993; Rozbruch & Ilizarov, 2006). In general, bone may form more slowly in adults and need slower rates of distraction, whereas children may benefit from rates of more than 1 mm per day in order to avoid premature consolidation of the gap, especially at sites of metaphyseal lengthening (Aronson, 1997).

- *Frequency of distraction.* It is defined as the number of increments per day into which the rate of distraction is divided. More frequent rhythms of distraction lead to more favorable regenerate formation and cause fewer soft tissue problems. Therefore, distraction mechanisms must be developed to obtain a rhythm close to continue traction (Figure 2.18).

- *Age of the patient.* Older patients tend to heal more slowly, with greater delays occurring after the age of twenty years (Paley, 1990; Fischgrund *et al.*, 1994; Aronson, 1994). Paley (1990) compared the results of lengthening between 12 adults and 48 pediatric patients and reported that patients older than 20 years healed at one half the rate of patients younger than

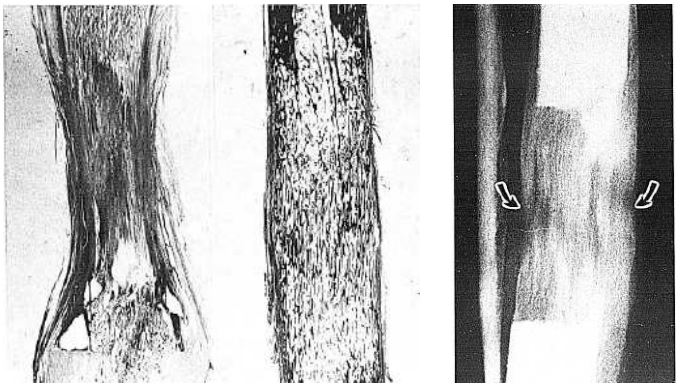

(a) (b)

Figure 2.18: a) Fibrous union with a distraction rate of 2 mm/day in 4 increments/day (left figure). Bony union with a distraction rate of 1 mm/day in 4 increments/day (right figure) (Ilizarov, 1990). b) With an autodistractor (60 steps/day) the central growth zone is hardly visible (Ilizarov, 1990).

20 years. Aronson *et al.* (2001) carried out an experimental study on rat models submitted to tibial mid-diaphyseal osteotomy. They found higher amounts of mineralized bone in the younger rats than in the elder ones.

- *Length of the distraction regenerate.* The rate of healing is directly proportional to the length of the distraction gap since the greater the lengthening, the longer the time needed for treatment. This is expressed as the healing index: number of days of treatment for each centimeter of new bone (Aldegheri *et al.*, 1985; De Bastiani *et al.*, 1987; Aldegheri *et al.*, 1989).

- *Fixator-related factors.* They affect the mechanical properties of the distraction appliance and the stability of the bone segment fixation. These parameters include the number, length, and diameter of the fixation pins, the rigidity of the distraction device, the material properties of the device, etc. Ilizarov (1989*a*), in his classic series of dog experiments, found that stable but not rigid, circular external fixation generated direct intramembranous bone formation in the distraction gap whereas in cases with insufficient fixation, new bone formed via cartilaginous tissue or resulted in fibrous nonunion.

- *Tissue-related factors.* Intrinsic parameters are also important factors that

affect the quality of the forming distraction regenerate. They include the type of bone as well as the tension developing within the soft tissue envelope, which includes muscles, ligaments, and fascia. With regard to the type of bone, metaphyseal sites generally heal faster than diaphyseal sites (Aronson, 1997). The femur has been shown to heal faster than the tibia (Price & Mann, 1991; Bonnard *et al.*, 1993), and tibia lengthened at two sites heal faster than those lengthened at only one site (Fischgrund *et al.*, 1994).

- *Device orientation.* It directly affects the distraction vector, relative to the anatomical axis of the bone segments to be distracted. Since the regenerate within the distraction gap is always formed along the axis of applied traction (Figure 2.19) (Ilizarov, 1989*a*), distraction appliances must be oriented carefully. This is especially important for lengthening of the femur, where the direction of distraction is not parallel to the anatomic axis of the bone (Samchukov *et al.*, 1998).

(a) (b)

Figure 2.19: a) Radiograph and b) photomicrograph of transverse distraction osteogenesis during Ilizarov's experiments (http://www.globalmednet.com/docdrom/Biol/DistPar/dp004.htm).

As observed, the successful application of the distraction osteogenesis technique is equally dependent on biological and biomechanical factors. This was first postulated by Ilizarov in his well known *"Ilizarov effects"* (Ilizarov, 1952; Ilizarov *et al.*, 1969; Ilizarov, 1971; Ilizarov *et al.*, 1983). The first Ilizarov principle or *"Law of Tension-Stress"* postulates that gradual traction creates stresses that

can stimulate and maintain regeneration of living tissues. The second Ilizarov principle theorized that the shape and mass of bones and joints are dependent on an interaction between mechanical loading and blood supply.

2.6 Clinical applications

Since Ilizarov's reintroduction of distraction in the orthopaedic therapy, new applications have emerged in the rest of the organism. One of the sites where this technique has also been introduced and is under investigation is the craniofacial skeleton. But perhaps one of the most exciting potential areas for future research is the application of distraction forces at different rates to regenerate both ligaments (Aston *et al.*, 1992) and articular cartilage (Lieberman & Friedlaender, 2005). Next, we summarize the main applications in long bones and mandibular distraction. Long bone distraction osteogenesis applications are:

- *Bone transport.* It was first introduced by Ilizarov for treating long bone defects that resulted from trauma, oncologic resection, or congenital anomalies (Ilizarov, 1971, 1988). The concept includes resection of pathologic bone followed by gradual transport of an osteotomized healthy bone segment (transport disk) via distraction device across the area of defect. After the transport disk reaches the opposite host bone segment, the intervening fibrous tissue is removed followed by application of compression between the transport and host bone segments at the docking site. Several bone transport techniques have been developed. According to Ilizarov, the techniques are divided into three groups based on the numbers of distraction-compression sites: monofocal, bifocal and trifocal.

  Congenital pseudoarthrosis of the tibia is ideally treated using the bone transport method of Ilizarov with open resection of the pseudoarthrosis and intramedullary fixation (Paley *et al.*, 1992).

- *Limb lengthening* (Figure 2.20). Congenital anomalies (birth defects) with limb reduction deficiencies like radial hemimelia[4], ulnar hemimelia, congen-

[4]Hemimelia: developmental anomaly characterized by the absence or gross shortening of the lower portion of one or more of the limbs.

ital short femur, fibular hemimelia, tibial hemimelia, are the commonest causes of one side limb shortening. However, other causes such as childhood fractures of the femur, osteomyelitis, neurological conditions like cerebral palsy, dysplasia (malformation) and destruction of the hip joint, residual paralytic poliomyelitis may also cause large amounts of bony shortening. For example, dramatic shortening exceeding 20 to 25 cm can occur when the lower femoral physis is damaged (http://www.ilizarov.org/ll.pdf).

Figure 2.20: Patient before treatment (left) and after lengthening and remodeling the shape of her leg (right) (Rozbruch & Ilizarov, 2006).

Likewise, lengthening of the forearm has been reported for a variety of indications, including radial agenesis, radiohumeral synostosis, ulnar dysplasia with dislocated radial head, growth arrest, epiphyseal dysplasia, disturbances from tumors or infection and Madelung's deformity (Raimondo *et al.*, 1999; Horii *et al.*, 2000; Launay *et al.*, 2004).

An interesting application of limb lengthening is the ability to lengthen both lower limbs and increase the height. This has the most logical application in achondroplastic dwarfism. Achondroplasia is the commonest form of short limbed dwarfism (Figure 2.21).

(a) (b)

Figure 2.21: Achondroplastic dwarf who underwent limb lengthening and achieved 31 cm of height without complications (Pombo-Arias, 1997).

- *Treatment of nonunions.* Despite advances in treatment protocols for fractures, some do not heal and result in non-unions. Moreover, mild shortening (up to 3 cm) is frequently found with nonunions in tibial fractures treated with plaster casting or functional cast bracing (http://www.ilizarov.org/ll.pdf). For this reason, these nonunions can be treated with distraction osteogenesis.

  Ilizarov differentiated three types of nonunions, based on clinical and radiographic findings: atrophic, normotrophic and hypertrophic. Atrophic nonunions with interposed fat, loose fibrous tissue or even muscle are clinically mobile and radiographically there is a thick radiolucent zone between bone ends. Hypertrophic nonunions are clinically stiff and radiographically expansive, with peripherally reactive bone formation and a thin radiolucent line between bone ends. Normotrophic nonunions are intermediate between atrophic and hypertrophic (Lieberman & Friedlaender, 2005).

  Hypertrophic nonunions can be successfully treated with distraction osteogenesis (Ilizarov *et al.*, 1972, 1973; Catagni *et al.*, 1994), whilst atrophic nonunions require either gradual compression of the site (to stimulate local

inflammatory resorption of the atrophic interface tissues and neovascularity) followed by distraction or local compression with simultaneous distraction osteogenesis at an adjacent site in the same bone to increase local and regional blood flow (Paley *et al.*, 1989).

- *Arthrodiastasis.* Distraction osteogenesis can also be used for gradual correction of angular joint deformities (arthrodiastasis) and can restore the movement to a stiff joint. Knee flexion contracture from a variety of etiologies can be stretched using either monolateral or ring fixators (Haggland *et al.*, 1993). Arthrodiastasis of the hip and elbow have also surprising success (Cañadell *et al.*, 1993; Lieberman & Friedlaender, 2005).

- *Foot reconstruction.* It has been undertaken for a variety of conditions including untreated, residual, or recurrent clubfeet[5] in adults (Figure 2.22), post-traumatic deformity and degenerative joint disease, failed ankle fusion and a variety of deformities such as vertical talus (Grant *et al.*, 1992; Paley, 1993; de la Huerta, 1994).

  These deformities can be corrected through soft tissue stretching (arthrodiastasis), osteotomies (distraction osteogenesis) or both (Grant *et al.*, 1992; Paley, 1993; de la Huerta, 1994). Many of these feet are considered preamputation and the Ilizarov method is used as a true salvage procedure. However, compared to other applications of the Ilizarov method, foot lengthening seems to be the most painful (Lieberman & Friedlaender, 2005).

- *Special indications.* The Ilizarov method has been used to correct infected spinal pseudoarthrosis (Graziano *et al.*, 1993) and for ligaments or stump lengthening amongst others (Ilizarov, 1990; Aston *et al.*, 1992) (Figure 2.23). Stumps can be elongated for improved prosthetic function. Likewise, the short cuboidal bones can also be elongated by the technique of corticotomy, stable external fixation, latency and distraction (Ilizarov, 1990).

On the other hand, a number of experiments and clinical investigations have demonstrated that gradual mechanical traction of bone segments at an osteotomy

[5]Clubfeet: congenital deformity of the foot.

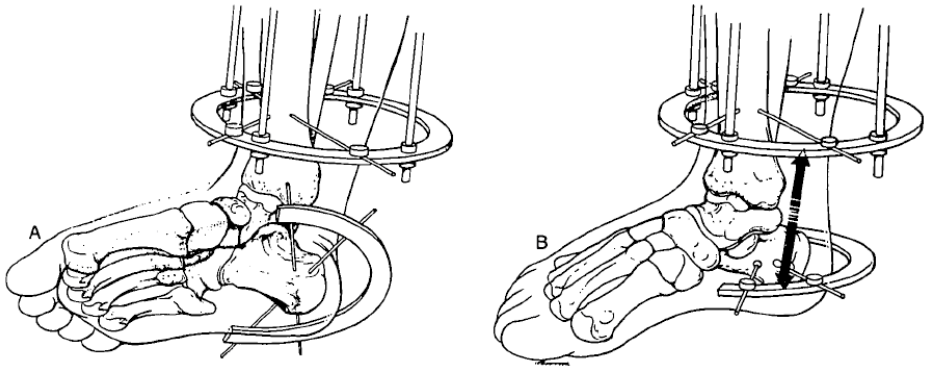

Figure 2.22: Before (a) and after (b) hindfoot clubfoot correction (Grant *et al.*, 1992)

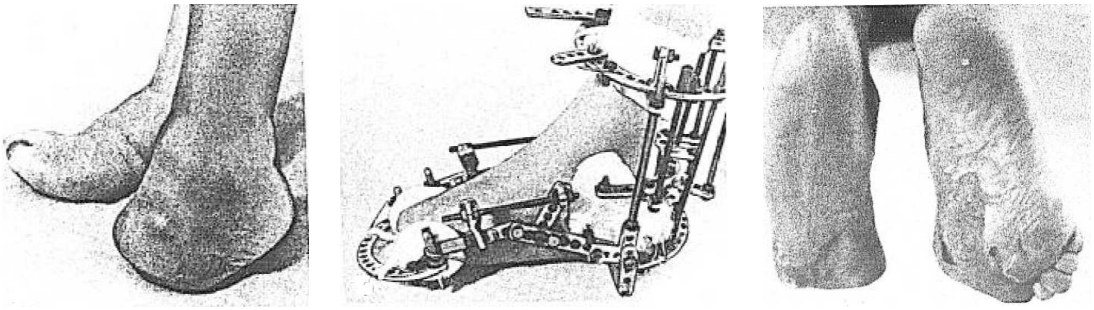

(a) (b) (c)

Figure 2.23: Stump elongation. a) Clinical appearance of a patient with a tarsometatarsal amputation; b) patient with the apparatus during elongation of the talus and calcaneus; c) final clinical appearance, plantar view (Ilizarov, 1990).

site created in the craniofacial region also regenerates new bone parallel to the direction of traction. The initial applications of distraction osteogenesis to the craniofacial skeleton were used on the mandible. However, it did not take long before distraction was applied to other bones, such as maxilla and midface:

- *Mandibular lengthening and widening.* This is the most commonly applied craniofacial osteodistraction technique over the past 10 years. The applications range from ramus lengthening to corpus lengthening and midline widening, using either internal or external devices (Samchukov *et al.*, 2001). This treatment is commonly used for patients with hemifacial microsomia (HFM). This pathology is a congenital asymmetrical malformation of both

the bony and soft-tissue structures of the cranium and face. It is the second most common facial birth defect after clefts, with an incidence in the range of 1 in 5000 (Converse *et al.*, 1973; Gorlin *et al.*, 1990).

- *Maxillary and midface distraction.* Maxillary and midface distraction are used for length and width deficiencies (Figure 2.24), such as midface hypoplasia[6] which is characterized by deficiency of skeletal height, width and anteroposterior relationships (Enlow, 1990).

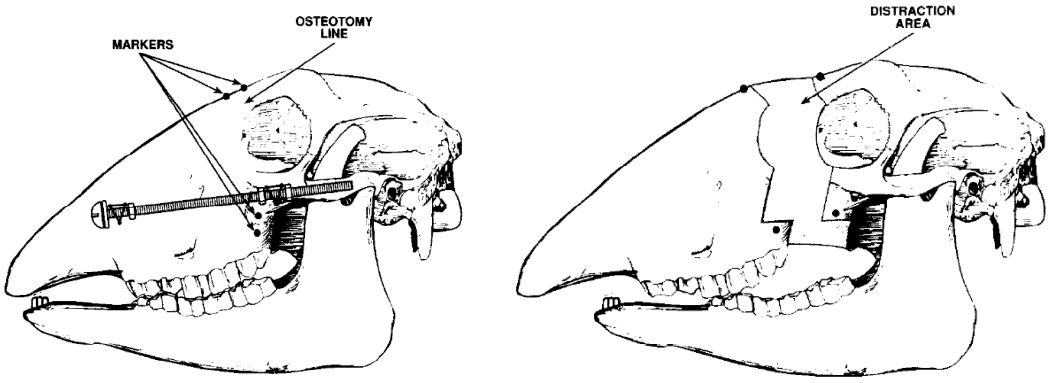

(a) (b)

Figure 2.24: Experimental surgical design. a) Diagram to show the osteotomy line and the expansion device b) Diagram to show the area of distraction after removal of the appliance and the increased distance between the bone markers (Rachmiel *et al.*, 1993).

- *Bone transport.* Although less commonly employed in the craniofacial region, bone transport is frequently used for correction of large mandibular defects, reconstruction of neocondyles, cleft lip and alveolar defects for dental implants.

- *Alveolar ridge* both in the mandible and maxilla (Figure 2.25). Alveolar deformities and defects may result from a variety of pathological processes including: developmental anomalies, such as cleft palate and congenital tooth absence, maxillofacial trauma, which often involves damage to the teeth and associated jaw structures, and periodontal disease leading to bone

[6]Hypoplasia: underdevelopment or incomplete development of a tissue or organ.

and tooth loss from the alveolar process. These deformities may be managed by a variety of surgical techniques, such as autogenous bone grafting, alloplastic augmentation, connective tissue grafting, or guided tissue regeneration (Chin, 1997; Lynch *et al.*, 2004). However, osteodistraction of the alveolar process may provide superior reconstruction of these types of defects and has provided successful results (Block *et al.*, 1996; Chin & Toth, 1996).

Alveolar bone can be distracted in all directions to gain both height and width. Alveolar small bone fragment distraction is done one or twice per day in 0.4 mm increments, well below the 1 or 2 mm per day used in long bones.

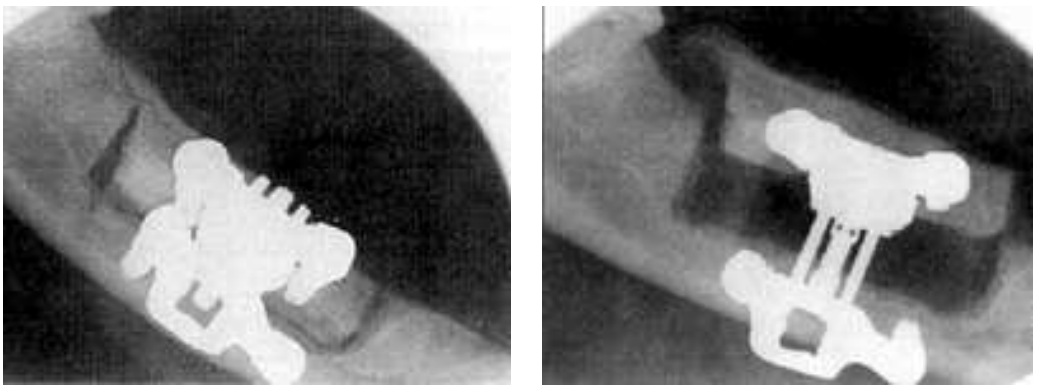

(a) (b)

Figure 2.25: Experimental mandibular alveolar ridge augmentation using osteodistraction, a) after segmental osteotomy and b) after completion of distraction (Block *et al.*, 1996). Note increased height of the alveolar process and newly formed bony tissues filling the intersegmentary gap.

- *Periodontal ligament (PDL) distraction.* This method is based on distraction of the periodontal ligament and produces rapid tooth movement with minimal complications (Liou & Huang, 1998; Samchukov *et al.*, 2001). This technique involves premolar extraction followed by undermining of the interseptal bone distal to the canine in order to reduce bony resistance on the compression site. A force is then applied to the tooth to be moved, resulting in PDL compression on one site and tension on the other side. Osteoblasts begin to deposit along the stretched periodontal fibers, thereby

forming long bony trabeculae horizontally and parallel to the path of tooth movement. This process is different from tooth movement into regenerate bone. The former involves movement of both tooth and bone as new bone is generated whilst the latter involves remodelling of bone as a tooth is moved into new bone.

- *Cranial distraction.* Cranial bones respond to tensional stresses in a similar manner as long bones, and are characterized by formation of a typical distraction regenerate (Barone *et al.*, 1993; Losken *et al.*, 1998; Samchukov *et al.*, 2001). Based on the results of experimental studies, several distraction osteogenesis techniques have now been applied clinically for reconstruction of cranial deformities and cranial vault defects.

Chapter 3

Numerical simulation of long bone distraction osteogenesis

3.1 Introduction

In chapter 1 we have seen several different models to simulate bone distraction. All these models are based on existing ones proposed for bone healing due to the similarities between these two processes (Lammens *et al.*, 1998; Jensen, 2002). In fact, distraction osteogenesis has been considered as a particular form of fracture healing, since a high rate of osteogenesis occurs and a high amount of callus forms during this procedure (Ilizarov, 1983, 1989*a*).

In this chapter, we present a general formulation of living tissues, which is based on a mathematical model previously proposed for bone fracture healing (Gómez-Benito *et al.*, 2005, 2006; García-Aznar *et al.*, 2007). This model has been extended since it was not able to simulate some mechanical conditions during distraction osteogenesis, such as the effect of the distraction rate. In particular, the cellular maturation stage has been considered in the process of cell differentiation. In the first part of this chapter, the mathematical model is described. In the second part, an example of application is performed in order to test the reliability of the model under different mechanical environments: the effect of the distraction rate on the regenerate during long bone lengthening.

3.2 Description of the model

The model here presented considers as state variables the concentration c^i of five cell phenotypes: mesenchymal stem cells (MSCs) (s), fibroblasts (f), cartilage cells (c), bone cells (b) and dead cells (d). These cells are associated to their corresponding skeletal tissues, which are considered non-diffusive: granulation tissue (g), fibrous tissue (f), cartilage tissue (c), bone (b) and debris tissue (d). This tissue production is described as a function of the cell type, cellular concentration and matrix production rate per cell (Figure 3.1) (Gómez-Benito *et al.*, 2005):

$$\frac{\partial V^i_{\text{matrix}}}{\partial t} = c^i \cdot Q^i \tag{3.1}$$

where V^i_{matrix} is the volume fraction of tissue i, c^i is the cell concentration and Q^i is the matrix production rate per cell. Model constant values are reported in section 3.5.

The evolution of these skeletal cells in a control volume δV is governed by the continuity equation (Gómez-Benito *et al.*, 2005):

$$\frac{DN}{dt} = [\frac{dc(\mathbf{x},t)}{dt} + c(\mathbf{x},t)\nabla \cdot \mathbf{v}] \cdot \delta V \tag{3.2}$$

where N is the number of cells in a control volume δV ($N = c\delta V$), D/dt is the material derivative, DN/Dt is the rate of change in the number of cells, t is time, $c(\mathbf{x},t)$ is the cell density, $\mathbf{v}$ is the growth rate and $\mathbf{x}$ is the spatial coordinate.

According to equation (3.2), the number of cells can be modified through a change in the cell concentration ($\frac{dc(\mathbf{x},t)}{dt}$) or volume growth rate ($\nabla \cdot \mathbf{v}$) (Figure 3.1). Regarding the former, the evolution of the concentration of the different cell types is described through the evolution of each cell type i:

$$\frac{dc(\mathbf{x},t)}{dt} = \sum_i \frac{dc^i(\mathbf{x},t)}{dt} \qquad i = s, f, c, b, d \tag{3.3}$$

The latter or tissue growth was considered as the combined effect of two phenomena: proliferation of MSCs and chondrocytes hypertrophy (Figure 3.1) (Gómez-Benito *et al.*, 2005). Therefore, we use the following expression:

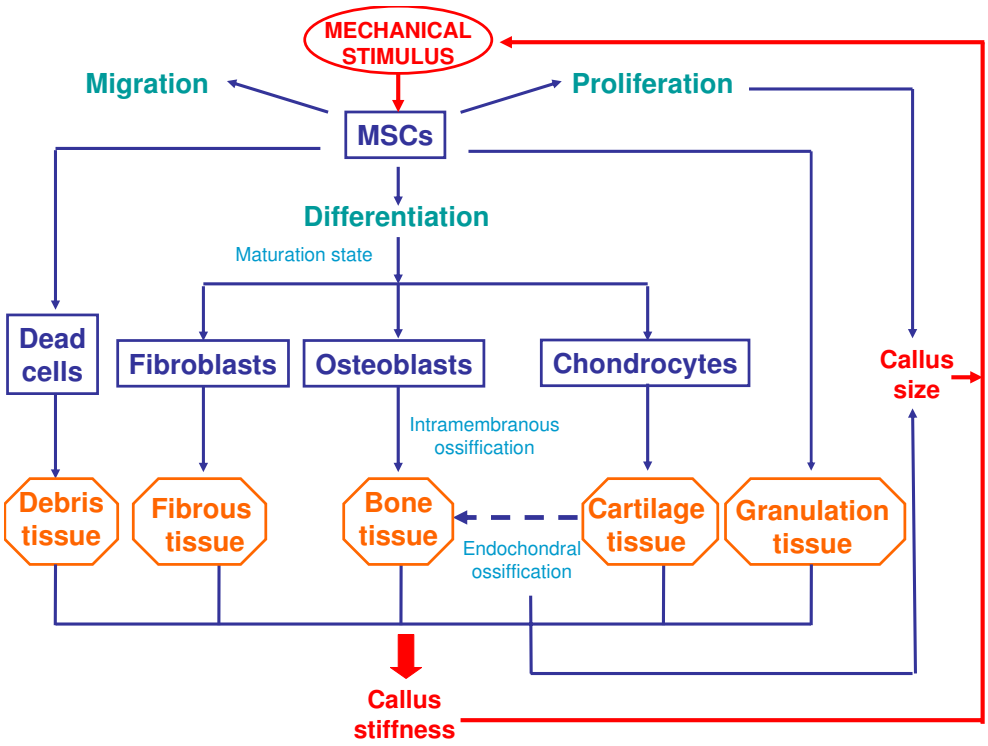

Figure 3.1: Scheme of the main events in the mechanobiological model (cell proliferation, migration, differentiation and tissue growth), guided by the mechanical stimulus.

$$\nabla \cdot \mathbf{v} = g^{v}_{\text{endochondral}}(\Psi, t) + f^{v}_{\text{proliferation}}(c^s, \Psi) \tag{3.4}$$

where $g^{v}_{\text{endochondral}}(\Psi, t)$ represents the callus growth produced during endochondral ossification and $f^{v}_{\text{proliferation}}(c^s, \Psi)$ is due to MSCs proliferation.

All events are assumed to be controlled by a single mechanical stimulus (Figure 3.1) identified here with the second invariant of the deviatoric strain tensor (Ψ) (Gómez-Benito *et al.*, 2005; García-Aznar *et al.*, 2007):

$$\Psi(\mathbf{x}, t) = J_2 = \sqrt{(\varepsilon_I - \varepsilon)^2 + (\varepsilon_{II} - \varepsilon)^2 + (\varepsilon_{III} - \varepsilon)^2} \tag{3.5}$$

where ε_I, ε_{II} and ε_{III} are principal strains, and $\varepsilon = (\varepsilon_I + \varepsilon_{II} + \varepsilon_{III})$ is the hydrostatic strain.

Next, the rules that govern the cellular evolution of each cell phenotype as

well as tissue growth are going to be described.

3.2.1 Cell balance

Mesenchymal stem cells

MSCs concentration ($c^s(\mathbf{x},t)$) was assumed to change by proliferation, migration and differentiation (Figure 3.1) (Gómez-Benito *et al.*, 2005):

$$\frac{dc^s(\mathbf{x},t)}{dt} = f^s_{\text{proliferation}}(c^s,\Psi) + f^s_{\text{migration}}(c^s,h^i) - f^s_{\text{differentiation}}(\Psi,t) \tag{3.6}$$

being $f^s_{\text{proliferation}}$, $f^s_{\text{migration}}$ and $f^s_{\text{differentiation}}$ the functions that define the rate of variation of c^s due to proliferation, migration and differentiation respectively, Ψ the mechanical stimulus, h^i the microcrack volume fraction in specie i per unit volume and $\mathbf{x}$ the spatial coordinate.

The first term in equation (3.6) ($f^s_{\text{proliferation}}$) controls MSCs proliferation. It is modeled as a function of its concentration (c^s) and the mechanical stimulus Ψ(**x**,t) (equation (3.7)): stem cells are assumed to proliferate by mitosis and this proliferation is considered to increase with mechanical stimulus. Proliferation function could have been chosen constant although there are some experimental works suggesting that mechanical strain increases cell proliferation (Smith & Roberts, 1980; Li *et al.*, 1997; Song *et al.*, 2007). In fact, proliferation during distraction osteogenesis exceeds that in nondistracted fracture healing as the stimulus is much higher (Aronson *et al.*, 1997*a*). We have chosen a saturation function to take into account that proliferation increases with the mechanical stimulus, but with a limit ($\alpha_{\text{proliferation}}$) (Gómez-Benito *et al.*, 2005):

$$f^s_{\text{proliferation}} = \frac{\alpha_{\text{proliferation}} \cdot \Psi(x,t)}{\Psi(x,t) + \Psi_{\text{proliferation}}} \cdot c^s \tag{3.7}$$

with $\alpha_{\text{proliferation}}$ and $\Psi_{\text{proliferation}}$ model constants (section 3.5).

With respect to the second term of equation (3.6) ($f^s_{\text{migration}}$), in this work, we have considered as a first approach, cell migration as random, nondirected, and following a standard diffusion equation known as Fick's law:

$$f^s_{\text{migration}} = -\nabla \cdot (\mathbf{D}(h^i) \cdot \nabla c^s) \tag{3.8}$$

where $\mathbf{D}$ is the diffusion coefficient (section 3.5).

And finally, the third term in equation (3.6) ($f^s_{\text{differentiation}}$) accounts for the MSCs differentiation process. In this manuscript, differentiation is assumed to be dependent on the daily average value of the mechanical stimulus and time (Cullinane *et al.*, 2003),

$$f^s_{\text{differentiation}} = \begin{cases} h_{\text{intramembranous}} & \text{if} \quad m^b = 1 \\ g_{\text{differentiation}} & \text{if} \quad m^c = 1 \\ f^f_{\text{differentiation}} & \text{if} \quad m^f = 1 \\ -c_s & \text{if} \quad \Psi > \Psi_{death} \\ 0 & \text{otherwise} \end{cases} \tag{3.9}$$

where $h_{\text{intramembranous}}$, $g_{\text{differentiation}}$ and $f^f_{\text{differentiation}}$ are the expressions that define the evolution to osteoblasts, chondrocytes and fibroblasts, respectively.

The dependence of the previous expressions on time and stimulus is defined through what is called the maturation state of the cells (m^i). It is biologically plausible to assume that MCSs will differentiate only if they have been subjected to a specific mechanical environment for a period of time (Roder, 2003). Once this state has been reached, it is said that the cell is fully matured (m^i=1). Whilst fully matured cells follow an irreversible differentiation pathway resulting in stable cell phenotypes, incomplete mature cells (m^i<1) can reverse their differentiation (cell plasticity) (Pacifici *et al.*, 1990; Ishizeki *et al.*, 1992; Asahina *et al.*, 1993; Nakase *et al.*, 1994). In order to evaluate the temporal evolution of the maturation state of the cell type i (m^i), different approaches can be used. In this case, the number of days a cell needs to mature fully at a constant stimulus level (Figure 3.2) is defined by $N_i = A_i \Psi^{b_i}$, where A_i and b_i are constants dependent on the cell phenotype (Table 3.1). Both constants A_i and b_i have been adjusted according to the maturation times proposed in previous parametric studies (Gómez-Benito *et al.*, 2005) and different experimental evidences (Roberts *et al.*, 1982; Turner

Table 3.1: Constants that describe the maturation process of each cell population (Roberts *et al.*, 1982; Turner *et al.*, 1994; Li *et al.*, 2000; Cullinane *et al.*, 2003; Gómez-Benito *et al.*, 2005).

	Bone cells	Fibroblasts	Cartilage cells
A_i	$1.13 \cdot 10^3$	3.47	137.08
b_i	1.81	-1.36	1.05

et al., 1994; Li *et al.*, 2000; Cullinane *et al.*, 2003). For instance, cartilage cells usually appear in moderate deviatoric strain environments at 15-20 days after fracture in humans (Cullinane *et al.*, 2003) and by day 7 in rats (Iwaki *et al.*, 1997). In the case of fibroblasts, a high tensile strain is known to stimulate their formation (Ilizarov, 1989*b*; Li *et al.*, 1997, 2000; Choi *et al.*, 2004). Indeed, in environments with marked mechanical instability (high distraction rates or non stable fixations, for instance) there is a tendency to the formation of a fibrous union (Ilizarov, 1989*b*; Li *et al.*, 1997, 2000; Choi *et al.*, 2004). And bone cells have been observed in stable mechanical environments (Turner *et al.*, 1994).

To consider the effect of the load history, we proposed, as a first approach, to follow a linear cumulative law similar to Miner's fatigue damage accumulation rule (Miner, 1945):

$$m^i = \sum_j \frac{n_j}{N_i(\Psi_j)} \tag{3.10}$$

where m^i is the maturation level of the cell i and n_j is the number of cycles produced at strain level Ψ_j.

Bone cells

Bone cell concentration ($c^b(\mathbf{x}, t)$) was assumed to depend only on the differentiation process, assuming its proliferation and migration negligible with respect to that of MSCs (Figure 3.1) (Gómez-Benito *et al.*, 2005):

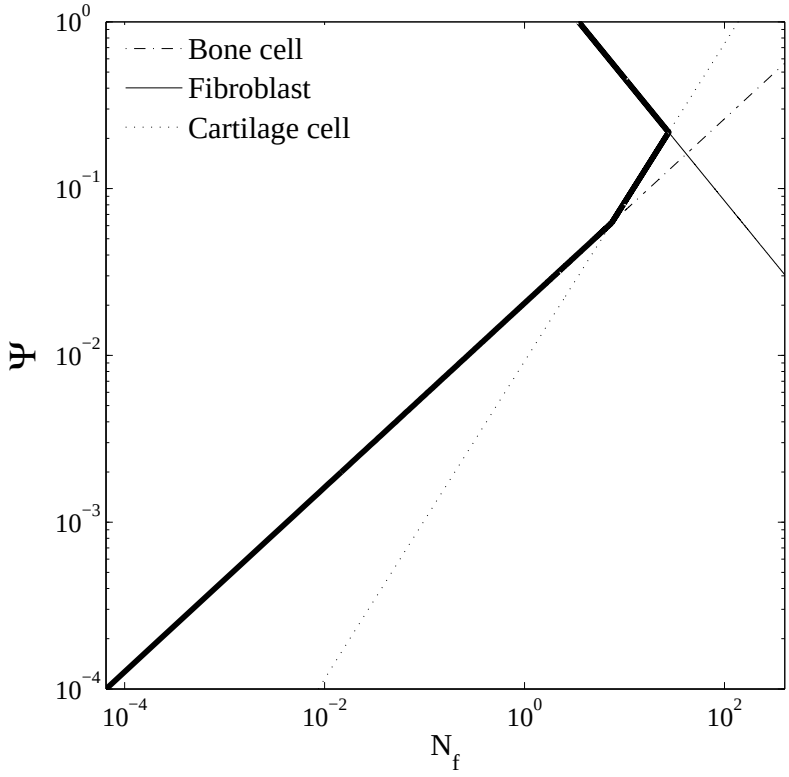

Figure 3.2: Number of days (N_f) that bone cells, fibroblasts and cartilage cells need to differentiate as a function of the mechanical stimulus Ψ.

$$\frac{dc^b(\mathbf{x},t)}{dt} = f^b_{\text{differentiation}}(\Psi, m^b) \tag{3.11}$$

$$f^b_{\text{migration}} = 0 \tag{3.12}$$

$$f^b_{\text{proliferation}} = 0 \tag{3.13}$$

The bone cell differentiation pathway can be either by intramembranous or endochondral ossification, through direct differentiation of MSCs or following cartilage apoptosis and matrix calcification, respectively. These two different bone cell pathways have been defined through the functions $h_{\text{intramembranous}}$ and $h_{\text{endochondral}}$, which distinguish between intramembranous and endochondral ossification:

$$f^b_{\text{differentiation}} = h_{\text{intramembranous}}(\Psi, m^b) + h_{\text{endochondral}}(\Psi, m^b) \tag{3.14}$$

where Ψ is the mechanical stimulus and m^b the maturation level of precursor cells to become bone cells.

In both cases, bone cells require an osteogenic mechanical environment and vascular ingrowth (Fang *et al.*, 2005). The first aspect can only occur if precursor cells have completely matured (m^b=1) for the case of intramembranous ossification or if cartilage has calcified for the case of endochondral ossification. Figure 3.3 shows the differentiation pathway of MSCs to bone cells, from pre-osteoblasts to fully mature osteocytes. On the other hand, the complex process of vascular ingrowth has been simplified and modeled through a diffusion equation, not modeling the vascular invasion directly, but its effect: the advance of the ossification front:

$$h_{\text{vascularization}} = D_b \nabla^2 c^b \tag{3.15}$$

with D_b the diffusion coefficient in the ossification process (section 3.5). Therefore, with the previous equation we assume that bone cells can only be deposited next to existing bone cells, assuming that these are sufficiently vascularized.

We also considered that cells can directly differentiate to bone cells if they reach a threshold level (c^b_{min}), which we assume to be indicative of sufficient level of vascularization.

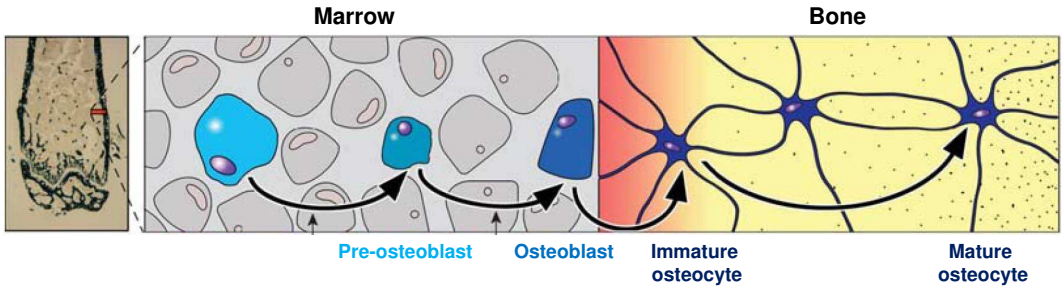

Figure 3.3: The mesengenic process for bone cells, after Robling *et al.* (2006)

With these assumptions, focusing on the intramembranous ossification, we use:

$$h_{\text{intramembranous}} = \begin{cases} h_{\text{vascularization}} & \text{if} \quad [(c^b < c^b_{min})\&(m^b = 1)] \\ c^s & \text{if} \quad [(c^b > c^b_{min})\&(m^b = 1)] \\ 0 & \text{otherwise} \end{cases} \tag{3.16}$$

where m^b is the normalized maturation state of MSCs to bone cells and c^i the cell concentration.

Endochondral ossification has been modeled analogously:

$$h_{\text{endochondral}} = \begin{cases} h_{\text{vascularization}} & \text{if} \quad [(m^b = 1)\&(c^b < c^b_{min})] \\ c^c & \text{if} \quad [(m^b = 1)\&(c^b > c^b_{min})] \\ 0 & \text{otherwise} \end{cases} \tag{3.17}$$

Cartilage cells

Cartilage cell concentration ($c^c(\mathbf{x}, t)$) was also assumed to change only by the differentiation process (Figure 3.1) (Gómez-Benito *et al.*, 2005). Its concentration increases by MSCs differentiation into this cell phenotype and decreases through the endochondral ossification:

$$\frac{dc^c(\mathbf{x}, t)}{dt} = f^c_{\text{differentiation}}(\Psi, t) = g_{\text{differentiation}} - h_{\text{endochondral}} \tag{3.18}$$

$$f^c_{\text{migration}} = 0 \tag{3.19}$$

$$f^c_{\text{proliferation}} = 0 \tag{3.20}$$

The endochondral ossification has been modeled with equation (3.17) whilst the direct differentiation of MSCs to chondrocytes follows the following rule:

$$g_{\text{differentiation}} = \begin{cases} c^s & \text{if } (m^c = 1) \\ 0 & \text{otherwise} \end{cases} \tag{3.21}$$

Fibroblasts

Similarly, fibroblast concentration ($c^f(\mathbf{x},t)$) was only dependent on differentiation rules, assuming their proliferation and migration negligible:

$$\frac{dc^f(\mathbf{x},t)}{dt} = f^f_{\text{differentiation}}(\Psi,t) \tag{3.22}$$

$$f^f_{\text{migration}} = 0 \tag{3.23}$$

$$f^f_{\text{proliferation}} = 0 \tag{3.24}$$

Differentiation of MSCs to fibroblasts has been modeled:

$$f^f_{\text{differentiation}} = \begin{cases} c^s & \text{if } (m^f = 1) \\ 0 & \text{otherwise} \end{cases} \tag{3.25}$$

Dead cells

Finally, if the mechanical stimulus reaches a limit value MSCs can also die:

$$\text{if } \Psi > \Psi_{\text{death}}, \quad \frac{dc^d}{dt} = c^s \tag{3.26}$$

where Ψ_{death} is the stimulus level above which MSCs will die (section 3.5).

3.2.2 Callus growth

Tissue growth is developed, as a first approximation, under the small deformation assumption. We are aware that distraction in the first days is a large deformation process since interfragmentary movements represent as much as 100% of the size of the gap in these first days. However, after 5 days of distraction, strains are reduced up to 20%. On the basis of this hypothesis and following equation (3.4), the total tissue growth is assumed to be computed as the sum of the proliferation of MSCs and chondrocytes hypertrophy (equation (3.4)) (Gómez-Benito *et al.*, 2005).

Regarding the former, it is assumed that the concentration of mesenchymal cells can increase due to proliferation, from zero to a maximum or saturation cell

density (c^s_{max}) without having to increase the callus size. Once this concentration is reached, the only way cells have to proliferate further is by increasing the callus size at a constant level of cell concentration (equation (3.4)):

$$f^v_{\text{proliferation}}(c^s, \Psi) = \begin{cases} 0 & \text{if} \quad (c^s < c^s_{max}) \\ \frac{f^s_{\text{proliferation}}}{c^s_{max}} & \text{if} \quad (c^s = c^s_{max}) \end{cases} \tag{3.27}$$

with $f^s_{\text{proliferation}}$ the proliferation function defined in equation (3.7) and c^s_{max} the normalized saturation value of stem cell density (section 3.5).

The second growth mode is assumed to be due to the hypertrophy of chondrocytes. These cells undergo an increase of volume before calcification and programmed cell death to allow osseous tissue to develop (endochondral ossification). Growth due to chondrocytes hypertrophy (equation (3.4)) is described by the following expression (Gómez-Benito *et al.*, 2005):

$$g^v_{\text{endochondral}}(c^c, \Psi) = \frac{-1}{c^c(\mathbf{x}, t)} \cdot \frac{\partial c(\mathbf{x}, t)}{\partial t} = -\frac{g_{\text{growth}}}{c^c(\mathbf{x}, t)} \tag{3.28}$$

where g_{growth} is:

$$g_{\text{growth}} = \begin{cases} \dfrac{\Psi - \Psi_{\text{calcified}}}{\Psi_{\text{bone}} - \Psi_{\text{calcified}}} k_{\text{hyper}} & \text{if } (\Psi < \Psi_{\text{calcified}}) \& (c^c > c^c_{min}) \\ 0 & \text{otherwise} \end{cases} \tag{3.29}$$

with $\Psi_{\text{calcified}}$, k_{hyper} and c^c_{min} constants of the model (section 3.5).

3.3 Material properties

The different tissues (granulation tissue, fibrous tissue, cartilage, calcified cartilage and bone tissue) govern the mechanical properties of the distraction gap and hence the associated gap stiffness. Tissues are assumed to be poroelastic and isotropic, each one with a constant proportion of the main components (Gómez-Benito *et al.*, 2005): collagen type I (c_I), II (c_{II}), and III (c_{III}), water, ground

substance (g_s) and mineral (m_i) (Table 3.2). The material properties, elastic modulus (E) and Poisson's ratio (ν) are determined through a mixture rule (Lacroix, 2000; Ament & Hofer, 2000) from the volume proportion of those components (v_x):

$$\begin{aligned} E(MPa) &= 20000v_{mi} + 280v_{cI} + 175v_{cII} + 100v_{cIII} + 0.7v_{gs} \\ \nu &= 0.33v_{mi} + 0.48v_{coll} + 0.49v_{gs} \end{aligned} \tag{3.30}$$

For instance, Griffin *et al.* (1997) determined an elastic modulus of 20 GPa and a Poisson's ratio of 0.33 for the mineral. Farquhar *et al.* (1990) obtained the elastic modulus of collagen II in the range of 135-205 MPa and Simha *et al.* (1999) a value of 160 MPa. Sasaki & Odajima (1996) measured the Young's modulus of collagen I in a sheep, obtaining a value of 430 MPa and van der Rijt *et al.* (2006) predicted a value of type I collagen fibrils ranging from 250 MPa to 450 MPa. For the collagen I we have taken an elastic modulus of 280 MPa which is in the range of previous estimations. Using a composites model theory, Simha *et al.* (1999) predicted a Young's modulus and a Poisson's ratio for the ground substance of 0.7 MPa and 0.49 respectively and a Poisson's ratio of the collagen of 0.48.

The Young's modulus and Poisson's ratio calculated through equation (3.30) as well as the volume proportions of each component of the different tissues are shown in Table 3.2.

Table 3.2: Tissue composition (% volume, the rest is water) and material properties of the different tissues (Gómez-Benito *et al.*, 2005; Reina-Romo *et al.*, 2009).

Volume composition	Bone tissue	Cartilage	Calcified cartilage	Fibrous tissue	Granulation tissue
Collagen I	0.2848	0.	0.	0.1861	0.018
Collagen II	0.	0.135	0.135	0.	0.
Collagen III	0.	0.	0.	0.	0.
Ground substance	0.0352	0.079	0.079	0.07885	0.082
Mineral	0.43	0.	0.015	0.	0.
E (MPa)	939.76	23.68	53.68	52.16	5.1
ν	0.2959	0.1035	0.1085	0.1280	0.0488

The values of the permeability are different for each tissue type. For hard tissues, we assume a constant permeability distinguishing between cortical bone, woven bone and calcified cartilage, with values of $7{\cdot}10^{-15}$, $7{\cdot}10^{-11}$ and $3.5{\cdot}10^{-12}$ mm^2. In soft tissues (granulation tissue, fibrous tissue, cartilage tissue and debris tissue) permeability is calculated from composition and porosity, following the model proposed by Levick (1987). The main aspects of these relationships are summarized in appendix A.

3.3.1 Tissue damage

Damage is incorporated in the model through the variable d^i. This variable quantifies the macroscopic mechanical degradation and is related to the density of internal microcracks (h^i). In general, the relation between both variables can be expressed as (Doblaré & García-Aznar, 2006):

$$f(d^i) = h^i. \tag{3.31}$$

The continuum damage variable d^i is normalized between [0,1] where 0 represents an intact matrix and 1 a completely disrupted matrix. Although damage could affect all tissues, we assume that it only occurs in the granulation and debris tissues due to their relative low resistant properties. We assume that granulation or debris tissues are locally disrupted when the maximum value of the mechanical stimulus in their corresponding tissues reaches a limit stimulus Ψ_{damage}. In this case, we assume that the disrupted volume fraction is 0.95, that is, only a small residual stiffness is considered for these tissues in mechanically demanding environments (Gómez-Benito *et al.*, 2005):

$$d^i = \begin{cases} 0 & \text{if} \quad \Psi < \Psi_{\text{damage}} \\ 0.95 & \text{otherwise} \end{cases} \tag{3.32}$$

The rigidity reduction of the granulation tissue as a result of the damage is given by:

$$E^g_{\text{new}} = E^g_0(1 - d^i) \tag{3.33}$$

with E^g_0 the Young's modulus of the intact granulation matrix.

3.4 Numerical implementation

In this chapter, as a first approach we will consider a free stress state as initial condition for each day analyzed. We assume therefore that the daily relaxation period is enough for the tissues to grow and adapt to their new mechanical environment. This assumption is used in all existing models of distraction osteogenesis (Idelsohn *et al.*, 2006; Isaksson *et al.*, 2007; Boccaccio *et al.*, 2007, 2008) and will be deeply analyzed in chapter 4. Also, as commented above, the mathematical formulation has been developed under the small deformations assumption although, it has been implemented in an updated Lagrangian finite element code and, thus, the reference configuration is updated at each increment.

Therefore, the formulation previously presented has been solved, under the small deformations assumption within an updated Finite Element code. In this formulation all variables are referred to the current configuration (i.e. from the end of the previous time step). The simulation process starts from an initial geometry and initial conditions (Figure 3.4). Next, four un-coupled finite element analyses are solved in the commercial program ABAQUS (Hibbit & Sorensen, 2002):

- *A poroelastic analysis* to determine the mean and maximum value of the mechanical stimulus (equation (3.5)) at each integration point,
- *A thermoelastic analysis* to model the distracted callus growth (equation (3.4)), using the similarity between growth and thermal deformation (Gómez-Benito *et al.*, 2005). In this analysis the thermal expansion coefficient is related to $1/c^s_{max}$ (equation (3.27)) and to $1/c^c$ (equation (3.28)) for growth due to proliferation or to endochondral ossification respectively. The temperature is related to $f^s_{\text{proliferation}}$ for the first growth mode and to g_{growth} for the second growth mode.
- *A first diffusion analysis* to simulate MSCs migration (equation (3.8)),
- *A second diffusion analysis* to model the vascularization and the advance of the

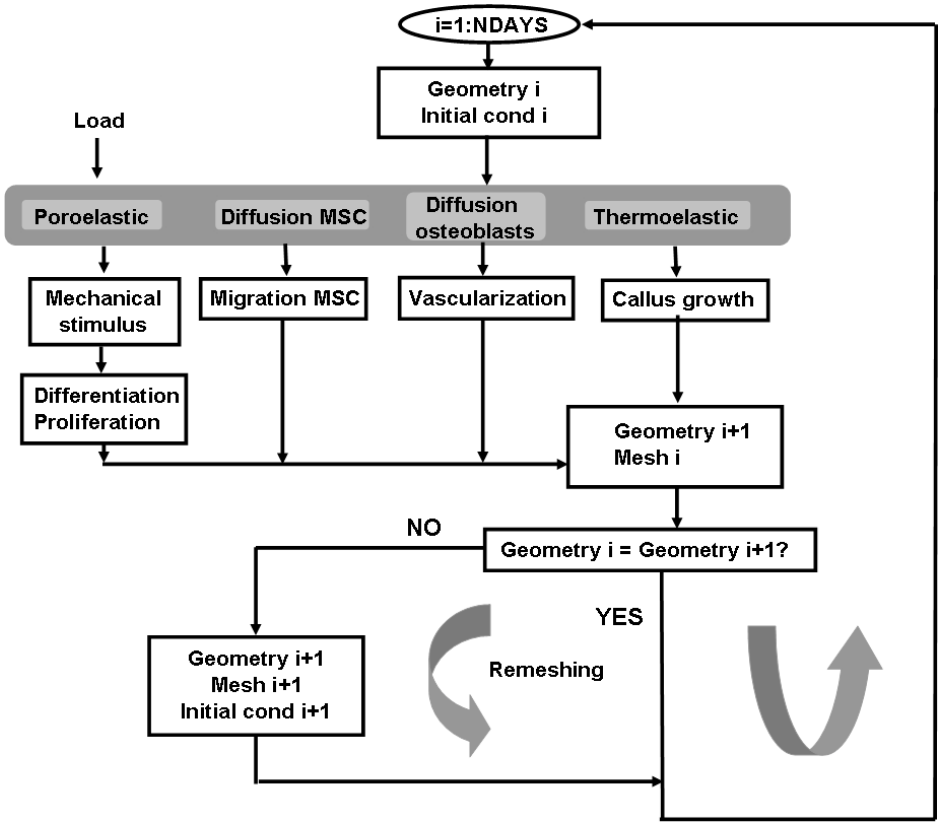

Figure 3.4: Scheme of the computational implementation.

ossification front (equation (3.15)).

A new geometry is defined by the nodal displacements obtained in the thermoelastic analysis. Nodal values (cell concentration and extracellular matrix composition) are updated with the equations that govern the differentiation and proliferation processes. These are function of the mechanical stimulus (Ψ) determined in the poroelastic analysis. Finally, a remeshing step is performed in Ansys® in order to adapt the mesh to the large geometry changes that take place during the process of distraction osteogenesis (Figure 3.5). In order to reduce the computational cost, the mesh is finer in the corticotomy gap. The remeshing is applied to the deformed geometry (Figure 3.5b), state variables are then interpolated to the new geometry with Matlab® (Figure 3.5c and d) and the new values are used as initial conditions for the following step. This numerical implementation is followed in both the distraction and consolidation phases.

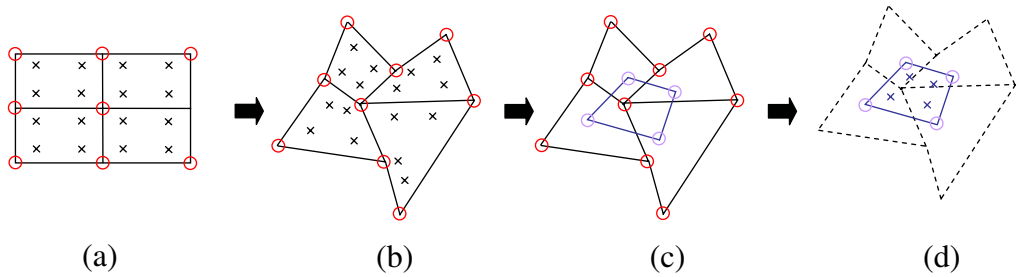

Figure 3.5: Remeshing implementation. a) Old mesh integration points before the loading process; b) old mesh nodes after the loading process; c) new mesh nodes; d) new mesh integration points. Old elements are drawn with dashed lines and new elements are drawn with solid lines.

3.5 Model parameters

All the parameters used in the simulations have been estimated from the literature and have been tested in sensitivity analyses:

- Ψ_{bone}=0.03 is the stimulus level below which bone tissue may be formed through the endochondral ossification.
- Ψ_{death}=1 is the stimulus level above which MSCs will die (Claes *et al.*, 1997; Gómez-Benito *et al.*, 2005).
- Ψ_{damage}=0.6 is the stimulus level above which disruption of granulation tissue takes place.
- $\Psi_{\text{calcified}}$=0.06 is the stimulus level below which cartilage begins to calcify before endochondral ossification occurs.
- $\alpha_{\text{proliferation}}$=0.6 day^{-1} and $\Psi_{\text{proliferation}}$=0.2 are the parameters that define the stem cell proliferation
- c^s_{max}=1 is the normalized saturation value of stem cell density (Wilsman *et al.*, 1996; Gómez-Benito *et al.*, 2005).
- k_{hyper}=0.01 second^{-1} is the parameter that controls the volume increase produced during normalized cartilage cell calcification (Wilsman *et al.*, 1996; Gómez-Benito *et al.*, 2005).

- Q^s=0.3 mm^3/(stem cell·day), Q^b=0.3 mm^3/(osteoblast·day), Q^c=0.2 mm^3/(chondrocyte·day), Q^f=0.5 mm^3/(fibroblast·day) is the amount of matrix synthesized per stem cell, osteoblast, chondrocyte or fibroblast and unit time.

- c^b_{min}=0.2 is the minimum concentration of bone cells that indicates when blood supply is completed at the ossification front and osteoblasts can differentiate directly from stem cells.

- c^c_{min}=0.6 is the equilibrium value of normalized cartilage cell concentration (Wilsman *et al.*, 1996; Gómez-Benito *et al.*, 2005).

- D=1 mm^2/day is the diffusion coefficient that controls stem cell migration.

- D_b=4 mm^2/day is the constant that defines the diffusion coefficient in the ossification process.

3.6 Example of application

As explained in chapter 2, mechanical factors, such as axial alignment, stability and distraction rate affect both the quality and quantity of the regenerated bone (Ilizarov, 1989*a*). For example, nonunions may occur when the bone ends move too much (Ilizarov, 1989*a*; Tajana *et al.*, 1989; Fischgrund *et al.*, 1994), the distraction rate is higher than the optimal (Ilizarov, 1989*b*; Tajana *et al.*, 1989; White & Kenwright, 1990; Choi *et al.*, 2004), the frequency of distraction is not adequate (Ilizarov, 1989*b*), there is no latency phase (Ilizarov, 1989*a*,*b*; White & Kenwright, 1990) or due to damage of the bone marrow and periosteal soft tissues (Ilizarov, 1989*a*).

Therefore, in this section, the mechanobiological model is applied to different mechanical environments in order to elucidate if mechanics may be an important factor that determines the main features of distraction osteogenesis. In particular, we analyze the effect of different distraction rates.

3.6.1 Influence of the distraction rate

Among all the mechanical factors, numerous researchers (Ilizarov, 1989*a*; White & Kenwright, 1990; Aronson, 1993; Choi *et al.*, 1997; Farhadieh *et al.*, 2000; al Ruhaimi, 2001; King *et al.*, 2003) have discussed the special importance of the distraction rate. According to all these studies, the recommended distraction rate is approximately 1 mm/day for long bones of large animals (Ilizarov, 1989*a*,*b*, 1990; Aronson, 1993; Choi *et al.*, 1997; Farhadieh *et al.*, 2000; al Ruhaimi, 2001; King *et al.*, 2003). A slower rate can result in a premature bony union while a faster rate can delay bony bridging producing nonunions or malunions (Ilizarov, 1989*a*,*b*, 1990). Therefore, here we have focused on analyzing how the distraction rate influences on the mechanical conditions and tissue regeneration by exploring the potential of the mathematical algorithm previously described to simulate clinically observed distraction rate related phenomena that occur during distraction osteogenesis.

Experimental set-ups

The mechanobiological model proposed in section 3.2 was used to compare our computational results with data from an *in vivo* experiment performed by Brunner *et al.* (1994) in sheep, where the bone segment transport over an intramedullary nail was evaluated. A diaphyseal defect created in the central region of the tibia was reduced through the ossification process induced in the upper part by distraction osteogenesis. The defect was stabilized with a nail.

Figure 3.6 represents the real geometry of the ovine tibia and the finite element model used. As the geometry of the ovine tibia is almost cylindrical in shape, the numerical implementation was performed in an axisymmetric finite element model of the diaphysis. We assumed rotational symmetry along the long bone axis (y) and mirror-image symmetry with respect to the plane of the osteotomy (x) and, therefore, only one-quarter of the total geometry was modeled. The geometrical dimensions of one-quarter of the finite element model of the tibia are shown in Figure 3.7a. Five distinct regions were modeled: the distracted gap, the marrow cavity, the periosteum, the cortical bone and the nail. Initially, the dimension of the gap was 1 mm. The nail was modeled with a diameter of 7 mm,

and the cortical bone with an inner diameter of 14 mm and an outer diameter of 20 mm. The contact between the marrow cavity and the nail was assumed to be frictionless.

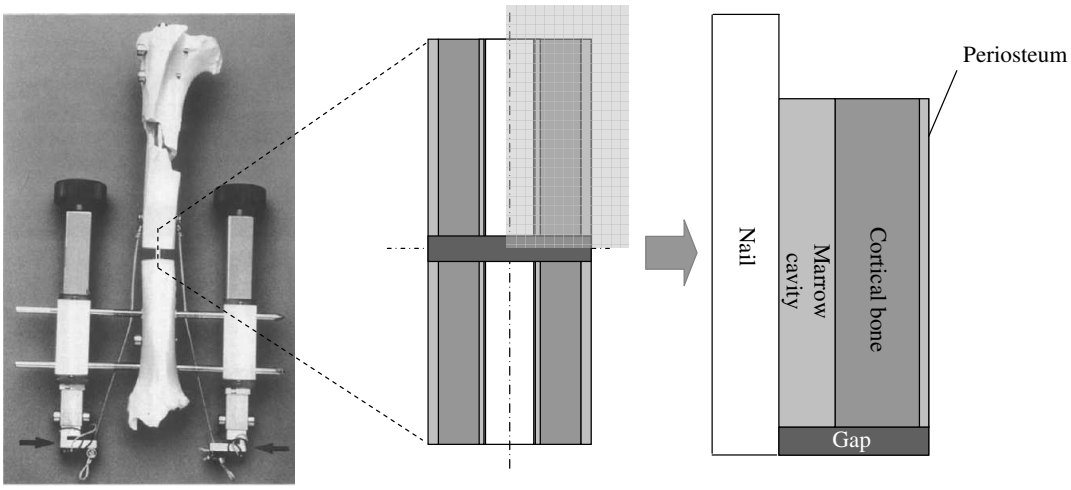

Figure 3.6: Scheme of the geometry and conditions in which the distraction process took place (Brunner *et al.*, 1994).

With regard to the boundary conditions needed for the numerical implementation described in section 3.4, the periosteum was assumed to be impermeable and hence zero fluid flow was prescribed at this boundary (Li *et al.*, 1987) (Figure 3.7b).

The mechanical stimulation consisted of an applied displacement on the top of the cortical bone (Figure 3.7b). The displacement was gradually applied for one minute and the final position maintained the rest of the day (relaxation period). This load history was repeated during the whole distraction process. During the consolidation period, the only active mechanical stimulation was due to the load derived from the normal activity of the animal, i.e. 500 N of static compressive load (Claes *et al.*, 1998). It was applied to the bone-nail complex through a rigid part located on top of the upper surface (which comprises the nail, marrow, cortical bone and periosteum) (Figure 3.7a). Therefore, in this model the nail shields the bone from the normal activity loads. Thus this load has been neglected during the distraction phase.

As initial conditions we considered in the diffusion analysis sources of MSCs

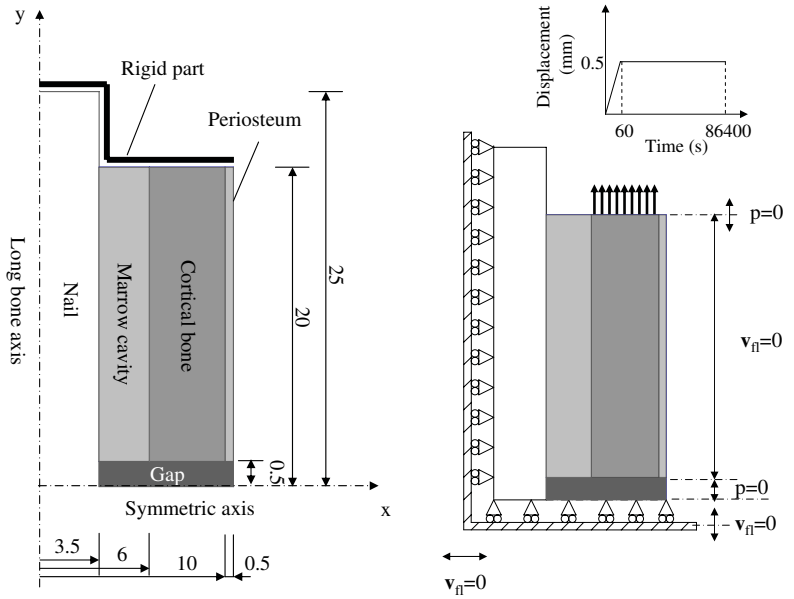

Figure 3.7: Scheme of the axysimmetric tibia model. a) Geometry (dimensions in mm), the rigid part was only modeled during the consolidation phase; b) boundary and loading conditions of the tibia model for the poroelastic analysis with p pore pressure and $\mathbf{v}_{fl}$ fluid velocity.

in the marrow cavity, periosteum and in the surrounding soft tissues (Gerstenfeld *et al.*, 2003) (Figure 3.8a). Hence, it was assumed that the process of corticotomy preserves the endosteum and periosteum. The initial boundary conditions for the ossification front modeled through the diffusion equation consisted on preosteoblastic sources in the areas of the endosteum and periosteum closest to the cortical bone (Figure 3.8b).

As result of the osteotomy, it was assumed initially that the gap tissue was entirely damaged and that damage was uniformly distributed in the corresponding extracellular matrix. Damage repair is not immediate since it depends on the rate of granulation tissue production and on the mechanical stimulus that controls tissue production and additional damage generation.

Although there are many factors influencing osteogenesis during limb lengthening, this study focused on the effect of the distraction rate on bone formation. The model here implemented was initially validated with the standard protocol,

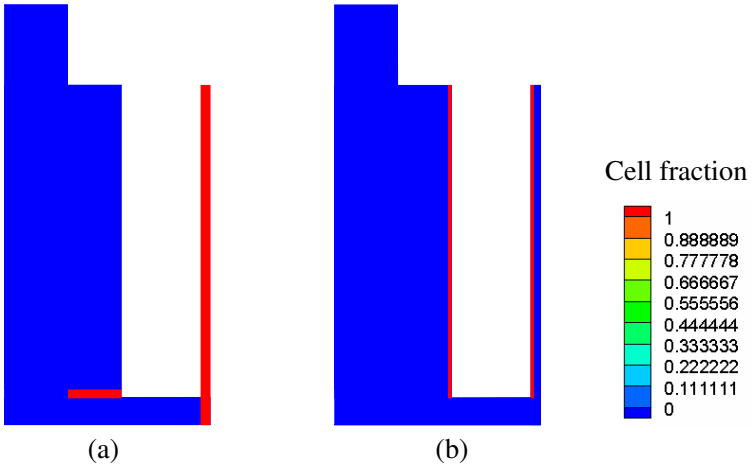

Figure 3.8: Initial conditions: a) MSCs; b) bone cells.

comparing qualitatively and quantitatively the computed reaction forces with realistic experimental results obtained by Brunner *et al.* (1994). This standard protocol considers a distraction rate of 1 mm/day, 20 days of distraction and 20 days of consolidation.

To analyze the capacity of this model to simulate bone regeneration under different distraction rates, values of 0.3 and 2 mm/day were applied. These rates are commonly used in the experiments found in the literature (Ilizarov, 1989*a*,*b*, 1990; Aronson, 1993; Choi *et al.*, 1997; Farhadieh *et al.*, 2000; al Ruhaimi, 2001; King *et al.*, 2003). The distraction length was kept constant (20 mm) and therefore the distraction and consolidation periods were modified accordingly. For the 2 mm/day distraction rate, the distraction protocol consists of 10 days of distraction followed by 10 days of consolidation. And for the 0.3 mm/day distraction rate, the protocol consists of 66 days of distraction followed by 66 additional days of consolidation.

The duration of the consolidation phase is chosen to be the same as the distraction period. It has been verified that fully mature cells have reached a stable phenotype that does not change by modifying the number of days of consolidation. Thus, the final outcome does not much depend on the duration of the consolidation period chosen in this work.

Normal distraction rate (1 mm/day): reaction forces estimation

First we simulated the standard protocol. The value of the computed reaction force has been represented in Figure 3.9, together with the experimental measurements (Brunner *et al.*, 1994). Figure 3.9 shows how, computationally, the reaction forces increase almost linearly. There is an initial steep increase of forces up to 50 N where tissue is being rapidly repaired from the initial damaged state, followed by a mild increase until day 16 where granulation tissue becomes gradually stiffer. Finally, there is another steep increase until the end of the transport, reaching approximately a force value of 230 N due to the appearance of cartilage and its subsequent calcification. Initially, the computational reaction force is within the experimental values, then, it increases at a lower ratio than experimental ones and by day 18 it starts increasing at a higher rate and becomes again within the curves measured by Brunner *et al.* (1994). The change in the slope of the reaction force predicted by the model is mainly due to the differentiation of MSCs to cartilage cells. This occurs mainly about day 15, thus, stiffness changes rapidly from the stiffness of the granulation tissue to the one of cartilage. Despite these differences, it is important to note that the experimental results showed a strong variability due to the interindividual variability and that the numerical ones are mostly within the upper and lower experimental bands.

In this standard protocol, during the entire process of distraction, the tissue distribution varies significantly. As it is directly related to the mechanical stimulus, both will be analyzed simultaneously. Initially, high values of the stimulus are predicted in the osteotomy site. The new tissue in this region is rapidly damaged leading to a gap filled with debris tissue. During the initial stage (1-10 days), the strain values decrease and the damaged tissue is progressively repaired and replaced by granulation tissue (Figure 3.10). This granulation tissue is synthesized by MSCs that migrate from the marrow cavity, periosteum and surrounding soft tissues to the interfragmentary gap. By day 10, the strain decreases further and bone tissue could be distinguished close to the periosteum and marrow. Finally, once the consolidation phase begins, the stimulus reduction is accelerated due to a higher stiffness of the solid matrix and to the loading conditions which only consist on the normal activity of the animal. In this phase, cartilage tissue

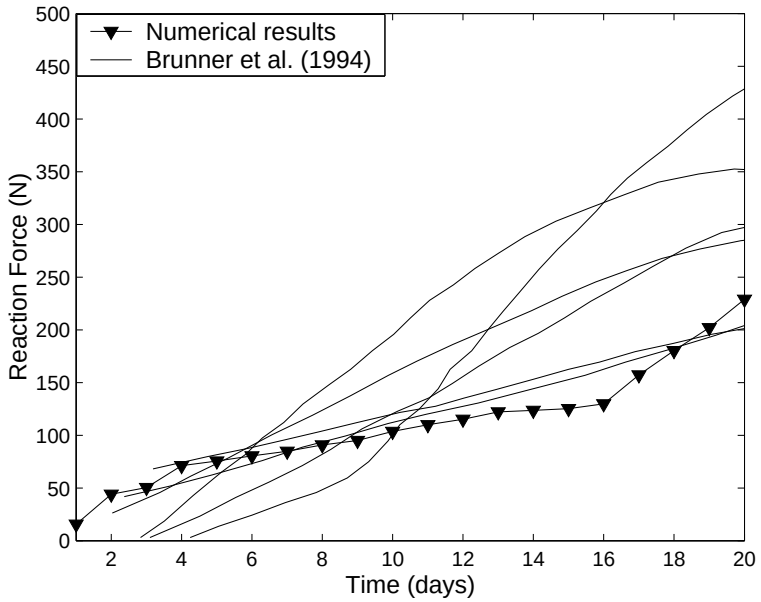

Figure 3.9: Comparison of the reaction forces calculated with the computational model and those measured experimentally (Brunner *et al.*, 1994).

is predicted to differentiate into mature woven bone. Regarding the ossification pattern, first, intramembranous ossification occurs and direct bone tissue appears in the gap. By day 20, endochondral ossification takes place until complete bony bridging.

Influence of different distraction rates

In the second case analyzed, the distraction rate is duplicated while keeping the distraction length constant (2 mm/day). In the case of successful bony bridging, higher rates would be of considerable benefit in clinical practice since they could lead to a reduction in the overall treatment time. However, as can be observed in Figure 3.11, when the distraction procedure is too rapid, the gap is gradually filled with fibrous tissue. This means that a malunion occurs at this level. Only a small amount of bone is formed close to the ends of the cortical bone. Necrotic tissue can be seen the first days of distraction. During the whole process three distinct zones are clearly visible: a necrotic and fibrous central region and a new bone area close to the cortex. It can also be seen that the latter is significantly smaller than in the standard protocol. Thus, increasing the distraction rate over a threshold

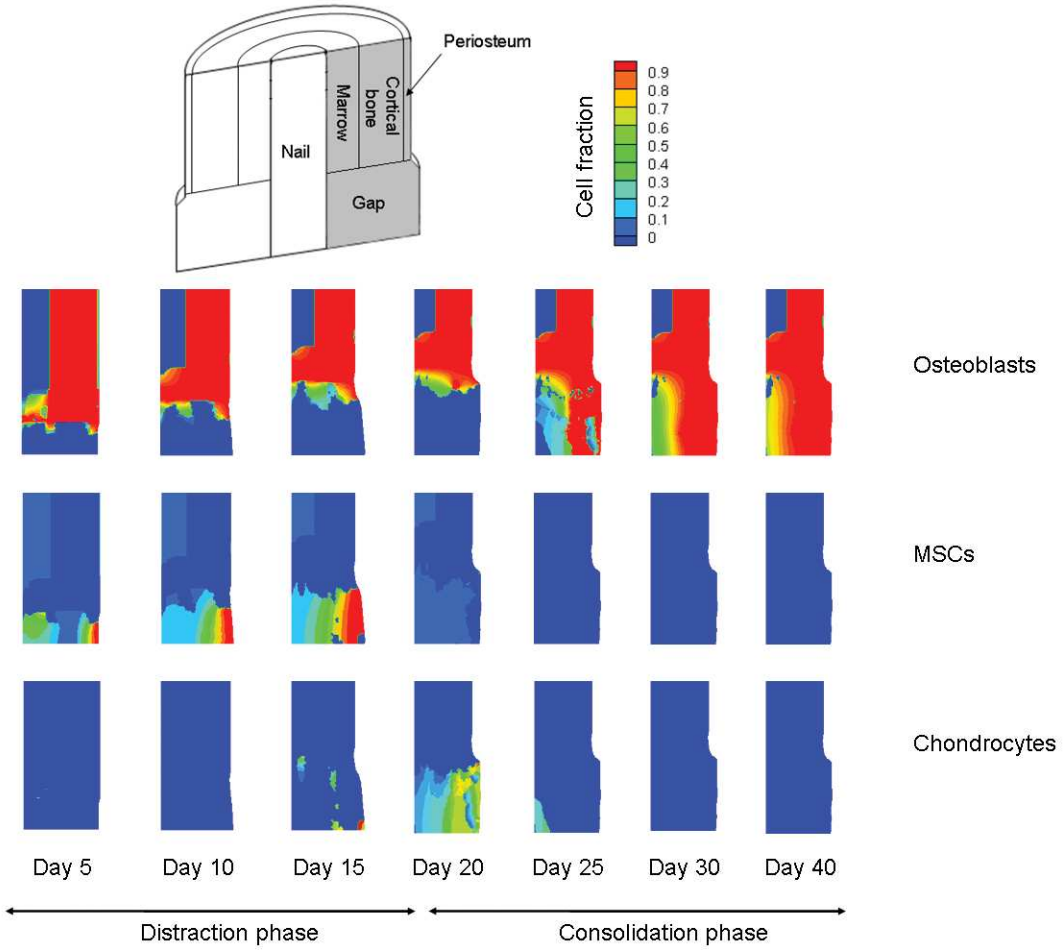

Figure 3.10: Cell distribution prediction at a distraction rate of 1 mm/day.

affects the proliferation and differentiation processes by altering the mechanical stimulus within the distraction gap, especially, in the first days. This induces malunion and the failure of the whole process. In this case, the computational results are also in concordance with the experimental ones.

Finally, a case with reduced distraction rate is analyzed. The results corresponding to a distraction rate of 0.3 mm/day are presented herein. This rate of distraction produces bony union from day 10 and does not allow the process of distraction to finish (Figure 3.12). Tissue structures offer resistance to distraction. Additional distraction may cause rupture of the consolidated bony bridge and produce pain. The volume of bone matrix increases with respect to the stan-

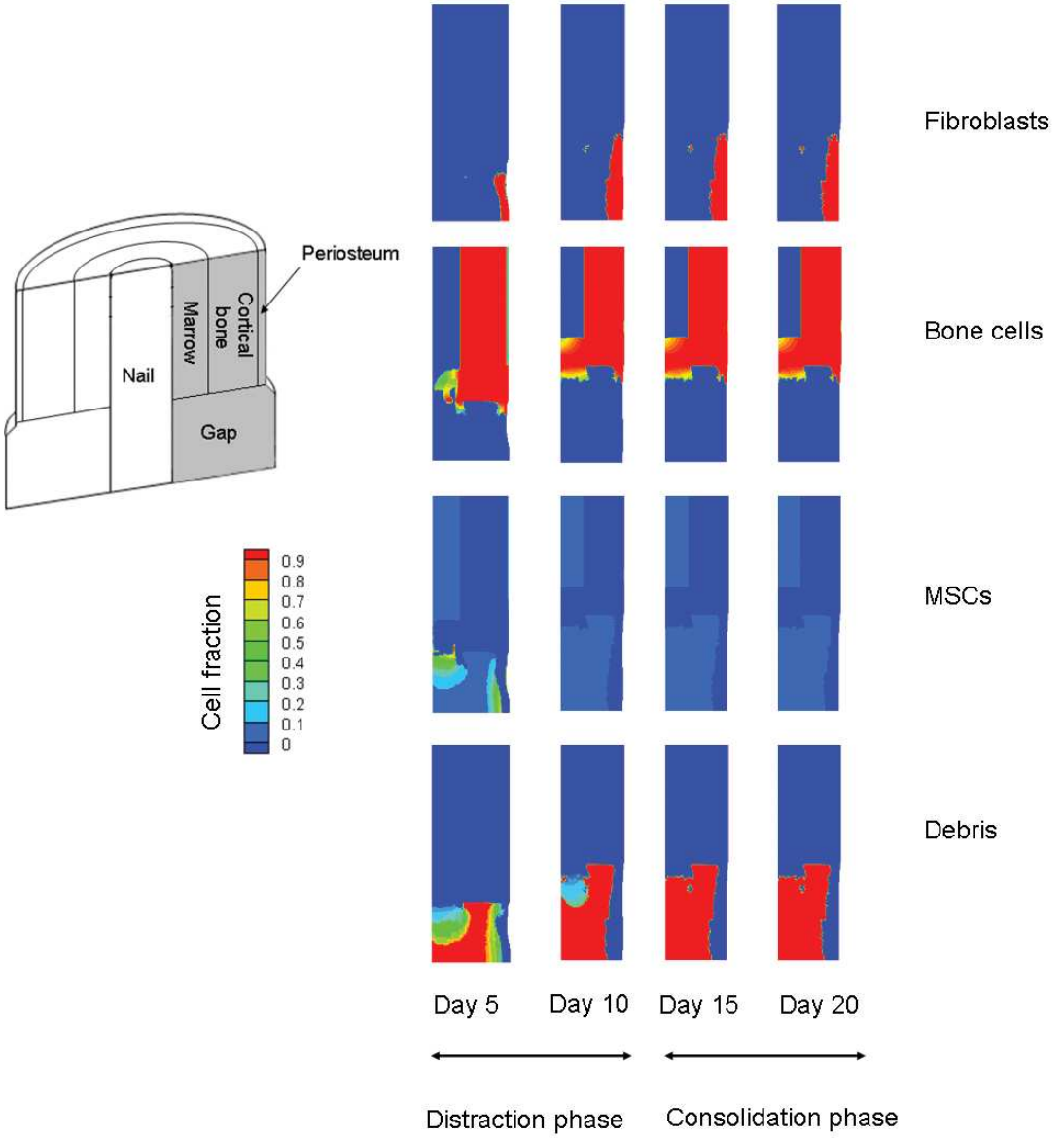

Figure 3.11: Prediction of the cell distribution for a distraction rate of 2 mm/day.

dard protocol and the debris tissue is rapidly repaired (Figure 3.13). Thus, the tissue becomes stiffer and the force needed to distract also increases.

The relative composition of bone cells in the distraction gap through the distraction period is summarized in Figure 3.13 for the three analyzed distraction regimens. Bone tissue composition in the osteotomy site indicates slow, mild

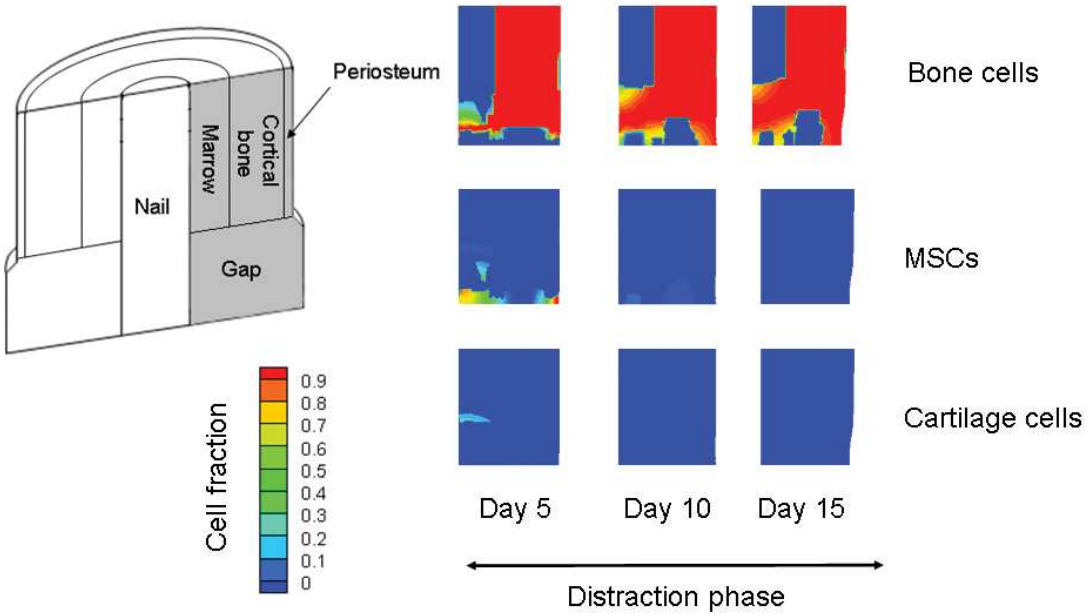

Figure 3.12: Prediction of the cell distribution for a distraction rate of 0.3 mm/day.

and rapid increase of bone content for distraction rates of 2, 1 and 0.3 mm/day respectively (Figure 3.13). A rate of 1 mm/day results in an initial slow rate of bone formation. By day 20, once endochondral ossification begins, its percentage increases rapidly at first until day 25 and then at a slow rate until the end of the consolidation period (90%). A lower rate of distraction (0.3 mm/day) results in a steeper increase from the beginning of the process. In this case, mechanical stimulation enhances bone formation and leads to a stiffer interfragmentary gap. Bone content is about 70% by day 10 and therefore does not allow the process of distraction to finish. In contrast, a 2 mm/day distraction rate slows down the differentiation and proliferation processes. It leads to a softer union and thus lower values of bone content (10%).

Discussion

In this section we have presented a mathematical model implemented in a Finite Element framework to study the spatial and temporal patterns of distraction osteogenesis near the osteotomy site. The main cellular events underlying

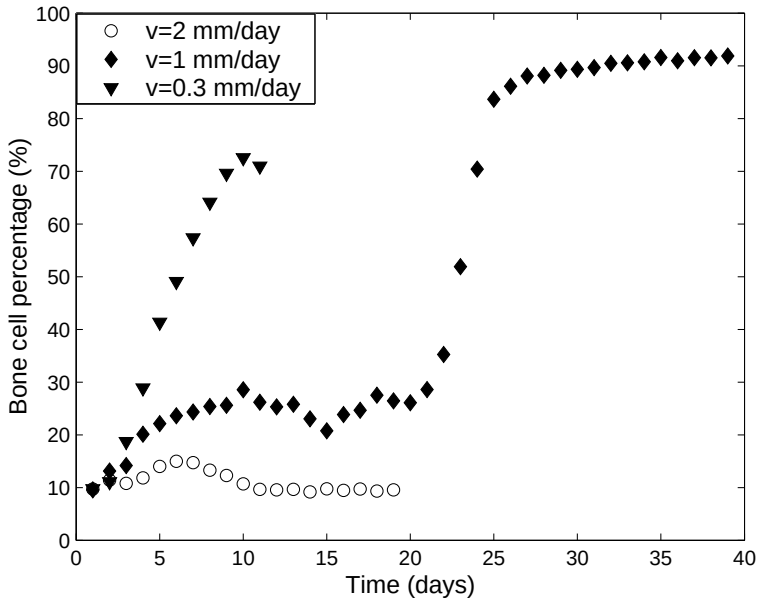

Figure 3.13: Bone volume fraction evolution in the gap throughout the distraction period for the different distraction rates analyzed.

in distraction osteogenesis have been implemented: proliferation, migration and differentiation as well as tissue growth and damage.

A mathematical model formulated earlier for fracture healing is basically used (Gómez-Benito *et al.*, 2005, 2006; García-Aznar *et al.*, 2007). Therefore, we assume that fracture healing and distraction osteogenesis share similar biological processes and strain-related bone tissue reactions. We have used this model and others based on different mechanoregulatory differentiation rules (Prendergast *et al.*, 1997; Claes & Heigele, 1999; Gómez-Benito *et al.*, 2005) to simulate the influence of different distraction rates. They were able to successfully predict the distraction osteogenesis process for distraction rates of 0.3 mm/day and 1 mm/day but not for 2 mm/day one. To improve those models, we have added the effect of the load history on the process of differentiation in the model by taking into account the maturation cell level, thus considering *cell plasticity* (Roder, 2003). We have also checked in different examples of fracture healing that this new extended model is also able to predict this regenerative process (Gómez-Benito *et al.*, 2005, 2006; García-Aznar *et al.*, 2007).

The results of this extended model have been compared with those reported

by Brunner *et al.* (1994) with the same distraction protocol (20 days of distraction followed by 20 days of consolidation), rate of distraction (1 mm/day) and animal model. Under these conditions, the computed evolution of the reaction force (Figure 3.9) shows the stiffening behavior exhibited experimentally. Initially, while the tissue is still soft, reaction forces are small. During the process of distraction, the calculated stimulus decreases, leading to a faster differentiation from granulation tissue to cartilage and bone. When the tissue becomes stiffer, the load transfer to the osteotomized bone increases. Figure 3.9 shows that not only is the trend of the reaction force very similar throughout the whole process but also the resulting quantitative values. The initial steep increase in the reaction force is due to the rapid process of repairing the damaged tissue. The second steep increase (from day 16) is due to cartilage formation, which is much stiffer than the granulation tissue (Figure 3.10).

In order to test the reliability of the implemented model we also compared with experimental results the tissue distribution obtained with different distraction rates. Our results agree with the experimental ones: a moderate distraction rate is needed for successful bony bridging while insufficient or excessive mechanical stimulation is adverse for distraction (Figures 3.14, 3.15 and 3.16).

With a distraction rate of 1 mm/day, numerically, bone tissue is formed in the areas close to the cortical bone and periosteum with an increase in bone density in those zones throughout the entire process. This is consistent with the experimental findings, where bone forms from the host bones to the center of the gap (Kojimoto *et al.*, 1988; Ohyama *et al.*, 1994; Richards *et al.*, 1998) (Figure 3.14). Similar results were presented by Isaksson *et al.* (2007) simulating the same distraction protocol with a different evolutive model.

With a distraction rate of 0.3 mm/day, there is an earlier increase in the average bone density (Figures 3.12, 3.13 and 3.15). Computationally, this lower rate of distraction is accompanied by lower mechanical stimulus which resulted in stimulated osteogenesis.

In contrast, a distraction rate of 2 mm/day produces nonunion (Li *et al.*, 2000). The deviatoric strain increases in the gap during the entire process of distraction osteogenesis, favoring the differentiation of MSCs to fibroblasts (Figure 3.11). Under this mechanical environment, the number of MSCs in the gap is limited

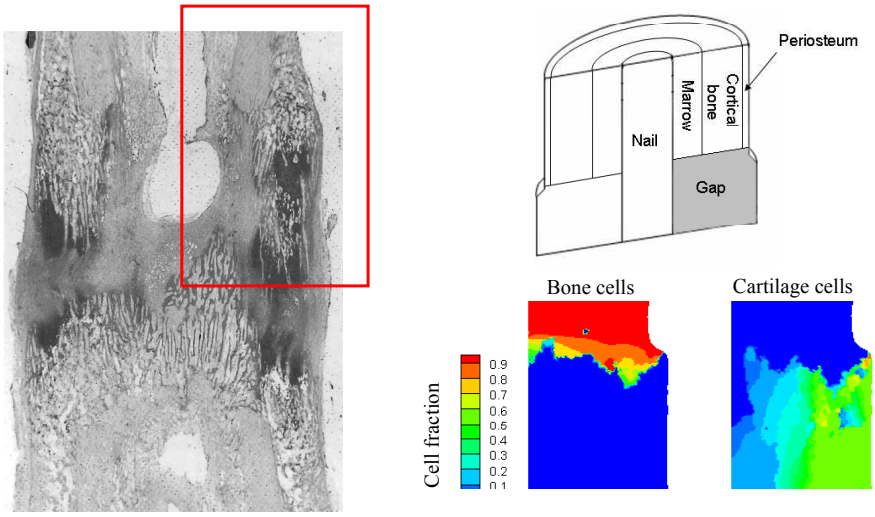

(a) (b)

Figure 3.14: Tissue distribution in a) rabbits at a distraction rate of 0.5 mm/day (Ohyama *et al.*, 1994) and b) numerical results at a distraction rate of 1 mm/day. Cartilage is shown in the central region whereas bone can be seen in the peripheral region.

and, consequently, they cannot contribute to the proliferation and differentiation processes producing a delay in bone tissue production (Figure 3.16). This is in agreement with most clinical results which consider that a rate of distraction of around 1mm/day produces the best effects on tissue regeneration (Ilizarov, 1989*a*; al Ruhaimi, 2001) (Figure 3.14). Nevertheless, higher distraction rates resulted in a predominantly fibrous interfragmentary gap (Choi *et al.*, 2004) (Figure 3.16).

Moreover, a parametric study has been performed in order to assess the sensitivity of the reaction force to the particular curves proposed for the maturation process (Figure 3.2). Those maturation curves have been increased and reduced up to a 20% for each cell type (Figure 3.17a) and the corresponding reaction forces have been computed (Figures 3.17b, 3.17c and 3.17d). Figures 3.17b and 3.17c show that the reaction force is almost unaffected by variations in the maturation curves of bone cells and fibroblasts. Variations in cartilage maturation periods produce reasonable changes that, however, do not alter neither the overall tendency of the reaction force nor the cells distributions (Figure 3.17d). Hence, the conclusions made in this chapter do not depend much on the specific values

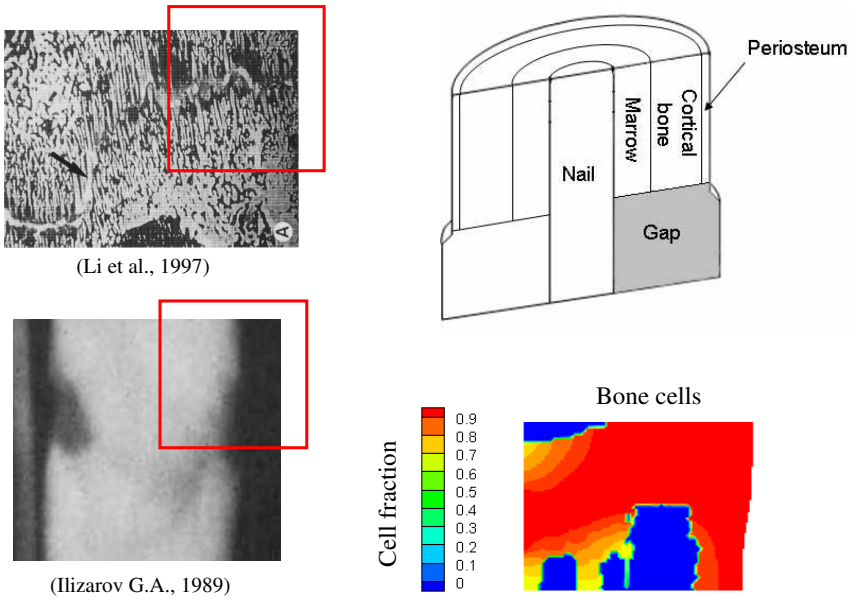

(a) (b)

Figure 3.15: Premature bony union in a) rabbits at a distraction rate of 0.3 mm/day (Li *et al.*, 1997) and dogs at a distraction rate of 0.5 mm/day (Ilizarov, 1989*b*) and b) numerical results at a distraction rate of 0.3 mm/day.

of the maturation curves.

Despite the experimental and computational results being similar, this work presents several limitations and assumptions that, at least, have to be revised in order to know their implications.

First, all the mathematical formulation is developed under the small deformations assumption. Nevertheless, distraction is a large deformation process since interfragmentary movements represent as much as 50% of the size of the gap. In this section, however, we have performed a first evaluation of the effect of some mechanical factors on the tissue distribution.

Second, the axisymmetric finite element model represents an idealized cylindrical bone under axial loading.

The third hypothesis is related to the mechanical stimulus chosen to regulate the process of cell proliferation and differentiation. Several studies have tried to identify the most appropriate stimulus or combination thereof with specific differentiation pathways of mesenchymal tissue (e.g. Pauwels (1960); Perren &

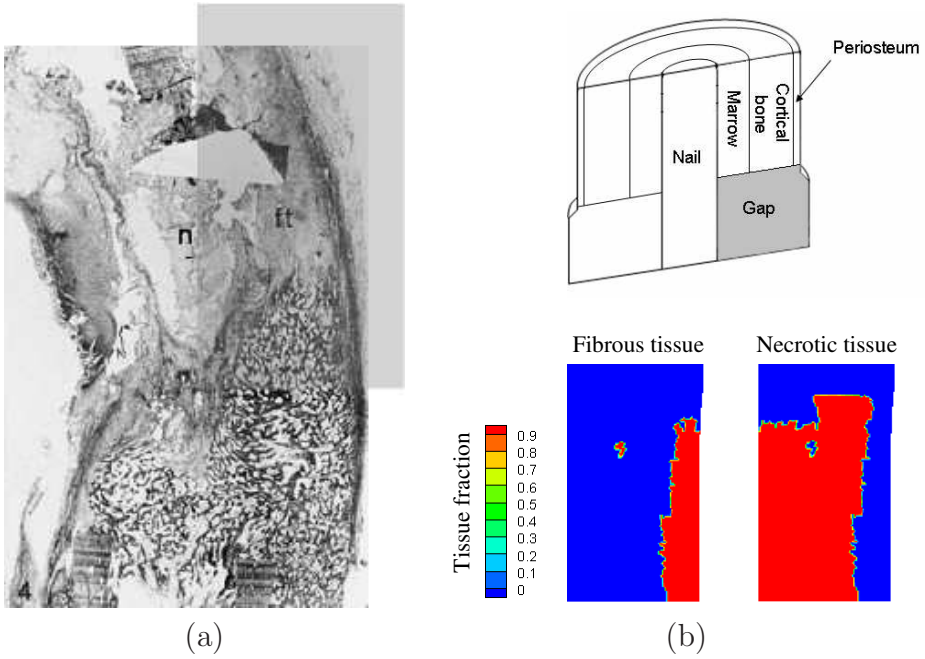

(a) (b)

Figure 3.16: Tissue distribution in a) rabbits at a distraction rate of 2.7 mm/day (Li *et al.*, 2000) and b) numerical results at a distraction rate of 2 mm/day. The central region is filled by fibrous tissue (ft) and some necrotic tissue (n).

Cordey (1980); Carter *et al.* (1998); Claes & Heigele (1999); Lacroix & Prendergast (2002*a*); Bailón-Plaza & van der Meulen (2003)). The second invariant of the deviatoric strain tensor is the simplest among them and provides similar results to experimental findings. For instance, chondrocyte biosynthesis was reported to be stimulated by shear loading in a flow-independent manner, demonstrating the potential for cells to respond to a purely deviatoric stress (Jin *et al.*, 1999). Moreover, Isaksson *et al.* (2006) concluded, in a comparison of different mechanical stimuli to describe normal fracture healing, that the most significant was the deviatoric component of the strain tensor. Most existing models of distraction osteogenesis (Idelsohn *et al.*, 2006; Isaksson *et al.*, 2007; Boccaccio *et al.*, 2007, 2008) are based on the mechanoregulation theory earlier presented by Prendergast *et al.* (1997) in which tissue differentiation is regulated by deviatoric strain in the solid phase and fluid flow in the interstitial fluid phase. Therefore, they are including the deviatoric component as well. Regarding the fluid flow, its contribution in distraction osteogenesis models is negligible. Mean value of fluid flow

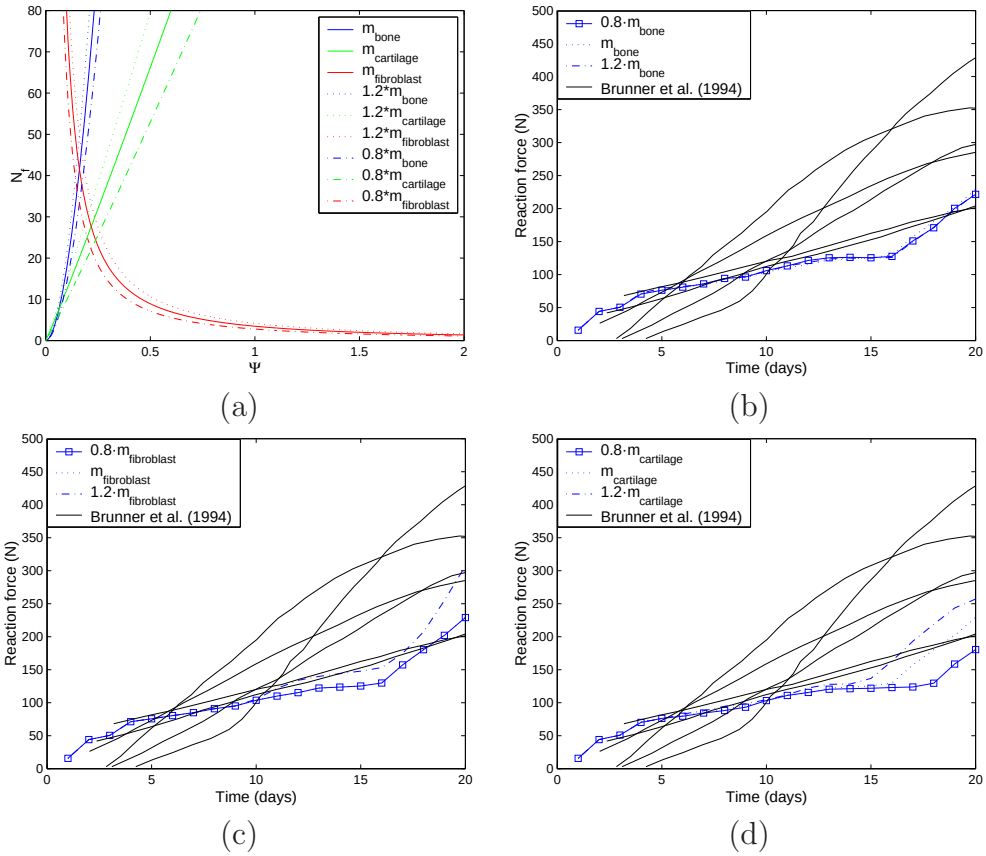

Figure 3.17: Parametric study of the maturation curves.

during distraction osteogenesis is nearly zero, under low rate of the load application, since it decays immediately after applying the imposed load. However, it is still not clear which is the actual stimulus that regulates cell proliferation and differentiation. In this work we considered the mean value of the mechanical stimulus during one day period for cell proliferation and differentiation. Differentiation of precursor cells to a specific cell phenotype can occur within several days (Le *et al.*, 2001) and therefore may not be controlled by a mechanical stimulation that lasts only a fraction of hour. Thus we consider the mean value of the mechanical stimulus to control these processes. This value is calculated with the evolution of the stimulus over the day of distraction (Figure 3.18). On the other hand, the maximum value of the mechanical stimulus is considered for tissue damage. This assumption seems to be logical since damage of material is always produced at the highest mechanical stimulus. Regarding cellular evolution, it

seems that cells sense the mean value during the entire process (Stokes *et al.*, 2006) although other authors consider its maximum value (Gardner & Mishra, 2003).

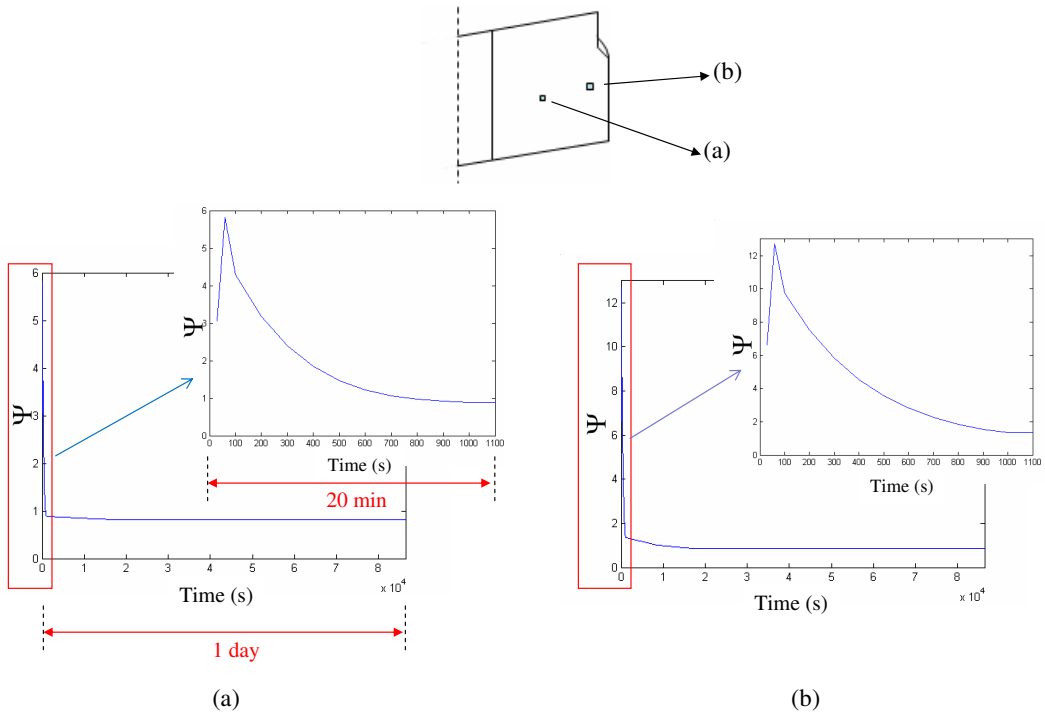

Figure 3.18: Relaxation behaviour of the second invariant of the deviatoric strain tensor over 1 day in two elements (a) and (b) of the distracted gap.

Another assumption made is that contact between nail and marrow is modeled as frictionless since experimentally no bone formation was observed in the nail (Isaksson *et al.*, 2007). There must be, however, some resistant force that opposes the displacement applied for distraction.

A further limitation of the model is related to the applied load. We assume that the external spindle used in the experiment is infinitely rigid since the displacement was directly applied to the cortical bone. Bending or torsion of the bone were neglected.

We also considered a free stress state as initial condition for each day analyzed numerically. We assumed therefore that the daily relaxation period is enough, in the three distraction protocols, for the tissues to grow and adapt to their new

mechanical environment. This hypothesis has been used in other models that simulate bone distraction (Isaksson *et al.*, 2007). Thus, residual stresses have been assumed to be negligible. The strain history has been considered to some extent through the evolution law that controls the maturation state of the cells. This effect will be deeply analyzed in chapter 4.

Finally, the normal daily activity of the sheep was not considered during distraction since its contribution to the overall mechanical stimulus is negligible. This is shown in Figure 3.19 where the stimulus distribution due to the normal daily activity of the animal (Figure 3.19a) and due to the applied distraction displacement (Figure 3.19b) is represented. This has been computed for the first day of distraction with a distraction rate of 1 mm/day. It can be seen that the relative contribution of walking during distraction is minimal (around 300 times smaller) and thus could be neglected in the distraction phase without altering tissue outcome.

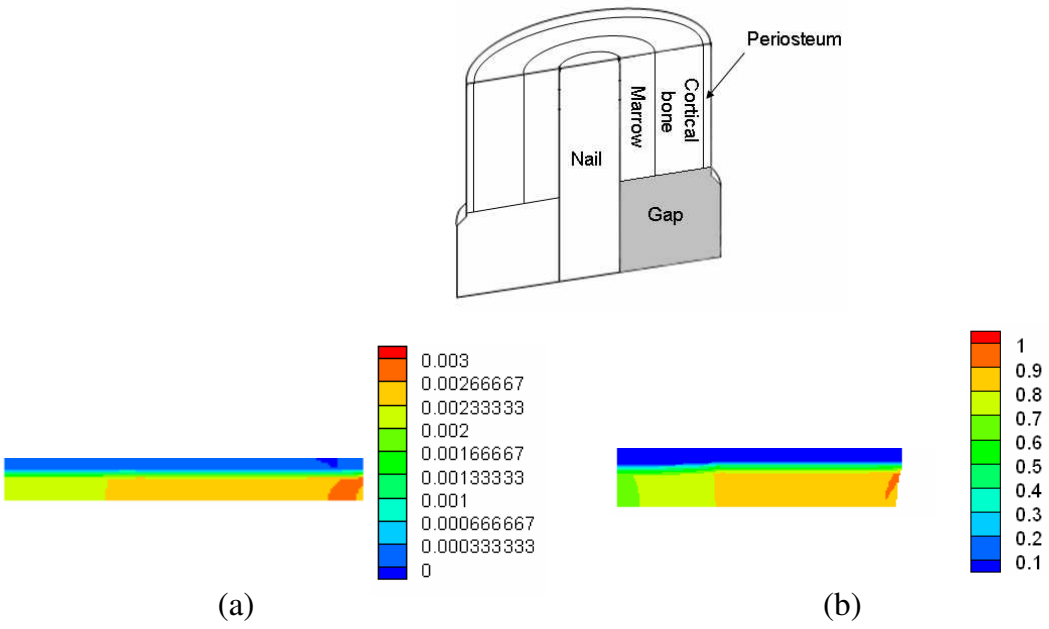

Figure 3.19: Stimulus level on the distracted gap one day after distraction, calculated (a) considering the normal daily activity of the animal and (b) the applied displacement derived from the distraction phase.

Moreover, temporal nature of tissue differentiation is modeled through the

maturation state variable since matrix production, and therefore stiffness of the distracted gap, are dependent on the maturation time of the corresponding cells. Nevertheless, reaction forces calculated with our computational model showed a change of the slope by day 16 approximately that did not match with experimental results (see Figure 3.9). This may be due to some factors in the real model that are not truly simulated. For instance, during the distraction process, the collagen fibers, which are the main component of the granulation tissue extracellular matrix (Bouletreau *et al.*, 2002*a*), are stretched out and consequently loose their normal wavy structure to get a rectilinear appearance oriented parallel to the distraction vector (Figure 2.8b) (Ilizarov, 1989*a*). These fibers provide, temporarily, mechanical resistance to the distracted gap and therefore may contribute to the increasing stiffness observed experimentally. This effect has not been included in our model yet.

As far as we know, this model is the first to examine nonunions computationally in distraction osteogenesis due to the application of different distraction rates. Current differentiation rules (Prendergast *et al.*, 1997; Claes & Heigele, 1999; Gómez-Benito *et al.*, 2005) are not able to predict delays in bony union when the distraction rate is very high (2 mm/day). Another advance over previous simulations is that it takes into account the influence of the strain history on the maturation state of the cells, as other authors have shown in previous works (Schriefer *et al.*, 2005). Further improvements of the model to include other aspects of cell biology as well as the extension of the model to other geometries will greatly enhance our understanding of the regulatory mechanisms involved in the distraction process. Chapter 4 will explore these aspects.

Chapter 4

Growth mixture model of distraction osteogenesis: effect of pre-traction stresses

4.1 Introduction

Until the early 80's, it was believed that biological organs were free of stress when all external loads were removed and hence considered that these tissues were not residually stressed (Gregersen *et al.*, 2000). However, nowadays, residual stresses have been widely investigated in the tissues of a number of organ systems and are thought to be a consequence of nonuniform growth, resorption and remodeling (Skalak, 1981; Skalak *et al.*, 1982; Fung, 1990*a*; Taber & Humphrey, 2001). The presence of residual stresses has been established, for example, in the cardiovascular system (see, e.g., Vaishnav & Vossoughi (1983); Fung (1984, 1985); Chuong & Fung (1986); Vaishnav & Vossoughi (1987); Liu & Fung (1988); Han & Fung (1996)), the gastrointestinal tract (see, e.g., Gregersen *et al.* (2000)) and the musculoskeletal system (see, e.g., Bertram *et al.* (1998); Popowics *et al.* (2002)). It has also been proposed that residual stresses may influence not only the biomechanical behavior of tissues, but also their local cell biology (e.g. Gregersen *et al.* (2000)).

Quantitative estimations of stress accumulation due to residual stresses during

the process of distraction can be found in the literature (Brunner *et al.*, 1994; Waanders *et al.*, 1998; Matsushita *et al.*, 1999; Richards *et al.*, 1999). During the process of distraction osteogenesis, stress accumulation is modulated by three effects: the mechanical elongation of the gap, the intrinsic viscoelastic nature of soft tissues in the interfragmentary gap (Leong *et al.*, 1979; Simpson *et al.*, 1996; Nakamura *et al.*, 1997; Matsushita *et al.*, 1999; Richards *et al.*, 1999; Aarnes *et al.*, 2002) and the tissue growth/differentiation inside the gap.

The notion of locally differential growth giving rise to residual stresses was suggested early by Skalak (1981) and then later by Chuong & Fung (1986) as an important feature of soft tissue growth. Since then, numerous studies have developed continuum growth models for single constituents (see, e.g., Huang (1994); Taber (1998); Chen & Hoger (2000); Epstein & Maugin (2000); Klisch *et al.* (2001); DiCarlo & Quiligotti (2002); Lubarda & Hoger (2002); Kuhl & P. (2003); Volokh (2004); Lappa (2005); Menzel (2005); Alastrué *et al.* (2007)) or mixtures (see, e.g., Preziosi & Farina (2002); Humphrey & Rajagopal (2003); Breward *et al.* (2003); Klisch *et al.* (2003); Garikipati *et al.* (2004)). In these models, growth has been defined either relative to a stress-free configuration (see, e.g., Rodriguez *et al.* (1994); Taber & Eggers (1996); Taber (1998); Garikipati *et al.* (2004); Ramasubramanian & Taber (2008)) or to a stressed configuration (for example, Klisch *et al.* (2001, 2003)). However, the inclusion of the effect of residual stresses in models of limb lengthening has not been considered yet. Existing mechanobiological models have used a zero pre-traction stress configuration as the daily reference state, assuming therefore no stress accumulation after each load step (Isaksson *et al.*, 2007; Boccaccio *et al.*, 2007, 2008).

Thus, the aim of this chapter is to develop a general macroscopic growth mixture formulation able to consider pre-traction stresses (stress level in the gap tissue before each distraction step) in bone distraction osteogenesis. First, we establish the typical governing equations (kinematics, constitutive relations and mass balance), then we particularize the model to the process of bone distraction osteogenesis and afterwards we apply the model to a clinical example in order to investigate the influence of pre-traction stresses and tissue growth on the outcome of limb lengthening. Finally, to analyze the potential of the new model proposed, we compare the pattern of limb lengthening in different animal species and a

human case.

4.2 Description of the model

In this model, we consider N types of tissues and M types of cells (Doblaré & García-Aznar, 2006). Moreover, each tissue is characterized by its apparent density (ρ^i) and, similarly, each type of cell is characterized by its concentration (c^i). The apparent density of tissue i can also be expressed as $\rho^i = \bar{\rho}^i \upsilon_m^i (1 - h^i)$ being $\bar{\rho}^i$ the real density of tissue i, υ_m^i its volume fraction and h^i the volume fraction of microcracks per unit volume of tissue i.

The macroscopic continuum formulation proposed is based on the incremental approach presented by Klisch *et al.* (2001). In our approach, each increment represents the daily loading from configuration Ω_k at time t_k to configuration Ω_{k+1} at time t_{k+1}, the end of the increment (Figure 4.1). In this model, the time-varying reference configuration represents the state prior to the growing process, after immediate application of the distraction displacement at time t_{k-1}, with an associated stress field ($\boldsymbol{\sigma}_{k-1}^{\text{post}}$).

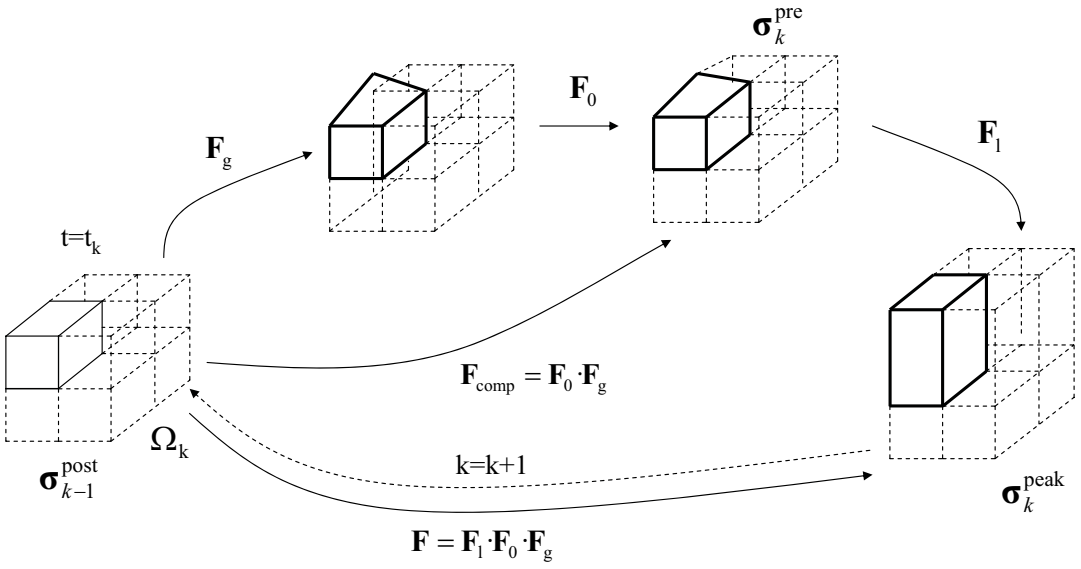

Figure 4.1: Scheme of the four configurations of interest during the daily incremental process in distraction osteogenesis for each point of the solid matrix (Skalak, 1981; Rodriguez *et al.*, 1994; Garikipati *et al.*, 2004).

The multiplicative decomposition of the deformation gradient tensor, advocated for growth theories by Rodriguez *et al.* (1994) and further elaborated in different works (see, e.g. Taber & Eggers (1996); Hoger (1997); Chen & Hoger (2000); Taber & Perucchio (2000); Klisch *et al.* (2001); DiCarlo & Quiligotti (2002); Quiligotti (2002); Klisch *et al.* (2003); Himpel *et al.* (2005)) is here used (Figure 4.1). On the basis of previous studies (Garikipati *et al.*, 2004; Davol *et al.*, 2008) and according to this hypothesis, the total deformation gradient is assumed to be composed of the elastic deformation associated to the external loads and that related to tissue growth or differentiation. From t_k to t_{k+1}, the incremental tensor associated to growth ($\mathbf{F}_\mathrm{g}$) accounts for the change in size and shape due to volumetric growth and for the new tissue produced or differentiated during the incremental growth process (Rodriguez *et al.*, 1994; Taber & Eggers, 1996; Taber, 1998; Garikipati *et al.*, 2004; Ramasubramanian & Taber, 2008). The tensor $\mathbf{F}_\mathrm{g}$ is, in general, incompatible, while the total gradient $\mathbf{F}$ has to be compatible. Therefore, an auxiliary tensor ($\mathbf{F}_0$) is needed to reach a compatible configuration ($\mathbf{F}_\mathrm{comp}$). Finally, the elastic strain associated to the loading process is additionally stored during the last configuration ($\mathbf{F}_\mathrm{l}$). Thus, the total deformation is described by the deformation gradients $\mathbf{F}_\mathrm{g}$, $\mathbf{F}_0$ and $\mathbf{F}_\mathrm{l}$ (see Figure 4.1), and the total composition of these tensors:

$$\mathbf{F} = \mathbf{F}_\mathrm{l} \cdot \mathbf{F}_0 \cdot \mathbf{F}_\mathrm{g}. \tag{4.1}$$

In order to compute the stress tensor, we assume tissues to be modeled as a mixture of a porous solid phase (s) and a mobile interstitial fluid (f). The solid phase corresponds to a mixture of the different tissues existing in the representative volume element under consideration. Employing the rule of mixtures, the total Cauchy stress $\boldsymbol{\sigma}$ results from the contribution of the hydrostatic pressure due to the fluid and a contribution of the solid constituents (as a first approach, isotropic behavior is assumed for the whole mixture). Then, the constitutive relation for the stress is formulated according to Humphrey & Rajagopal (2003), as a function of the response of the different tissues and their time-varying mass production. Mathematically, we have for all time t:

$$\boldsymbol{\sigma} = \boldsymbol{\sigma}_{\text{fl}} + \boldsymbol{\sigma}_{\text{eff}}, \tag{4.2}$$

$$\boldsymbol{\sigma}_{\text{fl}} = -p\mathbf{1}, \tag{4.3}$$

$$\boldsymbol{\sigma}_{\text{eff}} = \sum_{i=1}^{N} \upsilon^i_{m_0} \boldsymbol{\sigma}^i_k + \sum_{i=1}^{N} \frac{1}{\rho^i} \frac{1}{\det \mathbf{F}_k} \int_0^{t_k} \pi^i(\tau) \boldsymbol{\sigma}^i(\mathbf{F}_k, \tau) \det \mathbf{F}_k d\tau, \tag{4.4}$$

where $\boldsymbol{\sigma}_{\text{eff}}$ is the Cauchy stress tensor corresponding to the solid phase, $\boldsymbol{\sigma}_{\text{fl}}$ is the Cauchy stress tensor corresponding to the fluid phase, p represents the hydrostatic pressure field of the fluid, $\mathbf{1}$ the identity second order tensor, N is the number of tissues, $\upsilon^i_{m_0}$ is the initial volume fraction of tissue i, $\boldsymbol{\sigma}^i_k$ is the stress for each tissue i at time t_k, $\boldsymbol{\sigma}^i$ is the stress response for tissue i evaluated at time t_k with respect to the time $\tau \in [0,\ \mathrm{t}_k]$ in which the tissue was created, ρ^i its apparent mass density, π^i is the new matrix produced of tissue i per unit volume and time at time τ; τ is a dummy variable of integration over time and $\mathbf{F}_k$ is the total deformation gradient tensor calculated with respect to the reference state at time t_k.

The standard mass balance is posed for each tissue type i (Doblaré & García-Aznar, 2006). A sufficient amount of constituents (i.e. collagen) is considered to be available for tissue synthesis locally and their transport is neglected. Tissue components and tissues themselves are considered to be non-diffusive. Mass balance reads,

$$\begin{aligned} \frac{d\rho^i}{dt} + \rho^i \boldsymbol{\nabla} \cdot \mathbf{v} = \frac{d\bar{\rho}^i}{dt} \upsilon^i_m (1 - h^i) + \\ + \bar{\rho}^i \frac{d\upsilon^i_m}{dt}(1 - h^i) + \bar{\rho}^i \upsilon^i_m (-\frac{d(h^i)}{dt}) + \\ + \rho^i \boldsymbol{\nabla} \cdot \mathbf{v} = \pi^i \qquad i = 1, \ldots, N, \end{aligned} \tag{4.5}$$

where $\mathbf{v}$ is the macroscopic velocity vector of the solid skeleton, $\bar{\rho}^i$ is the real density of tissue i, υ^i_m is the volume fraction of tissue i, ρ^i its apparent mass density and π^i is the new volume produced of tissue i per unit volume and time. Moreover, we consider, as a first approach, that the total tissue production (π^i) is

the sum of the production of individual cells. Since we also consider that cells can remove other tissues, the net matrix production of tissue i per unit time can be written as the difference between its production and removal rates, both of which are positive by definition because of the continuous turnover *in vivo* (Doblaré & García-Aznar, 2006):

$$\pi^i = (c^i \beta^i_{\text{pr}} - \sum_{j=1, j\neq i}^{N} c^j \beta^i_j)\bar{\rho}^i, \tag{4.6}$$

where β^i_{pr} is the volumetric production rate of tissue i by the cell type i, β^i_j is the volume rate of tissue i removed by cells type j per unit time. Note that tissue production is indirectly controlled by the mechanical stimulus, since cellular differentiation and proliferation processes are regulated by this mechanical stimulus.

In a similar way, the cell balance (evolution of the number of cells per unit volume) for each cell type may be written as:

$$\frac{dc^i}{dt} + c^i \boldsymbol{\nabla} \cdot \mathbf{v} = \pi^i_c - \nabla \cdot \mathbf{m}^i_c \qquad i = 1, ..., M \tag{4.7}$$

being $\mathbf{v}$ the macroscopic velocity vector of the solid skeleton, c^i the concentration of the cell type i, $\mathbf{m}^i_c$ the mass flux of cell type i with respect to the solid, and π^i_c the net production of such cell type, which can have different origins: proliferation or differentiation. Differentiation can be either from different cells to this cell phenotype or from this type of cell to other types (including dead cells as a specific cell type and consequently considering the possibility of necrosis and apoptosis). Therefore, the net production of cells per unit time can be written as (Doblaré & García-Aznar, 2006):

$$\pi^i_c = c^i \alpha^i_{\text{pr}} + \sum_{k=1, k\neq i}^{M} c^k \alpha^i_k - \sum_{k=1, k\neq i}^{M} c^i \alpha^k_i \tag{4.8}$$

where M is the number of cell types, α^i_{pr} is the production of cells type i due to mitosis per unit time and cell and α^i_k is the production of cells type i from the differentiation of cells type k per unit time and cell.

4.2.1 Kinematics of growth

As in chapter 3, the mathematical formulation has been developed under the small deformations assumption at each time step. If the deformation gradient tensor is written in terms of the displacement gradient tensor $\mathbf{L}$ as $\mathbf{F}=\mathbf{1}+\mathbf{L}$, then equation (4.1) can be expanded to:

$$\mathbf{F} = (\mathbf{1} + \mathbf{L}_l)(\mathbf{1} + \mathbf{L}_0)(\mathbf{1} \ + \mathbf{L}_g) \tag{4.9}$$

$$\mathbf{F} = \mathbf{1} + \mathbf{L}_l + \mathbf{L}_0 + \ \mathbf{L}_g + \mathbf{L}_l\mathbf{L}_0 + \mathbf{L}_l\mathbf{L}_g + \mathbf{L}_0\mathbf{L}_g + \mathbf{L}_l\mathbf{L}_0\mathbf{L}_g \tag{4.10}$$

where the displacement gradient tensor $\mathbf{L} = \boldsymbol{\varepsilon} + \boldsymbol{\omega}$ is the sum of the linearized deformation and rotation tensors (0 means compatible, g growth and l elastic, see Figure 4.1). Under the small deformation assumption, equation (4.10) can be simplified as:

$$\mathbf{F} \simeq \mathbf{1} + \mathbf{L}_l + \mathbf{L}_0 + \mathbf{L}_g \tag{4.11}$$

Linearization of the multiplicative decomposition of the deformation gradient tensor (equation 4.11) leads to:

$$\boldsymbol{\varepsilon} = \frac{1}{2}\{(\mathbf{F} - \mathbf{1}) + (\mathbf{F} - \mathbf{1})^T\} = \boldsymbol{\varepsilon_l} + \boldsymbol{\varepsilon_0} + \boldsymbol{\varepsilon_g} \tag{4.12}$$

where $\mathbf{F}$ is the deformation gradient tensor (equation 4.11), $\mathbf{1}$ the second order identity tensor, T is the transpose operator and $\boldsymbol{\varepsilon}_l$, $\boldsymbol{\varepsilon}_0$, $\boldsymbol{\varepsilon}_g$ are the elastic, compatible and growth infinitesimal strain tensors respectively.

4.3 Constitutive equation

The model here proposed has been incorporated to the mechanobiological model described in section 3.2, considering the simplifications given by the kinematics of growth of section 4.2.1. Therefore the same state variables as in section 3.2 (concentration of the cell phenotypes, concentration of the skeletal tissues and the cellular maturation levels) as well as the same continuity equation of the skeletal tissues (equation (3.2)) are incorporated in this model. Further, in this model, it is assumed that the real density of the different tissues ($\bar{\rho}^i$) does not change over time:

$$\frac{\partial \bar{\rho}^i}{\partial t} = 0, \qquad i= g,\ f,\ c,\ b,\ d \quad \text{tissues}, \tag{4.13}$$

Following the previous description and considering these simplifications, the constitutive relation (4.2) for the stress can now be written as:

$$\boldsymbol{\sigma} = -p\mathbf{1} + \sum_{i=1}^{N} \upsilon^i_{m_0} \boldsymbol{\sigma}^i_k + \sum_{i=1}^{N} \frac{1}{\rho^i} \int_0^{t_k} \pi^i(\tau) \boldsymbol{\sigma}^i d\tau, \tag{4.14}$$

where $\boldsymbol{\sigma}^i = \boldsymbol{\sigma}^i(\boldsymbol{\varepsilon} - \boldsymbol{\varepsilon}_{\pi^i})$ is the stress response of tissue i evaluated at time t_k with respect to the time $\tau \in [0, t_k]$ in which the tissue was deposited with $\boldsymbol{\varepsilon}$, the total linearized strain tensor at time t_k, and $\boldsymbol{\varepsilon}_{\pi^i}$ is the strain level when the new matrix (π^i) was deposited at time τ ($\upsilon^i_{m_0}$, $\boldsymbol{\sigma}^i_k$ as in equation (4.4)).

According to (4.14) the stress response depends on the deformation experienced by each tissue type during the loading configuration evaluated at time t_k, on the strains generated during the growth process and on the new tissue produced at time τ.

The mass balance equation is now simplified as:

$$\frac{d\rho^i}{dt} + \rho^i \boldsymbol{\nabla} \cdot \mathbf{v} = \bar{\rho}^i \frac{dv_m^i}{dt}(1 - h^i) + \bar{\rho}^i v_m^i (-\frac{d(h^i)}{dt}) + \rho^i \boldsymbol{\nabla} \cdot \mathbf{v} = \pi^i$$

$$i = g,\ d \quad \text{tissues} \quad (4.15)$$

and

$$\frac{d\rho^i}{dt} + \rho^i \boldsymbol{\nabla} \cdot \mathbf{v} = \bar{\rho}^i \frac{dv_m^i}{dt} + \rho^i \boldsymbol{\nabla} \cdot \mathbf{v} = \pi^i \qquad i = c,\ b,\ f \quad \text{tissues} \qquad (4.16)$$

where h^i is evaluated with equations (3.31) and (3.32) and π^i with equation (4.6).

4.4 Numerical implementation

The formulation presented above has been solved in an updated Lagrangian finite element code. These equations are implemented at each load step k of the distraction process under the small deformation assumption considering boundary, initial and loading conditions. Next, we present the steps that have been numerically implemented in one increment (k to $k+1$) of the process equivalent to one day of distraction (see Figure 4.1):

1. Initialization: initially no growth is assumed and we impose the first distraction displacement in a poroelastic analysis to evaluate initial strains ($\boldsymbol{\varepsilon}(t_0)$) and post-traction stresses ($\boldsymbol{\sigma}_0$).

2. A remeshing process is employed to avoid the excessive distortion of the finite element mesh during the distraction process.

3. Growth analysis: once determined the strains ($\boldsymbol{\varepsilon}(t_k)$) and the corresponding stresses ($\boldsymbol{\sigma}_{k-1}^{\text{post}}$) for this step ($k$ to $k+1$) that includes poroelastic relaxation, new tissue is created and a compatibility analysis is performed to evaluate the new stress level ($\boldsymbol{\sigma}_k^{\text{pre}}$) that occurs as a consequence of tissue growth, differentiation and adaptation. In fact, given the mechanical stimulus computed from the poroelastic analysis, the matrix production rate $\pi^i(t_k)$ is

updated through (4.6). Both strain level ($\boldsymbol{\varepsilon}^i(t_k) = \boldsymbol{\varepsilon}(t_n)$) for the new tissue i formed and the matrix production ($\pi^i(t_k)$) are stored as state variables for each tissue i.

4. Update of the geometry: the new geometry is updated as well as the state variables at each nodal point according to the differentiation, proliferation and matrix production rules.

5. Two diffusion analyses are then performed in Abaqus (Hibbit & Sorensen, 2002): one to simulate MSCs migration and other to model vascularization ($\nabla \mathbf{m}_c^i$ in (4.7)) (Gómez-Benito *et al.*, 2005).

6. A new poroelastic analysis is implemented to determine the mean and maximum value of the mechanical stimulus at each nodal point. Equation (4.14) is solved with a user element subroutine in Abaqus (Hibbit & Sorensen, 2002) under the small deformations assumption.

   Assuming a linear elastic behavior of the solid matrix, the stresses can be computed as:

$$\boldsymbol{\sigma}(t_k) = -p\mathbf{1} + \sum_{i=1}^{N} \upsilon_{m_0}^i \boldsymbol{\sigma}_k^i + \sum_{i=1}^{N} \frac{1}{\rho^i} \sum_{n=1}^{n=k-1} \pi_n^i \mathbb{C}^i : [\boldsymbol{\varepsilon}(t_k) - \boldsymbol{\varepsilon}^i(t_n)]\Delta t_n \quad (4.17)$$

   where p represents the hydrostatic pressure field of the fluid, N is the number of tissues, $\upsilon_{m_0}^i$ is the initial volume fraction of tissue i, $\boldsymbol{\sigma}_k^i$ is the stress for each tissue i at time t_k, $\mathbb{C}^i$ is the elasticity tensor associated to tissue i, $\boldsymbol{\varepsilon}$ is the total strain tensor, n is the number of time increments from $t = 0$ to t_k, and π_n^i is the new tissue produced per unit time during the time increment n (if negative it means resorption).

   Note that in (4.17), when $k = n$ and $\pi_{k=n}^i \neq 0$, $\boldsymbol{\varepsilon}^i(t_n) = \boldsymbol{\varepsilon}(t_k)$ and, therefore, a null stress is associated to such tissue fraction. This is in agreement with the assumption that new tissue is deposited in an incremental unstressed state. Thus, only previously existing tissue will contribute to support stresses.

7. Go to step (2).

4.5 Examples of application

4.5.1 Validation of the model

Example of application

The same example of application as in section 3.6.1 is presented in order to compare the numerical results. Brunner *et al.* (1994) evaluated the bone segment transport over an intramedullary nail in 12 sheep. A diaphyseal defect created in the central region of the tibia was reduced through the ossification process induced in the upper part by distraction osteogenesis. The defect was stabilized with a nail. They measured the tensile force during limb lengthening, showing a daily incomplete relaxation of tissues within the distracted gap. In this experimental study, lengthening was started just after the osteotomy at a rate of 1 mm per day. The distraction protocol followed by Brunner *et al.* (1994) consisted of 20 days of distraction, immediately after the osteotomy, followed by 20 days of consolidation.

Considering an idealized cylindrical tibia, we represent its anatomy by an axisymmetric finite element model, and, therefore, only one-quarter of the actual geometry is modelled. The dimensions are shown in Figure 3.7a. The parameters required to model the diaphysis of the tibia are the diameter of the diaphysis, thickness of the periosteum and bone marrow, radius of the nail and size of the osteotomy gap. The initial size of the gap was 1 mm. The cortical bone was modeled with an inner radius of 6 mm and an outer radius of 10 mm, the thickness of the periosteum was set to 0.5 mm and the radius of the nail was 3.5 mm (Figure 3.7a) (Brunner *et al.*, 1994).

Boundary conditions of the axisymmetrical model consisted on rotational symmetry along the long bone axis and mirror-image symmetry with respect to the plane of the osteotomy (Figure 3.7b). Null fluid flow was prescribed at the periosteum, assuming therefore this boundary to be impermeable (Li *et al.*, 1987) (Figure 3.7b). Initial conditions consisted on a gap initially filled with debris tissue and on maximal tissue damage in that region to simulate the lack of the latency phase. The loading conditions during the distraction phase consisted of a

distracted displacement applied on the top of the cortical bone during one minute and maintained the rest of the day. The applied displacement was half the total value due to the symmetry conditions of the model. During the consolidation phase only the load derived from the normal activity of the animal was considered (500 N of compressive load (Claes & Heigele, 1999)). All tissues were assumed to be linear and biphasic with properties taken from literature (Table 4.1).

Table 4.1: Material properties of the tissue modelled in this study.

	E (MPa)	υ	κ (m^4/Ns)
Nail	$210{\cdot}10^3$	0.3	-
Bone Tissue	1000	0.29	$7{\cdot}10^{-14}$ [f,g]
Cartilage	5[a,b,c]	0.10	$2.13{\cdot}10^{-14}$ [i]
Calcified cartilage	57	0.11	$3.5{\cdot}10^{-15}$ [f,g,h]
Fibrous tissue	2[d]	0.13	$2.15{\cdot}10^{-14}$ [i]
Granulation tissue	1[e]	0.05	$1.5{\cdot}10^{-14}$ [i]
Debris tissue	0.05	0.05	$1.645{\cdot}10^{-14}$ [i]

a Charlebois *et al.* (2004); b Huang *et al.* (2001); c Akizuki *et al.* (1986); d Hori & Lewis (1982); e Leong & Morgan (2008); f Nafei *et al.* (2000); g Ochoa & Hillberry (1992); h Armstrong & Mow (1982); i Levick (1987)

The set of material properties included in this chapter is different in comparison with previous ones (Gómez-Benito *et al.*, 2005; García-Aznar *et al.*, 2007). In chapter 3, as we did not consider the effect of pre-traction stresses, we used mechanical properties very high to adjust the post-traction and relaxation results and to indirectly take into account the effect of these pre-traction stresses. Thus, for the Young's modulus of the cartilage, the literature displays a high variation, but generally values around 5 MPa are referenced for immature cartilage (Akizuki *et al.*, 1986; Huang *et al.*, 2001; Charlebois *et al.*, 2004). Regarding the granulation tissue, it is an extremely soft and fluid based tissue. Values around 1-2 MPa may be found in the literature (Isaksson *et al.*, 2007; Leong & Morgan, 2008). Also, the material properties are not determined through a mixture rule in this work, but instead they have a fixed value for each tissue type.

Results

In this section we present the pre-traction forces ($P_1 = F(\boldsymbol{\sigma}^{\text{pre}})$), post-traction forces ($P_2 = F(\boldsymbol{\sigma}^{\text{post}})$) and the peak forces ($P_3 = F(\boldsymbol{\sigma}^{\text{peak}})$). The former represents the force between the bone and the fixator before the daily traction displacements (Brunner *et al.*, 1994) (see Figure 4.2). Therefore, this force represents the resultant of the pre-traction stress field ($\boldsymbol{\sigma}^{\text{pre}}$) for each time increment (Figure 4.1). The post-traction force is the resultant force 20 minutes after the application of a new tensile displacement so this force takes into account the relaxation effect due to the poroelastic behaviour of the distracted gap tissues. Finally, the peak force is the resultant force right after the application of a tensile displacement.

Figures 4.3a, 4.3b and 4.3c represent the computed reaction force along the distraction steps before (P_1), immediately after (P_3) and 20 minutes after (P_2) the loading process and its comparison with experimental results (Brunner *et al.*, 1994). Post distraction and peak forces increase gradually until the end of the process up to a value of over 380 and 400 N, respectively, with a tendency that is in agreement with the experimental findings during the whole distraction phase (Figure 4.3b). Pre-traction forces also increase gradually through the distraction phase up to a value of 330 N (Figure 4.3a).

An interesting aspect is the analysis of both pre and post-traction forces simultaneously. As can be seen from Figure 4.4a the force increases each day and then slowly falls until it reaches a value slightly greater than the final force on the previous days. Three increments are shown in Figure 4.4b (increments 7, 8 and 9). It can be observed that there is a daily relaxation due to the poroelastic analysis and a change in stresses due to matrix growth, differentiation and adaptation.

Discussion

In this chapter, we have presented a mechanobiological model which incorporates the effect of pre-traction stresses and tissue growth (differentiation and adaptation is also considered) in the process of distraction osteogenesis. The model has been particularized to a case of long bone lengthening to assess its applicability. Despite being widely investigated in clinical and animal studies (Brunner *et al.*,

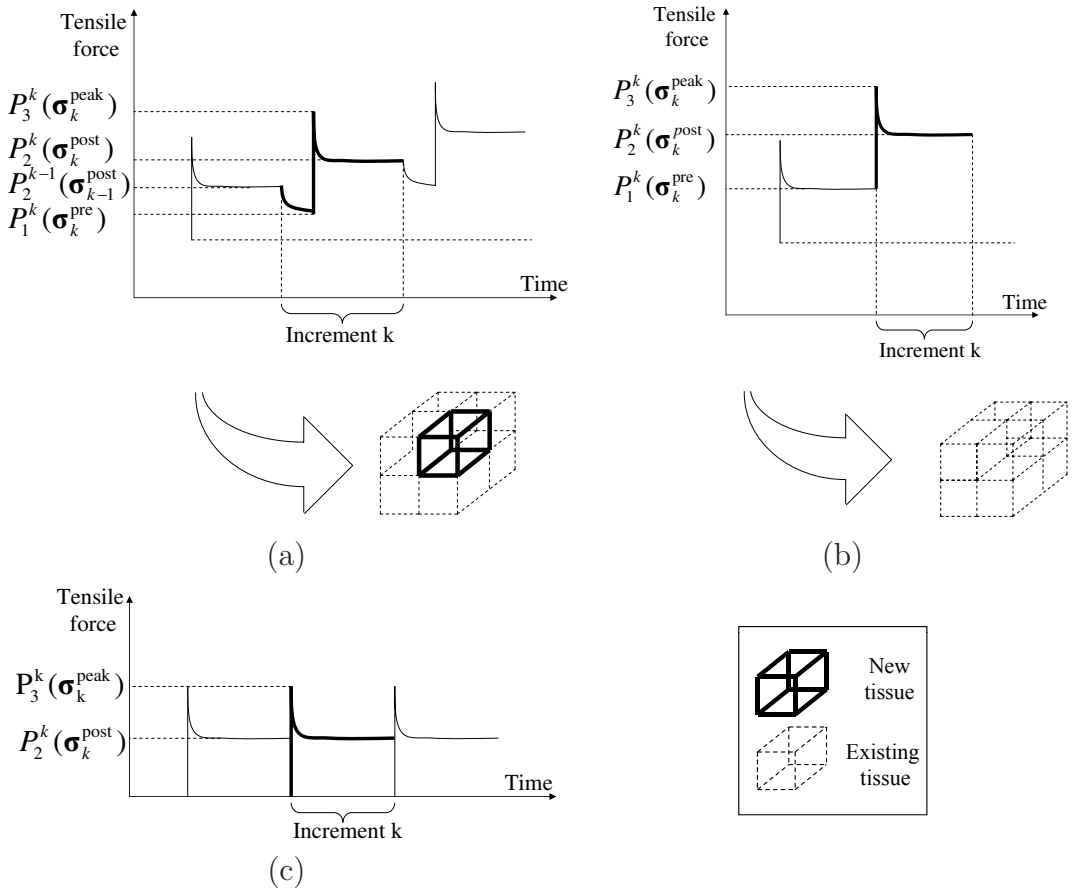

Figure 4.2: Growth and force relaxation. a) New tissue is produced and relaxation is due to both tissue deposition and poroelasticity. b) No matrix is deposited and force relaxation is only due to poroelasticity. c) No pre-traction stress is assumed so complete relaxation is considered from one step to the other as in Isaksson *et al.* (2007) and chapter 3; and pre-traction forces are null $\boldsymbol{\sigma}_k^{\text{pre}}=\mathbf{0}$.

1994; Waanders *et al.*, 1998; Matsushita *et al.*, 1999; Richards *et al.*, 1999) that a stress-free configuration prior to the daily distraction loading is unlikely in most tissues and is clearly not realistic, no model of distraction osteogenesis has included pre-traction stresses and tissue growth in a coupled mode yet.

A mathematical model is proposed and qualitatively validated, to some extent, by comparing reaction forces before and after the loading process with results yielded by experimental studies. Hence, the results of this model could be used as a first approach to measure the inelastic deformation of bone during lengthening.

Results predicted by the model show that pre-traction stresses directly affect

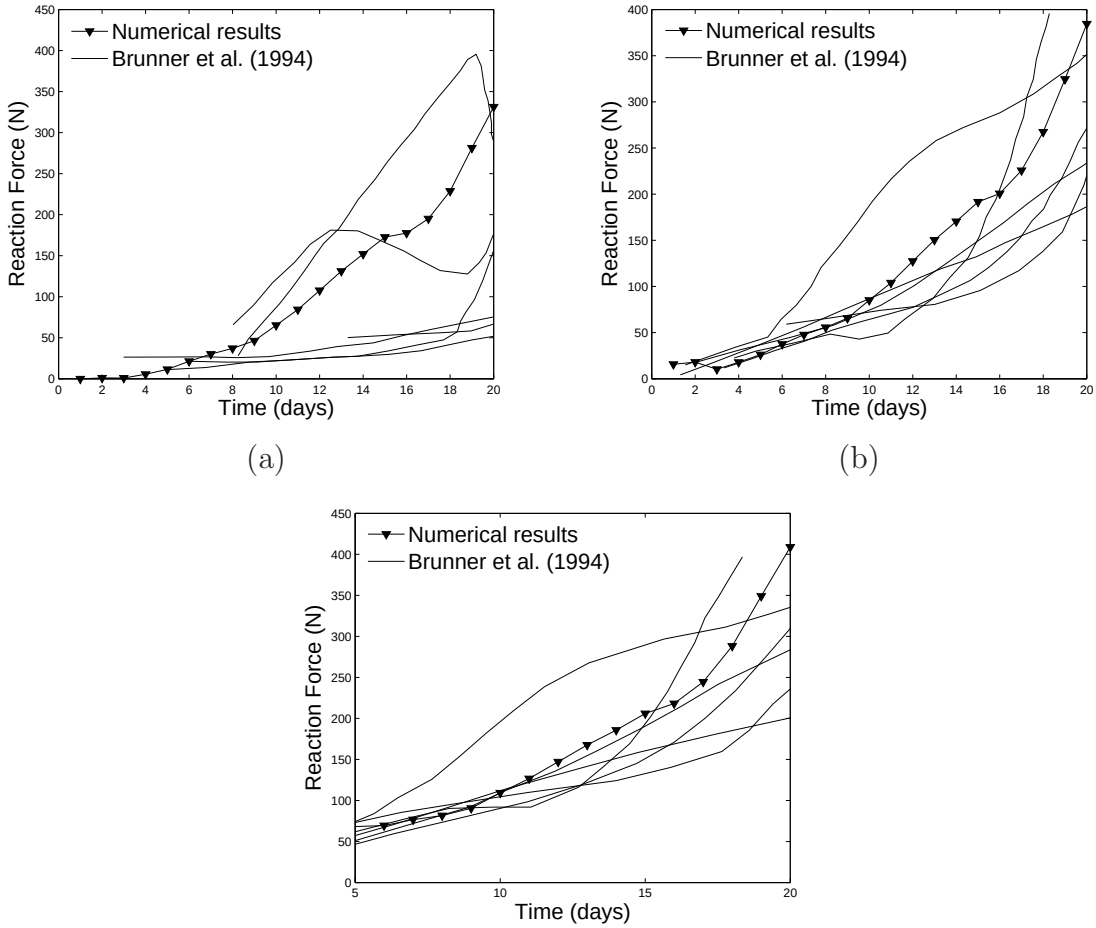

Figure 4.3: Reaction force during the loading process computed numerically and measured experimentally: a) pre-traction force; b) post-traction force; and c) peak force.

the reaction force evolution as shown in Figure 4.5 where the contribution of the pre-traction stresses to the post-traction reaction force is presented. It can be observed that the inclusion of pre-traction stresses in the model directly affects the reaction force by increasing its value.

Moreover, we have found that forces follow a pattern similar to experimental data (Figure 4.4): the maximum daily force decreases throughout the day until it reaches a value slightly greater than the initial force on the previous day; the mean daily force thus slightly increases. This drives to a stress accumulation in the long

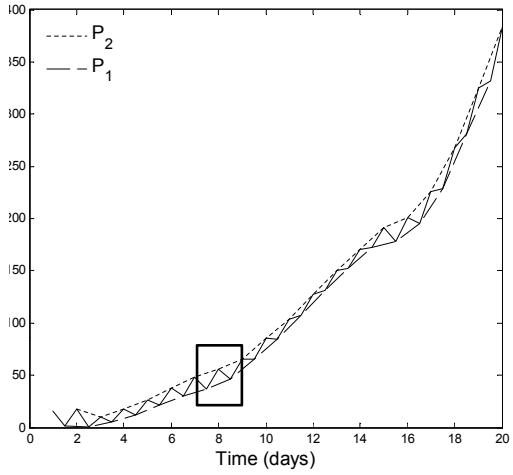

(a)

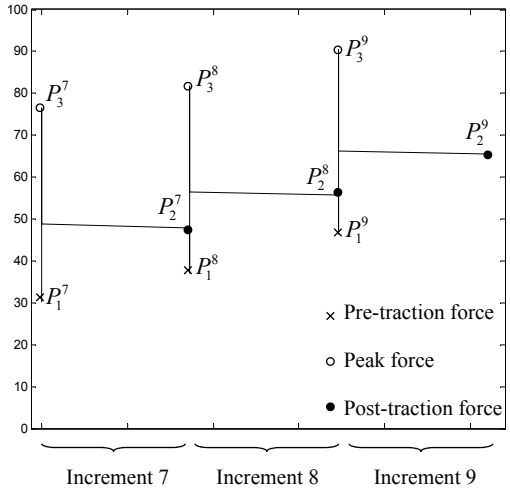

(b)

Figure 4.4: Evolution of the computed pre-traction (P_1) and post-traction (P_2) forces simultaneously: a) during the distraction process and b) during days 7, 8 and 9.

term. This effect is in agreement with many experimental findings (Forriol *et al.*, 1997; Waanders *et al.*, 1998; Gardner *et al.*, 1998; Matsushita *et al.*, 1999). In the model, the force relaxation is due to both the intrinsic poroelastic behaviour of the matrix and to matrix growth (also including differentiation and adaptation) (Figure 4.4b). The latter has been incorporated in the model following a mixture

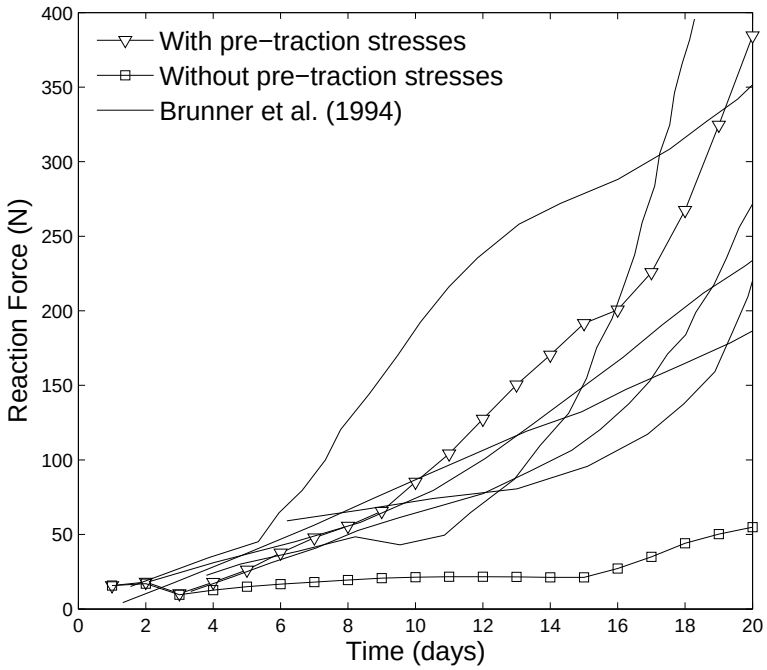

Figure 4.5: Post-traction forces computed with and without pre-traction stresses.

growth approach. Growth (or tissue adaptation) for each tissue is described in terms of the strains at which the new tissue is produced and is incorporated to the model pointwise. These strains are directly related to matrix deposition in such way that, if new tissue is produced at t=t_k, stresses will be non zero in the new created tissue for t>t_k (Figure 4.2a). By contrast, if no matrix is deposited, the daily relaxation of forces will be solely due to the intrinsic poroelastic behaviour of the matrix (Figure 4.2b).

In previous computational works (Isaksson *et al.*, 2007) and in the model described in chapter 3, the authors did not consider pre-traction stresses, and they also predicted a post-traction increasing behavior (Figure 3.9). However, in this case, models were not able to predict the pre-traction force increase with time, because they considered a zero pre-traction force along the whole distraction process (Figure 4.2c).

Another difference included in this work in comparison with previous ones (Gómez-Benito *et al.*, 2005; García-Aznar *et al.*, 2007; Reina-Romo *et al.*, 2009)

is the set of material properties chosen. If the material properties of this study (lower than those used in chapter 3 for some tissues) are used to simulate the model without pre-traction stresses, the reaction forces show values that are out of the experimental bands (Figure 4.5). This indicates that the influence of pre-traction stresses on the force prediction is crucial.

On the other hand, pre-traction stresses may have additional important implications (i.e. in tissue distribution), since they increase the mechanical stimulus that controls all the processes and consequently may affect to tissue damage, differentiation and tissue growth. Figure 4.6 shows the spatial distribution of the mechanical stimulus at days 5 and 10 of the distraction process considering pre-traction stresses (Figure 4.6a) and neglecting them (Figure 4.6b). As observed, the mechanical stimulus (second invariant of the deviatoric strain tensor) is higher when considering the pre-traction stresses (Figure 4.6a). Thus, tissue damage, which we assume to only depend on the maximum value of the mechanical stimulus, increases. Regarding differences in the differentiation processes, similar tissue outcomes are observed when considering pre-traction stresses and when neglecting them: there is an initial stage in which the gap was gradually filled with MSCs and a small amount of bone appeared next to the old bone matrix; a second period in which these precursor cells differentiated into cartilage cells, and a final stage in which further ossification took place and bony bridging occurred.

This model presents several limitations that need to be addressed. Firstly, it is clear that the fundamental aspect of this work is to assume that the relaxation stress that occurs in the pre-traction force is regulated by two combined effects: the poroelastic behaviour of tissue matrix and tissue growth (also considering differentiation and adaptation). This fact is consistent with the formulation proposed by Humphrey & Rajagopal (2003). Secondly, the mathematical formulation has been implemented under the small deformation assumption, although large strains are sometimes generated during distraction osteogenesis, specially during the first days. However, the mathematical formulation has been implemented in an updated Lagrangian code, so all variables are referred to the current (i.e. from the end of the previous increment) configuration of the system. Using this approach, this limitation is not very restrictive. In fact, taking into account that

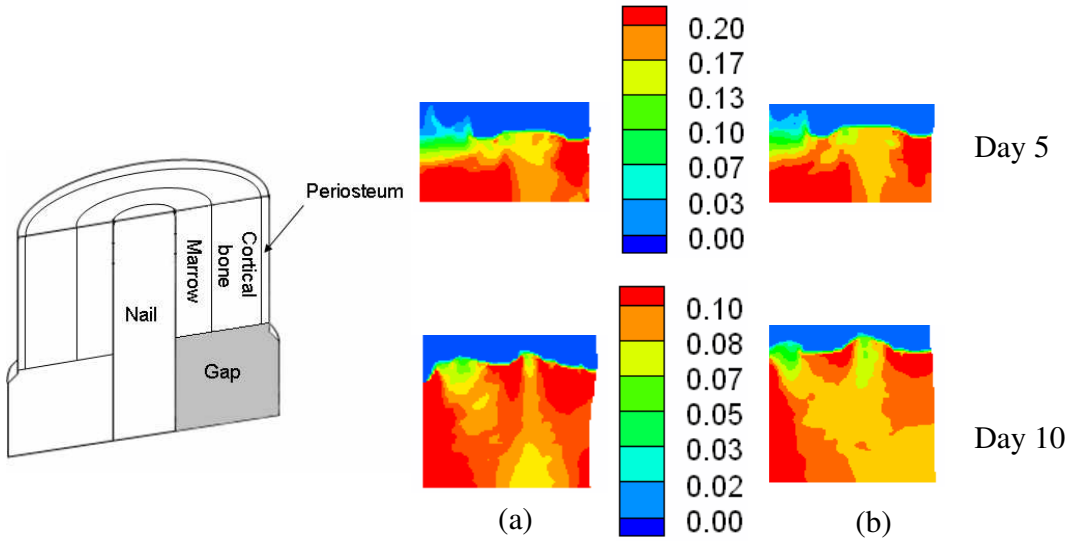

Figure 4.6: Spatial distribution of the mechanical stimulus (second invariant of the deviatoric strain tensor) at days 5 and 10 of the distraction process a) considering pre-traction stresses; b) neglecting pre-traction stresses.

a fixed displacement of 1 mm is applied in 2 time increments and that the gap size is 1 mm in this first step, initial deformations in each increment of around 50% are expected. Nevertheless these strains are reduced up to values around 7.5% in 5-10 days when the gap size is 5-10 mm. Deformations lower than 5% are expected from the 10^{th} day. Thus, we are underestimating the value of the strain tensor mainly in the initial stage of the distraction period. In the future, more accurate models should therefore include finite deformations in each increment in order to validate the growth mixture model. Thirdly, regarding the mechanical stimulus that controls all the biological processes, there is still no agreement as to whether cells respond to stress, strain, strain-rate, strain energy or any other mechanical quantities (Humphrey, 2001). Different mechanical stimuli such as strain energy and several measures of stress have been used to model tissue growth (see, e.g., Fung (1990*b*); Taber (1998); Lubarda & Hoger (2002); Kuhl *et al.* (2003); Garikipati *et al.* (2004); Menzel (2005); Himpel *et al.* (2005); Menzel (2006)). In bone healing, several studies have tried to identify the most appropriate stimulus or combination with specific differentiation pathways of skeletal cells (see, e.g., Pauwels (1960); Perren & Cordey (1980); Carter *et al.* (1998); Claes & Heigele

(1999); Lacroix & Prendergast (2002*a*); Bailón-Plaza & van der Meulen (2003)). The second invariant of the deviatoric strain tensor is the simplest among them and provides similar results to experimental findings (García-Aznar *et al.*, 2007). Moreover, Isaksson *et al.* (2006) concluded, in a comparison of different mechanical stimuli to describe normal fracture healing, that the most significant was the deviatoric component of the strain tensor. Fourthly, volumetric growth due to internal matrix production and external bone remodeling has been neglected and could be incorporated in future works. Fifthly, the solid matrix has been considered to be elastic. With a viscoelastic behavior of the matrix, force relaxation predicted by the model would be slightly higher. Future analysis should be done in this aspect to study the most appropriate matrix behavior. In addition, the solid matrix has been assumed to be isotropic and independent of the type of loading. Future work should be done to incorporate the tension-compression asymmetry in the material properties as well as the anisotropic behaviour. Further, quantitative validation of the results predicted by this model is limited since no additional studies have measured pre- and post-traction forces in sheep during distraction osteogenesis. Thus, in this work we have tried to perform a first semi-quantitative evaluation of the effect of the pre-traction stresses and tissue growth.

4.5.2 An interspecies computational study on limb lengthening

There is no ideal animal model for the study of all aspects involved in distraction osteogenesis. Rabbits are used in approximately 35% of musculoskeletal research studies (Neyt *et al.*, 1998). This is in part due to ease to house and manipulate, size, low cost and faster skeletal changes amongst others (Liebschner, 2004). However, they show fewer similarities with humans than dogs and sheep. Adult sheep offer the advantage of a body weight similar to that of humans and long bone dimensions suitable for the implantation of distractors. Also the amount of surrounding soft tissue in sheep is comparable to long bones in humans (Augat *et al.*, 1997). From a biological point of view, dogs are more suitable as a model for human bones (Gong *et al.*, 1964; Aerssens *et al.*, 1998), although they are less

acceptable due to increasing ethical issues (Pearce *et al.*, 2007).

Regarding the study of limb lengthening, many animal species have been used as experimental models such as rabbits (Kojimoto *et al.*, 1988; Waanders *et al.*, 1998), rats (Aronson *et al.*, 1997*b*; Yasui *et al.*, 1997), mice (Choi *et al.*, 2004), dogs (Ilizarov, 1989*a*,*b*, 1990; Aronson *et al.*, 1990) and sheep (Brunner *et al.*, 1994), amongst others. Some of these studies have provided quantitative estimations of stress accumulation due to residual stresses during the process of distraction (Brunner *et al.*, 1994; Waanders *et al.*, 1998; Matsushita *et al.*, 1999; Richards *et al.*, 1999). The substantial level of the stresses accumulated in the interfragmentary gap during the distraction process suggests that they should produce a large effect on the bone growth process during this technique.

There are still few computational studies in the field of bone distraction. Distraction of long bones has been numerically simulated in sheep (Isaksson *et al.*, 2007), humans (Morgan *et al.*, 2006), mice (Carter *et al.*, 1998) and rabbits (Richards *et al.*, 1998). In craniofacial distraction, models of mandibles of rats (Loboa *et al.*, 2005), humans (Samchukov *et al.*, 1998; Kofod *et al.*, 2005; Boccaccio *et al.*, 2007, 2008) and rabbits (Idelsohn *et al.*, 2006) have been developed. However, only the study performed in the previous section has included the effect of the pre-traction stresses in a single specie.

The aim of the present study is to evaluate the potential of the previously developed evolutive model described in section 4.2 by comparing the tissue pattern of limb lengthening in different animal species and the human case. In this sense, we explore if this model is able to qualitatively explain the differences in the lengthening patterns of tissue distributions found in animals of different size. This comparison was performed by simulating the spatial and temporal tissue changes in the distracted gap across species, computing their corresponding reaction forces and comparing the overall results with experimental findings.

We have assumed that the only parameter that depends on the type of specie is the cellular maturation period, according to experimental evidences (Table 4.2). It is well known that small animals, such as rabbits, have faster skeletal changes and bone turnover than larger animals (Newman *et al.*, 1995; Castañeda *et al.*, 2006). For instance, chondrocytes usually appear 15-20 days after fracture in humans (Cullinane *et al.*, 2003) and by day 7 in rats (Iwaki *et al.*, 1997).

Thus, maturation times of the rabbit were scaled by three to represent the faster progression of tissue development in the rabbit as compared to the sheep and human (Bailón-Plaza & van der Meulen, 2003; Roberts, 1988). The rest of parameters were considered specie-independent and were taken from previous works (Gómez-Benito *et al.*, 2005).

Experimental set-ups

To compare the process of distraction in different animals, different *in vivo* experiments were simulated. Firstly, the experiment carried out in sheep by Brunner *et al.* (1994), which has been simulated in the previous section to compute reaction forces. Here it will be extended further by analyzing tissue distributions.

Secondly, we simulated a rabbit tibia model. The numerical results were compared with those reported by Waanders *et al.* (1998). They measured the *in vivo* fixator forces in rabbit tibias. After a 6-day latency period, the rabbit tibia was distracted at a rate of 0.25 mm every 8 hours during 12 days.

Finally, a human tibia was analyzed and compared against the tensile force recorded by Matsushita *et al.* (1999). In this case, the lengthening process was started two weeks postoperatively at a rate of 0.5 mm every 12 hours during 20 days.

The latency phase was simulated by means of the initial conditions and directly affects to the actual Young's modulus of the gap (E). We assumed that, initially, tissue damage was totally repaired in the distraction gap (E=1 MPa) and that it was partially filled by mesenchymal stem cells when the latency phase occurs. In the sheep model, as no latency phase was employed, we assumed that the gap was initially filled with necrotic tissue and also that tissue damage was maximal in that region (d=0.95 and therefore E=0.05 MPa).

Other initial conditions consisted, in the diffusion analysis, of sources of MSCs in the marrow cavity, periosteum and in the surrounding soft tissues (Gerstenfeld *et al.*, 2003) (Figure 3.8a). The initial boundary conditions for the ossification front modeled through the diffusion equation consisted on preosteoblastic sources in the areas of the endosteum and periosteum closest to the cortical bone (Figure 3.8b).

A cylindrical geometry for the diaphysis of the tibia was assumed in all cases,

with the dimensions shown in Figure 4.7 and Table 4.2 (Brueton *et al.*, 1990; Brunner *et al.*, 1994; Claes & Heigele, 1999; Gómez-Benito *et al.*, 2007). In the sheep case, the nail was modelled assuming the nail/tissue interface to be frictionless.

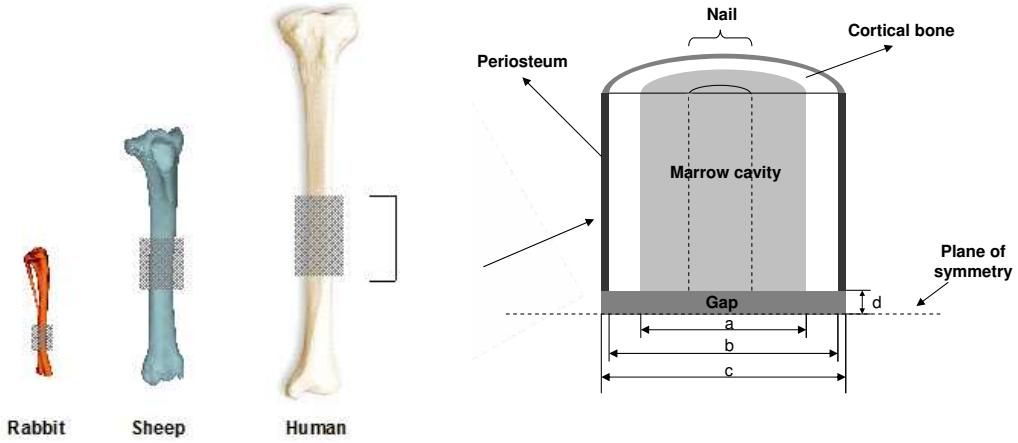

Figure 4.7: Scheme of the geometry of the tibia model.

Table 4.2: Geometrical values considered in the simulations, load derived from the normal activity of the animal and maturation levels for each animal model.

	Dimensions (mm)				Force	Maturation
	a	b	c	d	(N)	level
Sheep[1]	12	20	21	0.5	500[5]	m^i
Rabbit[2]	2.25	4.85	5.06	0.2	30[6]	$3{\cdot}m^i$ [8,9]
Human[3]	14	28	30	2.5[4]	800[7]	m^i

1 (Brunner *et al.*, 1994); 2 (Brueton *et al.*, 1990); 3 (Gómez-Benito *et al.*, 2007); 4 (Morgan *et al.*, 2006); 5 (Claes & Heigele, 1999); 6 (Gushue *et al.*, 2005); 7 (Jaeger & Vanitchatchavan, 1992); 8 (Bailón-Plaza & van der Meulen, 2003); 9 (Roberts, 1988)

According to each experimental set-up, mechanical loading consisted in the distraction phase on a displacement applied at a given frequency during 1 minute and maintained until the next distraction (8 hours, 12 hours or one day). During the consolidation period, the only active mechanical stimulation was due to the load derived from the normal activity of the animal. Values are reported in Table

4.2 for each animal considered. This load was neglected during the distraction phase and in the case of the sheep was applied to the bone-nail complex through a rigid part located on top of the upper surface (Figure 3.7a). In the remaining two cases (rabbit and human), the load was applied to a fixator which was simulated by means of a linear spring with only axial stiffness. Thus, a part of this load, proportional to the stiffness ratio between fixator and bone, was transmitted to the bone.

Boundary conditions were equal to those described in section 4.5.1: rotational symmetry along the long bone axis and mirror-image symmetry with respect to the plane of the osteotomy (Figure 3.7b). Null fluid flow was prescribed at the periosteum, assuming therefore this boundary to be impermeable (Li *et al.*, 1987) (Figure 3.7b).

Sheep model results

The computationally predicted reaction force in the sheep tibia has been already described and is shown in Figure 4.3b. With respect to the tissue distribution, during the first days, most of the damaged tissue in the gap was repaired and migration of MSCs from the marrow cavity, periosteum and surrounding soft tissues took place (Figure 4.8). By day 10, bone tissue could be seen close to the periosteum and marrow. Finally, once the consolidation phase had begun, cartilage tissue was predicted to differentiate into woven bone.

Rabbit model results

Figure 4.9 shows the computed reaction force in the rabbit model. Initially, numerical values increased due to the rapid migration of MSCs and also due to their quick proliferation (in 2-3 days) (Figure 4.10). By day 7-8, the gap was completely filled with granulation tissue and precursor cells started to differentiate into cartilage cells. Therefore, reaction forces increased rapidly due to the increasing stiffness in the tissue.

Regarding tissue distribution, during the first stage (1-10 days), the gap was gradually filled with migrating MSCs (Figure 4.10). The mechanical environment created in the gap allowed the maturation of these cells and their differentiation

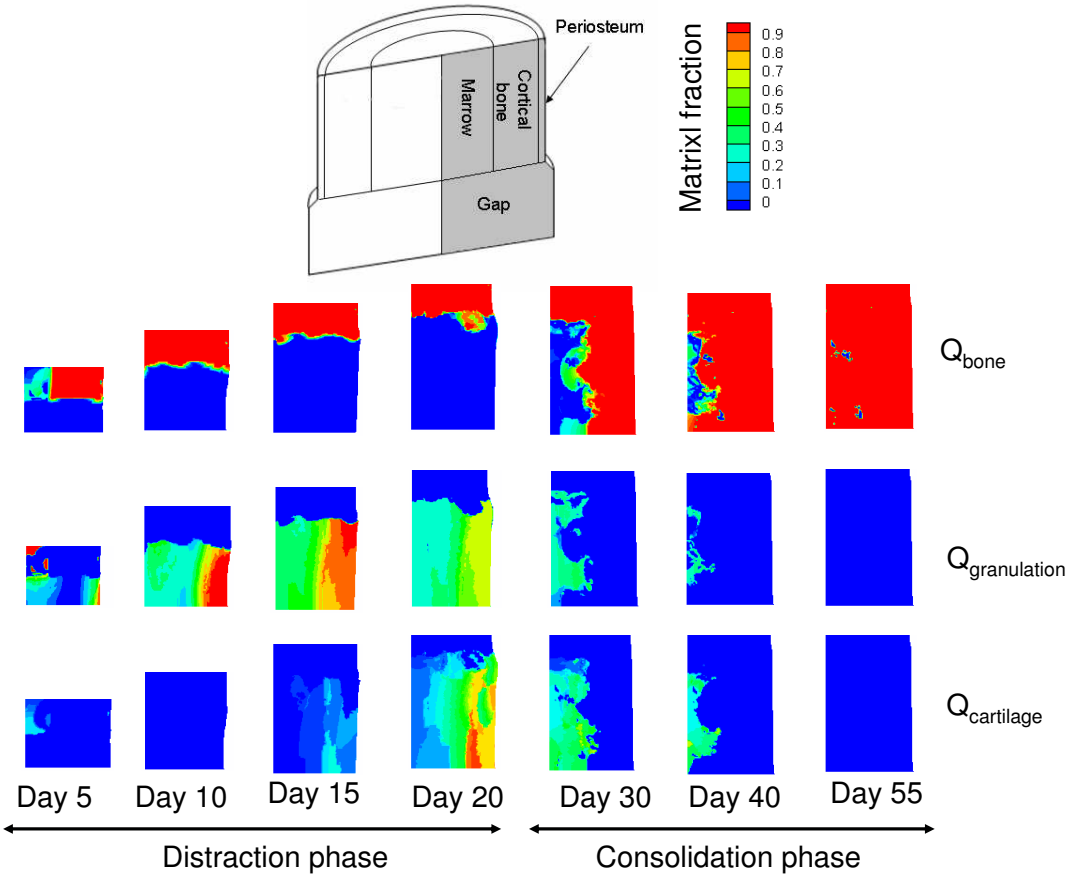

Figure 4.8: Tissue distribution prediction in the sheep tibia for a distraction rate of 1 mm/day.

into chondrocytes around day 7-8 (Kojimoto *et al.*, 1988). At the end of the distraction period, two distinct regions could be observed: a central cartilage region and a bony region close to the old bone matrix. During the consolidation period, endochondral ossification took place and the bone front gradually advanced until complete bony bridging of the gap was achieved (Figure 4.10).

Human case results

The reaction forces obtained in the human case are shown in Figure 4.11. Initially, during the first 13 days of distraction, there was a mild increase of the tensile force whilst the gap was gradually filled with granulation tissue. Once MSCs

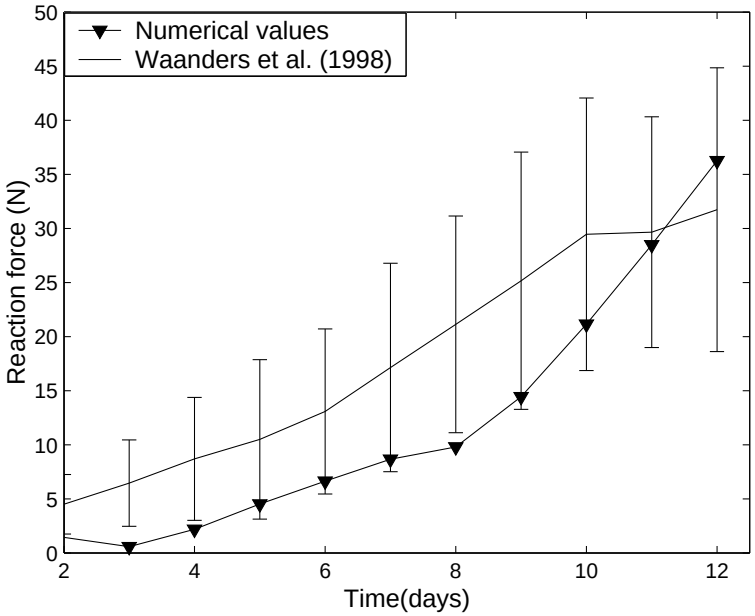

Figure 4.9: Comparison of the reaction forces calculated with the computational rabbit model and experimental measurements (Waanders *et al.*, 1998).

had matured, the differentiation process began and cartilage formation could be observed within the gap with the subsequent force increase.

The tissue pattern was very similar to that seen in the sheep model (Figure 4.12). Initially there was an active migration of MSCs towards the distracted gap, and by day 14-15 cartilage cells started to differentiate. Once the consolidation period had taken place, endochondral ossification occurred and bone cells gradually filled the gap.

Discussion

For the three animal models, our results are in agreement with those yielded by experimental studies. Moreover, the mechanically-based growth mixture model is able to qualitatively reproduce interspecies differences. First, the computed reaction force at the end of the distraction phase was one order of magnitude lower in the rabbit (35 N) than in the human (500 N) and sheep (400 N), which follows the trend of different experimental data (Brunner *et al.*, 1994; Waanders *et al.*, 1998; Matsushita *et al.*, 1999) (Figures 4.3b, 4.9 and 4.11). Secondly, more

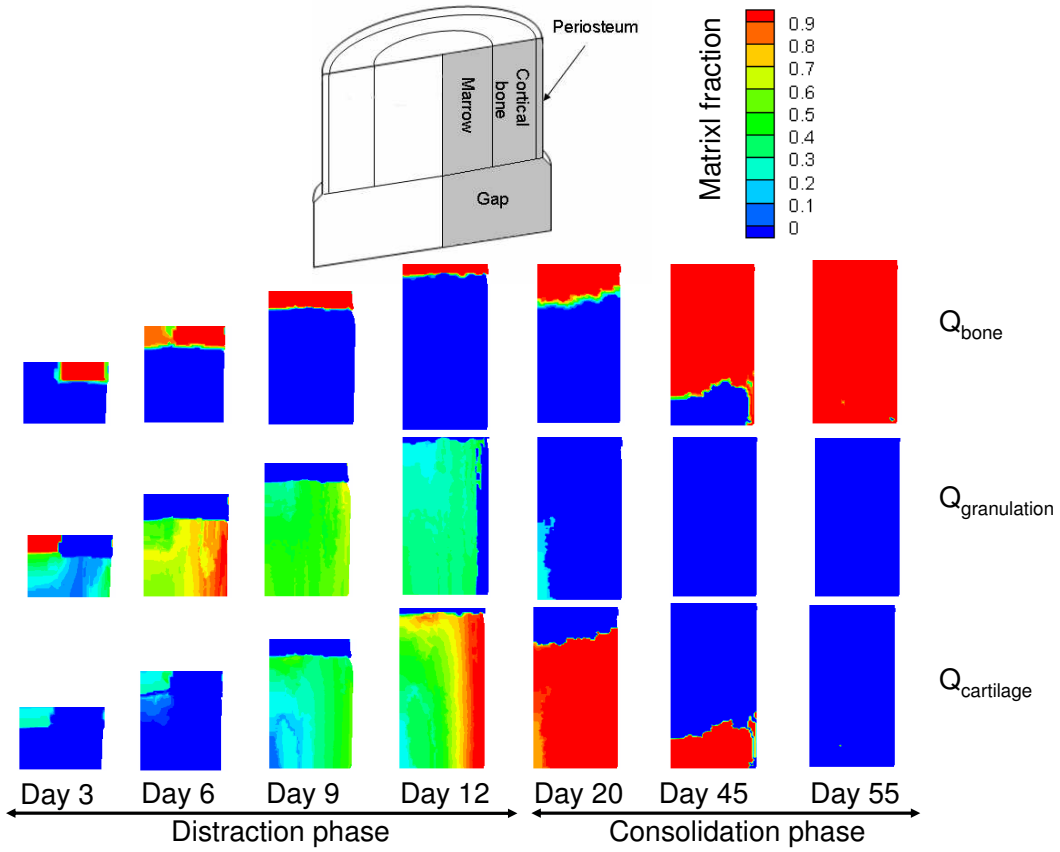

Figure 4.10: Tissue distribution prediction in the rabbit throughout the distraction and consolidation periods. There is no fibroblast differentiation during the process.

cartilage is formed in the rabbit than in the human and sheep cases: at the end of the distraction period, the volume fractions of cartilage in the gap are 0.34, 0.24 and 0.18 in the rabbit, sheep and human respectively. This is also in agreement with conclusions obtained by Li *et al.* (1999).

Comparing the three analyzed examples some similarities can also be found. First, the reaction force evolution is very similar: it gradually increases through the distraction period showing a noticeable change in the computed reaction forces when the production of cartilaginous matrix is active. This occurred in the range of days 14 and 16 in humans and in sheep and by day 8 in rabbits. This sudden change does not occur in the experimental results and may be due to some

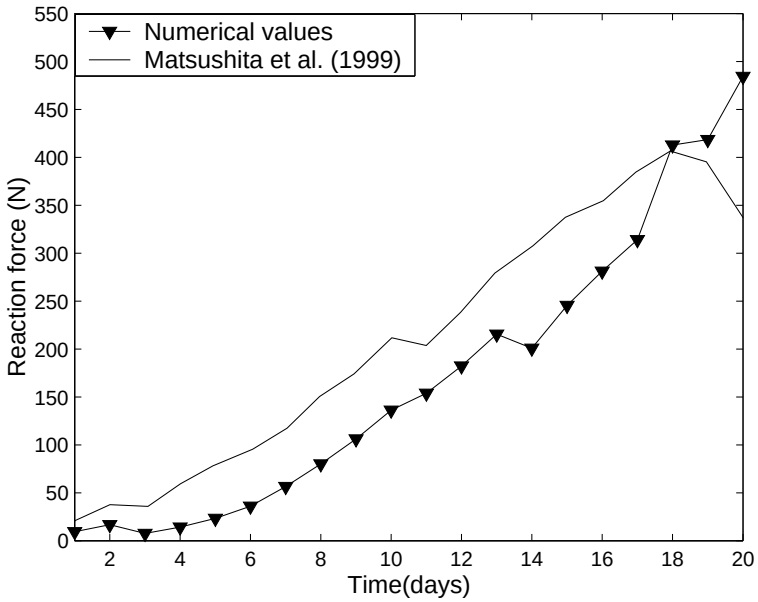

Figure 4.11: Comparison of the reaction forces calculated with the computational human model and those measured experimentally in the human tibia (Matsushita *et al.*, 1999).

effects that are not integrated in the model. For instance, during the distraction process, collagen fibers, which are the main component of the granulation tissue (Bouletreau *et al.*, 2002*a*), are stretched out and consequently loose their normal wavy structure to get a rectilinear appearance oriented parallel to the distraction vector (Ilizarov, 1989*b*; Wren & Carter, 1998). These fibers provide temporary mechanical resistance to the distracted gap and therefore may contribute to the increasing stiffness observed experimentally. A further difference could be found in the reaction force predicted by the model in the human case (Figure 4.11). Experimentally, around day 18, a decrease in the reaction force (directly related to the gap stiffness) was observed. This is probably due to the rupture of soft tissues (Matsushita *et al.*, 1999). These effects were not included and may cause some differences between the experimental and computational results in the reaction forces.

Secondly, regarding tissue distributions within the distracted gap, it can be observed that the tissue pattern evolved similarly for all the animal models analyzed (Figures 4.8, 4.10 and 4.12): there was an initial stage in which the gap was

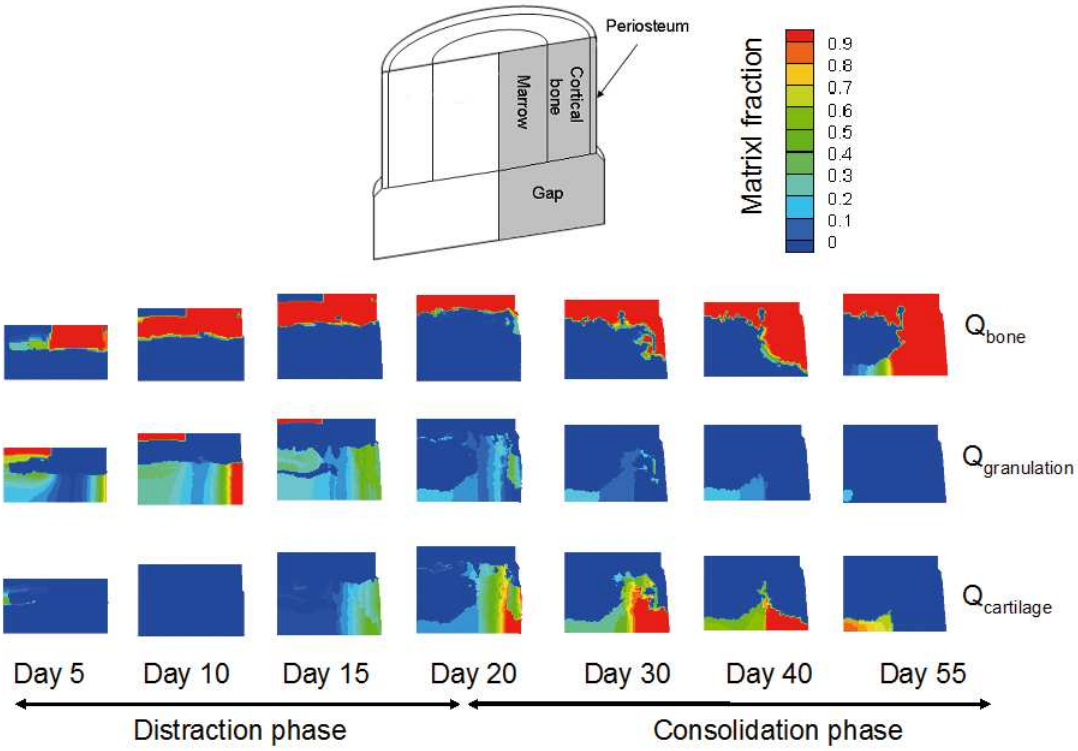

Figure 4.12: Tissue distribution prediction in the human tibia through the distraction and consolidation phases. There is no fibroblast differentiation during the process.

gradually filled with MSCs (Samchukov *et al.*, 2001) and a small amount of bone appeared next to the old bone matrix; a second period in which these precursor cells differentiated into chondrocytes, and a final stage in which further ossification took place and bony bridging occurred. However, in the case of the sheep and human, bony bridging occurred first in the periosteal callus. Comparing the results of the rabbit case (Figure 4.13) with three-dimensional microcomputed tomographies of the distraction gap of a rabbit subjected to the same protocol of distraction as in our rabbit model (Richards *et al.*, 1999), it can be seen that the bone tissue distribution is very similar: bone formation begins before completion of the distraction period and during the consolidation phase a significant increase in new bone was observed (Figure 4.13). This bone appears in our model as a mixture of endochondral and intramembranous ossification. Indeed, cartilage formation is observed in many experimental studies performed in small animals

(Ohyama *et al.*, 1994; Yasui *et al.*, 1997; Jazrawi *et al.*, 1998; Li *et al.*, 1999) as well as in larger ones (Peltonen *et al.*, 1992; de Pablos *et al.*, 1994; Fink *et al.*, 2003). This is also in agreement with existing computational models (Isaksson *et al.*, 2007; Boccaccio *et al.*, 2007, 2008). In the human case, comparison with experimental data has been very difficult since most available data only consist on bone measurements.

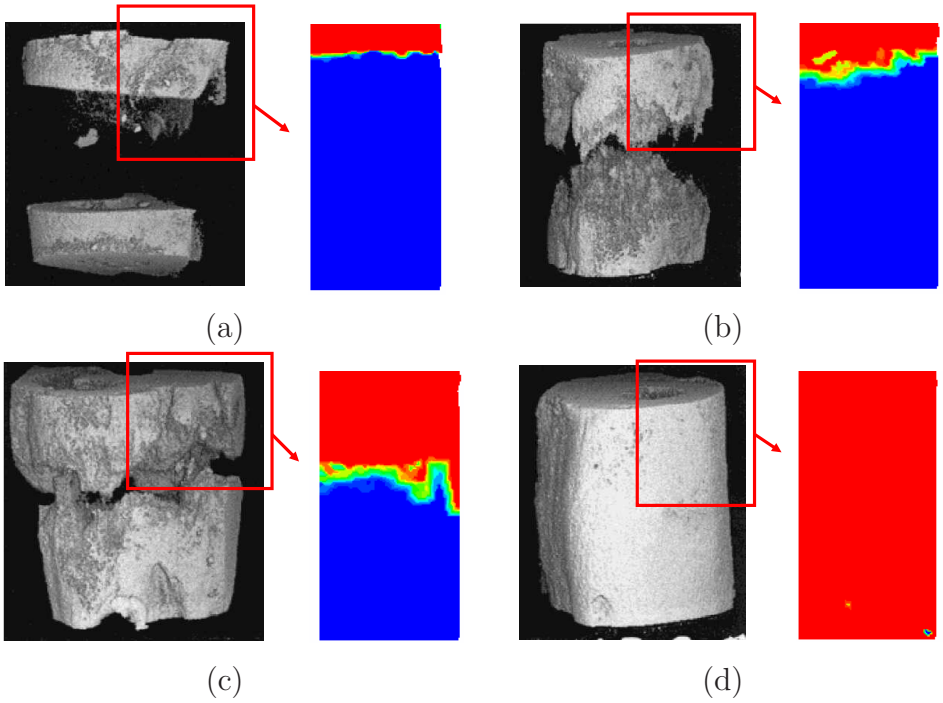

Figure 4.13: Comparison of bone turnover of the numerical results with three-dimensional microcomputed tomographies in the rabbit model (Richards *et al.*, 1999) at a) day 12; b) day 18; c) day 30; d) day 55 after the latency period.

In this study, the effect of the pre-traction stresses has been considered. However, comparing Figures 3.10 and 4.8, where the same experimental set-up has been modeled but with different mathematical models, it can be appreciated that tissue distributions are not affected significantly by the residual stresses. By contrast, considering residual stresses is crucial for a correct reaction force prediction and material properties adjust.

There are several limitations in the present study. The first one regards the mathematical formulation, which is developed under the small deformations as-

sumption. Nevertheless, distraction is a large deformation process since interfragmentary movements may represent as much as 100% of the size of the gap. However, after 5 days of distraction, strains are reduced up to 20%. Secondly, the latency phase is modelled by means of the initial conditions. An additional limitation is that we have only considered one cell type (MSC) as representative of all initial precursor cells and therefore a single tissue type (granulation tissue) as representative of the initial callus tissue in order to have a workable model with a limited number of tissues. Moreover, the named fibrous tissue represents in our model a final irreversible differentiated tissue that cannot evolve to other tissue types and that appears in cases of nonunion. The inclusion of additional tissue types would not alter significantly the overall results of this study and may only affect slightly to the mechanical properties of the distracted gap. Further, the same material properties have been considered for the three analyzed models. The interspecies tissue properties differences have been assumed comparable to that available in the literature for a single specie. Regarding the differences in cell-processes between species, we have assumed that the only parameter dependent on the type of specie is the maturation stage of the cells. However, other causes such as differences in inflammatory phases, proliferation rates, matrix production, surgical techniques that were applied or type of fixators amongst others may also contribute to the differentiation process.

As far as we know, no computational study has been performed yet analyzing the mechanical environment within the distraction gap for different animal models. In this section, a growth mixture model that includes pre-traction stresses was for the first time used in this study to compare tissue distribution as well as reaction forces in the human and the two animal species obtaining results that are in agreement with experimental studies. Hence, the ability of the model to predict different results corresponding to the two animal models and the human case indicates that interspecies differences can be predicted by a model that includes the effect of residual stresses. However, further studies are needed to completely corroborate the model because there is a lack of experimental measurements that allow to understand the main characteristics of bone healing in each specie.

Chapter 5

Numerical simulation of mandibular distraction osteogenesis

5.1 Introduction

Distraction osteogenesis is an effective way to grow new bone and has been widely used in the last decades to correct bone deformities, either congenital or acquired, bone length discrepancies and bony defects. Its application to the craniofacial skeleton has gained wide acceptance, since its clinical introduction by McCarthy *et al.* (1992), due to the huge possibilities this process offers.

In fact, the craniofacial skeleton is more amenable to the distraction technique than long bones. The bones of the craniofacial skeleton are much thinner than the long bones and the associated blood supply is richer. This is why the craniofacial skeleton with its rich blood supply can tolerate more liberal elevation of the periosteum as well as complete osteotomy which disrupts the endosteum (Aronson, 1994).

However, mandibular distraction osteogenesis (MDO) is often a more complex procedure than long bone lengthening (Gateño *et al.*, 2000). Bones must often be moved in three dimensions (Figure 5.1), as opposed to just one, as in a limb, and scarring must be kept to a minimum for aesthetic reasons. Also, the mandible is a

movable bone without fixed ends in contrast to long bones which are articulated at two joints. In fact, currently work has begun on the development of bidirectional and multidirectional devices as opposed to the most common unidirectional ones.

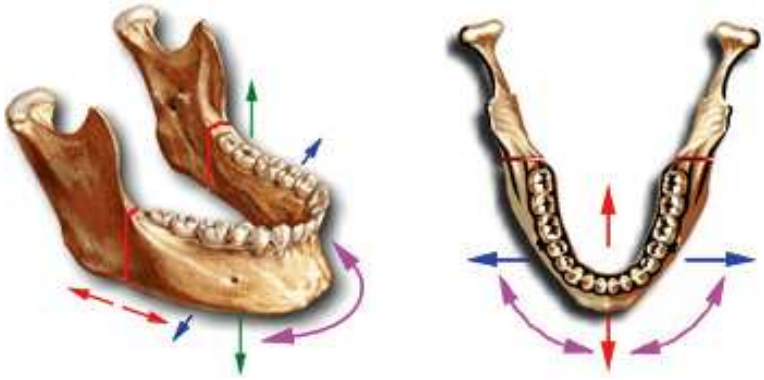

(a) (b)

Figure 5.1: Three-dimensional structure of the mandible.

Moreover, investigations into pre-operative computer planning, finite element modeling and mathematical modeling of mandibles and mandibular distraction osteogenesis have greatly improved as researchers attempt to better determine, in a non-invasive way, the most appropriate MDO procedure for each patient prior to surgery (Loboa *et al.*, 2005).

Previous studies of mandibular distraction osteogenesis have characterized the local bio-physical environment created within the osteotomy gap at different time points (Samchukov *et al.*, 1998; Loboa *et al.*, 2005; Kofod *et al.*, 2005; Cattaneo *et al.*, 2005; Boccaccio *et al.*, 2006) or during the whole process of distraction through mechanobiological models (Boccaccio *et al.*, 2007, 2008). However, none of these approaches have studied the temporo-spatial evolution of the different tissues during distraction osteogenesis and the biomechanics in patients with severe deformities.

This chapter is organized as follows. Firstly, a description of the anatomy of the mandible is presented, with a brief overview of the skull, lower jaw, temporomandibular joint and main masticatory muscles. Secondly, the clinical case is described, detailing the principal clinical aspects. Finally, we perform two different approaches. The former consists on a biomechanical analysis, where the strain field will be analyzed at the pre-distraction and post-distraction models and com-

pared with an idealized healthy case. The latter, consists of a temporo-spatial prediction of the main processes that occur during distraction osteogenesis of a mandible with severe hypoplasia of one of the ramus. In this case only the tissue distribution will be computed. In chapter 4, tissue distribution has been shown to not vary significantly with the inclusion of residual stresses and therefore the much simpler model described in chapter 3 will be implemented.

5.2 Anatomy of the mandible

In this section the mandible is briefly described, as well as the muscles and bones involved in the masticatory process.

This description will serve to posteriorly create the finite element model of the mandible. It is very important to correctly define the different muscle insertions as well as the boundary conditions of the mandible. Thus, the movements of the temporomandibular joint must be known.

To accomplish these objectives, firstly, we describe the main bones of the skull, that will serve as attachment for masticatory muscles. Secondly, we focus on the lower jaw of the mandible and afterwards a brief description of the temporomandibular joint is presented. Finally the main muscles involved in the masticatory processes are detailed.

5.2.1 The skull

The skull is the body's most complex bony structure, formed by *cranial* and *facial* bones, being 22 in all. The cranial bones, or cranium, enclose and protect the fragile brain and furnish attachments sited for head and neck muscles. The facial bones form the framework of the face, contain cavities for the special sense organs of sight, taste, and smell, provide openings for air and food passage, secure the teeth, and anchor the facial muscles of expression.

The cranial bones include the paired parietal and temporal bones and the unpaired frontal, occipital, sphenoid and ethmoid bones (Figure 5.2). The facial skeleton is made of 14 bones of which only the mandible and the vomer are unpaired. The maxillae, zygomatics, nasals, lacrimals, palatines, and inferior

conchae are paired bones (Figure 5.2). Through not really part of the skull, the hyoid bone, lies just inferior to the mandible in the anterior neck. This bone is unique in that it is the only bone of the body that does not articulate directly with any other bone. Instead, it is anchored by the narrow stylohyoid ligaments to the styloid processes of the temporal bones. The hyoid bone acts as a movable base for the tongue and serves as attachment points for neck muscles.

Most skull bones are flat bones. Except for the mandible, which is connected to the rest of the skull by a freely movable joint (the temporomandibular joint), all bones of the adult skull are firmly united by interlocking joints called sutures. The major skull sutures, the coronal, sagittal, squamous, and lamboid sutures connect cranial bones (Figure 5.2) whilst the remaining ones connect facial bones and are named according to the specific bones they connect. These suture lines have a saw-toothed or serrated appearance.

5.2.2 The mandible

The mandible (lower jaw) is the largest and strongest bone of the face. It has a body, which forms the chin, and two upright rami (Figure 5.3). Each ramus meets the body posteriorly at a *mandibular angle*. At the superior margin of each ramus are two processes separated by the *mandibular notch*. The anterior *coronoid process* is an insertion point for the large temporalis muscle that elevates the lower jaw during chewing. The posterior mandible condyle articulates with the mandibular fossa of the temporal bone, forming the temporomandibular joint on the same side.

The *mandibular body* serves for the reception of the lower teeth. Its superior border, called the *alveolar margin* contains the sockets in which the teeth are embedded. In the midline of the mandibular body there is a slight depression, the *mandibular symphysis* indicating where the two mandibular bones fused during infancy.

Large *mandibular foramina*, one of the medial surface of each ramus, permits the nerves (responsible for tooth sensation) to pass to the teeth in the lower jaw. Dentists inject lidocaine into these foramina to prevent pain while working on the lower teeth. The *mental foramina*, openings on the lateral aspects of the

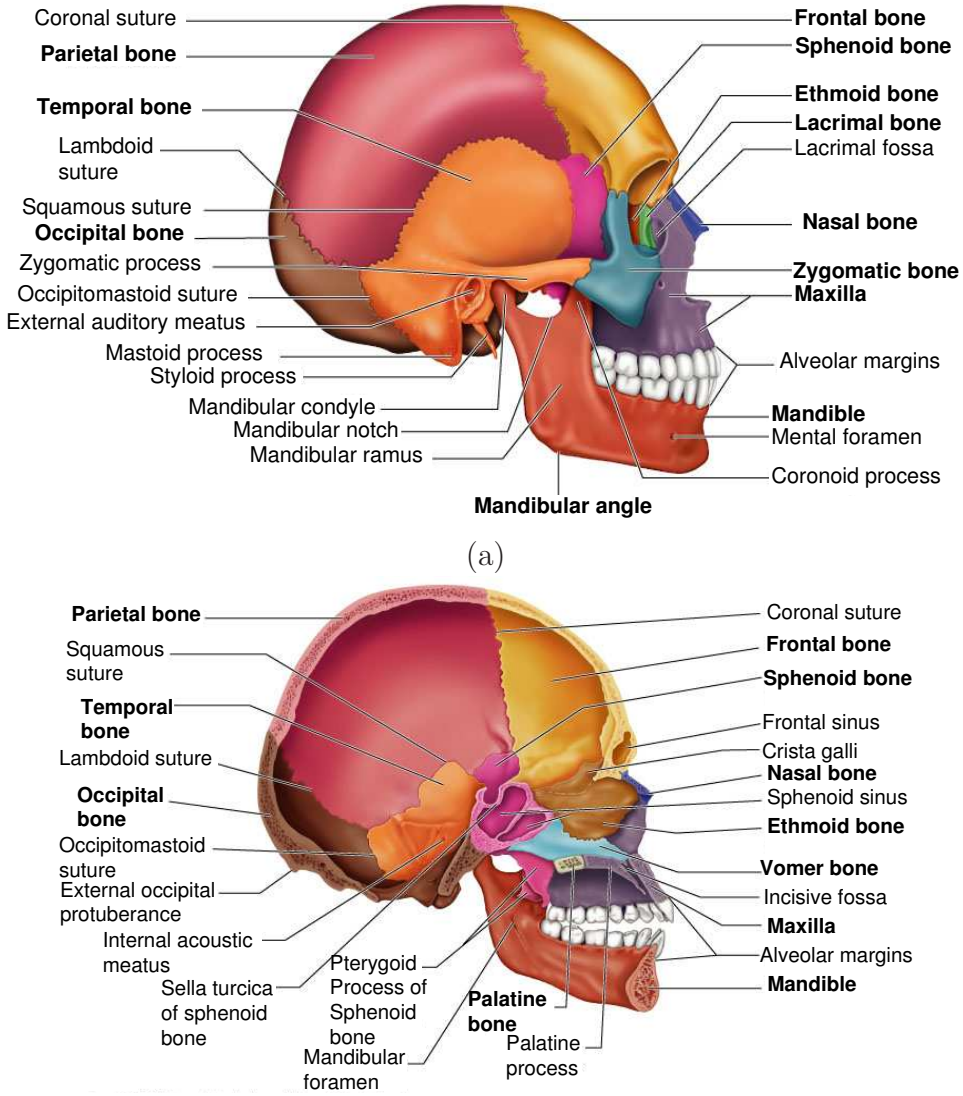

Figure 5.2: Anatomy of the lateral aspects of the skull. a) External anatomy of the right lateral aspect of the skull. b) Midsagittal view of the skull showing the internal anatomy of the left side of the skull (Marieb, 2004).

mandibular body, allows blood vessels and nerves to pass to the skin of the chin.

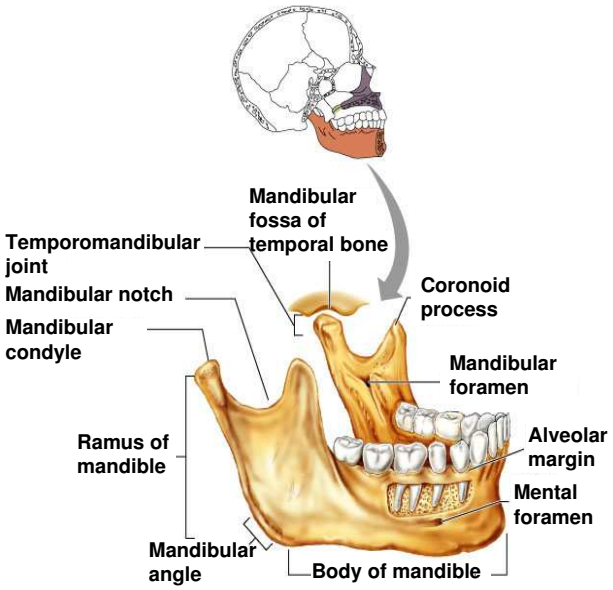

Figure 5.3: Detailed anatomy of the mandible (Marieb, 2004).

5.2.3 The temporomandibular joint

The temporomandibular joint (TMJ) lies just anterior to the ear. At this joint, the mandibular condyle articulates with the inferior surface of the squamous temporal bone (Figure 5.4). The mandibular condyle is egg shaped, whereas the articular surface of the temporal bone has a more complex shape. Posteriorly, it forms the concave mandibular fossa, anteriorly it forms a dense knob called the *articular tubercle*. The lateral aspect of the loose articular capsule that encloses the joint is thickened into a *lateral ligament*. Within the capsule, an articular disc divides the synovial cavity into superior and inferior compartments (Figure 5.4).

Two distinct kinds of movement occur at the TMJ. First the concave inferior disc surface receives the mandibular condyle and allows the familiar hinge-like movement of depressing and elevating the mandible while opening and closing

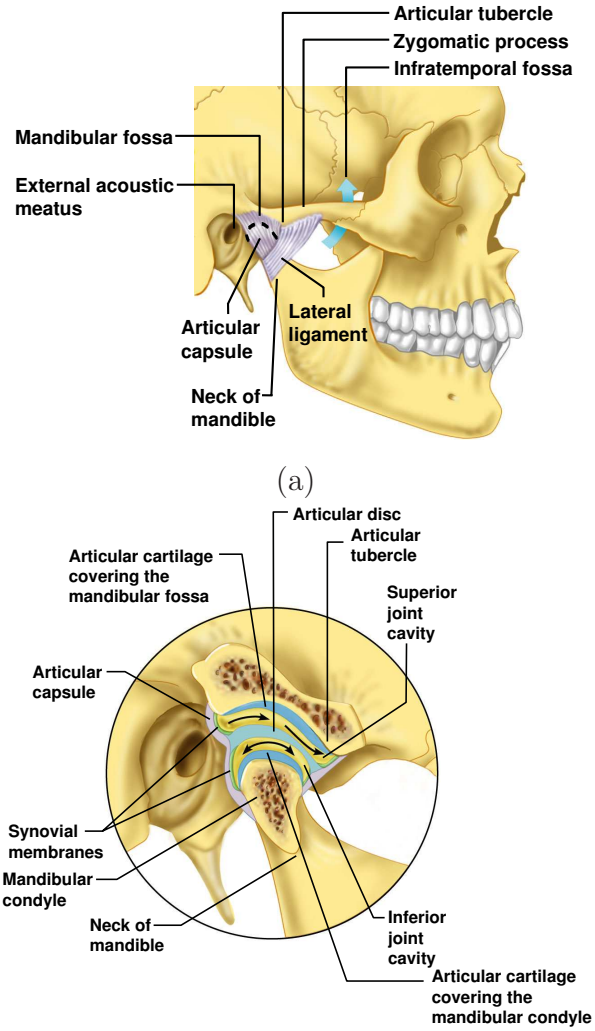

Figure 5.4: The temporomandibular joint (Marieb, 2004). a) Location of the joint in the skull showing important surrounding structures. b) Enlargement of a sagittal section through the joint, showing the articular disc, the superior and inferior compartments of the joint cavity and two movements that occur (arrows). The inferior joint cavity allows the mandibular condyle in opening and closing the mouth, whereas the superior joint cavity lets the mandibular condyle move forward to brace against the articular tubercle when the mouth opens wide.

the mouth. Secondly, the superior disc surface glides anteriorly along with the mandibular condyle when the mouth is opened wide. This anterior movement braces the condyle against the articular tubercle, so that the mandible is not

forced through the thin roof of the mandibular fossa when one bites hard foods. The superior compartment also allows this joint to glide from side to side. As the posterior teeth are drawn into occlusion during grinding, the mandible moves with a side to side movement called lateral excursion. This lateral jaw movement is unique to mammals.

5.2.4 The masticatory muscles

Four pairs of muscles are involved in mastication activities (chewing and biting), and all are innervated by the mandibular branch of cranial nerve V (see Table 5.1). The prime movers of jaw closure (and biting) are the powerful masseter and temporalis muscles (Figure 5.5). Grinding movements are brought about by the pterygoid muscles. The buccinator muscle also plays a role in chewing (Table 5.1 and Figure 5.5). Normally gravity is sufficient to depress the mandible, but if there is resistance to jaw opening, neck muscles such as the digastric and milohyoid are activated. Table 5.1 describes masticatory's muscle shape, their location relative to other muscles, origin and insertion, primary actions and innervations.

Forces developed by masticatory muscles

The approximate magnitude of the force developed by a muscle (F_i) during a given masticatory activity results as the product of the cross-sectional area of the muscle (X_i), a constant for skeletal muscles (K) and a scaled value of the muscle contraction relative to its maximum response for any task (EMG_i) (Korioth *et al.*, 1992):

$$F_i = EMG_i \cdot (X_i \cdot K) \tag{5.1}$$

where K=40 N/cm^2 (Weijs & Hillen, 1984; Reina *et al.*, 2007).

5.3 Clinical case description

This study was based on data from a 6-year-old male patient with unilateral mandibular hypoplasia of the right mandibular ramus, corresponding with a grade

Table 5.1: Muscles of mastication (Marieb & Hoehn, 2007).

Muscles of mastication	**Description**	**Insertion** O=origin I=insertion	**Action**	**Nerve innervation**
Masseter	Powerful muscle that covers lateral aspect of mandibular ramus	O=zigomatic arch and maxilla I=angle and ramus of mandible	Prime mover of jaw closure, elevates mandible	Trigeminal nerve
Temporalis	Fan-shaped muscle that covers parts of the temporal, frontal and parietal bones	O=temporal fossa I=coronoid process of mandible	Closes jaw; elevates and retracts mandible; synergist of pterygoids in side-to-side movements; mantains position of mandible at rest	Trigeminal nerve
Medial pterygoid	Deep-two headed muscle that runs along internal surface of mandible and is largely concealed by that bone	O=medial surface of lateral pterygoid plate of sphenoid bone, maxilla and palatine bone I=medial surface of mandible near its angle	Synergist of temporalis and masseter muscles in elevation of the mandible; acts with the lateral pterigoid muscle to protude mandible and to promote side-to-side (grinding) movements	Trigeminal nerve
Lateral pterygoid	Deep-two headed muscle; lies superior to medial pterygoid muscle	O=greater wing and lateral pterygoid plate of sphenoid bone I=condyle of mandible and capsule of TMJ	Protudes mandible; provides forward sliding and side-to-side grinding movements of the lower teeth	Trigeminal nerve
Buccinator	Thin, horizontal cheek muscle; principal muscle of cheek; deep to masseter	O=molar region of maxilla and mandible I=orbicularis oris	Trampoline-like action of buccinator muscles helps keep food between grinding surfaces of teeth during chewing	Facial nerve

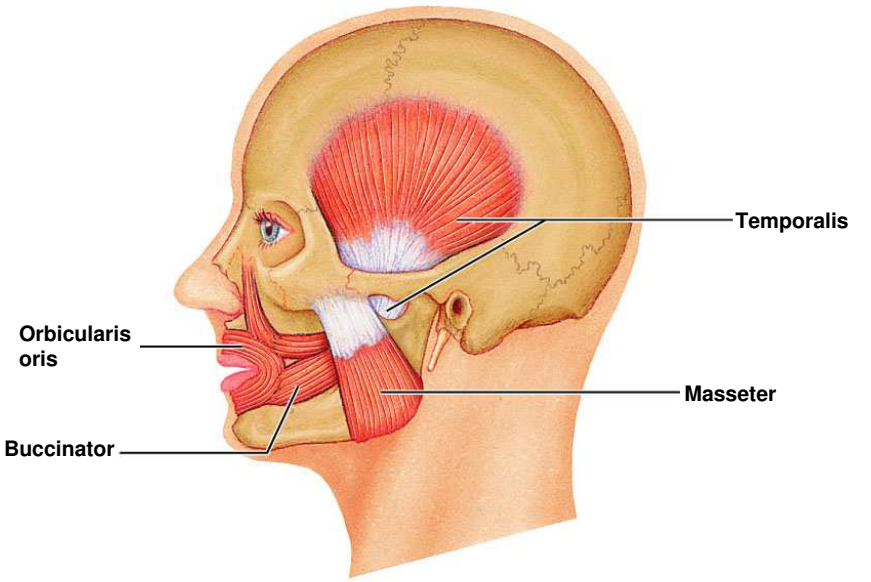

(a)

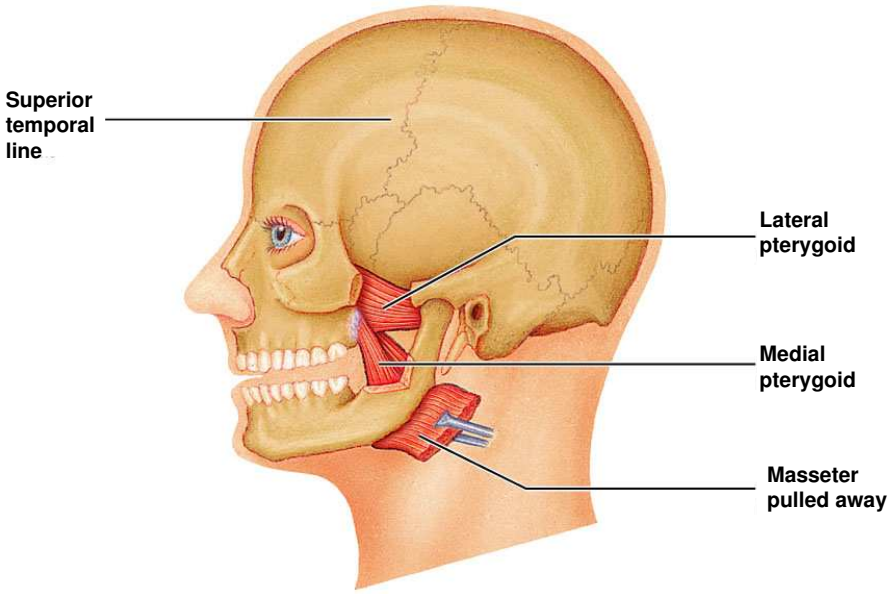

(b)

Figure 5.5: Muscles promoting mastication. a) Lateral view of the temporalis, masseter and buccinator muscles. b) Lateral view of the deep chewing muscles, the medial and lateral pterigoid (Marieb, 2004).

IIb according to Pruzanski criteria (Figure 5.6). This pathology is known as hemifacial microsomia (HFM) and consists of a congenital asymmetrical malformation

of both the bony and soft-tissue structures of the cranium and face. It varies in severity and emerges as a constellation of malformation of structures which arise from the first and the second branchial arch. It is the second most common facial birth defect after clefts (of the lip and palate), with an incidence of 1 in 5000 (Converse *et al.*, 1973; Gorlin *et al.*, 1990). It may affect aural, mandibular and dental development. Involvement is limited to one side most commonly, but bilateral involvement also occurs with more severe expression.

(a) (b)

Figure 5.6: Patient with hemifacial microsomia: a) before the treatment and b) after distraction osteogenesis.

The patient was treated with a multidirectional intraoral distraction device in order to correct the mandibular asymmetry (Figure 5.7). The treatment device consists of two distraction rods with gradually sliding clamps connected in the middle by a universal hinge (Figure 5.7). This hinge allows linear or angular correction in the sagittal plane and angular correction in the transverse, performed gradually. Therefore, the trajectory of bone segment movement can be changed during the distraction process.

This intraoral distraction device presents some advantages and disadvantages. As advantage we can mention its small dimensions and the absence of facial scars.

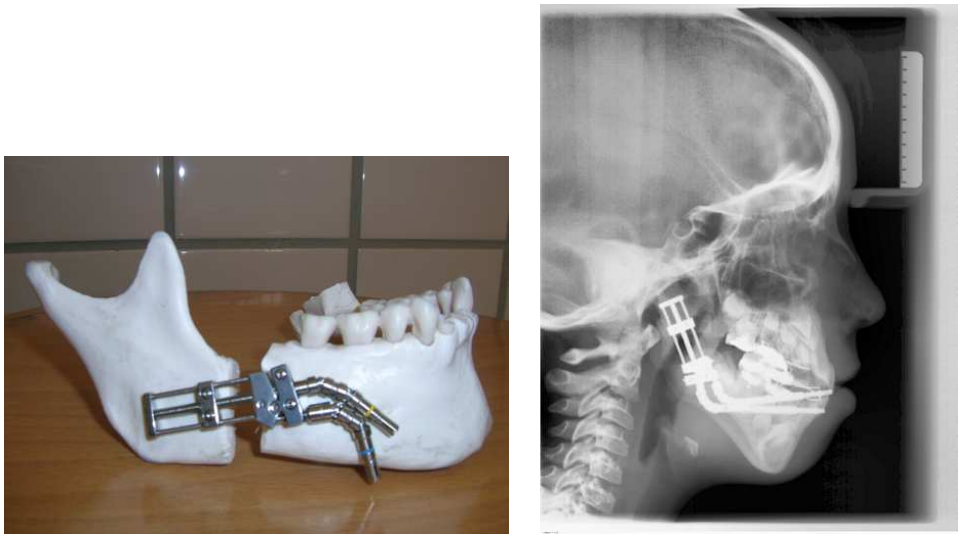

(a) (b)

Figure 5.7: a) Intraoral distraction device of the patient; b) Radiography of the patient showing the intraoral device used in the treatment.

However, one of the main limitations is related to the limited size of the device and the restricted access to the oral cavity.

Two different three-dimensional models of the patients' mandible were reconstructed from three-dimensional CT scans in the segmentation program MIMICS (Mimics, 2006). The *predistraction model* reflected the original morphology of the mandible before treatment and was used as the input geometry for the mechanobiological model (Figure 5.8a). The *postdistraction model* reflected the final morphology of the mandible after treatment (Figure 5.8b). In both cases, different regions were manually identified during the segmentation: cancellous bone, cortical bone and teeth. An additional 3D model, a *healthy idealized model*, was created. It was reconstructed from the pre-distraction model by symmetrically copying its non affected hemimandible (Figure 5.9a) with respect to the median plane at the symphyseal region (Figure 5.9b). These three geometries were meshed into finite element with 4-node tetrahedral elements (ANSYS ICEM®, Harpoon (2006)). Figure 5.10 shows the mesh of the different parts of the pre-distraction model.

In the following of the chapter two different analysis types are performed within this clinical case. First, a static analysis to analyze the strain field, mastication forces and reaction at condyles of the pre-distraction, post-distraction

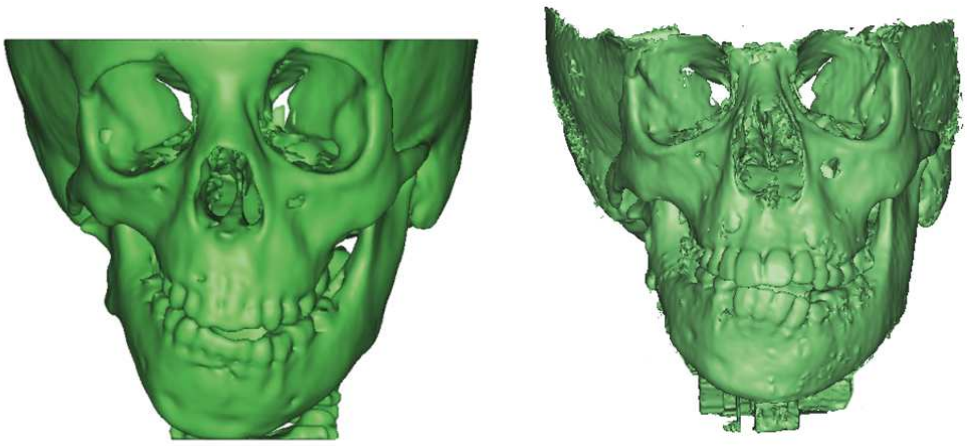

(a) (b)

Figure 5.8: a) Reconstructed geometry of the original morphology shows skeletal asymmetry due to hypoplasia of the right mandibular ramus; b) post distraction geometry of the patient.

(a) (b)

Figure 5.9: a) Geometry of the unaffected hemimandible and b) reconstruction of the *healthy* idealized mandible by applying an operation of symmetry with respect to the median plane in the symphyseal region.

and idealized healthy models. Secondly, a mechanobiological model to describe the evolution of the different tissues through the distraction process performed on the pre-distraction model.

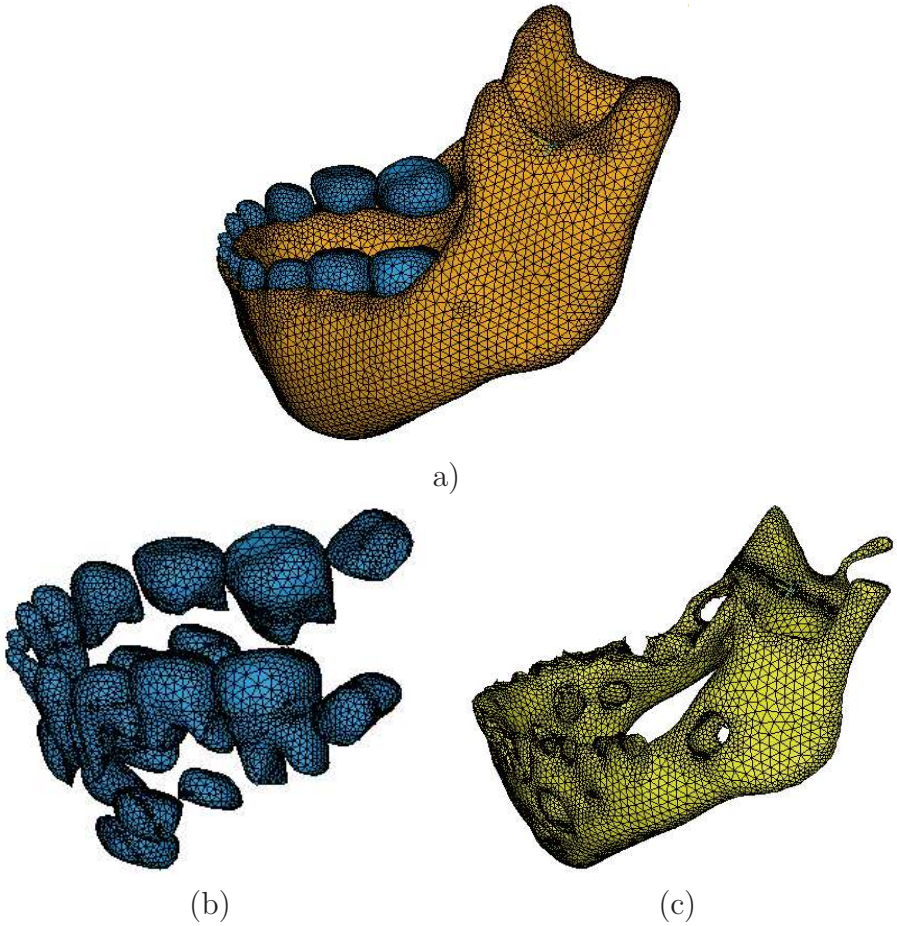

a)

(b) (c)

Figure 5.10: Finite element mesh of a) the mandible; b) the teeth and c) the cancellous bone of the affected mandible.

5.4 Biomechanical response of a mandible in a patient affected with hemifacial microsomia before and after distraction osteogenesis

In this section we aimed to compare the biomechanical behavior of the affected mandibles (pre- and post-distraction models) and the idealized healthy one during unilateral molar biting.

Three static finite element analysis were performed using the commercial software Abaqus®, simulating molar biting in different conditions: pre-distraction, post-distraction and idealized healthy mandibles. In the three analyzed models

(idealized healthy, pre-distraction and post-distraction), the different composing materials were all attributed linear elastic isotropic behavior. For bone tissue, we distinguished between cortical and cancellous bone, with respective values of the elastic modulus of 15750 MPa (Smit *et al.*, 2002) and 7900 MPa (Carter & Hayes, 1977) and Poisson's ratio of 0.325 (Smit *et al.*, 2002) and 0.3 (Carter & Hayes, 1977). The material properties of the teeth were assumed to be homogenous with values that correspond to those of the dentin (Craig & Peyton, 1958) (E=17600 MPa and ν=0.25).

5.4.1 Boundary and loading conditions

Functional loading

The model was loaded with force groups corresponding to the major masticatory muscles: superficial and deep masseter, medial and lateral pterygoid and the anterior, middle and posterior temporalis. The forces exerted by these muscles were imposed as external loads, distributed in the insertion area of each muscle. Figure 5.11 shows the nodes in which each force group was applied. In prescribing their values and orientations, we used the methodology of Korioth *et al.* (1992) (equation (5.1)). The orientation of the different forces is given by the unit vector coordinates of Table 5.2. These are referred to the global axes of Figure 5.11.

Table 5.2: Unit vector representing the orientation of the force produced by the muscles located in the right ramus of the mandible with respect to the global axes of Figure 5.11 (Korioth *et al.*, 1992)

Muscle	Force orientation		
	X	Y	Z
Sup masseter	-0.207	-0.419	0.885
Deep masseter	-0.546	0.358	0.758
Med pterygoid	0.486	-0.372	0.791
Lat inf pterygoid	0.630	-0.757	-0.174
Ant temporalis	-0.149	-0.044	0.988
Mid temporalis	-0.221	0.5	0.837
Post temporalis	-0.208	0.855	0.474

Significant differences exist between the degrees of right-left disproportion in

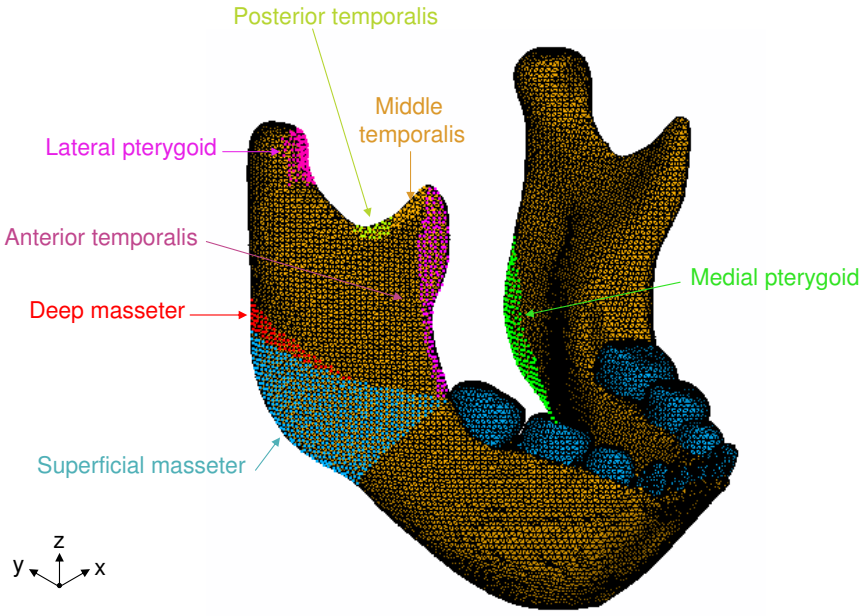

Figure 5.11: Insertions of the different portions of mastication muscles in the healthy idealized model.

masticatory muscles in hemifacial microsomia (Takashima *et al.*, 2003). In fact, the masticatory muscles on the affected side have been shown to exhibit varying degrees of hypoplasia or even to be altogether absent (Kane *et al.*, 1997; Marsh *et al.*, 1989; Murray *et al.*, 1984; Vento *et al.*, 1991). Therefore, the cross-sectional area of the different muscles must be defined in the affected and unaffected sides. This cross sectional area was calculated indirectly through the volume of the muscles and the fiber length (Van Eijden *et al.*, 1997). Van Eijden *et al.* (1997) measured the fiber lengths whilst Takashima *et al.* (2003) measured the volumes of the masticatory muscles in preadoslecent patients with hemifacial microsomia in both the affected and unaffected sides. Volumes, fiber length and cross-sectional area for each masticatory muscle of the unaffected side and affected sides are listed in Table 5.3. Note that Takashima *et al.* (2003) measured the volumes of the different muscles without considering the muscle portion (MP). Nelson (1986) did this muscle distribution and is also reported in Table 5.3. To completely calculate the force developed by the masticatory muscles, the muscle contraction values (EMG_i) must be defined for a given task. In this thesis only the activity of molar biting will be considered, since it is the most frequent biting in these

patients with anterior open bite. Values are reported in Table 5.3 for the ipsilateral and contralateral sides. Final forces values are summarized in Table 5.3 for the unaffected (U) and affected (A) sides in the case of molar biting.

Boundary conditions

Boundary conditions were imposed on the occlusal face of the molars and on the joint surface of the condyles. The former corresponded to a unilateral molar biting on the side in which the mastication takes place (right or left) and was simulated by simply restraining the vertical displacement of the molars that come in contact with the food. The latter aimed to reflect the mandibular fossa/condyle restriction and was simulated by fully restraining the movement along the normal direction of the top of the condyle. This was performed by creating a contact surface that simulates the mandibular fossa of temporal bone. Patients with grade IIb do not have any articular disc and thus the movement of the affected condyle was not restrained in both pre and post-distraction models. By contrast, in the ideal healthy model, both condyles are assumed to articulate and therefore their normal movement was also restrained.

5.4.2 Results

In this section we aim to compare the mandible strain field and deformed shape as well as the masticatory and reaction forces at the condyles for the three aforementioned cases: the *affected* mandibles (pre- and post-distraction) and the *idealized healthy* one during unilateral molar biting.

Before describing the results for the three different models, it suits to clarify that in the unilateral molar biting the term ipsilateral (working side) and contralateral (balancing side) refer to the side in which the food is situated and the opposite side, respectively.

Figure 5.12a shows the deformed and undeformed shape of the three analyzed mandibles for a molar biting on the right side. Viewed frontally, the mandible was rotated in a clockwise manner around the occlusal restraint in the pre and post-distraction models and in an anticlockwise direction in the healthy model. In the occlusal view, however, the displacement appears to be clockwise in the

Table 5.3: Volumes (measured in preadoslecent patients with HFM (Takashima *et al.*, 2003)), cross-sectional area (X_i) and fiber length (FL) of masticatory muscles of the unaffected (U) and affected (A) sides for patients suffering HFM; EMG_i for molar biting (Nelson, 1986) and final forces values developed by the masticatory muscles during molar biting in the unaffected and affected sides. I=ipsilateral, C=contralateral, MP=muscle portion.

Muscle	Volume $(cm^3)^1$		Part	MP[2]	FL $(cm)^3$	X_i (cm^2)		EMG_i [2]		F_i (N)[1,2,3,4]			
										U		A	
	U	A				U	A	I	C	I	C	I	C
Masseter	15.8	8.3	Superficial	0.7	2.46	4.89	2.57	0.56	0.20	109.54	39.12	57.57	20.56
			Deep	0.3	1.80	2.09	1.10	0.56	0.20	46.82	16.72	24.66	8.81
Medial Pterygoid	6.4	3.3		1	1.29	4.96	2.56	0.97	0.47	192.45	93.25	99.26	48.09
Lateral Pterygoid	6.1	3.5	Inferior	0.7	2.3	1.88	1.08	0.35	0.25	26.32	18.8	15.12	10.8
Temporal	10.3	5.6	Anterior	0.48	2.71	1.86	1.01	0.65	0.51	48.36	37.94	26.26	20.60
			Middle	0.29	2.64	1.12	0.61	0.60	0.53	26.88	23.74	14.64	12.93
			Posterior	0.23	2.57	0.89	0.48	0.54	0.54	19.22	19.22	10.47	10.47

1 (Takashima *et al.*, 2003)
2 (Nelson, 1986)
3 (Van Eijden *et al.*, 1997)
4 (Weijs & Hillen, 1984)

healthy model and anticlockwise in the two remaining models (Figure 5.12a).

The distribution of principal strains is shown in Figure 5.12b for the three models. Regions experiencing high magnitudes of tensile strains include the area around the occlusal restraint and the condyle of the working side in the healthy model (around 400 microstrains) and the condyle of the healthy ramus in the two other models.

In the healthy model, compressive strain was most severe (around -500 microstrains) around the occlusal bite point of the lingual border, the mandibular notch, the mandibular ramus of the working side and both condyles (Figure 5.12b).

By contrast, in the pre and post-distraction models, the articulated ramus of the mandible was subjected to higher magnitudes of tensile and compressive strains (around 3000 microstrains). Also, the lingual border experienced high values of compressive strain, mainly in the pre-distraction model.

Finally the total reaction forces found at the occlusal restraint are 255.1 N, 236 N and 362.7 N for the pre-distraction, post-distraction and idealized healthy models, respectively.

With regard to the molar biting with the left molar, for the affected models, results are not symmetrical with respect to those produced during the right molar biting, in contrast to the idealized healthy model (due to the symmetry in the geometry and boundary conditions). Viewed frontally, the pre-distraction mandible was rotated in a clockwise manner around the occlusal restraint and in an occlusal view in an anticlockwise manner as in the first load case. The post-distraction model also moves in the same directions in both perspectives. In addition, both tensile and compressive strains show higher strain magnitudes than the first load case. The symphyseal region experienced higher magnitudes of tensile strain on the labial surface than on the lingual side. Compressive strain, however, was found to be higher in magnitude in the lingual side than in the labial one. In this case, the mastication force resulted of 419.9 N, 303.9 N and 362.7 N for the pre-distraction, post-distraction and idealized healthy models, respectively. Figures are not shown due to their similarity to the first loading case.

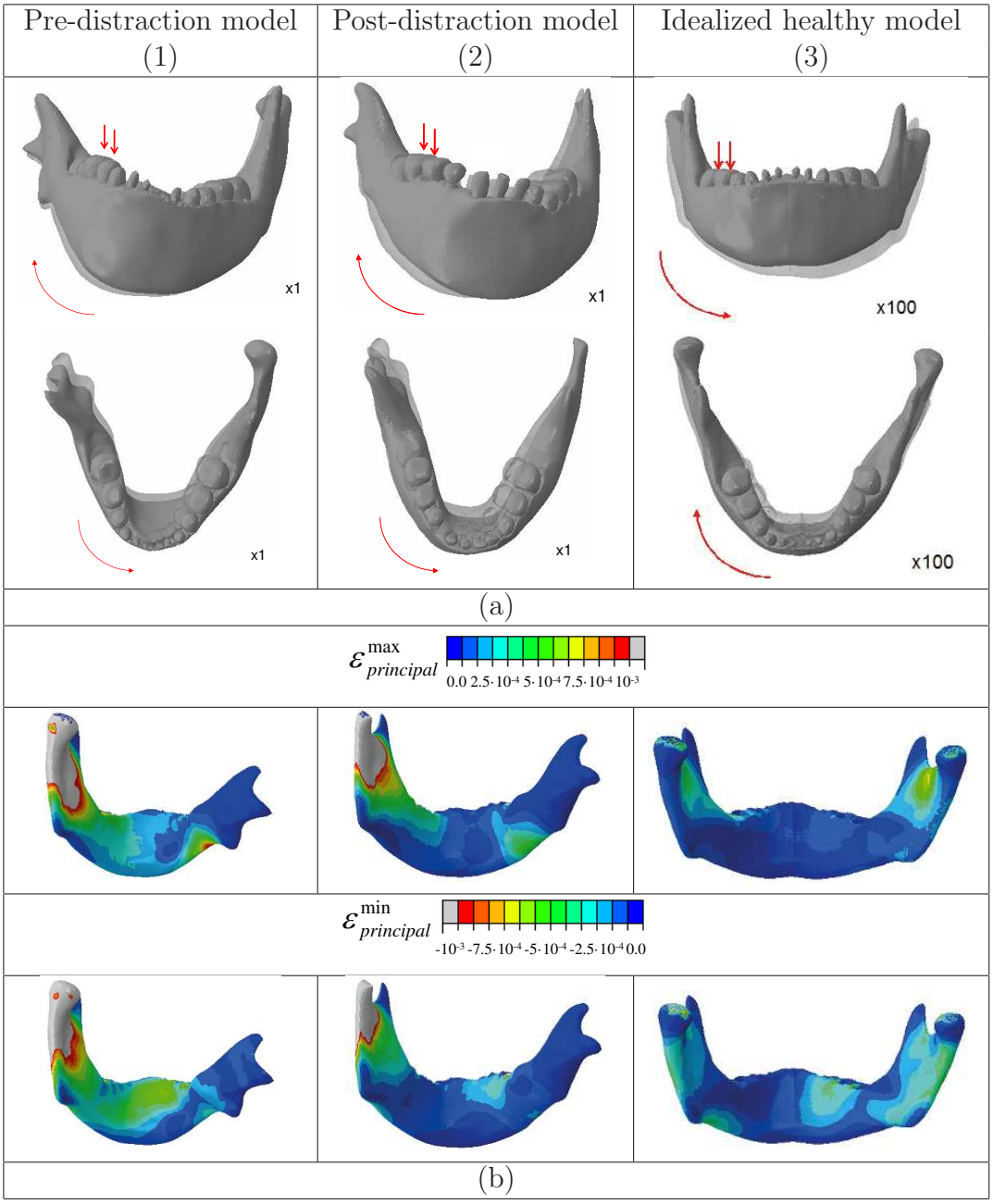

Figure 5.12: a) Frontal and occlusal (dorsal) views of the pre-distraction, post-distraction and idealized healthy mandibles in their undeformed state (light gray) and in their deformed state (dark gray) (magnified by a factor of 100 in the healthy model); b) Maximum (tensile) (ε_{pr}^{max}) and minimum (compressive) (ε_{pr}^{min}) principal strains of the hemimandibles in the pre-distraction, post-distraction and idealized healthy mandibles. Molar biting in the right side (which is the most common in this patient).

5.4.3 Discussion

In this study the distributions of tensile and compressive strains as well as the mastication forces and displacements were calculated in a mandible affected with HFM. Analysis of the principal strains in the healthy and affected mandibles reveals larger strains in the affected cases, compared to the healthy one. The distribution of strain is also much more symmetrical in the healthy case than in the affected models, both in tension and compression. However, from Figure 5.12b, it can be appreciated that strain distribution in the post-distraction model is qualitatively and quantitatively much more similar to the healthy model than the pre-distraction one. This reveals, to some extent, the success of the clinical procedure. In all cases strain magnitudes were lower than 3000 microstrains, which is within the physiological range measured experimentally. *In vivo* bone strains have been directly measured on the external surface of bones, obtaining values in the range of approximately $50-4000$ microstrains for most activities for various animals (Rubin & Lanyon, 1984), and up to 2500 microstrains in humans (Burr *et al.*, 1996; Frost, 1998).

The displacement field is very similar in the pre and post-distraction models for both load cases. By contrast, this deformed shape is not comparable to that of the healthy model, being similar to that computed by Korioth *et al.* (1992). The differences between the three models are mainly due to the different boundary conditions and forces exerted by the muscles. Unlike the healthy model, the affected TMJ of the post-distraction model was considered to not recover and hence to not articulate with the mandibular fossa of temporal bone, allowing rotations as a rigid body with high amplitudes. This is probably the critical point with regard to the deformed shape of the mandible.

In order to compare the different results, Table 5.4 summarizes the mandibular condylar forces in the balancing and working sides as well as the forces of mastication in all the analyzed cases. As observed, these results indicate a magnitude of the force transmitted through the healthy condyle of the same order for all the load cases and geometries analyzed. Many *in vivo* tests have measured mandibular condylar forces during jaw function. Breul *et al.* (1999), using magnetic resonance imaging (MRI) scans of the TMJ, show that the TMJ was

subjected to compressive forces during occlusion as well as during mastication. Results of our analysis also show compressive forces over the TMJ (Table 5.4). In addition, dos Santos (1995) came to the result that nearly 31% of the total force applied is supported by the TMJ and 69% by the occluding teeth. In our healthy case, 40% of the total force went through the TMJ and the remaining 60 % to the mastication forces.

Table 5.4: Reaction forces in the condyles ($\mathbf{F}$) and mastication forces ($\mathbf{F}_{\text{mastic}}$) in the different cases analyzed (I: ipsilateral; C: contralateral).

			$\mathbf{F}_x$ (N)	$\mathbf{F}_y$ (N)	$\mathbf{F}_z$ (N)	$\mathbf{F}$ (N)	$\mathbf{F}_{\text{mastic}}$ (N)
Healthy model	Mastication in left side	I	56.55	85.47	-57.54	117.53	-362.7
		C	-36.06	37.42	-116.4	127.47	
	Mastication in right side	I	-56.55	85.47	-57.54	117.53	-362.7
		C	36.06	37.42	-116.4	127.47	
Pre-distraction model	Mastication in healthy side	I	31.56	110	-35.81	119.91	-419.9
		C	0.	0.	0.	0.	
	Mastication in affected side	I	0.	0.	0.	0.	-255.1
		C	1.54	81.48	-116.6	142.26	
Post-distraction model	Mastication in healthy side	I	31.57	107.7	-134.5	175.17	-303.9
		C	0.	0.	0.	0.	
	Mastication in affected side	I	0.	0.	0.	0.	-236.3
		C	2.08	79.20	-121.5	145.05	

With regard to the mastication forces, we will focus on the first load case (mastication with the right molars) since patients with mandible asymmetries tend to chew with the osteotomy side (Naeije & Hofman, 2003). It can be seen that mastication forces are greater in the healthy model than in the affected ones which is in agreement with experimental evidences (Sato *et al.*, 1999). On the other hand, the bite force predicted in the healthy mandible (363 N) correlates well with the values measured for molar bite force in children of the same age (330 N, Sonnesen *et al.* (2001)). Bite forces measured in adult mandibles are also of the same order of magnitude (526 N (Korioth *et al.*, 1992); 569 N (Finn, 1978); 515 N (Nelson, 1986)) although higher since bite force increases with age (Bakke *et al.*, 1990; Kiliaridis *et al.*, 1993).

This study presents several limitations that need to be addressed. Firstly, the different constituents of the model were assumed linear elastic isotropic behavior

although mandibular bone should have been modeled as orthotropic. However, for a mandible loaded by occlusal forces, the orthotropic model is just 10 % more accurate than the much simpler isotropic model (Boccaccio *et al.*, 2006). Also, the teeth have been assigned one single material property being aware that they are composed of different materials (enamel, dentin, pulp and cementum). Secondly, only the main masticatory muscles have been included in this model. Others, such as neck muscles (digastric and milohyoid) also contribute to the masticatory process and should be considered in future works. Moreover, the possible strengthening of the muscles after distraction has not been included in the post-distraction model. Further, the cross sectional area of the muscles considered in this study has been taken from literature data. More accurate values could have been measured through MRI although this has not been done for ethical reasons. Finally, future work should model more precisely the TMJ.

In this study we have performed a biomechanical analysis in both healthy and altered conditions of a subject-specific mandible. It was found that the overall mechanical response of the pre-distraction model is very different from the healthy one and that the strain distribution of the post-distraction and healthy models was similar. This shows the success of the DO process from a biomechanical point of view. Also, the comparison of the different magnitudes measured in the different cases show that this model is a useful tool to understand the normal function and to predict changes due to alterations, such as those produced in cases of HFM. However, further works are needed in order to be able to pre-clinically test the mechanical consequences of a planned DO procedure.

5.5 Three dimensional simulation of mandibular distraction osteogenesis: mechanobiological analysis

The aim of this section is to apply the previously developed model of distraction osteogenesis (chapter 3) to investigate its ability to predict the main tissue patterns during the course of the three dimensional lengthening procedure of the mandible ramus. Considering the irregular shape of the mandible, it might be

questionable whether two-dimensional models adequately capture the structural characteristics of the bone.

5.5.1 Model description

This study was based on the same patient as in section 5.4. The three-dimensional model of the mandible corresponded with the original morphology of the mandible before treatment, i.e., predistraction model of section 5.3. Also, the same segmentation procedure was followed although, in this case, an additional region was identified: the gap. The right ramus of the predistraction model was virtually cut simulating the osteotomy at the location indicated by the surgeon (Figure 5.13). Four different regions were therefore identified during the segmentation procedure of this model: gap, cancellous bone, cortical bone and teeth (Figure 5.13).

With regard to the clinical distraction protocol, the full process includes a 7-day latency period and a phase of distraction of 20 days, followed by a consolidation period of 4 months. During the distraction phase, the mandible was distracted at a rate of 0.5 mm every 12 hours during 8 days, and to avoid pain, at a rate of 0.25 mm every 6 hours during the following 12 days. Changes in the angulation of the device were performed, at days 15, 17, 22 and 29 after the beginning of distraction. Thus, four angular changes of 7 degrees were done, with a total angular deformation of 28 degrees at the end of the distraction process.

5.5.2 Numerical implementation

The numerical implementation of the model includes four uncoupled finite element analyses combined with a remeshing process. The mathematical model applied is that described in Chapter 3, and therefore the numerical implementation is similar to that explained in section 3.4 although the remeshing process differs slightly. It consists on the following steps:

1. *Finite element analyses*: four un-coupled finite element analyses are implemented for each time step in the commercial programm Abaqus®: a poroelastic analysis to compute the mechanical stimulus, a thermoelastic

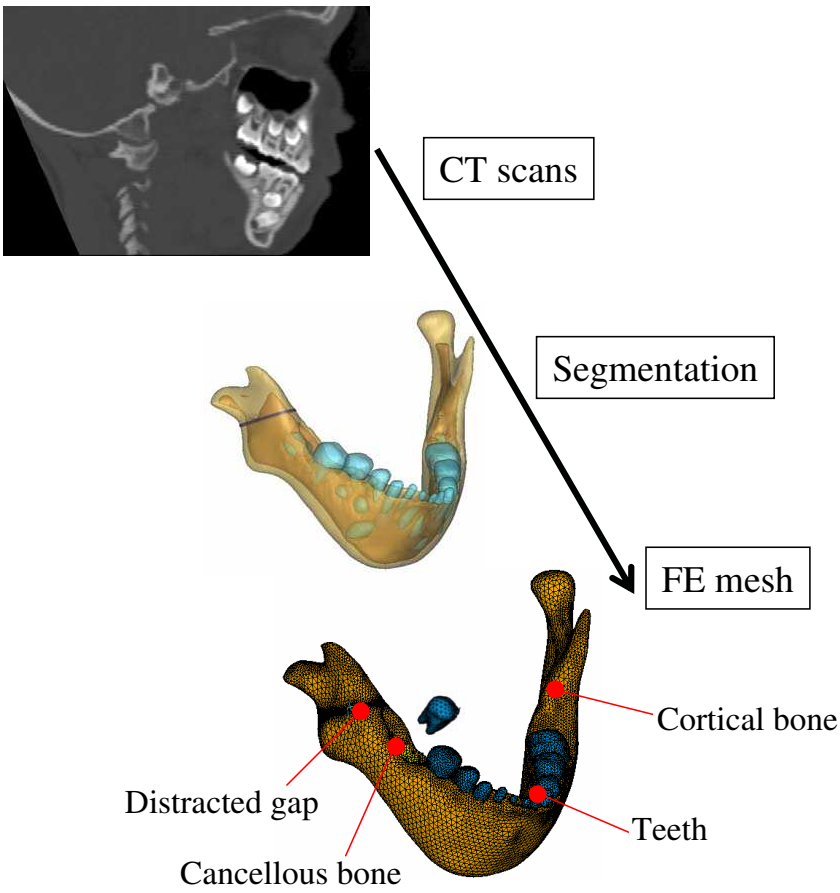

Figure 5.13: Procedure for generating a 3D FE model of the mandible from CT scans.

analysis to model callus growth and two diffusion analyses to simulate the MSC migration and to consider indirectly the vascularization. The new geometry of the gap is defined by the nodal displacements obtained in the thermoelastic analysis (Figure 5.14b).

2. *Update state variables.* Cell concentrations, extracellular matrices as well as cellular maturation levels are updated according to the equations that define the evolution of the different cells, the matrix production and the maturation levels (see chapter 3), respectively.

3. *Checking the old mesh.* Excessive distortion of the mesh may occur and thus the elements of the old mesh are checked regarding the angle of distorsion

and the aspect ratio. If all the elements pass the check go to step (1), otherwise go to step (4).

4. *Remeshing.* In this step the elements are remeshed in the commercial program Ansys® generating new undistorted elements located at the same position as the old ones (Figure 5.14c).

5. *Variables interpolation.* Given the old and the new meshes, the variables are then interpolated to the integration points of the new geometry with Matlab® and the new values are then used as initial conditions for the following step (Figure 5.14d) (go to (1)).

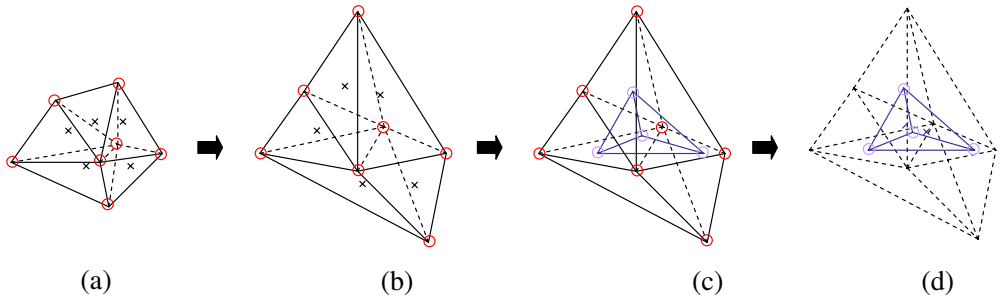

Figure 5.14: Remeshing implementation in 3D. a) Old mesh integration points before the loading process; b) old mesh nodes after the loading process; c) new mesh nodes; d) new mesh integration points.

In order to reduce the computational cost, these simulations are only performed in the gap. Therefore, for the gap we assumed biphasic behavior with the material properties reported in table 3.2. In the remaining regions of the model, as we are not interested in the evolution of tissues and cellular populations, we considered linear elastic isotropic behavior with the values summarized in section 5.4.

With regard to the boundary conditions needed for the numerical implementation, sources of MSCs were considered in the marrow cavity, periosteum and in the surrounding soft tissues for the diffusion analysis (Gerstenfeld *et al.*, 2003); the initial boundary conditions for the ossification front consisted of preosteoblastic sources in the areas of the endosteum and periosteum closest to the cortical bone.

Additionally, as the mandible is affected by a grade grade IIb according to Pruzanski criteria, the affected condyle does not articulate with the mandibular fossa and thus its movement is not restrained. The normal displacement of the healthy condyle, by contrast, is restrained as in section 5.4.1. The vertical displacement at the nodes of the surface of the right molars are also restrained according to clinical data.

5.5.3 Results

In this study, during the entire process of distraction, the tissue distribution varies significantly. Initially, due to the high values of the mechanical stimulus, part of the new tissue within the gap gets damaged at the osteotomy site leading to a gap mostly filled with debris tissue. During the initial stage (1-10 days), tissue damage is gradually reduced due to the decreasing values of the strain magnitudes allowing granulation tissue to be deposited (Figures 5.15 and 5.16). This granulation tissue is synthesized by MSCs that migrate from the marrow cavity, periosteum and surrounding soft tissues to the interfragmentary gap. At this time point small amounts of cartilage tissue appear in the distracted gap. As distraction proceeds, the low stimulated mechanical environment around the two bone fragments leads to bone formation. From day 15 until the end of the distraction process more amount of cartilage can be seen in the outer part of the callus. Immediately following completion of 20 mm, the distraction outcome shows a gap filled with cartilage tissue, constituting most of the regenerate surface. The area of new bone formation was located close to the host bones and the remaining gap was filled with cartilage tissue.

5.5.4 Discussion

The purpose of this study was to expand upon our previous axisymmetrical models to determine the patterns of tissue formation in a realistic, three dimensional geometry.

Finite element results show a tissue distribution within the gap that concurs with experimental evidences. In the first stage of the process, granulation tissue is gradually deposited in the gap, repairing the initial damage and replacing the

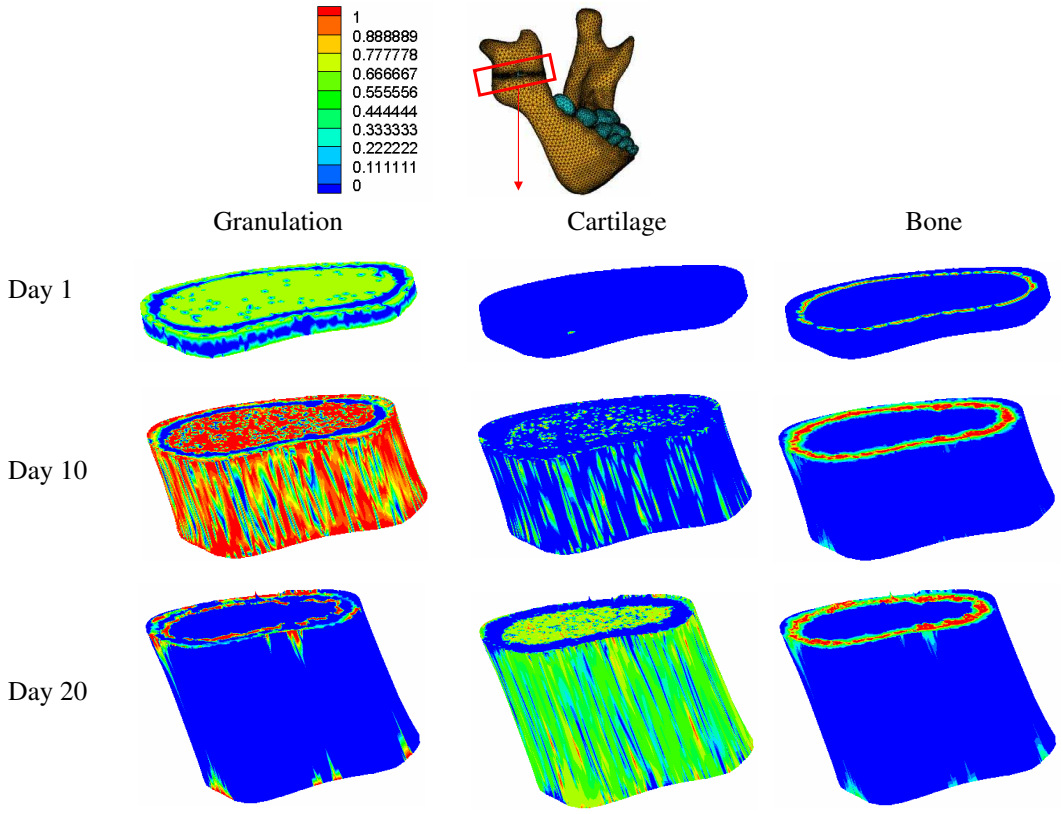

Figure 5.15: Tissue distribution in the mandible at days 1, 10 and 20 of the distraction procedure.

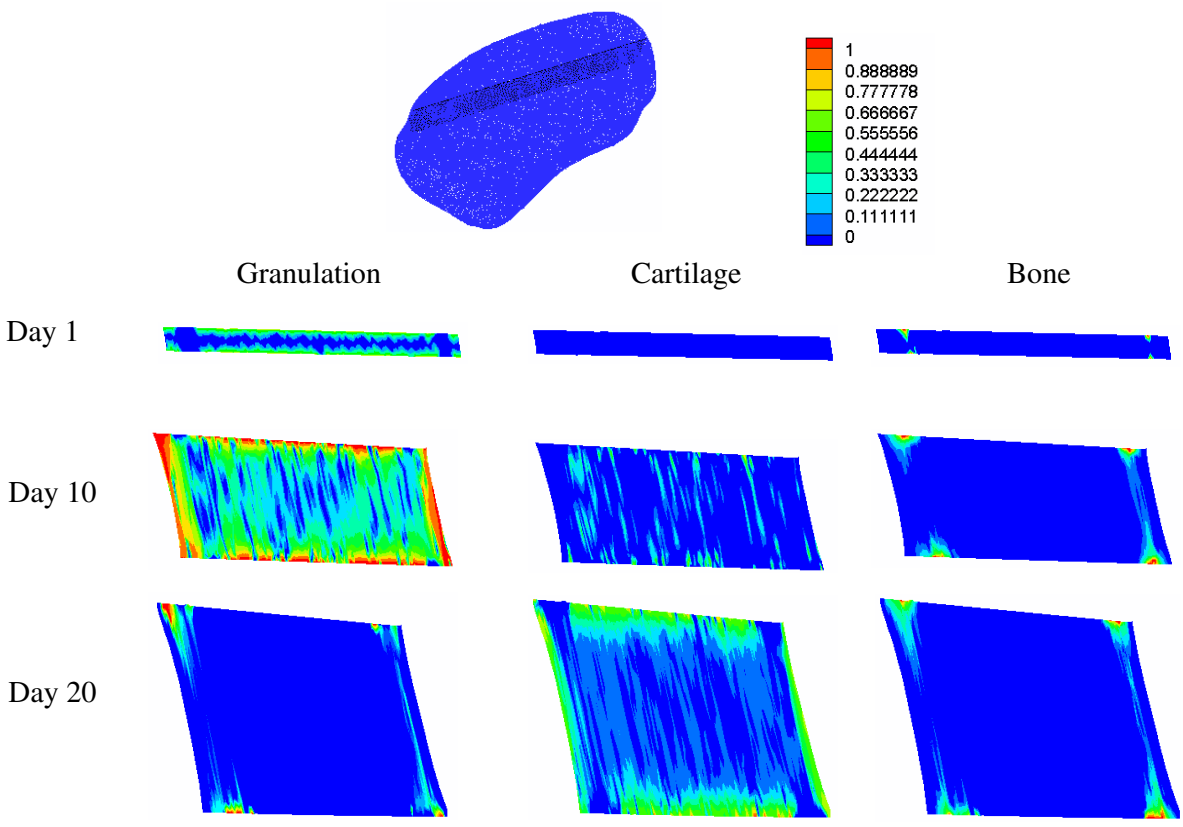

Figure 5.16: Sections through the thickness of the callus at days 1, 10 and 20 of the distraction procedure.

necrotic tissue. As distraction proceeds cartilage cells begin to mature and new bone appears next to the host bones.

Also, the geometry at the end of the distraction procedure was very similar to that obtained clinically (Figure 5.17). The CT scans used to reconstruct the mandible were taken at the end of the consolidation phase whilst the finite element mandible corresponds with the geometry of the lower jaw computed at the end of the distraction period. This might explain the small differences between both cases.

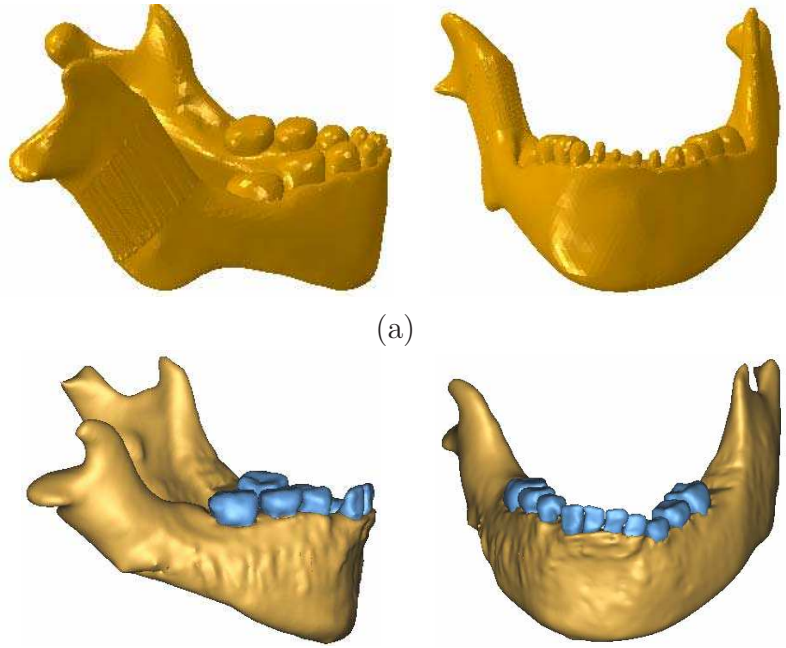

Figure 5.17: a) Finite element geometry after the distraction procedure; b) reconstructed mandible of the final morphology from CT scans.

Mechanobiological studies yet published in long bone simulations of distraction osteogenesis assume axisymmetric geometries (Isaksson *et al.*, 2007). In the mandible, Boccaccio *et al.* (2007, 2008) have performed three-dimensional approaches of the lengthening procedure in the symphysis. This part of the mandible is regular and very similar to long bone lengthening procedure. Their protocol of distraction last up to ten days. Thus, they did not need any remeshing process. In contrast, in this study the mandible ramus, which is much more

irregular in shape will be lengthened for 20 days a total of 20 mm. Therefore, we have improved on existing three dimensional numerical models of distraction osteogenesis by including the remeshing procedure.

This model presents several limitations that need to be discussed. Firstly, as already discussed in Chapter 3, all the mathematical formulation is developed under the small deformations assumption and a free stress state is assumed as initial condition for each day analyzed numerically. Secondly, the distraction orthodontic device has not been modelled, since the main goal of this study was to evaluate the tissue distribution outcome within the gap. Instead, the distracted displacement was directly applied on the top of the cortical bone. However, this simplification does not affect significantly the finite element prediction. Thirdly, only the distraction phase was simulated. Further studies should also consider the consolidation and latency periods. Fourthly, mastication loads were neglected, assuming them to be much smaller than the distracted loads.

This model presents a preliminar three dimensional approach of distraction osteogenesis from a computational perspective. Although it should be further extended in the future, it shows the enormous potential it offers. It could be used to study different aspects of the distraction procedure such as the effect of the distraction rate, the best placement of the corticotomy or the time of the device removal amongst others.

Chapter 6

Closure

6.1 Summary

This document presents a new model of distraction osteogenesis that predicts the spatial and temporal features of the process around the osteotomy site. The cellular events underlying distraction osteogenesis, namely proliferation, migration and differentiation as well as tissue growth and tissue damage have been implemented with a mathematical model formulated previously for fracture healing (Gómez-Benito *et al.*, 2005). This model has been extended further by introducing two new perspectives in the formulation of the differentiation processes. Firstly, the load history has been considered in the differentiation through a linear cumulative law similar to Miner's fatigue damage accumulation rule (Miner, 1945). This concept is based on the assumption that cells are able to change their differentiation pathway depending on the influences of the local mechanical environment. This potential reversibility is denoted as tissue *plasticity* (Roder, 2003). To validate the model, simulations have been performed in a wide variety of mechanical environments and have been compared to different experimental settings. It has been demonstrated that the model is able to explain classic results, such as the observed influence of the distraction rate on tissue outcome or the main interspecies differences.

Additionally to the above described new differentiation approach, another important feature of soft tissues, namely residual stresses is investigated in the field

of bone lengthening. In contrast to the previous simulations that consider a complete relaxation of the tissue during the daily loading process, here we assume that a stress free configuration prior to the daily loading is unlikely in most tissues and not realistic as observed in clinical and animal studies (Brunner *et al.*, 1994; Waanders *et al.*, 1998; Matsushita *et al.*, 1999; Richards *et al.*, 1999). In particular, we propose a new growth mixture model which assumes that stress relaxation is regulated by matrix production. In this sense, the formulation proposed considers that the strain response is regulated by the time varying matrix production, which is consistent with the formulation proposed by Humphrey & Rajagopal (2003).

Besides, computational simulations have also been implemented in three dimensional models. These studies are based on data from a young male patient with unilateral mandibular hypoplasia of the right mandibular ramus which was treated with distraction osteogenesis. The 3D model of the patients' mandible was reconstructed from three-dimensional CT and the process was successfully simulated following the clinical protocol of distraction.

6.2 Conclusions

The major conclusions of this thesis can be formulated as follows:

- The load history during cell differentiation has been shown to be crucial when predicting the effect of the distraction rate on the process of bone formation within the distraction gap. Previous studies have successfully simulated low distraction rates (Isaksson *et al.*, 2007) but have failed in predicting nonunions at high distraction rates, where the load history plays a decisive role.

- The rate of distraction was predicted to have an important effect on the outcome of distraction osteogenesis. Low distraction rates resulted in premature bony union, whereas a fast rate resulted in a fibrous union or nonunion.

- It has been shown that the inclusion of the pre-traction stresses in distraction osteogenesis models is necessary for a correct prediction of the force

required to distract with material properties in agreement with the literature. Existing models used high values of the material properties to be able to reproduce the stiffening behavior observed experimentally during the lengthening procedure.

- Although accurate force predictions during distraction osteogenesis with realistic material properties need the inclusion of pre-traction stresses, tissue distributions are not so much dependent on that showing similar results with and without residual stresses.

- The model consistently predicts tissue pattern in different animal species and a human case: the computed reaction force at the end of the distraction phase is one order of magnitude lower in the rabbit than in the human and sheep, and more cartilage is formed in the rabbit than in the human and sheep cases.

- The three dimensional simulation of the mandibular distraction osteogenesis process in a case of hemifacial microsomia has shown that the strain distribution in the post-distraction model is qualitatively and quantitatively much more similar to the healthy model than the pre-distraction one. This reveals, to some extent, the success of the clinical procedure from a biomechanical point of view.

6.3 Original contributions

For the development of this dissertation, the model of distraction osteogenesis has been developed in the commercial finite element software Abaqus®. In particular, this software was used to solve the poroelastic, thermoelastic and the two diffusive analyses explained in section 3.4. The poroelastic analysis has been implemented within two different subroutines. The former was coded to account for the load history in the differentiation process in a subroutine that defines the material's mechanical behavior (UMAT). The latter included the growth mixture model that considers the residual stresses in a User element subroutine (UEL) of Abaqus. All these subroutines were performed using Fortran 95. Besides, the

daily remeshing performed to avoid an excessive distorsion of the elements was implemented in Ansys® and Matlab®. Moreover, other softwares have been employed during this research. The management of CT scans has been made in Mimics®, the generation of meshes in Harpoon® and Ansys ICEM® and the visualization of results in Tecplot®.

The main contributions of this thesis are listed in the following points:

- A new approach to model cell differentiation was used through the load history. It abandons the classical view of a direct differentiation of stem cells commonly used in mechanobiological models of fracture healing and distraction osteogenesis.

- Computational simulation of distraction osteogenesis in bidimensional and three dimensional models. Both long bones and mandibles have been simulated. In both cases important geometric changes take place during the simulation and a remeshing is needed.

- Analysis of different mechanical environments in the process of distraction osteogenesis. In particular, the effect of the distraction rate on the outcome of the distraction procedure was evaluated.

- Interspecies analysis to assess the effect of different geometrical environments on bone regeneration during limb lengthening. Reaction forces and tissue distributions were computed in different animal species and the human case.

- Formulation of a growth mixture model that includes the pre-traction stresses in distraction osteogenesis. The model simulates the process of long bone lengthening assuming a non-free state prior to the daily loading process.

6.4 Publications

The main results of this work have been partially published in the following journals and conferences or are in preparation:

6.4.1 Journals

- Reina-Romo E., Gómez-Benito M.J., García-Aznar J.M., Domínguez J., Doblaré, M. (2009). Modeling Distraction Osteogenesis: Analysis of the distraction rate. *Biomechanics and Modeling in Mechanobiology.* 8: 323-35.

- Reina-Romo E., Gómez-Benito M.J., García-Aznar J.M., Domínguez J., Doblaré, M. Growth mixture model of distraction osteogenesis: effect of pre-traction stresses. *Biomechanics and Modeling in Mechanobiology.* In Press, DOI: 10.1007/s10237-009-0162-5.

- Reina-Romo E., Gómez-Benito M.J., García-Aznar J.M., Domínguez J., Doblaré, M. An interspecies computational study on limb lengthening. *Manuscript submitted for publication.*

- Reina-Romo E., Sampietro-Fuentes A., Gómez-Benito M.J., García-Aznar J.M., Domínguez J., Doblaré, M. Biomechanical response of a mandible in a patient affected with hemifacial microsomia before and after distraction osteogenesis. *Manuscript submitted for publication.*

- Reina-Romo E., Sampietro-Fuentes A., Gómez-Benito M.J., García-Aznar J.M., Domínguez J., Doblaré, M. Three-dimensional simulation of mandibular distraction osteogenesis: mechanobiological analysis. *In preparation.*

6.4.2 Conferences

- Reina E., Gómez-Benito M.J., García-Aznar J.M., Domínguez J., Doblaré, M. Modelo computacional de distracción ósea. CMNE/CILAMCE, Semni. Oporto, Portugal, June, 2007.

- Reina E., Gómez-Benito M.J., García-Aznar J.M., Domínguez J., Doblaré, M. Influence of distraction rate on the outcome of distraction osteogenesis: computational simulation. European Society of Biomechanichs Workshop 2007. Dublin, Ireland, August, 2007.

- Reina E., Gómez-Benito M.J., García-Aznar J.M., Domínguez J., Doblaré, M. Influencia de la velocidad de distracción en la regeneración ósea. Modelo computacional. 8^o Congreso Iberoamericano de Ingeniería Mecánica. Cusco, Peru, October, 2007.

- Reina-Romo E., Gómez-Benito M.J., García-Aznar J.M., Domínguez J., Doblaré, M. Simulating limb lengthening in an interspecies' analysis. Biomechanics and Biology of Bone Healing. Berlin, Germany, May 2008.

- Reina-Romo E., Gómez-Benito M.J., García-Aznar J.M., Domínguez J., Doblaré, M. Different animal models of bone distraction. 5^{th} European Congress on Computational Methods in Applied Sciences and Engineeering (ECCOMAS 2008). Venice, Italy, July 2008.

- Reina-Romo E., Gómez-Benito M.J., García-Aznar J.M., Domínguez J., Doblaré, M. Limb lengthening: Influence of the load history. 16^{th} Congress European Society of Biomechanics. Lucerne, Switzerland, July 2008.

- A. Sampietro Fuentes, E. Reina-Romo, M Ferrer Molina. Análisis biomecánico de la distracción ósea en mandíbula: comparativa clínico-experimental. 55 Reunión de la Sociedad Española de Ortodoncia. Valencia, Spain, June 2009.

- Reina-Romo E., Sampietro-Fuentes A., Gómez-Benito M.J., García-Aznar J.M., Domínguez J., Doblaré, M. Estudio tensional antes y después de la distracción osteogénica mandibular en una caso de microsomía hemifacial. Semni. Barcelona, Spain, July 2009.

- Reina-Romo E., Sampietro-Fuentes A., Gómez-Benito M.J., García-Aznar J.M., Domínguez J., Doblaré, M. Simulación numérica del proceso de distracción osteogénica mandibular en un caso de microsomía hemifacial. 9^o Congreso Iberoamericano de Ingeniería Mecánica, Las Palmas de Gran Canaria, Spain, November 2009.

6.5 Future work

Distraction osteogenesis is an active field which is continuously under investigation. In fact it still remains one of the most unknown phenomena of bone biology. Moreover, surgeons lack of established instructions to correctly define the specific patient planning of the process.

Therefore, the possible improvements in this field are innumerable, in both experimental and computational perspectives. In particular, several extensions of the model are planned for the future. These are summarized as follows:

1. Future work in the computational perspective:

    - Modeling the latency and remodeling phases.
    - Distraction osteogenesis is a clear example of large deformations. However, the lack of data about the real behavior of tissues involved in the regenerated gap under large deformations limits its current numerical application. Therefore, future work should focus on characterizing the mechanical behavior of these tissues under large deformations.
    - Simulating long bone lengthening in complex geometries and perform patient specific models. In particular, finite element simulations of bone distraction may be developed based on high order shape functions that properly represent the geometry (isogeometric analysis, NURBS). Also, these analyses can be extended and adapted to the the process of distraction, where a growing geometry takes place. In this case, the mesh could adapt to the changes of geometry that take place during the clinical procedure and therefore the remeshing could be avoided.
    - Another point to be improved regards cell migration, which has been simulated following a standard diffusion equation. However, it is well known that cell movement is not random and nondirected, but a much more complex phenomenon. For example, recently, cell motion has been found to be guided by the substrate compliance and prestrain (Lo *et al.*, 2000; Wong *et al.*, 2003; Schwarz & Bischofs, 2005). These aspects should be included in future works since cell migration plays a central role in distraction osteogenesis.

- Residual stresses have been assumed to be regulated by matrix production. However, future studies should also include an additional force relaxation due to volumetric growth.

- The growth process is assumed in our model to be solely due to proliferation of MSCs and chondrocytes hypertrophy (Gómez-Benito *et al.*, 2005). However, volumetric growth due to matrix production is not negligible and should be included in future models to achieve more realistic results.

- Related to the previous points, a micro-macro approach could be performed in order to introduce a higher magnification scale and thus reduce the number of parameters. Events such as cellular differentiation, proliferation and migration could be simulated at the microstructural level and later homogenized to the macro level.

- Moreover, we should further extend the model to study asymmetrical rules in the differentiation theory. There is currently an active discussion on whether cartilage forms in tensile environments such as distraction osteogenesis. Many studies report intramembranous ossification in the distracted gap (Ilizarov, 1989*a*,*b*; Aronson *et al.*, 1989; Delloye *et al.*, 1990; Shearer *et al.*, 1992; Ganey *et al.*, 1994; Schenck & Gatchter, 1994). However, almost all the existing mechanobiological models propose differentiation rules that are symmetrical with respect to the type of loading (Prendergast *et al.*, 1997; Gómez-Benito *et al.*, 2005) and therefore consider cartilage formation under tensile and compressive environments. In contrast, the tissue differentiation diagram proposed by Claes & Heigele (1999) includes this asymmetry and cartilage is only deposited in compressive environments. Therefore in Appendix B this differentiation theory has been applied and extended to the case of distraction osteogenesis to analyze whether existing asymmetrical mechanobiological rules are able to predict patterns in distraction osteogenesis that may be more realistic. The model has been validated to some extent, by simulating the effect of the fixator stiffness on the young regenerate bone after distraction osteogenesis

although further work is needed in order to fully validate the model.

2. Future work in the experimental perspective:

   - The validation issue is of main concern in models of distraction osteogenesis. The bibliography displays a large amount of data but with high variability. Therefore, in a close future, experiments of distraction osteogenesis must be performed in order to check the validity of all the assumptions and parameters chosen. Within this purpose, future work must be focused on:
     - Defining and preparing the animal experiments to be carried out, focusing on the type of specie, the distraction procedure aimed to perform, the different distraction protocols of interest and the parameters to be recorded through the process amongst others. For example, the force between the distracted gap and the fixator after pulling could be measured as well as the residual stresses stored in the bone after each daily lengthening procedure.
     - Distractor design and manufacturing. The optimum design must be carefully developed to ensure stability of the regenerate, as well as optimum clinical conditions.
     - Electronic instrumentation development to measure different magnitudes, such as load.

These future developments of the model reveal the interdisciplinary character of this process, since mechanical, biological as well as medical aspects need to be considered all together. The accomplishment of these goals would contribute to optimize the current treatment strategies. Presently, noninvasive procedures such as plain radiography have been used clinically to determine when the regenerate bone is capable of functional loading. However, the correlation between radiographic density and the biomechanical integrity of newly formed bone is poor. Therefore, more reliable quantitative and qualitative approaches need to be developed in order to determine the optimal protocol of distraction.

Appendix A

Permeability theory

A.1 Soft tissues permeability

The permeability (k) in soft tissues was computed from their composition, mainly the permeability of collagen fibrils (k_{col}) and ground substance (k_{gs}) (Levick, 1987):

$$k = \frac{1}{(1/k_{col}) + (1/k_{gs})} \tag{A.1}$$

The permeability of collagen fibers is determined as a function of the fiber radius, the volume they occupy and also the Kozeny coefficient which accounts for the effect of the friction between fluid and fibers. The permeability of the ground substance is a function of its content in glycosaminoglycans and proteoglycans. The permeability of these components is determined via the medium length of the fibers which form it. All these relations are correlated following the work of Levick (1987).

Permeability of collagen fibers is determined by:

$$k_{col} = \frac{(1 - V_{col}^h)^3 \cdot r_{col}^2}{4 \cdot G_{hb} \cdot (V_{col}^h)^2} \tag{A.2}$$

where r_{col} is the collagen fiber ratio which varies between 20, 30 and 50 nm according to the type of tissue, granulation, fibrous and cartilage (Levick, 1987); V_{col}^h is the effective volume occupied by the collagen fibers including interstitial

water; G_{hb} is the Kozeny coefficient which accounts for the friction effect between the fluid and the surfaces.

The effective volume occupied by the collagen fibers is slightly higher than its specific volume due to the water content in the fibers. Thus, the wet volume of collagen is:

$$V_{col}^{h} = V_{m}^{cI}(1 + \rho_c \cdot x_{cI}^{H_2O}) + V_{m}^{cII}(1 + \rho_c \cdot x_{cII}^{H_2O}) + V_{m}^{cIII}(1 + \rho_c \cdot x_{cIII}^{H_2O}) \quad \text{(A.3)}$$

where ρ_{col}=1.36 gr/cm^3, $x_{cI}^{H_2O}$=0.4 gr.water/gr.collagen I, $x_{cII}^{H_2O}$=$x_{cIII}^{H_2O}$=0.7 gr.water/gr. collagen II or III the mass of water in the interfibrillar space with respect to the dry collagen (Simha *et al.*, 1999).

The Kozeny coefficient is computed assuming the fibers are randomly distributed:

$$G_{hb} = \frac{2}{3}G_r + \frac{1}{3}G_p \quad \text{(A.4)}$$

with

$$G_p = \frac{2 \cdot V_p^3}{(1 - V_p) \cdot [2 \cdot ln(\frac{1}{1-V_p}) - 3 + 4(1 - V_p) - (1 - V_p)^2]} \quad \text{(A.5)}$$

and

$$G_r = \frac{2 \cdot V_p^3}{(1 - V_p) \cdot [ln(\frac{1}{1-V_p}) - \frac{1-(1-V_p)^2}{1+(1-V_p)^2}]} \quad \text{(A.6)}$$

where $V_p = V_{H_2O} - V_m^{ci} \cdot \rho_c \cdot x_{ci}^{H_2O}$ is the water volume, V_{H_2O}, minus the water in the interfibrillar space of the collagen fibers.

The permeability of the ground substance is a function of its content in glycosaminoglycans (GAG) and proteoglycans (PGP), which form it in a relation two and one. The permeability of these two components is determined by the medium length and radius of their fibers.

The specific length of the glycosaminoglycans per unit volume is assumed to be determined by:

$$l_{gag} = \frac{V_{gag}/r_{gag}^2}{(V_{gag}/r_{gag}^2) + (V_{pgp}/r_{pgp}^2)} \tag{A.7}$$

where r_{gag}=0.5nm and r_{pgp}=1.0nm are average radii of the fibers of glycosaminoglycans and proteoglycans respectively (Levick, 1987).

The specific length of the proteoglycans fibers is determined by:

$$l_{pgp} = 1 - l_{gag} \tag{A.8}$$

The permeability due to the glycosaminoglycans is obtained through the expression:

$$k_{gag} = a(V_{gag} \cdot \rho_{gag})^b \tag{A.9}$$

with a=1.3410^{-11} and b=-1.485 constants determined experimentally (Levick, 1987), ρ_{gs}= 1.54 gr/cm^3 glycosaminoglycans density.

The permeability associated to proteoglycans is:

$$k_{pgp} = \frac{(1 - V_{pgp})^3 \cdot r_{pgp}^2}{4 \cdot G_{hb} \cdot V_{pgp}^2} \tag{A.10}$$

being the resultant permeability of the ground substance:

$$k_{gs} = \frac{1}{(l_{gag}/k_{gag}) + (l_{pgp}/k_{pgp})} \cdot (1 - V_{col}^h) \cdot \xi \tag{A.11}$$

with ξ=0.7 the tortuosity.

Appendix B

Asymmetrical differentiation theories

B.1 Introduction

The role of chondrocytes in distraction osteogenesis is still controversial and objective of many experimental works. Whereas some studies report that the bone forms by intramembranous ossification and no endochondral ossification takes place (Ilizarov, 1989*a*,*b*; Aronson *et al.*, 1989; Delloye *et al.*, 1990; Shearer *et al.*, 1992; Ganey *et al.*, 1994; Schenck & Gatchter, 1994), others observe cartilage formation from the central fibrous tissue of the regenerate (Kojimoto *et al.*, 1988; White & Kenwright, 1990; Waanders *et al.*, 1994).

In the numerical model developed in this thesis, we have assumed that cartilage can be deposited in both tensile and compressive environments. This symmetry concept is also shared by other mechanobiological rules (Pauwels, 1941; Prendergast *et al.*, 1997; Gómez-Benito *et al.*, 2005). However, in order to analyze the effect of the asymmetry in the differentiation rules with respect to the type of loading (compression or tension), the model proposed by Claes & Heigele (1999) is used herein. This asymmetrical quantitative model has been developed to describe fracture healing patterns (compression loading) and successfully correlates new tissue formation with the local mechanical stimuli (Claes & Heigele, 1999; Shefelbine *et al.*, 2005). As explained in Chapter 1, this mechanical stimulus

is a combination of the dilatational and deviatoric strain. Very small dilatational strains (less than 0.85 %) and deviatoric ones (below 5%) allow bone formation, whereas tissue strains above 15% lead to fibrocartilage and connective tissue preventing bone healing (Figure B.1). As observed in Figure B.1, chondrogenesis only takes place in compressive dilatational strains (dilatational strain greater than -5% and below -0.85%) and moderate values of distortional strains (deviatoric strain less than 15 %).

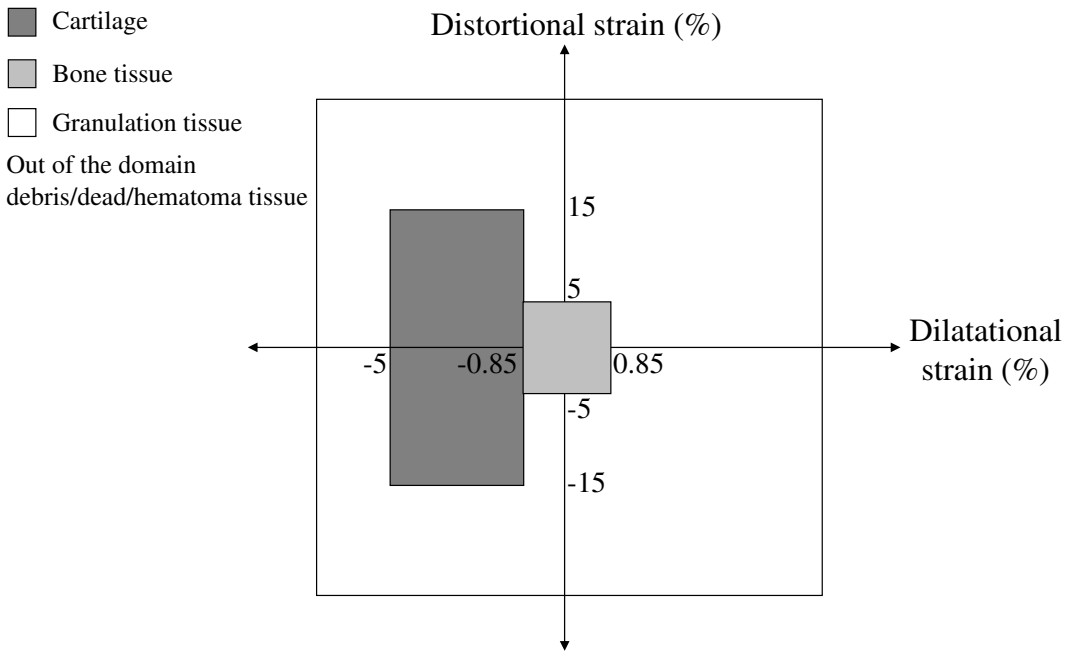

Figure B.1: Relationship between mechanical stimuli and bone formation (adapted from Claes & Heigele (1999)).

Despite the good results of this model in fracture healing cases (Claes & Heigele, 1999; Shefelbine *et al.*, 2005), it has never been applied to distraction osteogenesis. Therefore, in this appendix the model of Claes & Heigele (1999) will be extended to the case of bone lengthening and validated to some extent by evaluating the effect of the fixator stiffness on the maturation of the young regenerate bone after distraction osteogenesis. To do so, firstly a brief introduction is presented from an experimental perspective. Secondly, the mechano-regulation algorithm early proposed by Claes & Heigele (1999) has been extended to successfully simulate tensile environments such as distraction osteogenesis. And finally, a

sheep tibia model is implemented, using the finite element framework and results are compared against *in vivo* experimental data (Claes *et al.*, 2000).

B.2 Effect of the fixator stiffness on the young regenerate bone after distraction osteogenesis

Clinical and experimental studies have shown that several mechanical factors influence the course of bone healing. During limb lengthening, the mechanical behaviour of the distractor device is of particular importance since most of the load is transmitted through it. It directly affects the magnitude of the interfragmentary movement and callus size (Goodship & Kenwright, 1985; Goodship *et al.*, 1993; Claes *et al.*, 1997; Schell *et al.*, 2005). A stiff fixation minimizes interfragmentary movements and results in limited stimulation of callus formation. A flexible fixation can enhance the callus formation, thus improving the healing process, whereas an unstable fixation can lead to a nonunion (Kenwrigh & Goodship, 1989; Claes *et al.*, 1995). The specific range of movements which effectively stimulates young distraction callus is unknown (Claes *et al.*, 2000). The movement which occurs normally in this tissue during the maturation phase can be estimated from *in vitro* or *in vivo* measurements of fixators used in distraction osteogenesis (Schneider *et al.*, 1992; Podolsky & Chao, 1993; Claes *et al.*, 2000; Duda *et al.*, 2003).

Choosing the appropriate external fixator and design is as important as the actual execution of frame application. Although Ilizarov often attributed special biological effects to the ring external fixator with tensioned wires, distraction osteogenesis and even bone transportation can be successfully accomplished using monolateral, half-pins frames (Dahl & Fischer, 1991; Cañadell, 1993; de Pablos *et al.*, 1994) or even intramedullary rods (Brunner *et al.*, 1994). The choice of an external fixator is determined by the surgeon's experience and preference, the complexity of the problem, the patient's ability and tolerance, and the number of sites requiring treatment (Price & Mann, 1991; Saxby & Nunley, 1992). Each type of external fixator exhibits individual mechanical qualities that may or not

enhance osteogenesis and generalized healing (Paley *et al.*, 1990; Calhoun *et al.*, 1992*b*; Podolsky & Chao, 1993; Hamanishi *et al.*, 1994). For example, monolateral fixators are stable enough to distract the osteogenic zone but are limited by an inherent cantilever design that imparts eccentric loads to the bone and may result in undesirable angulation of the lengthened segment (Figure B.2b). Also, the application of the Ilizarov ring fixator to some anatomic localizations as well as the correction of angular deformities is difficult. In this sense, the Ilizarov ring fixator with half pins modifications (Green, 1991; Green *et al.*, 1992) is more versatile. This system promotes gradual mechanical forces and movements of bone in any plane (frontal, sagittal or transverse) or direction (axial, angular, translational, rotational or any combination) at an unlimited number of treatment sides, including the potential to cross and protect active joints (Golyakhovsky & Frankel, 1991; de la Huerta, 1994; Herzenberg *et al.*, 1994*b*,*c*). However, biplane or triplane deformities cannot be corrected with these hybrid fixators and require the use of the specialized Taylor Spatial Frame fixator to generate motion in two or three planes at the same time.

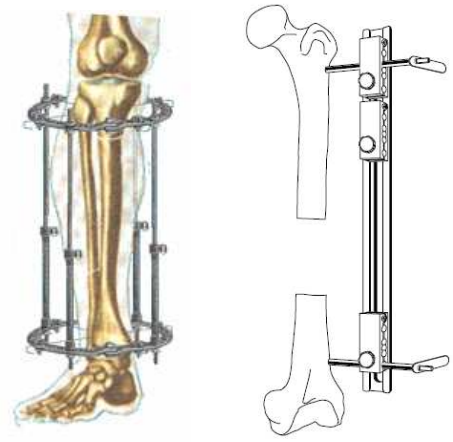

(a) (b)

Figure B.2: a) Ilizarov external fixator; b) Monolateral external fixator.

Numerous experimental studies (Goodship & Kenwright, 1985; Goodship *et al.*, 1993; Claes *et al.*, 1997; Schell *et al.*, 2005) as well as computational ones (Lacroix & Prendergast, 2002*b*; Isaksson *et al.*, 2006; Gómez-Benito *et al.*, 2006; García-Aznar *et al.*, 2007) have demonstrated the close link between interfrag-

mentary movement and bone consolidation during fracture healing. Far less research has been performed experimentally in distraction osteogenesis (Ilizarov, 1989*a*). And, as far as the authors know, no computational study has yet simulated the effect of the fixator stiffness on distraction osteogenesis. Therefore, this appendix aims to evaluate the effect of the stiffness of the fixator device on the interfragmentary movements and tissue outcome during the consolidation phase.

B.3 Description of the model

The model proposed by Claes & Heigele (1999) will be extended herein to simulate clinically observed fixator stiffness related phenomena that occur during distraction osteogenesis. Improvements have been performed on the original model (Claes & Heigele, 1999) (Figure B.1) in order to take into account the asymmetry in both distortional and dilatational strains. In fact, the model does not consider differences under tensile and compression distortional strains (Figure B.1). Nevertheless, it has been observed in the literature that bone formation is faster in distraction osteogenesis (tensile environment) than in fracture healing (compressive environment) (Aronson, 1991). Also, blood supply, which is closely related to osteogenesis, is much greater in distraction osteogenesis than fracture healing (Aronson, 1993). The tissue differentiation diagram of Claes & Heigele (1999) was adapted to determine tissue differentiation in tensile mechanical environments (Figure B.1). Four main areas can be distinguished on the modified diagram (Figure B.3). Firstly, a tissue destruction area, when the dilatational (Ψ_{dil}) or deviatoric strain (Ψ_{dev}) is too high (usually out of the physiological range) (-0.3>Ψ_{dil} >0.3, -0.3>Ψ_{dev} >0.3). Secondly, a cartilage area, with relatively high-dilatational compressive strain (-0.05< Ψ_{dil} <-0.0085, -0.15< Ψ_{dev} <0.15). Thirdly, a bony area, with small amounts of dilatational and deviatoric strain. This is the area modified with respect to the original model. According to *in vitro* studies on osteoblasts, cell culture osteoblasts try to avoid surface strains larger than 4% by turning away from the principal strain axis (Neidlinger Wilke *et al.*, 1994). Thus, the bone formation area in compressive environments is: -0.0085< Ψ_{dil} <0, -0.05< Ψ_{dev} <0 (Figure B.1) (Claes & Heigele, 1999). However, in highly stimulated tensile environments such as distraction osteogenesis bony

tissue is also deposited under higher mechanical stimulus. During the distraction process, bone columns increase in length and diameter so that the central soft interzone keeps the same length, around 4 mm long (Aronson *et al.*, 1990). Thus, tissue level strains produced within the 4 mm distracted gap when a displacement of 1 mm is applied is around 25 %. Therefore, in tensile environments such as distraction osteogenesis, much larger strains may activate bone cells. Our bony region in this case is: $0< \Psi_{dil} <0.034$, $0< \Psi_{dev} <0.2$ (Figure B.1). In the remaining zones of the diagram, granulation tissue is expected to be deposited under physiological mechanical loads ($-0.3<\Psi_{dil} <0.3$, $-0.3<\Psi_{dev} <0.3$).

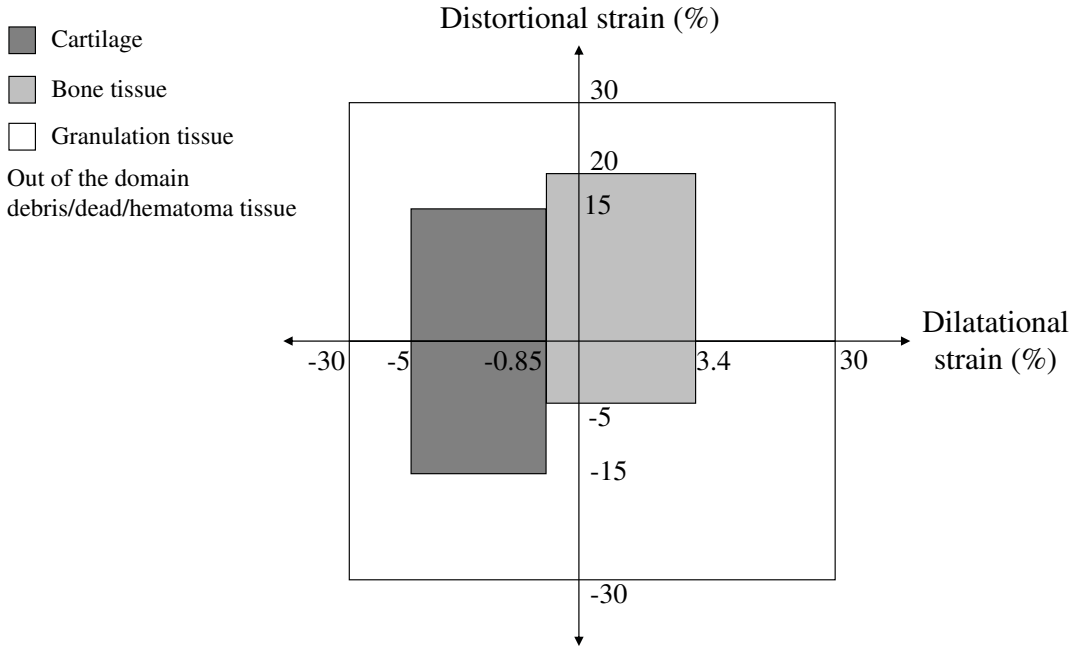

Figure B.3: Modified model of Claes & Heigele (1999) used in this study.

The numeric values for the regions were chosen based on previous *in vivo* measurements, and modelling simulations (Claes & Heigele, 1999; Shefelbine *et al.*, 2005). Note that the diagram distinguishes between bone formation under tensile environments and compressive ones. In fact, tissues do not behave similarly under tensile or compressive loads.

The remaining cellular events underlying distraction osteogenesis (cell proliferation, migration and tissue growth) were formulated and numerically imple-

mented as described in Chapter 3.

B.4 Experimental set-up

The model previously described has been applied to an experimental study performed by Claes *et al.* (2000). Using distraction principles, they performed a segmental bone transport model to examine the effect of the stiffness of the axial fixator on the maturation time of the callus after completion of the distraction process. Bone transport consists on restoring a segmental bony defect by moving one bone segment relative to another (Figure B.4).

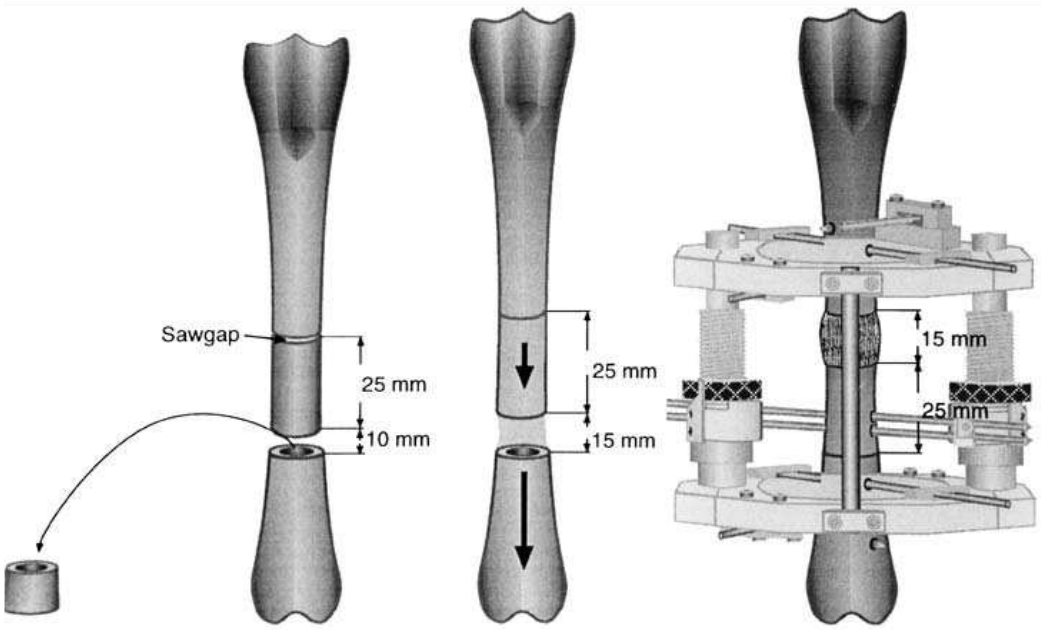

Figure B.4: Diagram of the operative procedure: left, creation of the mid-diaphyseal defect; middle, adjustment of the length of the defect to 15 mm; and right, daily segmental bone transport of 1 mm in two steps (Claes *et al.*, 2000).

During the experimental study, Claes *et al.* (2000) used 32 skeletally-mature female sheep, aged three years or older, with a mean weight of 80 $\pm$ 10 kg. They created a mid-diaphyseal bony defect of 15 mm in sheep tibias and after four days of latency, they performed bone transport at 1 mm per day in two increments during 15 days. Afterwards, during the consolidation period, they

analyzed four different cases. These four groups differed only in the stability of the bone fragment fixation. The distracted tibiae were placed in a fixator that permitted relatively marked axial mobility between the bone fragments; this mobility was accomplished by introducing variable stiffness fixators which differed on the allowed axial interfragmentary movement (IFM): 0 (control group), 0.5, 1.2 and 3 mm. The load-displacement curve of the fixator shows three distinct slopes (Figure B.5). From 0 to 120 N the axial stiffness of the fixator is 915 N/mm. From 120 N to approximately 130 N it equalled that of the springs, 7.69 N/mm, which allowed full axial movement within a small load range. At 130 N the bolts prohibited further axial displacement of the rings and the stiffness returned to 989 N/mm in all variable stiffness groups. The axial stiffness of the fixator used in the control group was 1065 N/mm.

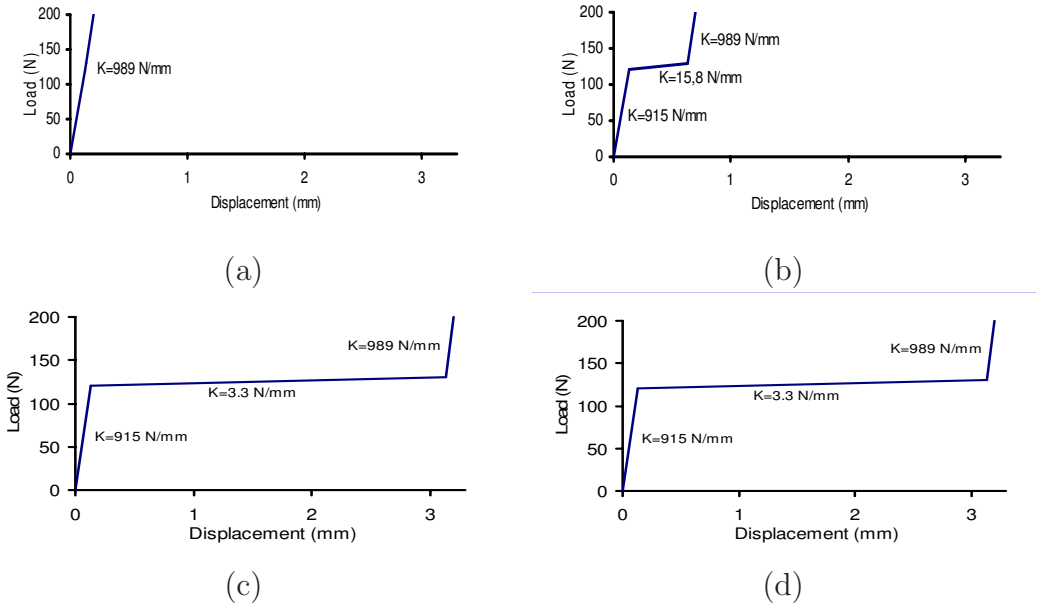

Figure B.5: Displacement-load curve of the external fixator with different IFM allowed: a) IFM=0 mm (control group); b) IFM=0.5 mm; c) IFM=1.2 mm; d) IFM=3 mm.

The clinical process of bone transport is performed in the diaphysis of the sheep tibia. The diaphysis of the tibia was assumed to be cylindrical. Also, just axial loads were considered. Therefore, it is assumed, as a first approach, a two dimensional axisymmetric finite element model of the ovine tibia (Figure B.6),

which is based on the geometry of the tibia from the experimental data (Claes & Heigele, 1999). Initially, the dimension of the gap was 1 mm. The cortical bone was modelled with an inner diameter of 12 mm and an outer diameter of 16 mm and the periosteum with a width of 0.5 mm.

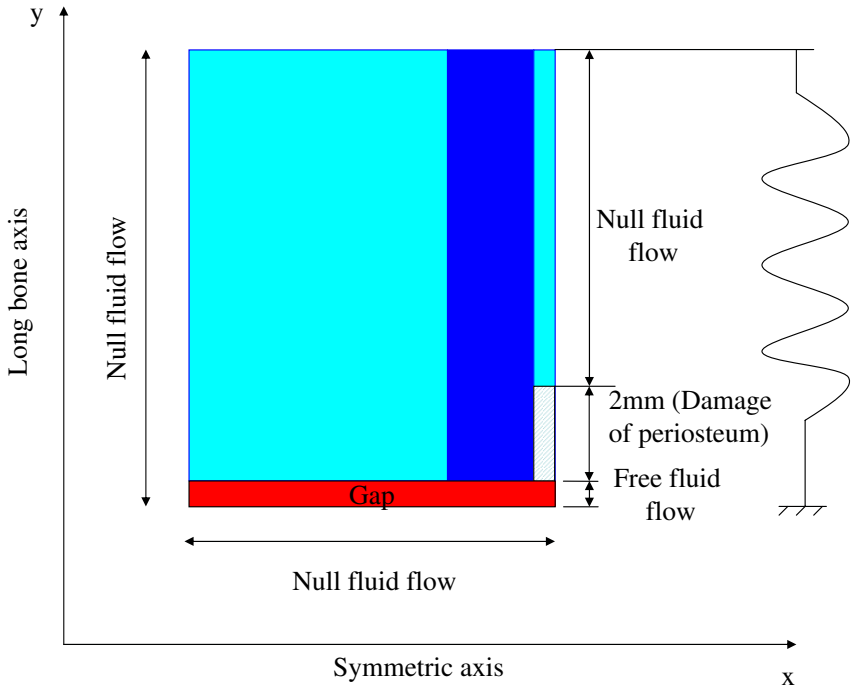

Figure B.6: The initial two-dimensional axisymmetric finite element model and indications of the different callus regions (Claes & Heigele, 1999).

B.5 Boundary and loading conditions

The mechanical stimulation during the distraction period consisted of an applied displacement on the top of the cortical bone. A displacement of 0.5 mm was gradually applied for one minute and the final position maintained during 12 hours. An additional displacement step of 0.5 mm is then performed during 1 minute and maintained until the end of the day. This load history was repeated during the whole distraction process. During the consolidation period, the only active mechanical stimulation was due to the load derived from the normal activity of the animal (500 N of compressive load (Duda *et al.*, 1998)).

With regard to the boundary conditions, the periosteum was assumed to be impermeable and hence zero fluid flow was prescribed at this boundary (Li *et al.*, 1987). In the diffusion analysis we considered sources of MSCs in the marrow cavity and the surrounding soft tissues (Gerstenfeld *et al.*, 2003). Consequently, it was assumed that the process of corticotomy preserves the endosteum. However, it did not preserve the periosteum and therefore we assumed it to not contribute to MSCs source and to be damaged for 2 mm around the plane site of the osteotomy (Figure B.6) (Claes *et al.*, 2000). The initial boundary conditions for the ossification front modeled through the diffusion equation consisted on preosteoblastic sources in the areas of the endosteum and periosteum closest to the cortical bone.

Also, the tissue in the interfragmentary gap was assumed to be totally damaged at the beginning of the distraction period since, according to experimental data, the four days of latency were not enough for recruitment of MSCs and reparation of the tissue. As observed in Figure B.6, the fixator was simulated by means of a variable stiffness linear spring with only axial stiffness.

B.6 Results

In this part of the appendix, we have determined first the tissue distribution during the distraction phase, assuming the fixator to be infinitely rigid. Afterwards, the evolution of the interframentary movement as well as the distribution of tissues is computed during the consolidation phase for the four types of fixator simulated.

The tissue distribution during the distraction period is very similar to that described in the previous examples although no cartilage formation takes place (Figure B.7). During the initial stage of the distraction phase, the initial damaged tissue is gradually repaired by the migrating MSCs. At the end of the distraction period two clearly distinct zones can be distinguished: a central soft tissue area and a peripherical bone tissue. This bone has been formed through intramembranous ossification close to the existing host bone. Also, during the distraction period, as the distraction gap increased, bone front advanced while the soft tissue interzone remained almost constant, about 3 mm long. This is in concordance

with experimental evidences (Aronson *et al.*, 1990).

Figures B.8, B.9, B.10 and B.11 show the spatial distribution of the different tissues during the consolidation period for the 0, 0.5, 1.2 and 3 mm fixator groups. The healing process is very similar in the three first cases (0, 0.5 and 1.2 mmm groups). Bone front advances progressively until filling completely the gap with a rate that decreases with increasing IFM allowed by the fixator. For instance complete bony bridging occurs at day 40 in the control group whilst in the 1.2 mm group it takes around 60 days to complete bony bridging. In all these cases, most bone tissue is formed via intramembranous ossification. By contrast, in the 3 mm group, nonunion occurs at the end of the consolidation phase. The interfragmentary gap is filled with necrotic tissue with two bone surrounding zones.

The IFM evolution shows a decreasing behavior for all the simulated cases (IFM= 0, 0.5, 1.2 and 3 mm groups) except for the most flexible one (IFM=3 mm), which is almost constant (Figure B.12). This large displacement allowed in the 3 mm group damages the tissue within the interfragmentary gap from the beginning of the consolidation phase. Since the highly stimulated mechanical environment is maintained through the whole process, this tissue does not evolve further and therefore does not change its stiffness. This is in agreement with experimental data since experimentally, the slowest reduction of the IFM was found in the 3.0 mm group. In the three remaining groups (0, 0.5 and 1.2 mm groups) a gradual decrease in the interfragmentary movement was computed reaching final values of 0.042, 0.046 and 0.082 mm respectively, which was indicative of complete bony union. At the beginning of the consolidation period, there is a high interfragmentary motion for these three simulated cases until the second week. This interfragmentary motion increases with the IFM allowed by the fixator. After the two first weeks, there is a rapid decrease of interfragmentary motion in the 0.5 mm group and a mild decrease in the other two groups until the fifth week. After that, a very low interfragmentary motion can be observed in all the simulated cases which is indicative of the complete healing process.

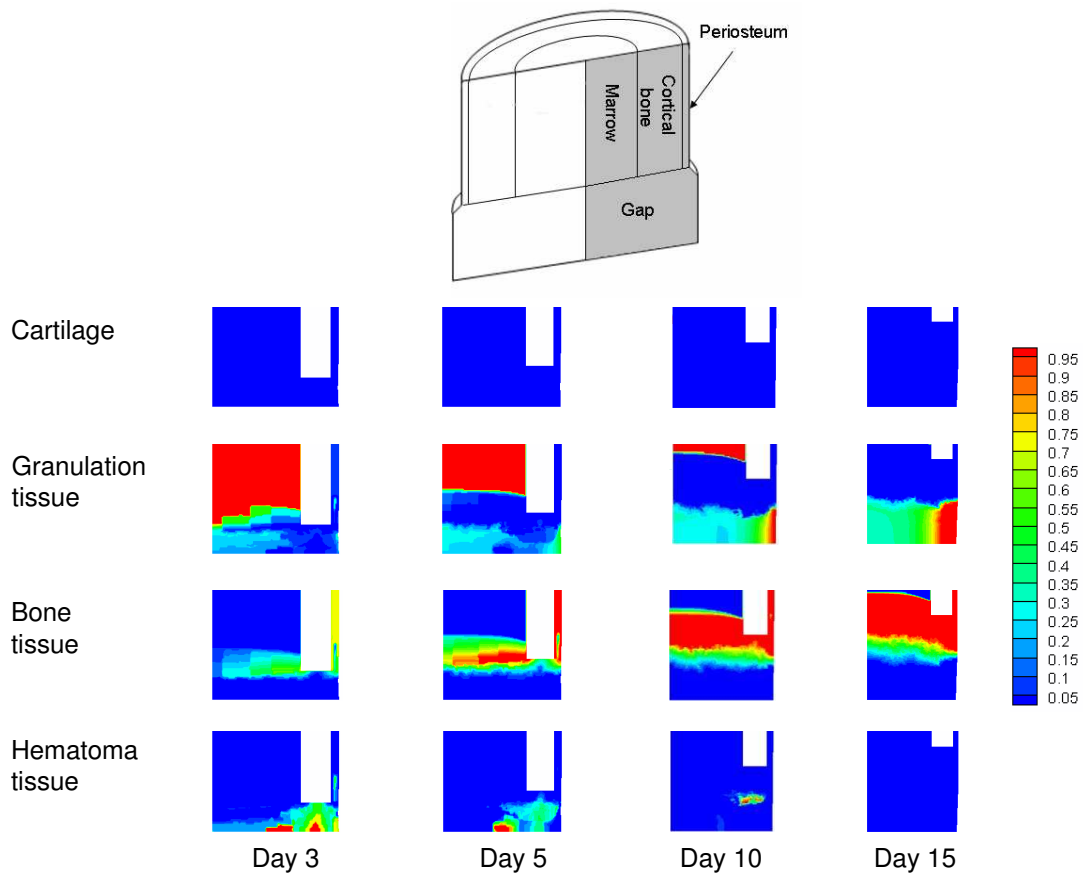

Figure B.7: Evolution of the different tissues within the distraction gap during the distraction phase for the four computed cases. Days are computed from the beginning of the distraction phase (the 4-day latency period is not considered in the model).

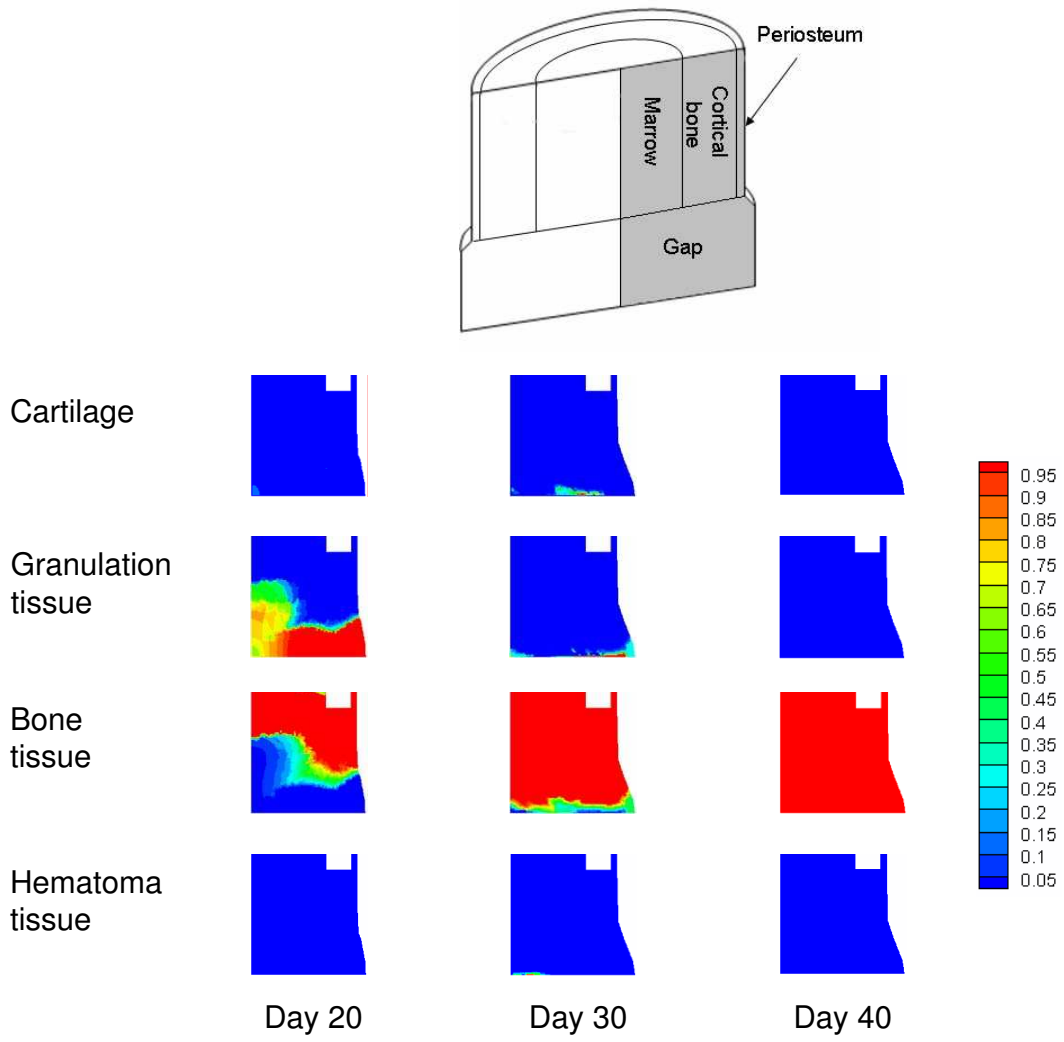

Figure B.8: Evolution of the different tissues within the distraction gap during the consolidation phase for the control group (IFM =0 mm). Days are computed from the beginning of the distraction phase.

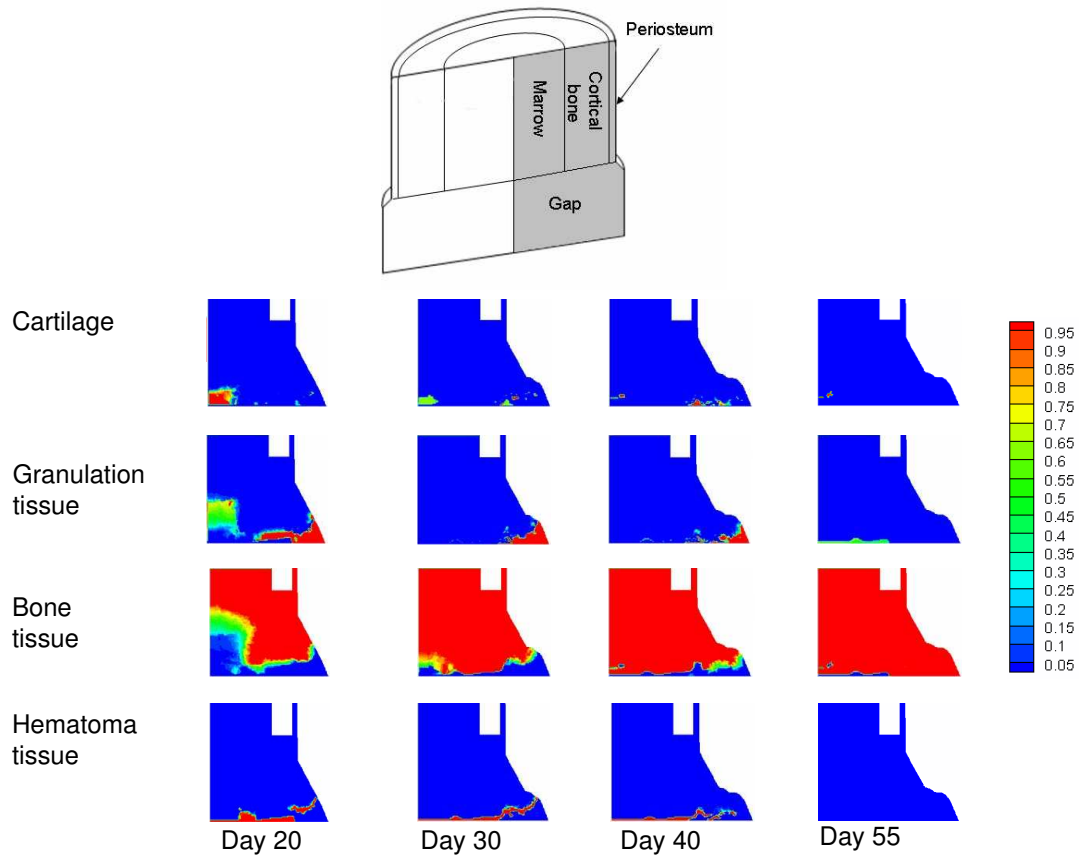

Figure B.9: Evolution of the different tissues within the distraction gap during the consolidation phase for the 0.5 mm group. Days are computed from the beginning of the distraction phase.

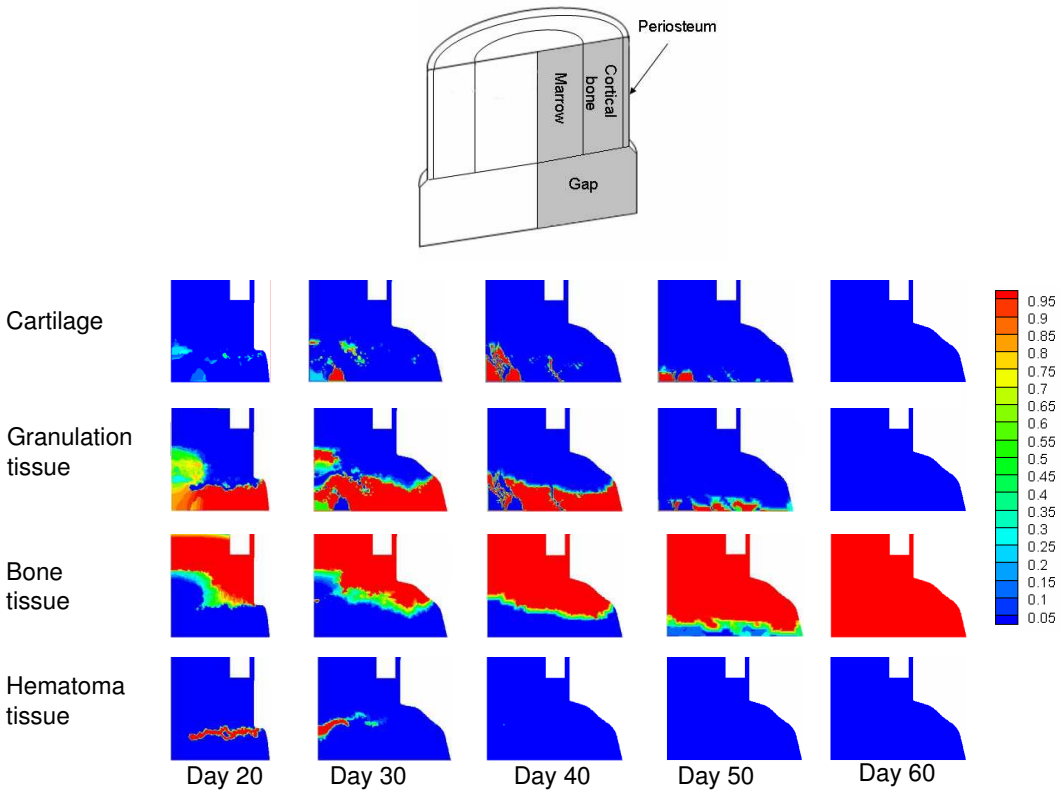

Figure B.10: Evolution of the different tissues within the distraction gap during the consolidation phase for the 1.2 mm group. Days are computed from the beginning of the distraction phase.

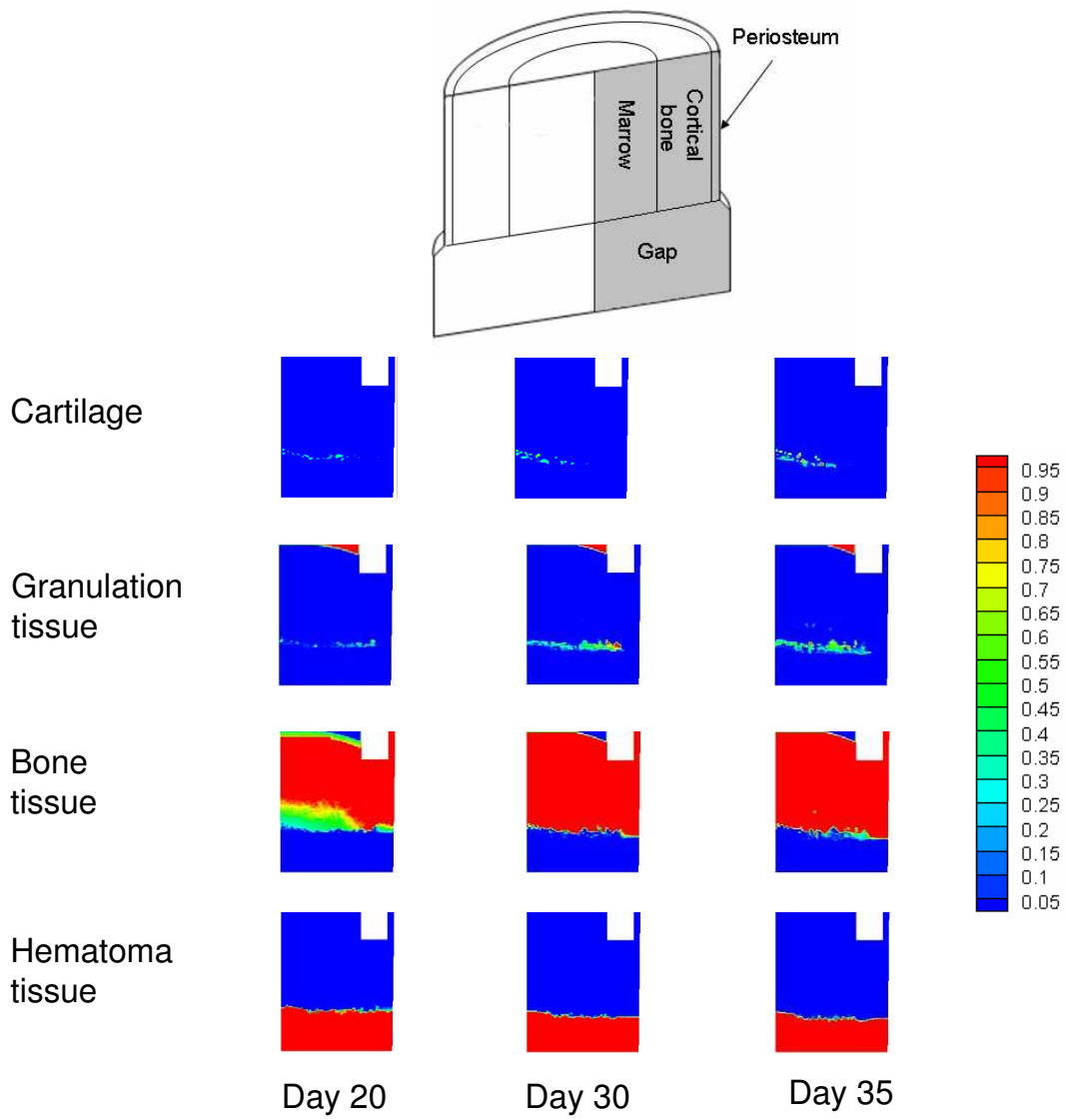

Figure B.11: Evolution of the different tissues within the distraction gap during the consolidation phase for the 3 mm group. Days are computed from the beginning of the distraction phase.

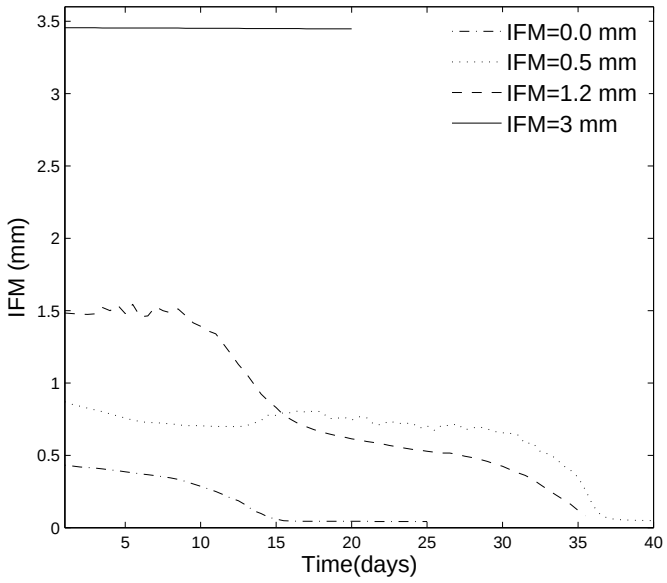

Figure B.12: Evolution of the IFM in the distraction callus with healing time in the four groups analyzed during the consolidation period.

B.7 Discussion

We have extended a previously developed differentiation model (Claes & Heigele, 1999) by incorporating tension-compression asymmetry to simulate the effect of the fixator stiffness on bone evolution during the consolidation phase. This new differentiation theory was introduced in the mechanobiological model described in chapter 3 to take into account the influence of tensile/compressive environments on the healing process, using finite element analysis. Moreover, the model considers that the mode of bone formation in tensile environments is primarily intramembranous ossification whilst under compressive loads endochondral ossification is the main mode (Claes & Heigele, 1999). In this sense, the mechanical stimulus that activates bone tissue formation is higher under tension than compression. This effect is not considered in other mechanobiological models in which both intramembranous and endochondral ossification occur in tensile and compressive environments (Prendergast *et al.*, 1997; Gómez-Benito *et al.*, 2005). In distraction osteogenesis (Ilizarov, 1989*a*,*b*, 1992; Aronson, 1991, 1994; Aronson

et al., 1990) or at implant interfaces (Geris *et al.*, 2004), where shear loads predominate, many experimental studies demonstrate the direct differentiation of mesenchymal stem cells into bone tissue through intramembranous ossification.

In order to test the reliability of the new extended model, four different fixators were simulated during the consolidation phase of a common distraction process. For the four analyzed cases, our results are in agreement with experimental ones: a stiff fixator promotes bone formation while the excessive motion induced by very flexible fixators is adverse for bony bridging. Also, decreasing the stiffness of the fixator increased callus size until the critical stiffness that leads to nonunion. Figure B.13 shows a comparison of the computed IFM with the experimental values measured by Claes *et al.* (2000). Experimental IFM values at the beginning and end of the consolidation period are similar to those computed numerically. These results show that the qualitative trend of the IFM values is predicted, with a much larger IFM in the 3 mm group than in the control group. In the 3 mm group , the distraction gap was mostly filled with poorly differentiated tissue (necrotic) whilst in the control group, which had much less motion between the bone ends, there was substantially more osteogenic activity in the distraction space. At the end of the consolidation period, a non union or pseudoarthrosis is predicted in the 3 mm group as compared to the complete bony union of the control group.

Moreover, the extended model is able to qualitatively reproduce tissue distributions within the gap in the four cases (Figures B.8, B.9, B.10 and B.11). During the bone transport procedure, bone tissue forms in the areas close to the cortical bone and periosteum. This bone front advances trough the consolidation period with a rate that increases as the fixator stiffness decreases. However, in the case with most mobility between the bone ends (3 mm group) osteogenic activity is least and nonunion occurs. This is in concordance with experimental findings. Figure B.14a shows the histology of the interfragmentary gap at the end of the consolidation phase in the 3 mm group. It can be observed that tissue distribution is very similar to the computed numerically (Figure B.14b). In this case, nonunion occurs and the interfragmentary gap is filled with a central necrotic tissue that does not evolve further. However, some amount of bone is close to the original one. Computationally, this lower stiffness of the fixator is

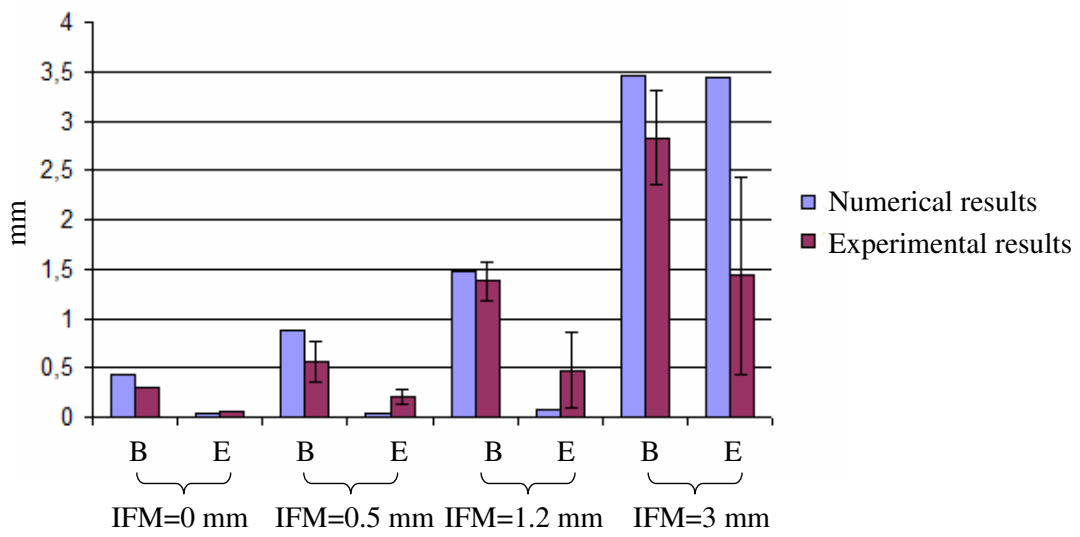

Figure B.13: Interfragmentary movement in the 0, 0.5, 1.2 and 3 mm groups at the beginning (B) and end (E) of the consolidation phase. Comparison with experimental results (Claes *et al.*, 2000).

accompanied by higher mechanical stimulus which resulted in tissue damage and nonunion. In contrast, a stiffer fixator, such as that used in the control group, resulted in stimulated osteogenesis. This is observed in Figures B.15a and B.15b where complete bony bridging occurs at the end of the consolidation period both experimentally and numerically. This is in agreement with most clinical results which consider that stable fixators produce the best effects on tissue regeneration whilst excessive displacement within the fixator promotes necrotic tissue formation (Ilizarov, 1989*a*).

Comparing the four analyzed examples some similarities can also be found. First, the evolution of the IFM shows in all cases the same decreasing tendency. Second, except in the 3 mm group where a nonunion occurs, the tissue pattern as well as the process of bone formation is very similar. And thirdly bone is synthesized through intramembranous ossification by direct differentiation of MSCs to bone cells in both the distraction and consolidation periods.

This model however presents some limitations that need to be discussed. Firstly, only four different tissues have been modeled (bone, cartilage, granulation and necrotic tissue). This makes bony and necrotic tissue the final differentiation

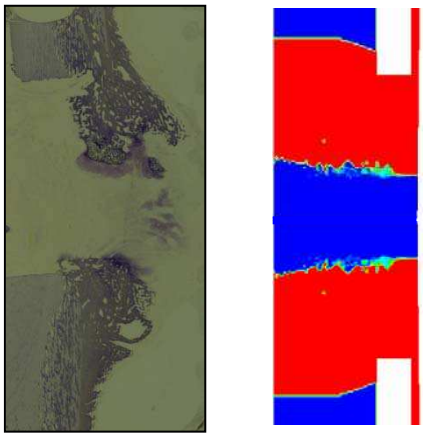

(a) (b)

Figure B.14: IFM=3mm: a) experimental; b) numerical.

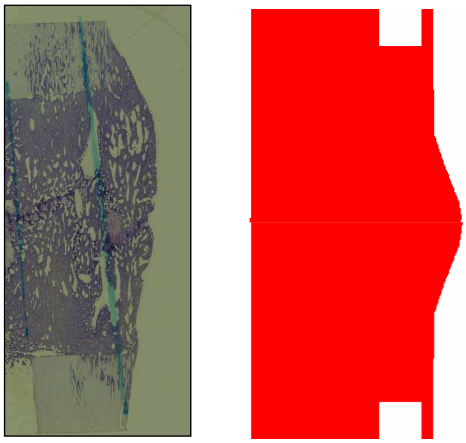

(a) (b)

Figure B.15: IFM=0mm: a) experimental; b) numerical.

pathways of the model during normal course of bone healing or nonunion, respectively. This is a clear limitation while computing the IFM in the 3 mm group since final tissue outcome cannot evolve further and thus the IFM is maintained through the whole period of bone consolidation (Figure B.13). If an additional tissue is introduced in the model so that it is deposited in highly stimulated environments (i.e., nonunion), the model would be able to show a more realistic evolution of the tissue stiffness and consequently of the IFM. Also the fixator has been modeled with a variable stiffness spring within finite element analysis and

the ovine tibia has been assumed to be cylindrical. Further improvements should be done to incorporate the real geometry of both the fixator and the tibia. Finally, the boundaries between the regions in the modified differentiation diagram (Figure B.3) were chosen according to experimental evidences and certainly affect the final results. In particular in this model, the boundary of the bone formation has been defined to depend on the type of loading. In tensile environments, *in vivo* studies have demonstrated that in highly stimulated environments such as distraction osteogenesis bone formation takes place with a speed that is twice that found in compressive environments (Aronson, 1991). Therefore, the boundaries of the intramembranous region are variable and dependant on the direction of the applied load. The other boundaries in this model were not sensible to the direction of the imposed loads. Future studies, however, will explore the sensitivity of theses boundaries.

Numerous models have been proposed to predict tissue differentiation during distraction osteogenesis. However, as far as we know, until now no asymmetrical model was used to predict the effect of the fixator stiffness on tissue outcome and the evolution of the interfragmentary movement. This study adapted a model that had previously been used to simulate fracture healing (Claes & Heigele, 1999) and computed the sequence of events in four cases with different external fixators.

Bibliography

Aarnes, G. T., Steen, H., Kristiansen, L. P., Ludvigsen, P. & Reikeras, O. (2002). Tissue response during monofocal and bifocal leg lengthening in patients. *J Orthop Res.* **20**, 137–41.

Abbott, L. C. (1927). The operative lengthening of the tibia and fibula. *J Bone Joint Surg.* **9**, 128–152.

Abbott, L. C. & Saunders, J. B. (1939). The operative lengthening of the tibia and fibula. A preliminary report on the further development of the principles and technique. *Ann Surg.* **110**, 961–991.

Adams, M. A., Burton, K., Bogduk, N. & Dolan, P. (2006). *The Biomechanics of Back Pain.* Elsevier Health Sciences, ISBN 0443100683.

Aerssens, J., Boonen, S., Lowet, G. & Dequeker, J. (1998). Interspecies differences in bone composition, density, and quality: potential implications for in vivo bone research. *Endocrinology.* **139**, 663–70.

Akizuki, S., Mow, V. C., Müller, F., Pita, J. C., Howell, D. S. & Manicourt, D. H. (1986). Tensile properties of human knee joint cartilage: I. Influence of ionic conditions, weight bearing, and fibrillation on the tensile modulus. *J Orthop Res.* **4**, 379–9.

al Ruhaimi, K. A. (2001). Comparison of different distraction rates in the mandible: an experimental investigation. *Int J Oral Maxillofac Surg.* **30**, 220–227.

Alastrué, V., Peña, E., Martínez, M. A. & Doblaré, M. (2007). Assessing the use of the "opening angle method" to enforce residual stresses in patient-specific arteries. *Ann Biomed Eng.* **35**, 1821–37.

Aldegheri, R., DeBastiani, G. & Renzi-Brivio, L. (1985). Allungamento diafisario dell'arto inferiore. *Chir Ozgani Mov.* **70**, 111.

Aldegheri, R., Trivella, G. & Lavini, F. (1989). Epiphyseal distraction. Hemichondrodiatasis. *Clin Orthop Relat Res.* **241**, 128–36.

Altman, G. H., Horan, R. L., Martin, I., Farhadi, J., Stark, P. R., Volloch, V., Richmond, J. C., Vunjak-Novakovic, G. & Kaplan, D. L. (2002). Cell differentiation by mechanical stress. *FASEB J.* **16**, 270–2.

Ament, C. & Hofer, E. P. (1996). On the importance of the osteogenic and vasculative factors in callus healing. In *Proceedings of the 5^{th} Meeting of the International Society for Fracture Repair.*

Ament, C. & Hofer, E. P. (2000). A fuzzy logic model of fracture healing. *J Biomech.* **33**, 961–8.

Anderson, R. (1936). Femoral bone lengthening. *Am. J. Surg.* **31**, 479–483.

Andreykiv, A., van Keulen, F. & Prendergast, P. J. (2007). Simulation of fracture healing incorporating mechanoregulation of tissue differentiation and dispersal/proliferation of cells. *Biomech Model Mechanobiol,* **7**, 443–461.

Armstrong, C. G. & Mow, V. C. (1982). Variations in the intrinsic mechanical properties of human articular cartilage with age, degeneration, and water content. *J Bone Joint Surg Am.* **64**, 88–94.

Aronson, J. (1991). *The biology of distraction osteogenesis. In: Maiocchi AB, Aronson J, editors, Operative Principles of Ilizarov. Fracture Treatment, Nonunion, Osteomyelitis, Lengthening, Deformity Correction.* Baltimore, Williams and Wilkins.

Aronson, J. (1993). Temporal and spatial increases in blood flow during distraction osteogenesis. *Clin Orthop Relat Res.* **301**, 124–131.

Aronson, J. (1994). Experimental and clinical experience with distraction osteogenesis. *Cleft Palate Craniofac J.* **31**, 473–81.

Aronson, J. (1997). Limb-lengthening, skeletal reconstruction, and bone transport with the Ilizarov method. *J Bone Joint Surg Am.* **79**, 1243–58.

Aronson, J., Gao, G. G., Shen, X. C., McLaren, S. G., Skinner, R. A., Badger, T. M. & Lumpkin, C. K. J. (2001). The effect of aging on distraction osteogenesis in the rat. *J Orthop Res.* **19**, 421–7.

Aronson, J., Good, B., Stewart, C., Harrison, B. & Harp, J. (1990). Preliminary studies of mineralization during distraction osteogenesis. *Clin Orthop Relat Res.* **250**, 43–9.

Aronson, J., Harrison, B., Stewart, C. & Harp, J. (1989). The histology of distraction osteogenesis using different external fixators. *Clin Orthop Relat Res.* **241**, 106–16.

Aronson, J. & Shen, X. (1994). Experimental healing of distraction osteogenesis comparing metaphyseal and diaphyseal sites. *Clin Orthop Rel Res.* **301**, 25–30.

Aronson, J., Shen, X. C., Gao, G. G., Miller, F., Quattlebaum, T., Skinner, R. A., Badger, T. M. & Lumpkin, C. K. J. (1997*a*). Sustained proliferation accompanies distraction osteogenesis in the rat. *J Orthop Res.* **15**, 563–9.

Aronson, J., Shen, X. C., Skinner, R. A., Hogue, W. R., Badger, T. M. & Lumpkin, C. K. J. (1997*b*). Rat model of distraction osteogenesis. *J Orthop Res.* **15(2)**, 221–6.

Asahina, I., Sampath, T. K., Nishimura, I. & Hauschka, P. V. (1993). Human osteogenic protein-1 induces both chondroblastic and osteoblastic differentiation of osteoprogenitor cells derived from newborn rat calvaria. *J Cell Biol.* **123**, 921–33.

Aston, J. W. J., Williams, S. A., Allard, R. N., Sawamura, S. & Carollo, J. J. (1992). A new canine cruciate ligament formed through distraction histogenesis. Report of a pilot study. *Clin Orthop Relat Res.* **280**, 30–6.

Augat, P., Merk, J., Genant, H. K. & Claes, L. (1997). Quantitative assessment of experimental fracture repair by peripheral computed tomography. *Calcif Tissue Int.* **60**, 194–9.

Bailón-Plaza, A. & van der Meulen, M. C. (2001). A mathematical framework to study the effects of growth factor influences on fracture healing. *J Theor Biol.* **212**, 191–209.

Bailón-Plaza, A. & van der Meulen, M. C. (2003). Beneficial effects of moderate, early loading and adverse effects of delayed or excessive loading on bone healing. *J Biomech.* **36**, 1069–77.

Bakke, M., Holm, B., Jensen, B. L., Michler, L. & Möller, E. (1990). Unilateral, isometric bite force in 8-68-year-old women and men related to occlusal factors. *Scand J Dent Res.* **98**, 149–58.

Barone, C. M., Ferder, M., Jimenez, D. F., Grossman, L., Hall, C., Strauch, B. & Argamaso, R. V. (1993). Distraction of the frontal bone outside the cranial plane: a rabbit model. *J Craniof Surg.* **4**, 177–181.

Barton, J. R. (2007). On the treatment of ankylosis by the formation of artificial joints. 1827. *Clin Orthop Relat Res.* **456**, 9–14.

Bateman, J. F., Lamandé, S. R. & Ramshaw, J. A. M. (1996). *Collagen superfamily. In Extracellular Matrix, vol. 2 (ed. W. D. Comper).* Amsterdam: Harwood Academic Publishers.

Beaupré, G. S., Giori, N. J., Blenman-Fyhrie, P. R. & Carter, D. R. (1992). Modeling fracture healing: the influence of mechanical loading on tissue differentiation. In *World Congress of Biomechanics, Bruxelles.*

Bertram, J. E., Polevoy, Y. & Cullinane, D. M. (1998). Mechanics of avian fibrous periosteum: tensile and adhesion properties during growth. *Bone.* **22**, 669–675.

Blenman, P. R., Carter, D. R. & Beaupré, G. S. (1989). Role of mechanical loading in the progressive ossification of a fracture callus. *J Orthop Res,* **7**, 398–407.

Block, M. S., Cervini, D., Chang, A. & Gottsegen, G. B. (1995). Anterior maxillary advancement using tooth-supported distraction osteogenesis. *J Oral Maxillofac Surg.* **53**, 561–5.

Block, M. S., Chang, A. & Crawford, C. (1996). Mandibular alveolar ridge augmentation in the dog using distraction osteogenesis. *J Oral Maxillofac Surg.* **54**, 309–14.

Block, M. S., Daire, J., Stover, J. & Matthews, M. (1993). Changes in the inferior alveolar nerve following mandibular lengthening in the dog using distraction osteogenesis. *J Oral Maxillofac Surg.* **51**, 652–60.

Boccaccio, A., Lamberti, L., Pappalettere, C., Carano, A. & Cozzani, M. (2006). Mechanical behavior of an osteotomized mandible with distraction orthodontic devices. *J Biomech.* **39**, 2907–18.

Boccaccio, A., Pappalettere, C. & Kelly, D. J. (2007). The influence of expansion rates on mandibular distraction osteogenesis: a computational analysis. *Ann Biomed Eng.* **35**, 1940–60.

Boccaccio, A., Prendergast, P. J., Pappalettere, C. & Kelly, D. J. (2008). Tissue differentiation and bone regeneration in an osteotomized mandible: a computational analysis of the latency period. *Med Biol Eng Comput.* **46**, 283–98.

Bonnard, C., Favard, L., Sollogoub, I. & Glorion, B. (1993). Limb lengthening in children using the Ilizarov method. *Clin Orthop Relat Res.* **293**, 83–8.

Bosch, P., Musgrave, D. S., Lee, J. Y., Cummins, J., Shuler, T., Ghivizzani, T. C., Evans, T., Robbins, T. D. & Huard. (2000). Osteoprogenitor cells within skeletal muscle. *J Orthop Res.* **18**, 933–44.

Bost, F. C. & Larsen, L. J. (1956). Experiences with lengthening of the femur over an intramedullary rod. *J. Bone and Joint Surg.* **38-A**, 567–584.

Bouletreau, P. J., Warren, S. M. & Longaker, M. T. (2002*a*). The molecular biology of distraction osteogenesis. *J Craniomaxillofac Surg.* **30**, 1–11.

Bouletreau, P. J., Warren, S. M., Spector, J. A., Peled, Z. M., Gerrets, R. P., Greenwald, J. A. & Longaker, M. T. (2002*b*). Hypoxia and VEGF up-regulate BMP-2 mRNA and protein expression in microvascular endothelial cells: implications for fracture healing. *Plast Reconstr Surg.* **109**, 2384–97.

Breul, R., Mall, G., Landgraf, J. & Scheck, R. (1999). Biomechanical analysis of stress distribution in the human temporomandibular-joint. *Ann Anat.* **181**, 55–60.

Breward, C. J., Byrne, H. M. & Lewis, C. E. (2003). A multiphase model describing vascular tumour growth. *Bull Math Biol.* **65**, 609–40.

Brighton, C. T., Lorich, D. G., Kupcha, R., Reilly, T. M., Jones, A. R. & Woodbury, R. A. (1992). The pericyte as a possible osteoblast progenitor cell. *Clin Orthop Relat Res.* **275**, 287–99.

Broom, N. D. & Silyn-Roberts, H. (1990). Collagen-collagen versus collagen-proteoglycan interactions in the determination of cartilage strength. *Arthritis Rheum.* **33**, 1512–1517.

Brueton, R. N., Brookes, M. & Heatley, F. W. (1990). The vascular repair of an experimental osteotomy held in an external fixator. *Clin Orthop Relat Res.* **257**, 286–304.

Brunner, U. H., Cordey, J., Schweiberer, L. & Perren, S. M. (1994). Force required for bone segment transport in the treatment of large bone defects using medullary nail fixation. *Clin Orthop Relat Res.* **301**, 147–155.

Bucci, L. (1995). *Nutrition Applied to Injury Rehabilitation and Sports Medicine.* CRC Press.

Buck, B. E., Malinin, T. I. & Brown, M. D. (1989). Bone transplantation and human immunodeficiency virus. An estimate of risk of acquired immunodeficiency syndrome (AIDS). *Clin Orthop Relat Res.* **240**, 129–36.

Burger, E. H. (2001). *Experiments on cell mechanosensitivity: bone cells as mechanical engineers. Bone Mechanics Handbook, chapter 28.* CRC Press Boca Raton.

Burr, D. B., Milgrom, C., Fyhrie, D., Forwood, M., Nyska, M., Finestone, A., Hoshaw, S., Saiag, E. & Simkin, A. (1996). In vivo measurement of human tibial strains during vigorous activity. *Bone.* **18**, 405–10.

Burrill, A. M. (1998). *A New Law Dictionary and Glossary.* The Lawbook Exchange.

Calhoun, J. H., Evans, E. B. & Herndon, D. N. (1992*a*). Techniques for the management of burn contractures with the Ilizarov fixator. *Clin Orthop Relat Res.* **280**, 117–24.

Calhoun, J. H., Li, F., Ledbetter, B. R. & Gill, C. A. (1992*b*). Biomechanics of the Ilizarov fixator for fracture fixation. *Clin Orthop Relat Res.* **280**, 15–22.

Cañadell, J. (1993). Bone lengthening: experimental results. *J Pediatr Orthop B.* **2**, 8–10.

Cañadell, J., Gonzales, F., Barrios, R. H. & Amillo, S. (1993). Arthrodiastasis for stiff hips in young patients. *Int Orthop.* **17**, 254–8.

Caplan, A. I. & Boyan, B. D. (1994). *Bone volume 8, mechanisms of bone development and growth, Chapter: Endochondral bone formation: the lineage cascade.* CRC, Press.

Cara del Rosal, J. A. (1992). *Influencia de la vascularización sobre el callo de elongación.* PhD thesis, Universidad de Navarra.

Carter, D. R. (1987). Mechanical loading history and skeletal biology. *J Biomech.* **20**, 1095–109.

Carter, D. R. & Beaupré, G. S. (2001). *Skeletal Function and Form: Mechanobiology of Skeletal Development Aging, and Regeneration.* Cambridge University Press, ISBN 052179000X.

Carter, D. R., Beaupré, G. S., Giori, N. J. & Helms, J. A. (1998). Mechanobiology of skeletal regeneration. *Clin Orthop Relat Res.* **355S**, S41–S55.

Carter, D. R. & Hayes, W. C. (1977). The compressive behavior of bone as a two-phase porous structure. *J Bone Joint Surg Am.* **59**, 954–62.

Castañeda, S., Largo, R., Calvo, E., Rodríguez-Salvanés, F., Marcos, M. E., Díaz-Curiel, M. & Herrero-Beaumont, G. (2006). Bone mineral measurements of subchondral and trabecular bone in healthy and osteoporotic rabbits. *Skeletal Radiol.* **35**, 34–41.

Catagni, M. A., Guerreschi, F., Holman, J. A. & Cattaneo, R. (1994). Distraction osteogenesis in the treatment of stiff hypertrophic nonunions using the Ilizarov apparatus. *Clin Orthop Relat Res.* **301**, 159–63.

Cattaneo, P. M., Kofod, T., Dalstra, M. & Melsen, B. (2005). Using the Finite Element Method to model the biomechanics of the asymmetric mandible before, during and after skeletal correction by distraction osteogenesis. *Comput Methods Biomech Biomed Engin.* **8**, 157–65.

Charlebois, M., Mckee, M. D. & Buschmann, M. D. (2004). Nonlinear tensile properties of bovine articular cartilage and their variation with age and depth. *J Biomech Eng.* **126**, 129–137.

Cheal, E. J., Mansmann, K. A., DiGioia, A. M., Hayes, W. C. & Perren, S. M. (1991). Role of interfragmentary strain in fracture healing: ovine model of a healing osteotomy. *J Orthop Res.* **9**, 131–42.

Chen, Y. & Hoger, A. (2000). Constitutive functions for elastic materials in finite growth and deformation. *J Elast.* **59**, 175–193.

Chin, M. (1997). Alveolar process reconstruction using distraction osteogenesis. In *International congress on Cranial and Facial Bone Distraction Processes, Paris, France.*

Chin, M. & Toth, B. A. (1996). Distraction osteogenesis in maxillofacial surgery using internal devices: review of five cases. *J Oral Maxillofac Surg.* **54**, 45–53.

Choi, I. H., Ahn, J. H., Chung, C. Y. & Cho, T. J. (2000). Vascular proliferation and blood supply during distraction osteogenesis: a scanning electron microscopic observation. *J Orthop Res.* **18**, 698–705.

Choi, I. H., Shim, J. S., Seong, S. C., Lee, M. C., Song, K. Y., Park, S. C., Chung, C. Y., Cho, T. J. & Lee, D. Y. (1997). Effect of the distraction rate on the activity of the osteoblast lineage in distraction osteogenesis of rat's tibia. Immunostaining study of the proliferating cell nuclear antigen, osteocalcin, and transglutaminase C. *Bull Hosp Jt Dis.* **56**, 34–40.

Choi, P., Ogilvie, C., Thompson, T., Miclau, T. & Helms, J. H. (2004). Cellular and molecular characterization of a murine non-union model. *J Orthop Res.* **22**, 1100–1107.

Chuong, C. J. & Fung, Y. C. (1986). On residual stresses in arteries. *J Biomech Eng.* **108**, 189–92.

Cierny, G. r. & Zorn, K. E. (1994). Segmental tibial defects. comparing conventional and Ilizarov methodologies. *Clin Orthop Relat Res.* **301**, 118–23.

Claes, L., Augat, P., Suger, G. & Wilke, H. J. (1997). Influence of size and stability of the osteotomy gap on the success of fracture healing. *Orthop Res.* **15**, 577–84.

Claes, L., Laule, J., Wenger, K., Suger, G., Liener, U. & Kinzl, L. (2000). The influence of stiffness of the fixator on maturation of callus after segmental transport. *J Bone Joint Surg Br.* **82**, 142–8.

Claes, L. E. & Heigele, C. A. (1999). Magnitudes of local stress and strain along bony surfaces predict the course and type of fracture healing. *J Biomech.* **32**, 255–266.

Claes, L. E., Heigele, C. A., Neidlinger-Wilke, C., Kaspar, D., Seidl, W., Margevicius, K. J. & Augat, P. (1998). Effects of mechanical factors on the fracture healing process. *Clin Orthop Relat Res.* **355S**, S132–S147.

Claes, L. E., Wilke, H. J., Augat, P., Rübenacker, S. & Margevicius, K. J. (1995). Effect of dynamization on gap healing of diaphyseal fractures under external fixation. *Clin Biomech.* **10**, 227–234.

Codivilla, A. (1905). On the means of lengthening, in the lower limbs, the muscles and tissues which are shortened through deformity. *Am J Orthop Surg.* **2**, 353.

Converse, J. M., Coccaro, P. J., Becker, M. & Wood-Smith, D. (1973). On hemifacial microsomia. The first and second branchial arch syndrome. *Plast Reconstr Surg.* **51**, 268–79.

Cope, J. B., Samchukov, M. L. & Cherkashin, A. M. (1999). Mandibular distraction osteogenesis: a historic perspective and future directions. *Am J Orthod Dentofac Orthop.* **115**, 448–60.

Cowin, S. C. (1999). Structural changes in living tissues. *Meccanica.* **34**, 379–98.

Cowin, S. C., Moss-Salentijn, L. & Moss, M. L. (1991). Candidates for the mechanosensory system in bone. *J Biomech Eng.* **113**, 191–7.

Craig, R. G. & Peyton, F. A. (1958). Elastic and mechanical properties of human dentin. *J Dent Res.* **37**, 710–718.

Cullinane, D. M., Salisbury, K. T., Alkhiary, Y. & Eisenberg, S. (2003). Effects of the local mechanical environment on vertebrate tissue differentiation during repair: does repair recapitulate development. *J Exp Biol,* **206**, 2459–2471.

Culmann, K. (1864). *Die Graphische Statik.* Verlag von Meyer & Zeller, Zurich.

Dahl, M. T. & Fischer, D. A. (1991). Lower extremity lengthening by Wagner's method and by callus distraction. *Orthop Clin North Am.* **22**, 643–9.

Dahl, M. T., Gulli, B. & Berg, T. (1994). Complications of limb lengthening. A learning curve. *Clin Orthop Relat Res.* **301**, 10–8.

Darwin, C. (1859). *The origin of species.* John Murray.

Davol, A., Bingham, M. S., Sah, R. L. & Klisch, S. M. (2008). A nonlinear finite element model of cartilage growth. *Biomech Model Mechanobiol.* **7**, 295–307.

De Bari, C., DellAccio, F., Tylzanowski, P. & Luyten, F. P. (2001). Multipotent mesenchymal stem cells from adult human synovial membrane. *Arthritis Rheum.* **44**, 1928–1942.

De Bastiani, G., Aldegheri, R., Renzi-Brivio, L. & Trivella, G. (1987). Limb lengthening by callus distraction (callotasis). *J Pediatr Orthop.* **7**, 129–34.

de la Huerta, F. (1994). Correction of the neglected clubfoot by the Ilizarov method. *Clin Orthop Relat Res.* **301**, 89–93.

de Pablos, J., Barrios, C., Alfaro, C. & Cañadell, J. (1994). Large experimental segmental bone defects treated by bone transportation with monolateral external distractors. *Clin Orthop Relat Res.* **298**, 259–65.

Delloye, C., Delefortrie, G., Coutelier, L. & Vincent, A. (1990). Bone regenerate formation in cortical bone during distraction lengthening: an experimental study. *Clin Orthop.* **250**, 34–42.

DiCarlo, A. & Quiligotti, S. (2002). Growth and balance. *Mech Res Commun.* **29**, 449–456.

Diefenderfer, D. L. & Brighton, C. T. (2000). Microvascular pericytes express aggrecan message which is regulated by BMP-2. *Biochem Biophys Res Commun.* **269**, 172–178.

Doblaré, M. & García-Aznar, J. M. (2006). On numerical modelling of growth, differentiation and damage in structural living tissues. *Arch Comput Methods Eng.* **13**, 471–513.

dos Santos, J. J. (1995). Supportive conservative therapies for temporomandibular disorders. *Dent Clin North Am,* **39**, 459–77.

Duda, G., Eckert-Hubner, K., Sokiranski, R., Kreutner, A., Miller, R. & Claes, L. (1998). Analysis of inter-fragmentary movement as a function of musculoskeletal loading conditions in sheep. *J Biomech.* **31**, 201–210.

Duda, G. N., Sporrer, S., Sollmann, M., Hoffmann, J. E., Kassi, J. P., Khodadadyan, C. & Raschke, M. (2003). Interfragmentary movements in the early phase of healing in distraction and correction osteotomies stabilized with ring fixators. *Langenbecks Arch Surg,* **387**, 433–40.

Ehrlich, P. J. & Lanyon, L. E. (2002). Mechanical strain and bone cell function: a review. *Osteoporos Int,* **13**, 688–700.

Enlow, D. H. (1990). *Facial growth.* Ed 3, Philadelphia, WB Saunders.

Epstein, M. & Maugin, G. A. (2000). Thermomechanics of volumetric growth in uniform bodies. *Int J Plast.* **16**, 951–978.

Eroschenko, V. P. & di Fiore, M. S. H. (2007). *DiFiore's Atlas of Histology with Functional Correlations*. Lippincott Williams & Wilkins, ISBN 0781770572.

Fang, T. D., Salim, A., Xia, W., Nacamuli, R. P., Guccione, S., Song, H. M., Carano, R. A., Filvaroff, E. H., Bednarski, M. D., Giaccia, A. J. & Longaker, M. T. (2005). Angiogenesis is required for successful bone induction during distraction osteogenesis. *J Bone Miner Res.* **20**, 1114–24.

Farhadieh, R. H., Gianoutsos, M. P., Dickinson, R. & Walsh, W. R. (2000). Effect of distraction rate on biomechanical , mineralization, and histologic properties of an ovine mandible model. *Plast Reconstr Surg.* **105**, 889–895.

Farquhar, T., Dawson, P. R. & Torzilli, P. A. (1990). A microstructural model for the anisotropic drained stiffness of articular cartilage. *J. Biomech. Eng.* **112**, 414–425.

Fink, B., Pollnau, C., Vogel, M., Skripitz, R. & Enderle, A. (2003). Histomorphometry of distraction osteogenesis during experimental tibial lengthening. *J Orthop Trauma.* **17**, 113–8.

Finn, R. A. (1978). Relationship of vertical maxillary dysplasias, bite force, and integrated EMG. In *Abstracts of Conference on Craniofacial Research. Center for human Growth and Development. University of Michigan, Ann Arbor.*

Fischgrund, J., Paley, D. & Suter, C. (1994). Variables affecting time to bone healing during limb lengthening. *Clin Orthop Relat Res.* **301**, 31–7.

Fonseca, R. J. (2000). *Oral and maxillofacial surgery.* Elsevier Health Sciences, ISBN 0721696317.

Forriol, F., Goenaga, I., Mora, G., Viñolas, J. & Canadell, J. (1997). Measurement of bone lengthening forces; an experimental model in the lamb. *Clin Biomech.* **12**, 17–21.

Frierson, M., Ibrahim, K., Boles, M., Bote, H. & Ganey, T. (1994). Distraction osteogenesis: a comparison of corticotomy techniques. *Clin Orthop.* **301**, 19–24.

Frost, H. M. (1963). *Bone remodeling dynamics.* Charles C. Thomas, Springfield, IL.

Frost, H. M. (1998). A brief review for orthopedic surgeons: fatigue damage (microdamage) in bone (its determinants and clinical implications). *J Orthop Sci.* **3**, 272–81.

Fung, Y. C. (1984). *Biodynamics: Circulation.* New York: Springer-Verlag.

Fung, Y. C. (1985). *What principle governs the stress distribution in living organs? in Fung YC, Fukada E, Wang JJ (eds): Biomechanics in China, Japan, and USA.* Beijing, China, Science press.

Fung, Y. C. (1990*a*). *Biomechanics: Motion, Flow, Stress, and Growth.* New York: Springer-Verlag.

Fung, Y. C. (1990*b*). *Biomechanics: Mechanical Properties of Living Tissues.* Springer, Berlin.

Fung, Y. C. (1993). *Biomechanics: Mechanical Properties of Living Tissues, Second edition.* Springer Verlag, New York.

Ganey, T. M., Klotch, D. W., Sasse, J., Ogden, J. A. & Garcia, T. (1994). Basement membrane of blood vessels during distraction osteogenesis. *Clin Orthop Relat Res.* **301**, 132–8.

García-Aznar, J. M., Kuiper, J. H., Gómez-Benito, M. J., Doblaré, M. & Richardson, J. B. (2007). Computational simulation of fracture healing: influence of interfragmentary movement on the callus growth. *J Biomech.* **40**, 1467–1476.

Gardner, M. J., van der Meulen, M. C., Demetrakopoulos, D., Wright, T. M., Myers, E. R. & Bostrom, M. P. (2006). In vivo cyclic axial compression affects bone healing in the mouse tibia. *J Orthop Res,* **24**, 1679–1686.

Gardner, T. N., Evans, M., Simpson, H. & Kenwright, J. (1998). Force-displacement behaviour of biological tissue during distraction osteogenesis. *Med Eng Phys.* **20**, 708–15.

Gardner, T. N. & Mishra, S. (2003). The biomechanical environment of a bone fracture and its influence upon the morphology of healing. *Med Eng Phys.* **25**, 455–464.

Garikipati, K., Arruda, E. M., Grosh, K., Narayanan, H. & Calve, S. (2004). A continuum treatment of growth in biological tissue: the coupling of mass transport and mechanics. *J Mech Phys Solids.* **52**, 1595–1625.

Gateño, J., Teichgraeber, J. F. & Aguilar, E. (2000). Computer planning for distraction osteogenesis. *Plast Reconstr Surg.* **105**, 873–82.

Gebhardt, W. (1901). lber funktionell wichtige Anordnungsweisen der groberen und feineren Bauelemente des Wirbeltierknochens. I, Allgemeiner Teil. *Wilhelm Roux' Arch Entwickl Mech Org,* **11**, 383–498.

Geris, L., Andreykiv, A., Van Oosterwyck, H., Vander Sloten, J., van Keulen, F., Duyck, J. & Naert, I. (2004). Numerical simulation of tissue differentiation around loaded titanium implants in a bone chamber. *J Biomech.* **37**, 763–769.

Geris, L., Gerisch, A., Maes, C., Carmeliet, G., Weiner, R., Vander Sloten, J. & Van Oosterwyck, H. (2006). Mathematical modeling of fracture healing in mice: comparison between experimental data and numerical simulation results. *Med Biol Eng Comput,* **44**, 280–9.

Geris, L., Gerisch, A., Sloten, J. V., Weiner, R. & Oosterwyck, H. V. (2008). Angiogenesis in bone fracture healing: a bioregulatory model. *J Theor Biol,* **251**, 137–58.

Geris, L., Van Oosterwyck, H., Vander Sloten, J., Duyck, J. & Naert, I. (2003). Assessment of mechanobiological models for the numerical simulation of tissue differentiation around immediately loaded implants. *Comput Methods Biomech Biomed Engin,* **6**, 277–88.

Geris, L., Vandamme, K., Naert, I., Vander Sloten, J., Duyck, J. & Van Oosterwyck, H. (2009). Numerical simulation of bone regeneration in a bone chamber. *J Dent Res,* **88**, 158–63.

Geris, L., Vander Sloten, J. & Van Oosterwyck, H. (2008). Mathematical modelling of bone regeneration including angiogenesis: design of treatment strategies for atrophic nonunions. In *Transactions of the 54th Annual Meeting of the Orthopaedic Research Society, New Orleans.*

Gerstenfeld, L. C., Culliname, D. M., Barnes, G. L., Graves, D. T. & Einhorn, T. A. (2003). Fracture healing as a post-natal development process: molecular, spatial, and temporal aspects of its regulation. *J Cell Biochem.* **88**, 873–884.

Gil-Albarova, J., de Pablos, J., Franzeb, M. & Cañadell, J. (1992). Delayed distraction in bone lengthening. Improved healing in lambs. *Acta Orthop Scand.* **63**, 604–6.

Glowacki, J. & Mulliken, J. B. (1985). Demineralized bone implants. *Clin Plast Surg.* **12**, 233–41.

Golyakhovsky, V. & Frankel, V. H. (1991). Ilizarov bone transport in large bone loss and in severe osteomyelitis. *Bull Hosp Jt Dis Orthop Inst.* **51**, 63–73.

Gómez-Benito, M. J., Fornells, P., García-Aznar, J. M., Seral, B., Seral-Iñigo, F. & Doblaré, M. (2007). Computational comparison of reamed versus unreamed intramedullary tibial nails. *J Orthop Res.* **25**, 191–200.

Gómez-Benito, M. J., García-Aznar, J. M., Kuiper, J. H. & Doblaré, M. (2005). Influence of fracture gap size on the pattern of long bone healing: a computational study. *J Theor Biol.* **235**, 105–119.

Gómez-Benito, M. J., García-Aznar, J. M., Kuiper, J. H. & Doblaré, M. (2006). A 3D computational simulation of fracture callus formation: influence of the stiffness of the external fixator. *J Biomech Eng.* **128**, 290–299.

Gong, J. K., Arnold, J. S. & Cohn, S. H. (1964). Composition of trabecular and cortical bone. *Anat Rec.* **149**, 325–31.

Goodman, S., Song, Y., Doshi, A. & Aspenberg, P. (1994). Cessation of strain facilitates bone formation in the micromotion chamber implanted in the rabbit tibia. *Biomaterials,* **15**, 889–893.

Goodship, A. E. & Kenwright, J. (1985). The influence of induced micromovement upon the healing of experimental tibial fractures. *J Bone Joint Surg Br.* **67**, 650–5.

Goodship, A. E., Watkins, P. E., Rigby, H. S. & Kenwright, J. (1993). The role of fixator frame stiffness in the control of fracture healing. An experimental study. *J Biomech.* **26**, 1027–35.

Gorlin, R. J., Cohen, M. M. J. & Levin, L. S. (1990). *Syndromes of the head and neck.* New York: Oxford University Press.

Grant, A. D., Atar, D. & Lehman, W. B. (1992). The Ilizarov technique in correction of complex foot deformities. *Clin Orthop Relat Res.* **280**, 94–103.

Graziano, G. P., Herzenberg, J. E. & Hensinger, R. N. (1993). The halo-Ilizarov distraction cast for correction of cervical deformity. Report of six cases. *J Bone Joint Surg Am.* **75**, 996–1003.

Green, S. A. (1991). The Ilizarov method: Rancho technique. *Orthop Clin North Am.* **22**, 677–88.

Green, S. A., Harris, N. L., Wall, D. M., Ishkanian, J. & Marinow, H. (1992). The Rancho mounting technique for the Ilizarov method. A preliminary report. *Clin Orthop Relat Res.* **280**, 104–16.

Gregersen, H., Kassab, G. S. & Fung, Y. C. (2000). The zero stress state of the gastrointestinal tract: biomechanical and functional implications. *Dig Dis Sci.* **45**, 2271–2281.

Griffin, L. V., Gibeling, J. C., Martin, R. B., Gibson, V. A. & Stover, S. M. (1997). Model of flexural fatigue damage accumulation for cortical bone. *J Orthop Res.* **15(4)**, 607–614.

Guerrero, C. (1990). Expansion mandibular quirurgica. *Rev Venez Ortod.* **48**, 1–2.

Guldberg, R. E., Caldwell, N. J., Guo, X. W., Goulet, R. W., Hollister, S. J. & Goldstein, S. A. (1997). Mechanical stimulation of tissue repair in the hydraulic bone chamber. *J Bone Miner Res.* **12**, 1295–302.

Gushue, D. L., Houck, J. & Lerner, A. L. (2005). Rabbit knee joint biomechanics: motion analysis and modeling of forces during hopping. *J Orthop Res.* **23**, 735–42.

Habal, M. B. (1994). New bone formation by biological rhythmic distraction. *J Craniofac Surg.* **5**, 344–7.

Haggland, G., Rydholm, U. & Sunden, G. (1993). Ilizarov technique in the correction of knee flexion contracture: report of four cases. *J Pediatr Orthop B.* **2**, 170–172.

Hamanishi, C., Yoshii, T., Totani, Y. & Tanaka, S. (1994). Lengthened callus activated by axial shortening. Histological and cytomorphometrical analysis. *Clin Orthop Relat Res.* **307**, 250–4.

Han, H. C. & Fung, Y. C. (1996). Direct measurement of transverse residual strains in aorta. *Am J Physiol.* **270**, H750–H759.

Harpoon (2006). *Sharc Lt. Richard Bardwell. Empress Business Centre.* Manchester, UK.

Havlik, R. J. & Bartlett, S. P. (1994). Mandibular distraction lengthening in the severely hypoplastic mandible: a problematic case with tongue aplasia. *J Craniofac Surg.* **5**, 305–10.

Heller, O. (1998). *Management of Medical Technology: Theory, Practice, and Cases.* Springer, ISBN 0792380541.

Hertling, D. & Kessler, R. M. (2006). *Management of Common Musculoskeletal Disorders: Physical Therapy Principles and Methods.* Lippincott Williams & Wilkins.

Herzenberg, J. E., Davis, J. R., Paley, D. & Bhave, A. (1994*a*). Mechanical distraction for treatment of severe knee flexion contractures. *Clin Orthop Relat Res.* **301**, 80–8.

Herzenberg, J. E., Scheufele, L. L., Paley, D., Bechtel, R. & Tepper, S. (1994*b*). Knee range of motion in isolated femoral lengthening. *Clin Orthop Relat Res.* **301**, 49–54.

Herzenberg, J. E., Smith, J. D. & Paley, D. (1994*c*). Correcting torsional deformities with Ilizarov's apparatus. *Clin Orthop Relat Res.* **302**, 36–41.

Hibbit, K. & Sorensen, I. (2002). *Theory Manual, v. 6.3.* HKS inc. Pawtucket, RI, USA.

Himpel, G., Kuhl, E., Menzel, A. & Steinmann, P. (2005). Computational modelling of isotropic multiplicative growth. *Comput Model Eng Sci.* **8**, 119–134.

Hoger, A. (1997). Virtual configurations and constitutive equations for residually stressed bodies with material symmetry. *J Elast.* **48**, 125–144.

Holbein, O., Neidlinger-Wilke, C., Suger, G., Kinzl, L. & Claes, L. (1995). Ilizarov callus distraction produces systemic bone cell mitogens. *J Orthop Res.* **13**, 629–38.

Hori, R. Y. & Lewis, J. L. (1982). Mechanical properties of the fibrous tissue found at the bone-cement interface following total joint replacement. *J Biomed Mater Res.* **16**, 911–27.

Horii, E., Nakamura, R., Nakao, E., Kato, H. & Yajima, H. (2000). Distraction lengthening of the forearm for congenital and developmental problems. *J Hand Surg [Br].* **25**, 15–21.

Huang, C. Y., Mow, V. C. & Ateshian, G. A. (2001). The role of flow-independent viscoelasticity in the biphasic tensile and compressive responses of articular cartilage. *J Biomech Eng.* **123**, 410–7.

Huang, Z. (1994). The equilibrium equations and constitutive equations of the growing deformable body in the framework of continuum theory. *Int J Non-Linear Mech.* **39**, 951–962.

Humphrey, J. D. (2001). Stress, strain, and mechanotransduction in cells. *J Biomech Eng.* **123**, 638–641.

Humphrey, J. D. & Rajagopal, K. R. (2003). A constrained mixture model for arterial adaptations to a sustained step change in blood flow. *Biomech Model Mechanobiol.* **2**, 109–26.

Hyodo, A., Kotschi, H., Kambic, H. & Muschler, G. (1996). Bone transport using intramedullary fixation and a single flexible traction cable. *Clin Orthop Relat Res.* **325**, 256–68.

Idelsohn, S., Planell, J. A., Gil, F. J. & Lacroix, D. (2006). Development of a dynamic mechano-regulation model based on shear strain and fluid flow to optimize distraction osteogenesis. *J Biomech.* **39S**, S1–S684.

Ilizarov, G. A. (1952). A method of uniting bones in fractures and an apparatus to implement this method. In *USSR Authorship Certificate 9847 1.*

Ilizarov, G. A. (1971). Basic principles of transosseous compression and distraction osteosynthesis. *Ortop Travmatol Protez.* **32**, 7–15.

Ilizarov, G. A. (1983). Experimental theoretical and clinical aspects of transosseous osteosynthesis. In *Abstracts of the First International Symposium on Transosseous Osteosynthesis. Medi Surgical Video, Milan, Italy, pp. 17.*

Ilizarov, G. A. (1988). The principles of the Ilizarov method. *Bull Hosp Jt Dis Orthop Inst.* **48**, 1.

Ilizarov, G. A. (1989*a*). The tension-stress effect on the genesis and growth of tissues. Part I: the influence of stability of fixation and soft-tissue preservation. *Clin Orthop.* **238**, 249–81.

Ilizarov, G. A. (1989*b*). The tension-stress effect on the genesis and growth of tissues. Part II: the influence of the rate and frequency of distraction. *Clin Orthop.* **239**, 263–85.

Ilizarov, G. A. (1990). Clinical application of the tension-stress effect for limb lengthening. *Clin Orthop Relat Res.* **250**, 8–26.

Ilizarov, G. A. (1992). *Transosseous Osteosynthesis*. Heidelberg: Springer-Verlag.

Ilizarov, G. A. & Gracheva, V. I. (1971). Bloodless treatment of congenital pseudoarthrosis of the crus with simultaneous elimination of shortening using dosed distraction. *Orthop Traumatol Protez.* **32**, 42–6.

Ilizarov, G. A., Kaplunov, A. G., Degtiarev, V. E. & Lediaev, V. I. (1972). Treatment of pseudarthroses and ununited fractures, complicated by purulent infection, by the method of compression-distraction osteosynthesis. *Ortop Travmatol Protez.* **33**, 10–4.

Ilizarov, G. A., Lediaev, V. I. & Degtiarev, V. E. (1973). Operative and bloodless methods of repairing defects of the long tubular bones in osteomyelitis. *Vestn Khir Im I I Grek.* **110**, 55–9.

Ilizarov, G. A., Lediaev, V. I. & Shitin, V. P. (1969). The course of compact bone reparative regeneration in distraction osteosynthesis under different conditions of bone fragment fixation (experimental study). *Eksp Khir Anesteziol.* **14**, 3–12.

Ilizarov, G. A. & Ledyaev, V. I. (1992). The replacement of long tubular bone defects by lengthening distraction osteotomy of one of the fragments. 1969. *Clin Orthop Relat Res.* **280**, 7–10.

Ilizarov, G. A., Schreiner, A. A., Imerlishvili, I. A., Bakhlykov, Y. N., Onirkova, A. M. & Marterl, I. I. (1983). On the problem of improving osteogenesis conditions in limb lengthening. In *Abstracts of First International Symposium on Experimental and Clinical Aspects of Transosseous Osteosynthesis, USSR, 20-22*.

Ilizarov, G. A. & Soybelman, L. M. (1969). Some clinical and experimental data concerning lengthening of lower extremities. *Exp Khir Arrestar.* **14**, 27.

Isaksson, H., Comas, O., Van Donkelaar, C. C., Mediavilla, J., Wilson, W., Huiskes, R. & Ito, K. (2007). Bone regeneration during distraction osteogenesis: mechano-regulation by shear strain and fluid velocity. *J Biomech.* **40**, 2002–11.

Isaksson, H., van Donkelaar, C. C., Huiskes, R. & Ito, K. (2008). A mechano-regulatory bone-healing model incorporating cell-phenotype specific activity. *J Theor Biol.* **252**, 230–46.

Isaksson, H., Wilson, W., van Donkelaar, C. C., Huiskes, R. & Ito, K. (2006). Comparison of biophysical stimuli for mechano-regulation of tissue differentiation during fracture healing. *J Biomech.* **39**, 1507–16.

Ishizeki, K., Kuroda, N. & Nawa, T. (1992). Morphological characteristics of the life cycle of resting cartilage cells in mouse rib investigated in intrasplenic isografts. *Anat Embryol (Berl).* **185**, 421–30.

Iwaki, A., Jingushi, S., Oda, Y., Izumi, T., Shida, J. I., Tsuneyoshi, M. & Sugioka, Y. (1997). Localization and quantification of proliferating cells during rat fracture repair: detection of proliferating cell nuclear antigen by immunochemistry. *J Bone Miner Res.* **12**, 96–102.

Jaeger, R. J. & Vanitchatchavan, P. (1992). Ground reaction forces during termination of human gait. *J Biomech.* **25**, 1233–6.

Jazrawi, L. M., Majeska, R. J., Klein, M. L., Kagel, E., Stromberg, L. & Einhorn, T. A. (1998). Bone and cartilage formation in an experimental model of distraction osteogenesis. *J Orthop Trauma.* **12**, 111–6.

Jensen, O. T. (2002). *Alveolar Distraction Osteogenesis.* Quintessence Pub. Co., ISBN 0867154144.

Jin, M., Levenston, M., Frank, E. & Grodzinsky, A. (1999). Regulation of cartilage matrix metabolism by dynamic tissue shear strain. *Trans Orthop Res Soc.* **24**, 169.

Jones, C. B., Dewar, M. E., Aichroth, P. M., Crawfurd, E. J. & Emery, R. (1989). Epiphyseal distraction monitored by strain gauges. Results in seven children. *J Bone Joint Surg Br.* **250**, 61–72.

Junqueira, L. C. & Carneiro, J. (2005). *Basic histology: Text & Atlas.* McGraw-Hill Professional, ISBN 0071440917.

Kallio, T. J., Vauhkonen, M. V., Peltonen, J. I. & Karaharju, E. O. (1994). Early bone matrix formation during distraction. A biochemical study in sheep. *Acta Orthop Scand.* **65**, 467–71.

Kane, A. A., Lo, L. J., Christensen, G. E., Vannier, M. W. & Marsh, J. L. (1997). Relationship between bone and muscles of mastication in hemifacial microsomia. *Plast Reconstr Surg.* **99**, 990–7.

Kaplan, F. S., Hayes, W. C., Keaveny, T. M., A., B., Einhorn, T. A. & Iannotti, J. P. (1994). *Form and function of bone, in "Orthopaedic Basic Science".* American Academy of Orthopaedic Surgeons, Columbus, Ohio.

Karp, N. S., Thorne, C. H. M., McCarthy, J. & Sissons, H. (1990). Bone lengthening in the craniofacial skeleton. *Ann Plast Surg.* **24**, 231–237.

Kelly, D. J. & Prendergast, P. J. (2005). Mechano-regulation of stem cell differentiation and tissue regeneration in osteochondral defects. *J Biomech.* **38**, 1413–22.

Kempson, G. E., Tuke, M. A., Dingle, J. T., Barrett, A. J. & Horsfield, P. H. (1976). The effects of proteolytic enzymes on the mechanical properties of adult human articular cartilage. *Biochim Biophys Acta.* **428**, 741–760.

Kenwrigh, J. & Goodship, A. E. (1989). Controlled mechanical stimulation in the treatment of tibial fractures. *Clin Orthop Relat Res.* **241**, 36–47.

Kenwright, J., Spriggins, A. J. & Cunningham, J. L. (1990). Response of the growth plate to distraction close to skeletal maturity. Is fracture necessary? *Clin Orthop Relat Res.* **250**, 61–72.

Kenwright, J. & White, S. H. (1993). A historical review of limb lengthening and bone transport. *Injury.* **24**, S9–19.

Khaleel, A. & Pool, R. D. (2003). (i) Congenital pseudoarthrosis and lengthening. *Curr Orthop.* **17**, 411–417.

Kiliaridis, S., Kjellberg, H., Wenneberg, B. & Engström, C. (1993). The relationship between maximal bite force, bite force endurance, and facial morphology during growth. A cross-sectional study. *Acta Odontol Scand.* **51**, 323–31.

King, N. S., Liu, Z. J., Wang, L. L., Chiu, I. Y., Whelan, M. F. & Huang, G. J. (2003). Effect of distraction rate and consolidation period on bone density following mandibular osteodistraction in rats. *Arch Oral Biol.* **48**, 299–308.

Kirienko, A., Villa, A. & Calhoun, J. H. (2003). *Ilizarov Technique for Complex Foot and Ankle Deformities.* Informa Health Care, ISBN 0824747895.

Klapp, R. & Block, W. (1930). *Die Knochenbruchbehandlung mit Drahtzugen.* Stuttgart, Ferd Elnke.

Klisch, S. M., Chen, S. S., Sah, R. L. & Hoger, A. (2003). A growth mixture theory for cartilage with application to growth-related experiments on cartilage explants. *J Biomech Eng.* **125**, 169–179.

Klisch, S. M., Van Dyke, T. J. & Hoger, A. (2001). A theory of volumetric growth for compressible elastic biological materials. *Math Mech Solids.* **6**, 551–575.

Kofod, T., Cattaneo, P. M. & Melsen, B. (2005). Three-dimensional finite element analysis of the mandible and temporomandibular joint on simulated occlusal forces before and after vertical ramus elongation by distraction osteogenesis. *J Craniofac Surg.* **16**, 421–9.

Kojimoto, H., Yasui, N., Goto, T., Matsuda, S. & Shimomura, Y. (1988). Bone lengthening in rabbits by callus distraction. *J Bone Joint Surgery Br.* **70-B**, 543–9.

Komuro, Y., Takato, T., Harii, K. & Yonemara, Y. (1994). The histologic analysis of distraction osteogenesis of the mandible in rabbits. *Plast Reconstr Surg.* **94**, 152–9.

Korioth, T. W. P., Romilly, D. P. & Hannam, A. G. (1992). Three-dimensional finite element stress analysis of the dentate human mandible. *Am J Phys Anthropol.* **88**, 69–96.

Kuhl, E., Menzel, A. & Steinmann, P. (2003). Computational modeling of growth. *Comput Mech.* **32**, 71–88.

Kuhl, E. & P., S. (2003). Mass- and volumetric-specific views on thermodynamics for open systems. *Proc R Soc London,* **459A**, 2547–2568.

Lacroix, D. (2000). *Simulation of tissue differentiation during fracture healing.* PhD thesis, University of Dublin.

Lacroix, D. & Prendergast, P. J. (2002*a*). A mechano-regulation model for tissue differentiation during fracture healing: analysis of gap size and loading. *J Biomech.* **35**, 1163–1171.

Lacroix, D. & Prendergast, P. J. (2002*b*). Three-dimensional simulation of fracture repair in the human tibia. *Comput Methods Biomech Biomed Eng.* **5**, 369–76.

Lacroix, D., Prendergast, P. J., Li, G. & Marsh, D. (2002). Biomechanical model to simulate tissue differentiation and bone regeneration: application to fracture healing. *Med Biol Eng Comput.* **40**, 14–21.

Lammens, J., Liu, Z., Aerssens, J., Dequeker, J. & Fabry, G. (1998). Distraction bone healing versus osteotomy healing: a comparative biochemical analysis. *J Bone Miner Res.* **13**, 279–86.

Lanyon, L. E. (1987). Functional strain in bone tissue as an objective, and controlling stimulus for adaptive bone remodelling. *J Biomech.* **20**, 1083–93.

Lanyon, L. E. (1993). Osteocytes, strain detection, bone modeling and remodeling. *Calcif Tissue Int.* **53**, S102–6.

Lappa, M. (2005). A CFD level-set method for soft tissue growth: theory and fundamental equations. *J Biomech.* **38**, 185–90.

Launay, F., Jouve, J. L., Viehweger, E., Guillaume, J. M., Jacquemier, M. & Bollini, G. (2004). Progressive forearm lengthening with an intramedullary guidewire in children: report of 10 cases. *J Pediatr Orthop.* **24**, 21–5.

Le, A. X., Miclau, T., Hu, D. & Helms, J. A. (2001). Molecular aspects of healing in stabilized and non-stabilized fractures. *J Orthop Res.* **19**, 78–84.

Leong, J. C., Ma, R. Y., Clark, J. A., Cornish, L. S. & Yau, A. C. (1979). Viscoelastic behavior of tissue in leg lengthening by distraction. *Clin Orthop Relat Res.* **139**, 102–9.

Leong, P. L. & Morgan, E. F. (2008). Measurement of fracture callus material properties via nanoindentation. *Acta Biomater.* **4**, 1569–75.

Leung, K. S., Taglang, G. & Schnettler, R. (2006). *Practice of Intramedullary Locked Nails: New Developments in Techniques and Applications.* Birkhuser, ISBN 3540253491.

Levick, J. R. (1987). Flow through interstitium and other fibrous matrices. *Q. J. Exp. Physiol.* **72**, 409–438.

Li, G., Bronk, J. T., An, K. N. & Kelly, P. J. (1987). Permeability of cortical bone of canine tibiae. *Microvascular Res.* **34**, 302–310.

Li, G., Simpson, A. H. & Triffitt, J. T. (1999). The role of chondrocytes in intramembranous and endochondral ossification during distraction osteogenesis in the rabbit. *Calcif Tissue Int.* **64**, 310–7.

Li, G., Simpson, H. R. W., Kenwright, J. & Triffitt, J. T. (1997). Assessment of cell proliferation in regenerating bone during distraction osteogenesis at different distraction rates. *J Orthop Res.* **15**, 765–772.

Li, G., Simpson, H. R. W., Kenwright, J. & Triffitt, J. T. (2000). Tissues formed during distraction osteogenesis in the rabbit are determined by the distraction

rate: localization of the cells that express the mRNAs and the distribution of types I and II collagens. *Cell Biol Int.* **24**, 25–33.

Lieberman, J. R. & Friedlaender, G. E. (2005). *Bone Regeneration and Repair: Biology and Clinical Applications.* Humana Press, ISBN 0896038475.

Liebschner, M. A. (2004). Biomechanical considerations of animal models used in tissue engineering of bone. *Biomaterials.* **25**, 1697–714.

Liou, E. J. & Huang, C. S. (1998). Rapid canine retraction through distraction of the periodontal ligament. *Am J Orthod Dentofacial Orthop.* **114**, 372–82.

Liu, S. Q. & Fung, Y. C. (1988). Zero-stress states of arteries. *J Biomech Eng.* **110**, 82–4.

Lo, C. M., Wang, H. B., Dembo, M. & Wang, Y. L. (2000). Cell movement is guided by the rigidity of the substrate. *Biophys J,* **79**, 144–152.

Loboa, E. G., Beaupré, G. S. & Carter, D. R. (2001). Mechanobiology of initial pseudarthrosis formation with oblique fractures. *J Orthop Res,* **19**, 1067–1072.

Loboa, E. G., Fang, T. D., Parker, D. W., Warren, S. M., Fong, K. D., Longaker, M. T. & Carter, D. R. (2005). Mechanobiology of mandibular distraction osteogenesis: finite element analyses with a rat model. *J Orthop Res.* **23**, 663–70.

Losken, H. W., Mooney, M. P., Zoldos, J., Tschakaloff, A., Burrows, A. M., Smith, T. D., Cooper, G. M., Kapucu, M. R. & Siegel, M. I. (1998). Internal calvarial bone distraction in rabbits with delayed-onset coronal suture synostosis. *Plast Reconstr Surg.* **102**, 1109–19.

Lubarda, V. A. & Hoger, A. (2002). On the mechanics of solids with a growing mass. *Int J Solids Struct.* **39**, 4627–4664.

Lynch, S. E., Genco, R. J. & Marx, R. E. (2004). *Tissue Engineering: Applications in Maxillofacial Surgery and Periodontics.* Quintessence Pub. Co., ISBN 0867153466.

Malgaigne, J. F. (1847). *Traité des fractures et des luxations.* JB Bailliere.

Marieb, E. N. (2004). *Bone and skeletal tissues Part A. Human anatomy and physiology. Sixth edition. Power point lecture slide presentation by Vicen Austin. University of Kentucky.* Pearson Education Inc, publishing as Benjamin Cummings.

Marieb, E. N. & Hoehn, K. (2007). *Human anatomy & physiology.* Pearson Education, ISBN 0321372948.

Marsh, J. L., Baca, D. & Vannier, M. W. (1989). Facial musculoskeletal asymmetry in hemifacial microsomia. *Cleft Palate J.* **26**, 292–302.

Martin, R. B., Burr, D. B. & Sharkey, N. A. (1998). *Skeletal Tissue Mechanics.* Springer-Verlarg, New York.

Matsushita, T., Nakamura, K. & Kurokawa, T. (1999). Tensile force in limb lengthening: histogenesis or only mechanical elongation. *Orthopedics.* **22**, 61–3.

McCarthy, J. G., Schreiber, J., Karp, N., Thorne, C. H. & Grayson, B. H. (1992). Lengthening the human mandible by gradual distraction. *Plast Reconstr Surg.* **89**, 1–8.

Menzel, A. (2005). Modelling of anisotropic growth in biological tissues. A new approach and computational aspects. *Biomech Model Mechanobiol.* **3**, 147–71.

Menzel, A. (2006). *Anisotropic remodeling of biological tissue, in Mechanics of Biological Tissue.* Eds. Holzapfel and Ogden, Springer.

Meyer, U., Meyer, T., Schlegel, W., Scholz, H. & Joos, U. (2001). Tissue differentiation and cytokine synthesis during strain-related bone formation in distraction osteogenesis. *Br J Oral Maxillofac Surg.* **39**, 22–9.

Mimics, . (2006). *Materialise.* Leuven, Belgium.

Miner, M. A. (1945). Cumulative fatigue damage. *Transactions, American Society of Mechanical Engineers,* **67**, A159–A164.

Moore, M. H., Guzman-Stein, G., Proudman, T. W., Abbott, A. H., Netherway, D. J. & David, D. J. (1994). Mandibular lengthening by distraction for airway obstruction in treacher-collins syndrome. *J Craniofac Surg.* **5**, 22–5.

Moreo, P., García-Aznar, J. M. & Doblaré, M. (2008). Modeling mechanosensing and its effect on the migration and proliferation of adherent cells. *Acta Biomater,* **4**, 613–21.

Morgan, E. F., Longaker, M. T. & Carter, D. R. (2006). Relationships between tissue dilatation and differentiation in distraction osteogenesis. *Matrix Biol.* **25**, 94–103.

Mosheiff, R., Cordey, J., Rahn, B. A., Perren, S. M. & Stein, H. (1996). The vascular supply to bone in distraction osteoneogenesis: an experimental study. *J Bone Joint Surg Br.* **78**, 497–8.

Mow, V. C. & Ateshian, G. A. (1997). *Friction, Lubrication, and Wear of Diarthrodial Joints. In: Basic Orthopaedic Biomechanics, V.C. Mow and W.C. Hayes (eds).* Raven Press, New York, 2^{nd} ed.

Mow, V. C. & Ratcliffe, A. (1997). *Structure and function of articular cartilage and meniscus. In: Mow VC, Hayes WC (eds) Basic orthopaedic biomechanics.* Lippincott-Raven, New York.

Mulder, M., Small, N., Botma, Y., MacKenzie, J. & Ziady, L. (2002). *Basic Principles of Wound Care.* Pearson South Africa, ISBN 1868911365.

Murray, J. E., Kaban, L. B. & Mulliken, J. B. (1984). Analysis and treatment of hemifacial microsomia. *Plast Reconstr Surg.* **74**, 186–99.

Murray, J. H. (1996). Distraction histiogenesis: principles and indications. *J Am Acad Orthop Surg.* **4**, 317–327.

Naeije, M. & Hofman, N. (2003). Biomechanics of the human temporomandibular joint during chewing. *J Dent Res.* **82**, 528–31.

Nafei, A., Danielsen, C. C., Linde, F. & Hvid, I. (2000). Properties of growing trabecular ovine bone. Part I: mechanical and physical properties. *J Bone Joint Surg Br.* **82**, 910–20.

Nakamura, K., Matsushita, T., Okazaki, H. & Kurokawa, T. (1997). Soft tissue responses to limb lengthening. *J Orthop Sci.* **2**, 191–197.

Nakase, T., Takaoka, K., Hirakawa, K., Hirota, S., Takemura, T., Onoue, H., Takebayashi, K., Kitamura, Y. & Nomura, S. (1994). Alterations in the expression of osteonectin, osteopontin and osteocalcin mRNAs during the development of skeletal tissues in vivo. *Bone Miner.* **26**, 109–22.

Neidlinger Wilke, C., Holbein, O., Grood, E., Morike, M. & Claes, L. (1994). Effects of cyclic strain on proliferation, metabolic activity and alignment of human osteoblasts and fibroblasts. In *Abstract Book, 40th Annual Meeting, ORS.*

Nelson, G. J. (1986). *Three dimensional computer modeling of human mandibular biomechanics.* PhD thesis, University of British Columbia.

Newman, E., Turner, A. S. & Wark, J. D. (1995). The potential of sheep for the study of osteopenia: current status and comparison with other animal models. *Bone.* **16**, 277S–284S.

Neyt, J. G., Buckwalter, J. A. & Carroll, N. C. (1998). Use of animal models in musculoskeletal research. *Iowa Orthop J,* **18**, 118–23.

Ng, K. W., Mauck, R. L., Statman, L. Y., Lin, E. Y., Ateshian, G. A. & Hung, C. T. (2006). Dynamic deformational loading results in selective application of mechanical stimulation in a layered, tissue-engineered cartilage construct. *Biorheology.* **43**, 497–507.

Nöth, U., Osyczka, A. M., Tuli, R., Hickok, N. J., Danielson, K. G. & Tuan, R. S. (2002). Multilineage mesenchymal differentiation potential of human trabecular bone-derived cells. *J Orthop Res.* **20**, 1060–9.

Ochoa, J. A. & Hillberry, B. M. (1992). Permeability of bovine cancellous bone. In *Transactions of the 38th ORS, Washinton DC.*

Ohyama, M., Miyasaka, Y., Sakurai, M., Yokobori, A. J. & Sasaki, S. (1994). The mechanical behavior and morphological structure of callus in experimental callotasis. *Biomed Mater Eng.* **4**, 273–81.

Osyczka, A. M., Noth, U., Danielson, K. G. & Tuan, R. S. (2002). Different osteochondral potential of clonal cell lines derived from adult human trabecular bone. *Ann N Y Acad Sci.* **961**, 73–77.

Pacifici, M., Golden, E. B., Oshima, O., Shapiro, I. M., Leboy, P. S. & Adams, S. L. (1990). Hypertrophic chondrocytes. The terminal stage of differentiation in the chondrogenic cell lineage? *Ann N Y Acad Sci.* **599**, 45–57.

Paley, D. (1988). Current techniques of limb lengthening. *J Pediatr Orthop.* **8**, 73–92.

Paley, D. (1990). Problems, obstacles, and complications of limb lengthening by the Ilizarov technique. *Clin Orthop Relat Res.* **250**, 81–104.

Paley, D. (1993). The correction of complex foot deformities using Ilizarov's distraction osteotomies. *Clin Orthop Relat Res.* **293**, 97–111.

Paley, D., Catagni, M., Argnani, F., Prevot, J., Bell, D. & Armstrong, P. (1992). Treatment of congenital pseudoarthrosis of the tibia using the Ilizarov technique. *Clin Orthop Relat Res.* **280**, 81–93.

Paley, D., Catagni, M. A., Argnani, F., Villa, A., Benedetti, G. B. & Cattaneo, R. (1989). Ilizarov treatment of tibial nonunions with bone loss. *Clin Orthop Relat Res.* **241**, 146–65.

Paley, D., Fleming, B., Catagni, M., Kristiansen, T. & Pope, M. (1990). Mechanical evaluation of external fixators used in limb lengthening. *Clin Orthop Relat Res.* **250**, 50–7.

Paley, D., Herzenberg, J. E., Paremain, G. & Bhave, A. (1997). Femoral lengthening over an intramedullary nail. A matched-case comparison with Ilizarov femoral lengthening. *J Bone Joint Surg Am.* **79**, 1464–80.

Paterson, D. (1990). Leg-lengthening procedures. A historical review. *Clin Orthop Relat Res.* **250**, 27–33.

Pauwels, F. (1941). *Grundriβ einer Biomechanik der Frankturheilung.* In: 34^{th} Kongress der Deutschen Orthopdischen Gessellschaft. Ferdinand Enke Verlag, Stuttgart, (Biomechanics of the Locomotor Apparatus) translated by Maquet, P., Furlong, R.(Eds), Springer, Berlin.

Pauwels, F. (1960). Eine neue Theorie über den Einfluss mechanischer Reize auf die Differenzierung der Stützgewebe. *Z Anat Entwicklungsgeschichte.* **121**, 478–515.

Pearce, A. I., Richards, R. G., Milz, S., Schneider, E. & Pearce, S. G. (2007). Animal models for implant biomaterial research in bone: a review. *Eur Cell Mater.* **13**, 1–10.

Peltier, L. F. (1990). *Fractures: a history and iconography of their treatment. San Francisco.* Norman Publishing.

Peltonen, J. I., Kahri, A. I., Lindberg, L. A., Heikkila, P. S., Karaharju, E. O. & Aalto, K. A. (1992). Bone formation after distraction osteotomy of the radius in sheep. *Acta Orthop Scand.* **63**, 599–603.

Perren, S. M. (1979). Physical and biological aspects of fracture healing with special reference to internal fixation. *Clin Orthop.* **138**, 175–195.

Perren, S. M. & Cordey, J. (1980). *The concept of interfragmentary strain* pp. 63–77. Current concepts of internal fixation of fractures. Springer-Verlarg, Berlin.

Pietrzak, W. S. (2008). *Musculoskeletal Tissue Regeneration: Biological Materials and Methods.* Humana Press, ISBN 1588299090.

Pittenger, M. F., Mackay, A. M., Beck, S. C., Jaiswal, R. K., Douglas, R., Mosca, J. D., Moorman, M. A., Simonetti, D. W., Craig, S. & Marshak, D. R. (1999). Multilineage potential of adult human mesenchymal stem cells. *Science.* **284**, 143–7.

Podolsky, A. & Chao, E. Y. (1993). Mechanical performance of Ilizarov circular external fixators in comparison with other external fixators. *Clin Orthop Relat Res.* **293**, 61–70.

Pombo-Arias, M. (1997). *Tratado de Endocrinología Pediátrica.* Ediciones Díaz de Santos, ISBN 8479782943.

Popowics, T. E., Zhu, Z. & Herring, S. W. (2002). Mechanical properties of the periosteum in the pig, Sus scrofa. *Arch Oral Biol.* **47**, 733–741.

Prendergast, P. J., Huiskes, R. & Soballe, K. (1997). Biophysical stimuli on cells during tissue differentiation at implant interfaces. ESB Research Award 1996. *J Biomech.* **30**, 539–48.

Preziosi, L. & Farina, A. (2002). On Darcy's law for growing porous media. *Int J Non-Linear Mech.* **37**, 485–491.

Price, C. T. & Mann, J. W. (1991). Experience with the Orthofix device for limb lengthening. *Orthop Clin North Am.* **22**, 651–61.

Putti, V. (1934). Operative lengthening of the femur. *Surg Gynecol Obstet.* **58**, 318.

Putti, V. (1990). The operative lengthening of the femur. 1921. *Clin Orthop Relat Res,* **250**, 4–7.

Quiligotti, S. (2002). On bulk growth mechanics of solid-fluid mixtures: kinematics and invariance requirements. *Theor Appl Mech.* **28-29**, 277–288.

Rachmiel, A., Potparic, Z., Jackson, I. T., Sugihara, T., Clayman, L., Topf, J. S. & Forté, R. A. (1993). Midface advancement by gradual distraction. *Br J Plast Surg.* **46**, 201–7.

Raimondo, R. A., Skaggs, D. L., Rosenwasser, M. P. & Dick, H. M. (1999). Lengthening of pediatric forearm deformities using the Ilizarov technique: functional and cosmetic results. *J Hand Surg [Am].* **24**, 331–8.

Ramasubramanian, A. & Taber, L. A. (2008). Computational modeling of morphogenesis regulated by mechanical feedback. *Biomech Model Mechanobiol.* **7**, 77–91.

Reilly, T. M., Seldes, R., Luchetti, W. & Brighton, C. T. (1998). Similarities in the phenotypic expression of pericytes and bone cells. *Clin Orthop.* **346**, 95–103.

Reina, J. M., García-Aznar, J. M., Domínguez, J. & Doblaré, M. (2007). Numerical estimation of bone density and elastic constants distribution in a human mandible. *J. Biomech.* **40**, 828–836.

Reina-Romo, E., Gómez-Benito, M. J., García-Aznar, J. M., Domínguez, J. & Doblaré, M. (2009). Modeling distraction osteogenesis: analysis of the distraction rate. *Biomech Model Mechanobiol.* **8**, 323–35.

Richards, M., Goulet, J. A., Schaffler, M. B. & Goldstein, S. A. (1999). Temporal and spatial characterization of regenerate bone in the lengthened rabbit tibia. *J Bone Miner Res.* **14**, 1978–86.

Richards, M., Goulet, J. A., Weiss, J. A., Waanders, N. A., Schaffler, M. B. & Goldstein, S. A. (1998). Bone regeneration and fracture healing: experience with distraction osteogenesis model. *Clin Orthop Relat Res.* **355S**, S191–S204.

Riddle, R. C. & Donahue, H. J. (2009). From streaming-potentials to shear stress: 25 years of bone cell mechanotransduction. *J Orthop Res.* **27**, 143–9.

Roberts, W. E. (1988). Bone tissue interface. *J Dent Educ.* **52**, 804–9.

Roberts, W. E., Mozsary, P. G. & Klingler, E. (1982). Nuclear size as a cell-kinetic marker for osteoblast differentiation. *Am J Anat.* **165**, 373–84.

Robling, A. G., Castillo, A. B. & Turner, C. H. (2006). Biomechanical and molecular regulation of bone remodeling. *Annu Rev Biomed Eng.* **8**, 455–98.

Rockwood, C. A., Green, D. P., Bucholz, R. W., Heckman, J. D., Court-Brown, C. M., Koval, K. J. & Tornetta, P. (2006). *Rockwood and Green's Fractures*

in Adults: Rockwood, Green, and Wilkins' Fractures. Lippincott Williams & Wilkins, ISBN 0781746361.

Roder, I. (2003). *Dynamical Modeling of Hematopoietic Stem Cell Organization*. PhD thesis, Leipzig.

Rodriguez, E. K., Hoger, A. & McCulloch, A. D. (1994). Stress-dependent finite growth in soft elastic tissues. *J Biomech.* **27**, 455–67.

Roux, W. (1895). *Gesammelte abhandlungen über entwicklungsmechanik der organismen*. Wilhelm Engelmann, Leipzig.

Rozbruch, S. R. & Ilizarov, S. (2006). *Limb Lengthening and Reconstruction Surgery*. CRC Press, ISBN 0849340519, 9780849340512.

Rubin, C. T. & Lanyon, L. E. (1984). Dynamic strain similarity in vertebrates; an alternative to allometric limb bone scaling. *J Theor Biol,* **107**, 321–7.

Samchukov, M. L., Cope, J. B. & Cherkashin Mosby, A. M. (2001). *Craniofacial Distraction Osteogenesis*. Heidelberg: Springer-Verlag. Inc. St. Louis. 22-23.

Samchukov, M. L., Cope, J. B., Harper, R. P. & Ross, J. D. (1998). Biomechanical considerations of mandibular lengthening and widening by gradual distraction using a computer model. *J Oral Maxillofac Surg.* **56**, 51–9.

Sanz-Herrera, J. A., Moreo, P., García-Aznar, J. M. & Doblaré, M. (2009). On the effect of substrate curvature on cell mechanics. *Biomaterials,* **In press**.

Sasaki, N. & Odajima, S. (1996). Elongation mechanism of collagen fibrils and force-strain relations of tendon at each level of structural hierarchy. *J Biomech.* **29**, 1131–1136.

Sato, M., Ochi, T., Nakase, T., Hirota, S., Kitamura, Y., Nomura, S. & Yasui, N. (1999). Mechanical tension-stress induces expression of bone morphogenetic protein (BMP)-2 and BMP-4, but not BMP-6, BMP-7, and GDF-5 mRNA, during distraction osteogenesis. *J Bone Miner Res.* **14**, 1084–95.

Saxby, T. & Nunley, J. A. (1992). Metatarsal lengthening by distraction osteogenesis: a report of two cases. *Foot Ankle.* **13**, 536–9.

Schell, H., Epari, D. R., Kassi, J. P., Bragulla, H., Bail, H. J. & Duda, G. N. (2005). The course of bone healing is influenced by the initial shear fixation stability. *J Orthop Res.* **23**, 1022–8.

Schenck, R. K. & Gatchter, A. (1994). *Bone Formation and Repair, Chapter 27.* (Brighton C.T., Friedlaender G.E., Lane J.M.), American Academy of Orthopaedic Surgeons.

Schneider, E., Sasse, S., Schmidt, H. G. & Schmann, U. (1992). Biomechanics of the ring fixator–contributions of individual structural elements. *Spine.* **95**, 580–7.

Schriefer, J. L., Warden, S. J., Saxon, L. K., Robling, A. G. & Turner, C. H. (2005). Cellular accommodation and the response of bone to mechanical loading. *J Biomech.* **38**, 1838–1845.

Schwarz, U. S. & Bischofs, I. B. (2005). Physical determinants of cell organization in soft media. *Med Eng Phys.* **27**, 763–72.

Sevitt, S. (1981). *Bone repair and fracture healing in man.* London: Churchill Livingstone.

Shapiro, F. (1988). Cortical bone repair. The relationship of the lacunar-canalicular system and intercellular gap junctions to the repair process. *J Bone Joint Surg Am.* **70**, 1067–1081.

Shearer, J. R., Roach, H. I. & Parsons, S. W. (1992). Histology of a lengthened human tibia. *J Bone Joint Surg Br.* **74**, 39–44.

Shefelbine, S. J., Augat, P., Claes, L. & Simon, U. (2005). Trabecular bone fracture healing simulation with finite element analysis and fuzzy logic. *J Biomech.* **38**, 2440–50.

Simha, N. K., Fedewa, M., Leo, P. H., Lewis, J. L. & Oegema, T. (1999). A composites theory predicts the dependence of stiffness of cartilage culture tissues on collagen volume fraction. *J Biomech.* **32**, 503–509.

Simon, U., Augat, P., Utz, M. & Claes, L. (2003). Simulation of tissue development and vascularization in the callus healing process. In *Transactions of the 49th Annual Meeting of the Orthopaedic Research Society, New Orleans.*

Simpson, A. H., Cunningham, J. L. & Kenwright, J. (1996). The forces which develop in the tissues during leg lengthening. A clinical study. *J Bone Joint Surg Br.* **78**, 979–83.

Singare, S., Li, D., Liu, Y., Wu, Z. & Wang, J. (2006). The effect of latency on bone lengthening force and bone mineralization: an investigation using strain gauge mounted on internal distractor device. *Biomed Eng Online.* **5**, 18.

Skalak, R. (1981). *Growth as a finite displacement field.* In Proc. IUTAM Sym. on Finite Elasticity, ed. DE Carlson, RT Shield.

Skalak, R., Dasgupta, G., Moss, M., Otten, E., Dullumeijer, P. & Vilmann, H. (1982). Analytical description of growth. *J Theor Biol.* **94**, 555–77.

Smit, T. H., Huyghe, J. M. & Cowin, S. C. (2002). Estimation of the poroelastic parameters of cortical bone. *J Biomech,* **35**, 829–835.

Smith, R. K. & Roberts, W. E. (1980). Cell kinetics of the initial response to orthodontically induced osteogenesis in rat molar periodontal ligament. *Calcif Tissue Int.* **30**, 51–6.

Snyder, C. C., Levine, G. A., Swanson, H. M. & Browne, E. Z. J. (1973). Mandibular lengthening by gradual distraction. Preliminary report. *Plast Reconstr Surg.* **51**, 506–8.

Soballe, K., Hansen, E. S., B-Rasmussen, H., Jorgensen, P. H. & Bünger, C. (1992). Tissue ingrowth into titanium and hydroxyapatite coated implants during stable and unstable mechanical conditions. *J Orthop Res.* **10**, 285–299.

Song, G., Ju, Y., Soyama, H., Ohashi, T. & Sato, M. (2007). Regulation of cyclic longitudinal mechanical stretch on proliferation of human bone marrow mesenchymal stem cells. *Mol Cell Biomech.* **4**, 201–10.

Sonnesen, L., Bakke, M. & Solow, B. (2001). Bite force in pre-orthodontic children with unilateral crossbite. *Eur J Orthod.* **23**, 741–9.

Stokes, I. A., Aronsson, D. D., Dimock, A. N., Cortright, V. & Beck, S. (2006). Endochondral growth in growth plates of three species at two anatomical locations modulated by mechanical compression and tension. *J Orthop Res.* **24**, 1327–1334.

Taber, L. A. (1998). A model for aortic growth based on fluid shear and fiber stresses. *J Biomech Eng.* **120**, 348–54.

Taber, L. A. & Eggers, D. W. (1996). Theoretical study of stress-modulated growth in the aorta. *J Theor Biol.* **180**, 343–357.

Taber, L. A. & Humphrey, J. D. (2001). Stress-modulated growth, residual stress, and vascular heterogeneity. *J Biomech Eng.* **123**, 528–35.

Taber, L. A. & Perucchio, R. (2000). Modeling heart development. *J Elast.* **61**, 165–197.

Tagil, M. & Aspenberg, P. (1999). Cartilage induction by controlled mechanical stimulation in vivo. *J Orthop Res.* **17**, 200–204.

Tajana, G. F., Morandi, M. & M., Z. M. (1989). The structure and development of osteogenic repair tissue according to Ilizarov technique in man. Characterization of extracellular matrix. *Orthopedics.* **12**, 515–23.

Takashima, M., Kitai, N., Murakami, S., Furukawa, S., Kreiborg, S. & Takada, K. (2003). Volume and shape of masticatory muscles in patients with hemifacial microsomia. *Cleft Palate Craniofac J.* **40**, 6–12.

Thompson, D. W. (1917). *On growth and form.* Cambridge University Press, London.

Trueta, J. & Trias, A. (1961). The vascular contribution to osteogenesis. IV. The effect of pressure upon the epiphysial cartilage of the rabbit. *J Bone Joint Surg Br.* **43-B**, 800–13.

Turner, C. H., Forwood, M., Rho, J. Y. & Yoshikawa, T. (1994). Mechanical loading thresholds for lamellar and woven bone formation. *J. Bone Miner. Res.* **9**, 87–97.

Vaishnav, R. N. & Vossoughi, J. (1983). *Estimation of residual strain in aortic segments. In Biomedical engineering II: recent development: proceedings of the Second Southern Biomedical Engineering Conference.* Oxford: Pergamon Press.

Vaishnav, R. N. & Vossoughi, J. (1987). Residual stress and strain in aortic segments. *J Biomech.* **20**, 235–9.

van der Meulen, M. C. & Huiskes, R. (2002). Why mechanobiology? A survey article. *J Biomech.* **35**, 401–14.

van der Rijt, J. A., van der Werf, K. O., Bennink, M. L., Dijkstra, P. J. & Feijen, J. (2006). Micromechanical testing of individual collagen fibrils. *Macromol Biosci,* **6**, 697–702.

Van Eijden, T. M., Korfage, J. A. & Brugman, P. (1997). Architecture of the human jaw-closing and jaw-opening muscles. *Anat Rec.* **248**, 464–74.

Vento, A. R., LaBrie, R. A. & Mulliken, J. B. (1991). The O.M.E.N.S. classification of hemifacial microsomia. *Cleft Palate Craniofac J.* **28**, 68–76.

Volokh, K. Y. (2004). A simple phenomenological theory of tissue growth. *Mech Chem Biosyst.* **1**, 147–60.

von Meyer, G. H. (1867). Die architekter die spongiosa. *Arch Anat Physiol Wiss Med,* **34**, 615–628.

Waanders, N. A., Richards, M., Steen, H., Kuhn, J. L., Goldstein, S. A. & Goulet, J. A. (1998). Evaluation of the mechanical environment during distraction osteogenesis. *Clin Orthop Relat Res.* **349**, 225–34.

Waanders, N. A., Senunas, L. E., Steen, H., Goulet, J. A., Bonadio, J. & Goldstein, S. A. (1994). Bone formation in distraction osteogenesis: histologic and immunohistochemical findings. *Trans Orthop Res Soc.* **40**, 231.

Wagner, H. (1971). Operative beinverlangerung. *Chirurg.* **42**, 260.

Weijs, W. A. & Hillen, B. (1984). Relationship between the physiological cross-section of the human jaw muscles and their cross-sectional area in computer tomograms. *Acta Anat.* **118**, 129–38.

Weil, T. S., Van Sickels, J. E. & Payne, C. J. (1997). Distraction osteogenesis for correction of transverse mandibular deficiency: a preliminary report. *J Oral Maxillofac Surg.* **55**, 953–60.

White, S. H. & Kenwright, J. (1990). The timing of distraction of an osteotomy. *J Bone Joint Surg Br.* **72**, 356–61.

White, S. H. & Kenwright, J. (1991). The importance of delay in distraction of osteotomies. *Orthop Clin North Am.* **22**, 569–79.

Wiedemann, M. (1996). Callus distraction: a new method? A historical review of limb lengthening. *Clin Orthop.* **327**, 291.

Wilsman, N. J., Farnum, C. E., Leiferman, E. M., Fry, M. & Barreto, C. (1996). Differential growth by growth plates as a function of multiple parameters of chondrocytic kinetics. *J Orthop Res.* **14**, 927–36.

Wolff, J. (1892). *The Law of Bone Remodelling.* Das Gesetz derTransformation der Knochen, Kirschwald. Translated by Maquet, P., Furlong, R.

Wolfson, N., Hearn, T. C., Thomason, J. J. & Armstrong, P. F. (1990). Force and stiffness changes during Ilizarov leg lengthening. *Clin Orthop Relat Res.* **250**, 58–60.

Wong, J. Y., Velasco, A., Rajagopalan, P. & Pham, Q. (2003). Directed movement of vascular smooth muscle cells on gradient-compliant hydrogels. *Langmuir.* **19**, 1908–13.

Wren, T. A. & Carter, D. (1998). A microstructural model for the tensile constitutive and failure behavior of soft skeletal connective tissues. *J Biomech Eng.* **120**, 55–61.

Yasui, N., Kojimoto, H., Shimizu, H. & Shimomura, Y. (1991). The effect of distraction upon bone, muscle and periosteum. *Orthop Clin North Am.* **22**, 563–567.

Yasui, N., Kojimoto, H. Sasaki, K., Kitada, A., Shimizu, H. & Shimomura, Y. (1993). Factors affecting callus distraction in limb lengthening. *Clin Orthop Relat Res.* **293**, 55–60.

Yasui, N., Sato, M., Ochi, T., Kimura, T., Kawahata, H., Kitamura, Y. & Nomura, S. (1997). Three modes of ossification during distraction osteogenesis in the rat. *J Bone Joint Surg Br.* **79**, 824–30.

Yen, S. L. (1997). Distraction osteogenesis: application to dentofacial orthopedics. *Semin Orthod.* **3**, 275–83.

Ying, J. Y. (2001). *Nanostructured Materials: Applications to Sensors, Electronics, and Passivation Coatings*. Academic Press, ISBN 0127444513.

Young, H. E., Steele, T. A., Bray, R. A., Hudson, J., Floyd, J. A., Hawkins, K., Thomas, K., Austin, T., Edwards, C., Cuzzourt, J., Duenzl, M., Lucas, P. A. & Black, A. C. J. (2001). Human reserve pluripotent mesenchymal stem cells are present in the connective tissues of skeletal muscle and dermis derived from fetal, adult, and geriatric donors. *Anat Rec.* **264**, 51–62.

Younger, A. S. (1997). *The biomechanical properties of distraction callus created during Ilizarov tibial lengthening in sheep*. PhD thesis, Aberdeen (Scotland): Aberdeen University.

Younger, A. S., Mackenzie, W. G. & Morrison, J. B. (1994). Femoral forces during limb lengthening in children. *Clin Orthop Relat Res.* **301**, 55–63.

Zuk, P. A., Zhu, M., Mizuno, H., Huang, J., Futrell, J. W., Katz, A. J., Benhaim, P., Lorenz, H. P. & Hedrick, M. H. (2001). Multilineage cells from human adipose tissue: implications for cell-based therapies. *Tissue Eng.* **7**, 211–28.

Zvaifler, N. J., Marinova-Mutafchieva, L., Adams, G., Edwards, C. J., Moss, J., Burger, J. A. & Maini, R. N. (2000). Mesenchymal precursor cells in the blood of normal individuals. *Arthritis Res.* **2**, 477–88.